Seismic Assessment of Unreinforced Masonry Walls

A thesis
submitted in partial fulfillment
of the requirements for the Degree
of
Doctor of Philosophy
In Civil Engineering
by

Ludovikus Sugeng Wijanto

Department of Civil Engineering
University of Canterbury
Christchurch, New Zealand

December, 2007

CONTENTS

Chapter 7 : Interpretation of Performance Test Results

Chapter 8 :

Analysis of Unreinforced Masonry Walls Using Finite Element Method and Current Seismic Assessment Standard

Chapter 9 : Conclusions and Recommendations

ABSTRACT

This thesis focuses on the seismic performance of unreinforced masonry wall perforated with a door opening representing typical URM walls of many aged masonry buildings in Indonesia. To obtain a test result that will be able to represent the local conditions, the experiments have been conducted in the Research Institute for Human Settlements (RIHS) laboratory in Bandung-Indonesia.

Two 75 % unreinforced masonry (URM) walls with a 1½-wythe of solid clay-brick were constructed in Dutch bond configuration and tested until failure under quasi-static-reversed cyclic loading. Both units were loaded vertically by constant loads representing gravity loads on the URM wall's tributary area. Both models were constructed using local materials and local labours. Two features were taken into account. First, it accommodated the influence of flanged wall and second, the URM wall was built on the stone foundation. The first URM wall represent the plain existing URM building in Indonesia and second strengthened by Kevlar fibre.

It was observed from the test results that the URM wall Unit-1 did not behave as a brittle structure. It could dissipate energy without loss of strength and had a post-elastic behaviour in terms of "overall displacement ductility" value of around 8 to 10. As predicted, the masonry material was variable and non homogeneous which caused the hysteresis loop to be non symmetrical between push and pull lateral load directions. It can be summarized that Kevlar fibre strengthening technique is promising and with great ease of installation. Although Kevlar material is more expensive when compared to other fabrics as long as it was applied at the essential locations and in limited volumes, it can significantly increase the in-plane URM wall capacity. With appropriate arrangements of Kevlar fibre, a practicing engineer will be able to obtain a desired rocking mechanism in the masonry structure. Another advantage for the architectural point of view, very thin Kevlar fibres do not reduce the architectural space.

Studies have also been undertaken to analyze the in-plane response of plain URM wall before and after retrofiting using the current seismic standard and the Finite Element Method (FEM).

ACKNOWLEDGEMENTS

This experimental work reported in this thesis was conducted in the Research Institute for Human Settlements (RIHS) laboratory in Bandung-Indonesia and technical facilities from Department of Civil Engineering, University of Canterbury, New Zealand. I wish to express my deepest gratitude to Professor Athol J. Carr, Dr. José I. Restrepo and Dr. Takim Andriono, supervisors of this project, for their invaluable guidance, patient and continuous support on this research project.

This research was funded by private structural consultant company in Indonesia, PT. Gistama Intisemesta, and also a financial support from Department of Civil Engineering, University of Canterbury, New Zealand. Thanks are given to :

- Engineering Faculty of Trisakti University - Indonesia for encouraging and providing facilities to continue this doctoral program.
- The excellent assistance and very generous help from the technical laboratory staffs of RIHS laboratory in Bandung under the management of Mr Sadikin.
- Mr Suwandoyo for his assistance during preparation of experimental work and also technical discussion regarding Indonesian clay bricks.
- VSL Indonesia for their assistance to purchase the thread lock bars from Australia and stressing the bars during construction of URM Unit-1
- Fosroc Indonesia for their help in providing the Kevlar materials with exceptional price
- Directors and staffs of PT Gistama Intisemesta – Indonesia for supporting, helping and running the company in my absence pursuing this doctoral program.
- my fellow post-graduate students for their constructive discussion and friendship, in particular Jitendra and Iwan Sudarno.

Special thanks to Dr. Greg MacRae for contributing with useful advice and also Dr. Pam Hoat Joen for her fruitful advice and discussion in Hongkong and Jakarta.

Thanks are also given to B. Hutchinson for helping with the computer facilities and Bruce Steven for his enormous help to use ABAQUS programme. Ms Louise Barton for her help in academic administration is also acknowledged.

Finally, I would like to express my deepest gratitude to my wife, Sumi and my sons Stefan and Sean, for their loves, continuous supports and encouragements especially when they reside permanently to New Zealand in order to support me completely. They also helped with the experiments, correction and printing of the final draft of this thesis.

NOTATION

A_b	=	cross-sectional area of the brick
A_n	=	area of net mortared/grouted brick section
A_s	=	gross area of a section
A_t	=	area of the splitting section
A_v	=	shear area
C_{db}	=	stress distribution factor for brick
C_{dj}	=	stress distribution factor for mortar
E_A	=	absorbed strain energy
E_b	=	modulus of elasticity of brick
E_D	=	energy dissipated per cycle
E_{kf}	=	modulus of elasticity of Kevlar fibre
E_m	=	modulus of elasticity of masonry
E_{mc}	=	modulus of elasticity of mortar
E_s	=	modulus of elasticity of stone foundation
F	=	force in general
f_{ae}	=	expected vertical axial compressive stress
f'_{bt}	=	direct tensile strength of bricks
f'_c	=	compressive strength of concrete
f'_{cb}	=	compressive strength of bricks
f'_{dt}	=	diagonal tension strength, default assume 1/30 f'_m
f_{mc}	=	compressive strength of mortar
f'_m	=	compressive strength of the masonry
f_n	=	normal stress at the bed joint
f'_{pm}	=	compressive strength of the prism masonry
f'_s	=	compressive strength of the stone foundation
f'_t	=	uniaxial tensile strength
f'_{tb}	=	uniaxial tensile strength of the brick
f_{tkv}	=	tensile strength of Kevlar fibre
f'_{tm}	=	tensile strength of masonry
f'_y	=	yield strength of steel
G_{kvf}	=	shear modulus of Kevlar fibre
G_m	=	shear modulus of masonry

G_{mc}	=	shear modulus of mortar
G_s	=	shear modulus of stone foundation
g	=	acceleration of gravity (9.81 m/sec^2)
H	=	horizontal force
h	=	storey height
h_{eff}	=	effective wall or pier height
h_s	=	spandrel height
h_p	=	height of masonry prism
I_g	=	moment of inertia for the gross section representing uncracked behaviour
j	=	thickness of the mortar joint
K	=	stiffness in general
K_s	=	secant stiffness, or shear stiffness
k	=	lateral stiffness of wall or pier, N/mm
	=	constant factor
L	=	length of the brick
L_s	=	length of the spandrel
l_w	=	length of the wall
M_L	=	richter (local) magnitude
M_o	=	total overturning moment
M_S	=	surface wave magnitude
M_u	=	flexural strength
N	=	the axial compression force
P	=	axial force
P_{CE}	=	expected vertical axial compressive force
R	=	reaction force
T	=	thickness of brick unit
t	=	thickness of masonry wall or pier, mm
t_p	=	thickness of masonry prism, mm
u	=	horizontal displacement of a node
u,v,w	=	displacements in x,y,z directions
V	=	shear force
V_{bjs1}	=	bed joint sliding with bond plus friction
V_{bjs2}	=	bed joint sliding with friction only

V_c	=	elastic shear force
V_d	=	diagonal tension
V_{dt}	=	toe crushing
V_f	=	shear strength due to friction
V_n	=	design shear strength
V_s	=	shear force at which shear sliding occurs
V_t	=	shear force at which diagonal crack occurs
V_u	=	ultimate shear resistance, or design shear force according to principles of capacity design
V_y	=	yield shear force
W	=	weight
$W_{1,2,3}$	=	width of brick unit
α	=	factor equal to 0.5 for fixed-free cantilever wall, or equal to 1.0 for a fixed-fixed pier wall
β	=	non-dimensional factor equal to 0.67 for $l/h_{eff} < 0.67$, 1.0 for $l/h_{eff} > 1.0$ and interpolation β value when $0.67 \leq l/h_{eff} \leq 1.0$
γ	=	shear strain
Δ	=	displacement
Δ_m	=	maximum displacement
Δ_y	=	lateral displacement at first yield
Δ_{75}	=	lateral displacement corresponding to a force level of 0.75 V_y
δ	=	storey drift, equal to the ratio of the lateral displacement to the storey height
ε	=	normal/axial strain, defined as the change in length per unit length of a line segment in the direction under consideration, dimensionless
ε_{mc}	=	mortar strain
ε_m	=	masonry strain
μ	=	coefficient of friction
ρ	=	unit weight
σ	=	normal stress
σ_n	=	the normal stress at the bed joint
τ	=	shear stress
τ_{av}	=	average shear stress
τ_{FRP}	=	contribution of the FRP laminate in resisting shear

τ_m	=	shear strength of the masonry
	=	shear strength at the shear bond failure
τ_{max}	=	maximum shear stress
τ_o	=	shear stress at the shear bond failure
τ_{bo}	=	shear bond strength at zero normal stress
υ_b	=	Poisson's ratio of the brick
υ_m	=	Poisson's ratio of the masonry
υ_{mc}	=	Poisson's ratio of the mortar
υ_s	=	Poisson's ratio of the stone foundation
ξ	=	damping ratio

CHAPTER 1 :
INTRODUCTION

1.1 BACKGROUND

Masonry construction was very common from the beginning of the civil construction technique over the whole world. Clay bricks have been employed for at least 10,000 years. They were made from sun-dried bricks and widely used in Babylon, Egypt, Spain, South American, United States and elsewhere (Drysdale et al., 1994). Older buildings mostly consist of unreinforced masonry (URM) walls. The URM elements are constructed from hand-placed units of natural or manufactured material such as clay-brick etc. and one stacked atop another and jointed to each other with mortar. In this thesis masonry structures are built from clay bricks and jointed with mortar. There are numerous methods of clay-brick making, largely depending on local customs. The properties of bricks are influenced by the nature of the clays, methods of molding and the firing. Pure clays are useless for brick making unless they are mixed with a non-plastic material and this is different for every country or region. As the properties of clays vary throughout the world, it will be apparent that different kinds of bricks predominate in different regions. The wide variety of bricks that have resulted naturally produces a bewildering variety of properties.

Most of those older masonry buildings are designed primarily to resist gravity loads only since the provision for earthquake loading codes were not then established. It was observed in frequent earthquakes that older masonry structures perform poorly and most of those buildings would collapse in a major earthquake. The clay brick material is relatively heavy, brittle, of low tensile strength and show low ductility when subjected to seismic excitation. Some historical performance of unreinforced masonry buildings throughout past earthquakes shown on Figure 1.1. and can be detailed as follows :

- The United States has had historical earthquakes which caused extensive damage to masonry buildings. The San Francisco earthquake of April 18, 1906 with an estimated magnitude of 8.0 on the Richter scale, followed by the 1925 Santa Barbara earthquake having magnitude 6.3 on the Richter scale, the Long Beach earthquake on March 10, 1933 , the Northridge earthquake occurred on January 17, 1994, the Nisqually

earthquake of February 28, 2001 and one of the latest, the San Simeon, California earthquake of December 22, 2003. The observed seismic performance noted from these earthquakes, has resulted in a series of documents dealing with the seismic assessment and strengthening of masonry structures.

(a) Coalinga earthquake May 2, 1983

(b) Armenia earthquake December 7, 1988

(c) Loma Prieta earthquake October 17, 1989

(d) Northridge earthquake January 17, 1994

(e) Bengkulu earthquake –Indonesia June 4, 2000

(f) Nisqually earthquake February 28, 2001

Figure 1.1. Severe damages at URM buildings after an earthquake

- An earthquake of December 7, 1988, having a magnitude 0f 6.8 struck the Soviet Republic of Armenia. Cities such as Spitak and Leninakan suffered heavy damage.

Most of the buildings were of unreinforced masonry bearing wall construction and performed poorly over all. In the Erzincan earthquake, Turkey, on March 13,1992 with Richter Magnitude 6.8 a large percentage of unreinforced masonry bearing wall–structures were destroyed (Bruneau and Saatcioglu, 1994).

- A large number of the earthquakes in Indonesia have caused extensive damage to unreinforced masonry housings. The houses commonly consist of a half clay brick thickness and are constructed in accordance with common local practice without design for earthquake resistance. However, older masonry buildings with more than one wythe performed well suffering only minor or no damage at all when subjected of low to moderate earthquakes.

A number of common failures of URM buildings have been observed from around the world. Bruneau (1994), regrouped the failure performances as follows : lack of anchorage, anchor failure, in-plane failures, out-of-plane failure, combined in-plane and out-of-plane effects and diaphragm-related failures. Many older URM-buildings lack positive anchorage of the floors and roof to the URM-walls, which contribute to sudden failure under seismic excitation. Anchor failure depends on the material properties which are unsuitable to seismic resistance. The in-plane failure characterized by a shear crack pattern, where cracks are primarily along the mortar bed joints; some inclined cracks may also be developed. The exact crack pattern will, of course, depend on the wall boundary conditions and the aspect ratio of the URM elements. Seismic actions are bidirectional and the URM can perform in both in-plane and out-of-plane direction. Improperly anchorage of floor/roof diaphragms to the URM walls and out-of-plane failure can cause failure of the diaphragm transfer the horizontal seismic forces. The out-of-plane failure has been identified as the major cause of loss of life during the earthquakes.

From previous earthquake experience showing the vulnerability of URM buildings, the current regulations for construction and design in seismic prone areas throughout the world no longer recommend the use of unreinforced masonry structures. Considerable attention to the means of evaluation and strengthening of the all older masonry buildings that exists in seismic prone area is necessary. Most of the unreinforced masonry research is focused on the performance of existing rather than new structures.

1.2 OBJECTIVES OF THE RESEARCH WORK

The objective of this research was to quantify the performance of in-plane unreinforced masonry walls with door opening in the centre when subjected to gravity load and lateral seismic action. Another intention of this project was to enhance the seismic performance of URM walls using a surface coating material. The research model was to represent existing unreinforced masonry walls built in Indonesia in the 1900s. The research included of two 75% scale unreinforced masonry walls with a 1½-wythe of clay-brick and the clay-brick configuration generally used at that time i.e. Dutch bond configuration. Both models were tested in the Research Institute for Human Settlements (RIHS) laboratory in Bandung-Indonesia. Test unit-1 is an URM-wall representing an existing structural condition and test unit-2 was strengthened by high performance aramid fiber containing Kevlar material. Both units were tested until failure under quasi-static-reversed cyclic loading.

It was of particular interest to investigate :

- The in-plane strength and deformation capacity of perforated unreinforced masonry (URM) wall with door opening
- The advantage of using Kevlar as retrofit material for URM wall
- Review the test result using the ABAQUS program
- The relationship between the analysis and the experiment

The end result of the study will be recommendations for the assessment and strengthening of URM buildings using Kevlar material. Although this research was conducted in Indonesia and using local materials, it is expected that these research results are easily extrapolated to other seismic prone countries.

1.3 TERMINOLOGY

The initial phase of this study comprises a literature search where models proposed by research groups and/or adopted by codes (ASTM, NEHRP, FEMA, IBC, NZS, British Standards and Indonesian Standards) are being selected. A database of experimental tests was compiled. In the second phase of this study, critical parameters will be identified and a parametric analysis will be developed.

1.4 ORGANIZATION OF THESIS

This report is divided in 9 chapters. Chapter 2 describes the review of specific unreinforced masonry literature that relate to this research. A description of the clay brick materials used and their mechanical properties are detailed in chapter 3. The description of specimen design, construction techniques, instrumentations and testing procedures are detailed at chapter 4. Chapter 5 describes the test result of unit-1 which represents the existing URM wall and chapter 6 describes the test result of URM wall strengthened by Kevlar material. This is followed with interpretation of both performances of the test results in chapter 7. The analyses of the performance of both specimens using the current seismic assessment standard, the ABAQUS finite element program and the comparison with the test results are detailed in chapter 8.

Finally, a summary of the thesis and its conclusion are provided in chapter 9. Some suggestions for future research on the subject of URM walls are given.

CHAPTER 2 :
LITERATURE REVIEWS

2.1 INTRODUCTION

This chapter presents review of different studies incorporating the performances of unreinforced masonry walls. Not much research on unreinforced masonry walls has been conducted in Indonesia. Tests on URM walls have never been conducted in Indonesia until this research study. Studies have also been undertaken to model and analyze the response of URM walls due to gravity loading and lateral loading. This section will briefly summarize previous research relating to the material components of masonry, in-plane performance of URM walls, modeling and analysis of URM walls with and without strengthening.

In 1976, Beca Carter Hollings and Ferner consulting engineers, commissioned by the New Zealand Ministry of Foreign Affairs, under the aegis of the New Zealand Bilateral Assistance Program to Indonesia, carried out of the first confined masonry wall testing program in conjunction with preparing the Seismic Design Loadings Code for Indonesia. They tested 19 walls comprising of 11 red brick walls and 7 *batako* (trass lime blocks) walls. In-plane tests were conducted on 3 red brick walls and 3 *batako* walls and others were tested for face loadings. The test was not to try to exactly match theory with the observed behaviour, which is impracticable with a material of such inherent variability, but to provide recommendations of practical applicability to the common forms of masonry construction currently used in Indonesia. Upon completion of this program, a large number of recommendations were proposed for the use of infill walls both as structural walls and non-structural walls by Beca Carter (1981). The results of the in-plane loading tests indicated that infill walls could be used to resist lateral seismic loads even for low-grade masonry. Clay brick walls reinforced with practical columns at certain spacings could resist the seismic loads as face loading. From these tests some information was obtained about the strength data of the clay brick and mortars, which was used during the tests.

2.2. MECHANICAL PROPERTIES OF MASONRY MATERIALS

Masonry is a nonhomogeneous material consisting of bricks and mortar in filled joints. Both have certain strengths and deformation capabilities. Only a proper balance between the right type of mortar and the right type of brick can give a good result for bearing walls. The strength value of brickwork is also strongly influenced by the workmanship. This section will discuss the properties of the brick units, the mortar and their behaviour in masonry walls.

2.2.1. Masonry Units

Currently there are various types of masonry units produced from a variety of raw materials such as clay, calcium silicate (sand lime brick), stone and concrete and by a variety of production methods. Regarding its shape, however, clay brick is still produced in a rectangular shape for easy handling. In this research programme only clay brick material will be investigated. Clay brick as a building element is made of clay with or without a mixture of other substances, burned at an adequately high temperature to prevent it from crumbling again when soaked in water. Bricks can be classified as solid or hollow. Most building codes define a brick as solid if the net cross-sectional area in every plane parallel to a bearing surface is 75% or more of its gross cross-sectional are measured in the same plane. The hollow brick is defined if the cores, cells, or hollow spaces within the total cross-sectional area exceed 25% of the cross section of the unit.

Information of the mechanical properties of clay bricks is required when assessing existing URM buildings. The mechanical properties data for masonry units are interpreted in the following section.

2.2.1.1. Compressive Strength of Masonry Units

Compressive strength of masonry units was determined by a standardized procedure such as those of ASTM C-1314, NZS-366 1963, BS-3921 and SNI 15-2094-1991. This test will investigate the compressive strength of the masonry units itself and the value is increased by lateral confinement from the platens of the testing machine. This confinement also depends on the ratio of the height to thickness of the masonry unit. The compressive strength of masonry

unit depends on the strength of the raw materials and shown higher value compared to the compressive strength of masonry (Paulay and Priestley, 1992, Drysdale et al., 1994).

2.2.1.2. Tensile Strength of Masonry Units

Tensile strength describes the capacity of a masonry material unit when subjected to a maximum tension. There are several tensile strength tests that depend on the applied loading such as flexural tensile strength, splitting tensile strength and direct tensile strength. The flexural tensile strength test or modulus of rupture test (ASTM C-67) was measured on masonry units subjected to an axial load that is applied incrementally to the center between the two supports at the end of the masonry units. The splitting tensile strength test (ASTM C-1006) was measured by applying a line-load at both surfaces and longitudinally parallel to the length of the masonry unit. The axial tensile strength test was carried out on cylindrical specimens where the ratio of height to diameter is 1. Steel plates glued with epoxy resin on the top and bottom faces of the cylinders were used to apply the tensile force.

In the absence of tensile strength tests of the masonry units, Hilsdorf (1967) reported some correlation between the compressive strength and the power of two-thirds yields the direct tensile strength :

$$f_{t,axial} = 0.26\, f_{cb,cyl}^{0.67} \quad \text{..... (2.1)}$$

Other correlations are as follows :

$$f_{t,axial} = 0.72\, f_{cb,spliting} \quad \text{..... (2.2)}$$

$$f_{t,axial} = 0.50\, f_{cb,flexural} \quad \text{..... (2.3)}$$

Sahlin, 1971, reviewed of test data the ratio of the tensile strength to the compressive strength of bricks is around 1:20 for solid brick and 1:30 for hollow bricks. It was mentioned that the ratio of modulus of rupture varies roughly between 10% and 30 % of the compressive strength of clay brick. The tensile strength value is around 30% to 40% of the modulus of rupture.

2.2.1.3. Moisture Content and Absorption of Masonry Units

The property of bricks that has the biggest influence on the mortar is the suction rate. The absorption in the clay brick unit produces a suction effect that can draw water from mortar. The suction rate must be controlled to prevent excessive removal of water from the mortar.

The water absorbed by the bricks leaves cavities in the mortar, which fill with air and result in a weakened mortar on setting. ASTM C-67 specifies it as the initial rate of absorption value (IRA), which is normally defined as the amount of water absorbed by a dry masonry unit when partially immersed in water to a depth of 3 mm for a given period of one minute. Several tests have indicated that IRA values between 2.5 to 15 g/minute/dm^2 generally produce good bond strength with compatible mortar (Drysdale et al., 1994; ASTM C-67). Sahlin, 1971, reported that masonry units with low suction (less than 10 g/minute/dm^2) and reasonably rough surfaces, and mortar with reasonably high water retentivity more than 70% would probably give a good bond. Generally, the Indonesian brick has a high suction rate and the limit value of suction rate for Indonesia clay brick is not higher than 20 g/minute/dm^2 (UNIDO, Technical Paper No 11, 1978). Bricks of low strength must be soaked for about one to two minutes to bring the suction rate down to suggested level. The moisture content and the water absorption of the masonry unit have a considerable effect on the characteristic of the masonry. Masonry quality was improved by wetting the clay brick units for approximately 5 to 8 minutes in a container of water, before placing the mortar.

Clay bricks absorb moisture from the environment that can causes complex chemical reactions. Several researchers have conducted tests and have plotted relationships between moisture expansion versus time for clay and shale bricks as discussed at Drysdale et al., 1994. It is reasonable practice to assume that a linear relationship exists between expansion and the logarithm of time (Drysdale et al., 1994).

2.2.1.4. Creep and Shrinkage

A burnt clay product such as a brick has a very little movement itself but when combined with mortar some shrinkage of the brickwork can occur. The stronger the mortar the greater is the chance of such shrinkage becoming obvious. There are two kinds of shrinkage : free shrinkage and prevented shrinkage. Free shrinkage being a term for how much shorter a bar of mortar becomes during curing, it shortens very much in the first hours and the shortening decreases with a higher amount of lime and a smaller amount of cement. Prevented shrinkage is the stress, which is created in the mortar if it is not allowed to shrink. This can, if the stress is stronger than the tension strength lead to cracks in the mortar. For lime mortars these forces grow very slowly and are very small. The more cement that is added a mortar the faster will the stress grow and the higher values it will reach. Mortars of cement-sand can give stress

values of about 3 MPa within 3 to 4 days. When the amount of cement in a mortar increases the chance of cracks also increases. In reality, mortar is always prevented from shrinkage as it is kept in place by the bonding with the bricks.

2.2.2. Mortars

Although mortars form only a small proportion of brickwork as a whole, their characteristics have a big influence on the quality of the brickwork. Batching and mixing are also an essential factor that has a great influence on both strength and workability of mortars. Mortar is used as a means of sticking or bonding bricks together and to take up all irregularities in the bricks. To do this the mortar must be well workable so that all joints are filling completely. There are two things of importance for the workability, stiffness and plasticity. The stiffness is dependent upon how much water there is added to the mortar. How much water to add depends on what one is to use the mortar for, and does not say anything about the quality, but it is a characteristic of the condition. The plasticity is a term for how easy the mortar can be formed. A binder rich mortar has a better plasticity than a binder poor mortar. The grading of the aggregate also has a certain influence on the plasticity, the closer the grading is to the ideal curve the better the plasticity.

The water content is calculated after the water is added to the dry mortar. The moisture in the aggregate is not considered in this calculation. The water content in the aggregate was about 20 % by weight.

Curing of mortar cubes : according to ASTM C-270, should be stored as follows : Mortars where cement is the main binder, cubes must be cured in a relative humidity of 90 % or more and kept in the moulds for from 48 – 52 hours, in such a manner that the upper surfaces shall be exposed to the moist air. Different mortar strengths are obtained by changing the aggregate ratio. Mortars, which only contain lime as a binder normally, have a strength of 0.5 to 1 MPa, cement-lime mortars strength varies from 1 to 10 MPa and pure cement mortar strengths ranges from 10 to 20 MPa. Table 2.1. is shown the compressive strength of mortar, that conducted by UNIDO in Indonesia.

Various types of cement can be used for mortar, such as ordinary Portland cement or Masonry cement. Ordinary Portland cement should conform to ASTM C-150 standard and Masonry cement should conform to ASTM C-207 standard.

The sand for mortar should be clean, sharp and free from salt and organic contamination (Hendry et al., 1997). Most natural sand contains a small quantity of silt or clay. A small quantity of silt improves the workability. Specifications of sand should conform to ASTM C-144 standard, prescribe grading limits for the particle size distribution.

Mixing water for mortar should be clean and free from contaminants either dissolved or in suspension. Ordinary water will be suitable.

Table 2.1. Compressive Strength of Mortar Cubes 50 mm x 50 mm x 50 mm
Average of 3 Cubes - According to ASTM C-270 (UNIDO, 1978a)

Mortar No.	Mortar Composition					Compressive strength Average in kg/cm^2			
	Cement	Lime	Trass	Sand	r.c.	7 days	14 days	28 days	60 days
1		1	5			15	27	41	53
2	½	1	7			34	78	69	131
3	1			4		63	107	148	161
4		1		1	1	0	1	3	7
5		1		2		1	1	3	5
6	1	1		6		14	19	33	50
7		1		2	1	2	4	8	10
8	1			3		91	195	216	252
9	¼	1	5			7	13	23	28
10	1	1	12			7	18	31	38
11	1	1	10			16	33	45	67
12	1		6			27	47	54	84
13	1		4	1		50	74	102	117
14	1	1	7	3		16	26	34	49
15	1	1	9	3		16	29	47	57
16	½	1		4		9	12	17	23
17	1		2	2		75	105	123	141
18	1			2		214	312	303	404
19		1		3	1	0	1	3	9
20	½	1	5			45	77	109	117
21	½	1	4	6		8	13	21	28
22	1	1		4		45	63	77	77
23	½	1.5	10			22	50	71	95

Note : r.c. = red-cush

The modulus of elasticity of mortars, E_{mc}, can be related to its compressive strength, f'_{mc}, and may be approximated by $E_{mc} = 100\ f'_{mc}$. Poisson's ratio of most hydraulic cement and lime mortars is on the order of 0.2 and increases rapidly as the uniaxial strength of the mortar is approached.

2.2.3. Masonry

Clay-brick material with a relatively heavy specific gravity is capable of resisting axial load force but is weak in resisting tensile and shear load. In accordance with its character clay-brick becomes a structural element of low ductility. In the event of an earthquake an unreinforced masonry building often experiences damage so that unreinforced masonry construction is no longer recommended for buildings in seismic prone regions.

The tensile strength of masonry is very low, of the order of 1.5 to 2 % of its compressive strength. Normally brickwork strength is strongly correlated to the strength of the mortar. It appears that masonry strength may vary between the 1/3 power and the 2/3 power of the mortar strength when the elasticity modulus of brick and mortar are approximately equal (Sahlin, 1971).

> *Because of specific characteristics of each constituent masonry materials, especially the masonry unit, it is not easy to predict the mechanical characteristics of a specific masonry construction type by knowing only the characteristics of its constituent materials, mortar and masonry units. It is therefore of relevant importance that, for each type of masonry, experiments to correlate the strength characteristics of constituent materials with the characteristics of masonry are carried out* **(**Tomaževič, M., 1999)

2.2.3.1. Masonry Compressive Strength

The compressive strength of the masonry units was determined by a standardized procedure such as the prisms test (ASTM C-1314); whole or half brick and capped with a sulphur-pumice mixture (NZS-366 1963); prisms test with minimum three courses (AS/NZS 4456.5-1997), British Standard and Indonesian standard (SNI 15-2094-1991) which brick unit will be cut in half with a saw. Each cut part of the brick will be stacked on the other part and the

space between the two cut bricks are to be filled with 6 mm mortar. This test will investigate the compressive strength of the masonry in the normal direction of the mortar bed. ASTM C-1314 prism tests recommended a height to depth ratio between 1.3 and 5.0. Recommendations have been made to the standards association NZ along these lines for a test based on ratio of height to least lateral dimension greater than or equal to 3

The compressive strength of a masonry wall is affected by some factors, such as workmanship, the properties of the masonry units, the thickness of mortar joints, the age of mortar and also the suction rate (Sahlin, 1971). It is reported that increasing mortar joint thickness lowers the compressive strength and the normal joint thickness of 10 mm is recommended (Sahlin, 1971). In their book, Paulay and Priestley, 1992, as well as Drysdale et al., 1994, have concluded that the prism compressive strength of brick masonry (f'_m) is less compared with the unit compressive strength of a brick unit (f'_{cb}). The brick masonry strength normally is about 25% to 50% of the masonry unit strength, the lower value referring to low strength mortar and the higher strength for high strength mortar. The compressive strength of masonry is substantially less than the masonry unit strength because of the influence of the mortar. The ratio also tends to decrease with increasing masonry unit's strength. In addition, the prism compressive strength of brick (f'_{pm}) bound with mortar is larger compared with the mortar strength (f'_{mc}) (Figure 2.1.). Collapse will occur because of vertical shearing of the brick unit rather than disintegration of the mortar. The cause is a result of improper brick and mortar laying. Because the lesser strength and value of the elasticity modulus of mortar than that of the brick unit caused the axial and lateral tension (*Poisson's ratio)* of the mortar to become larger than the clay units. In line with the axial tension reaching the mortar's maximum strength (f'_{mc}), the mortar will experience a continued increasing of lateral shearing (Figure 2.2.a.). The joint effect of a lower elasticity modulus and a higher *Poisson's ratio* will tend to the lateral tensile strength of the mortar exceeding the lateral tension of the brick unit (Figure 2.2.b.). Because friction and adhesive strength on the mortar-brick joints force the lateral tension of the mortar and brick unit to change the lateral compressive strength on the mortar to equal to the lateral tensile strength on the brick unit (Figure 2.2.c.)

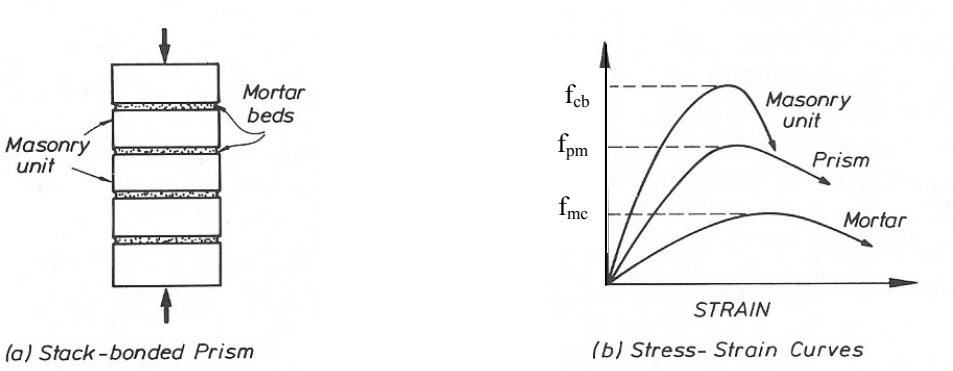

Figure 2.1. Correlation between stress-strain at masonry prism (Paulay and Priestley, 1992)

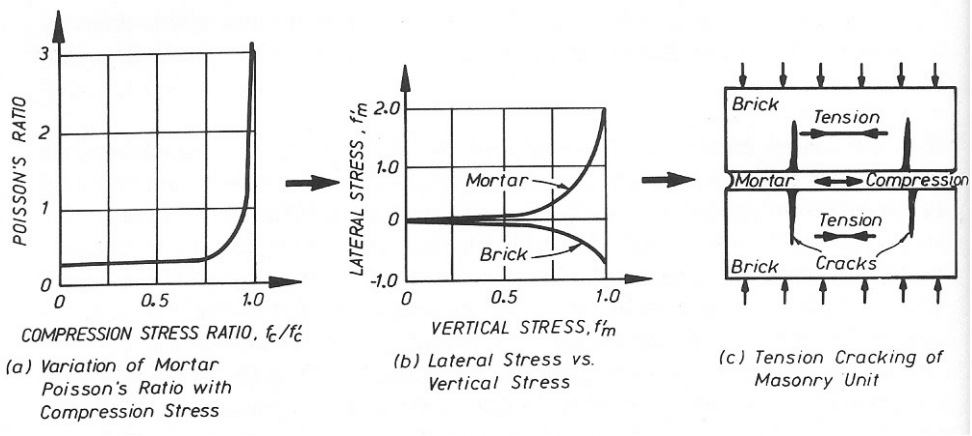

Figure 2.2. Mechanism of a collapse on the masonry prism (Paulay and Priestley, 1992)

The prism test recommends a height to thickness ratio of not more than 5 nor less than 1.3 (ASTM standard C-1314). The specimen contains five stack-bond prisms and was tested in axial compression. The procedure of the compressive testing of the axially loaded prisms was in accordance with ASTM Test Method ASTM C-1314. ASTM standard E-518 prescribes a horizontal flexural test method for determining the bond strength of masonry.

In 1978, United Nations Development Programme (UNDP) in cooperation with the Indonesian Directorate of Building Research focused on the extensive testing of brickwork specimens using local bricks and mortars. The aim of this research was to provide technical data for the establishment of the Indonesian Code of Practice for Brickwork Construction based on local practice. Compressive strength testing was conducted using a brickwork cube consist of 5 layers of bricks vertically and 2 layers horizontally. The specimens were tested after 7 days, 14 days, and 28 days (6 specimens each) and it was concluded that the compressive strength of brickwork had developed nearly 100% in 14 days. The compressive strength of brickwork varies between 2 to 3 MPa. The shear strength of brickwork is highly affected by the bonding between the brick and mortar. Table 2.2. are shown the classification compressive strength of brick masonry in Indonesia :

Table 2.2. Classification according to strength (SNI 15-2094-1991)

Class	Average minimum compressive strength of 30 pcs tested bricks		Allowable coefficient of variation (%)
	kg/cm^2	MPa	
25	25	2.5	25
50	50	5	22
100	100	10	22
150	150	15	15
200	200	20	15
250	250	25	15

Similar specimens to those used for compressive strength were loaded diagonally and the shear strength of Indonesian brickwork ranges between 0.05 to 0.19 MPa and the data were found to be very variable. The flexural tensile strength of brickwork varies between 0.02 to 0.12 MPa (UNIDO, 1978b, 1979). Since there were no available standard tests to evaluate the elastic modulus of brickwork in Indonesia, ASTM E-111 was adopted.

Recently, tests on the compressive strength of clay brick units were conducted in Indonesia by Basoenondo et al. using solid clay bricks produced traditionally in home industries from Cikarang. The compressive strengths were conducted using the Indonesian standard and give lower quality bricks with average compressive strength of approximately 4 MPa. The compositions of the mortar mix consisted of 0.95 part of water : 1 part of cement : 4 part of sand. (Basoenondo et al., 2003). There are many local clay-brick suppliers in Indonesia that the quality and the compressive strength vary greatly. A standardized clay brick quality and dimension are urgently needed for masonry units in Indonesia.

2.2.3.2. Masonry Flexural Tensile Strength

The tensile strength of masonry describes the capacity of a material when subjected to maximum tension. The tensile strength is governed by the bond between the mortar and the units as this is typically less than the tensile strength of either of the constituent materials. Masonry bond strength easily affected by workmanship and can vary depending on the correct match between the mortar and the unit properties, particularly the water retention of the mortar and the suction of the masonry units.

Two types of loading options are provided for the flexural test, as shown in Figure 2.3. :

- First, the specimens tested as horizontal beams with the transverse loads applied vertically
- Secondly, the specimen consists of at least five courses and tested in a vertical orientation and loaded in a manner that will induce equal and opposite's couples at the ends. (Bond-wrench method ; ASTM C-1072)

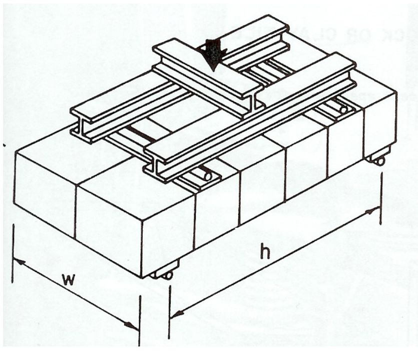

(a) Flexure test with transverse loading

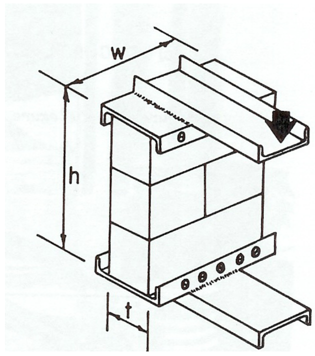

(a) Flexure test with eccentric loading

Figure 2.3. Methods of masonry flexural tensile strength

The Australian standard (SAA Masonry Code AS-3700) allows designers to assume a characteristic flexural tensile strength for masonry of 0.20 MPa. Hendry et al., 1997, reported the flexural tensile strength of clay brick ranges from about 0.2 to 0.8 MPa in the stronger direction.

Tomaževič, 1999, reported the correlation between the tensile, f_t, and compressive strength, f_m, of any type of masonry as :

$$0.03\ f_m \leq f_t \leq 0.09\ f_m \quad \ldots\ldots\ldots\ldots\ldots\ldots\ldots\ldots \quad (2.4)$$

The flexural tensile strength value from the tests for unreinforced masonry walls can be used for in-plane lateral forces and out-of-plane bending conditions.

2.2.3.3. Masonry Elastic Modulus

The elastic modulus or Young's modulus was characterized by linear proportionality between stress and strain in the elastic condition. It may be determined from measurements obtained from compression tests of masonry prisms or a prismatic masonry test. The ideal combination

of mortar and clay-brick is a clay-brick with elastic modulus equal to or nearly equal to that of the joint mortar. The Young's modulus of Elasticity is a result of a comparison between strain and stress as follows :

$$E_m = \sigma / \varepsilon_m \quad \ldots\ldots\ldots\ldots\ldots\ldots\ldots\ldots\ldots\ldots (2.5)$$

The minimal test information concerning the strain-tension of clay units has resulted in the assumption that the behaviour of clay bricks almost resembles linear elasticity material while concrete blocks are considered to behave in nonlinear way similar to the behaviour of concrete in general. The Young's modulus of elasticity of brick units also shows a very wide variety and basically depends on the type of material and value of the compressive strength. Typically, a secant modulus of elasticity, E_m, is described by the slope of the stress-strain curve between 5% and 33% of the masonry ultimate compressive strength of each prism test or prismatic test (FEMA-274 1997, UBC-97, ASTM E-111 and NEHRP, 2000).

Empirical linear relationships between the compressive elastic modulus and the equivalent compressive strength from some researches are usually assumed as follows :

$$E_m = k \cdot f'_m \quad \ldots\ldots\ldots\ldots\ldots\ldots\ldots\ldots\ldots\ldots (2.6)$$

Where k is a constant factor, E_m is elastic modulus of masonry in compression (MPa) and f'_m is specified compressive strength of masonry (MPa). Some of the correlations are shown in Table 2.3. and k factor for clay bricks vary in between $300 \leq k \leq 750$. This huge range factor is depend on the local raw material of clay brick.

Table 2.3. :

Correlation between modulus of elasticity of masonry and masonry compressive strength

No.	Reference	Elastic Modulus of Masonry in Compression
1	NEHRP 2000	Clay brick $E_m = 750 f'_m$
2	Tomaževič, 1999	Clay brick $200 f_{cb} \leq E_m \leq 2000 f_{cb}$
3	FEMA 273, 1997	Clay brick $E_m = 550 f'_m$
4	Sahlin (1971), Crisafulli et al (1995)	Clay brick $E_m = 300 f'_m$
5	Drysdale et al., 1994	Concrete $E_m = 750 f'_m$ Clay brick $E_m = 500\text{-}600 f'_m$
6	Paulay and Priestley, 1992	Concrete $E_m = 1000 f'_m$ Clay brick $E_m = 750 f'_m$

Without noticing the above differences, in a sensitive calculation towards the E_m value, attention should be paid to using a representative E_m value to avoid excessive strains, particularly considering the examples of clay bricks in Indonesia. Normally, the test result showed significant variation on the Young's modulus of clay brick. In his text book (Drysdale et al., 1994) has taken the maximum masonry compressive strain value as 0.003

2.2.3.4. Masonry Shear Strength

Shear specimens should be tested by a compression force applied along diagonal axis within the centroidal plane of the cross section. The diagonal compression test will be used to evaluate the masonry shear strength and the modulus of rigidity.

The basic form of the shear strength for unreinforced masonry is based on the Mohr Coulomb shear friction expression (Crisafulli et al. 1995; Hendry et al. 1997) as follow :

$$\tau_m = \tau_o + \mu\sigma_n \quad \ldots\ldots\ldots\ldots\ldots\ldots\ldots\ldots\ldots\ldots \quad (2.7)$$

where τ_m = shear strength at the shear bond failure; τ_o = shear bond strength at zero normal stress due to the adhesive strength of mortar; μ = coefficient of internal friction between brick and mortar; and σ_n = the normal stress at the bed joint. From the above formula, it has shown that there is a relation between shear strength and the normal stress.

Hendry et al. 1997, reported the shear strength limit value of clay brick is about 2.0 N/mm^2. The shear strength depends on the mortar strength. For high strength mortar (1:1/4:3) which has compressive strength between 20 to 50 N/mm^2, the value of τ_o will be approximately 0.3 N/mm^2 and 0.2 N/mm^2 for medium strength mortar (1:1:6). The average value of μ is 0.4 to 0.6. Sahlin, 1971, summarized that τ_o will be approximately 0.2 N/mm^2 and the average value of μ is 0.5.

In parametric form equation can be expressed :

$$V_n = f_n\,(f'_m, N) \quad \ldots\ldots\ldots\ldots\ldots\ldots\ldots\ldots\ldots\ldots \quad (2.8)$$

Where V_n represents the design shear strength, f'_m is a measure of masonry material properties and N is the axial compression force.

Types of shear failure are divided into three categories i.e. failure along the mortar and brick unit joints, failure of shear load and diagonal tensile cracks. Some methods of testing shear strength are shown in Figure 2.4.

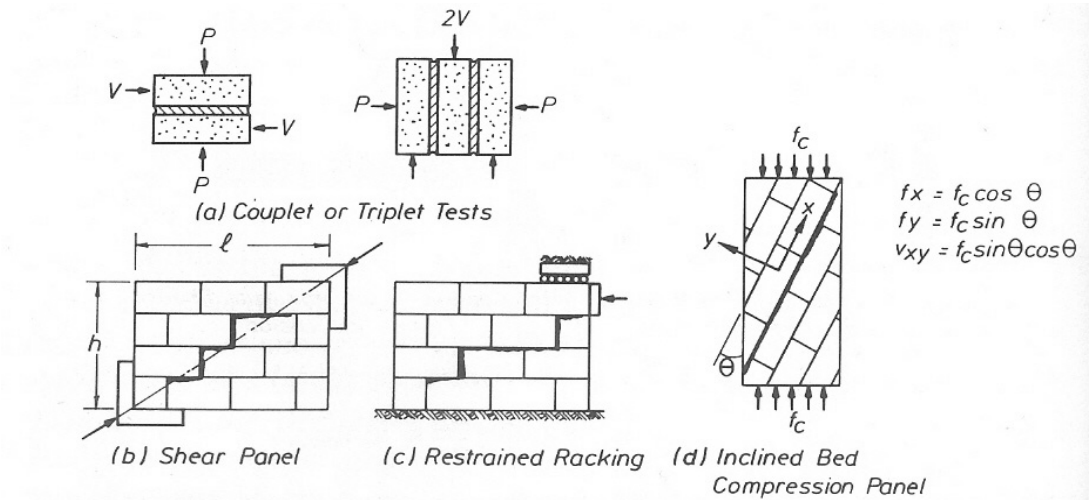

Figure 2.4. Methods of testing shear strength in masonry construction (Paulay and Priestley, 1992).

2.2.3.5. Masonry Shear Modulus

Masonry shear modulus of modulus of rigidity may be obtained from measurements of diagonal deformations in racking test specimens. In the absence of sufficient data, shear modulus, G_m, can be assumed vary from 6% to 25% of the Elastic modulus (Young's modulus). The shear modulus of elasticity, G_m, was taken from the coefficient from Alcocer and Klinger (1994) in between 0.1 – 0.3 times E_m (0.1 for high-strength units and 0.3 for weaker units). The shear modulus of uncracked unreinforced masonry can be estimated as $G_m = 0.4\ E_m$ in compression (FEMA 273) After cracking the shear stiffness is reduced substantially as sliding along bed joints develops or as diagonal tension cracks open. Some researchers reported that G_m value can be estimated through = 400 f'_m (Fattal and Cattaneo, 1977, Paulay and Priestley, 1992)

Tomaževič (1999), reported the correlation between the tensile and compressive strength for any type of masonry : $1000\ f_{ts} \leq G_m \leq 2700\ f_{ts}$. Most result indicated a G_m value close to 2000 f_{ts}.

2.3. PERFORMANCE OF UNREINFORCED MASONRY WALLS

2.3.1. General

There is a large number of existing URM buildings in the world and many experiences of URM structural performance reported after being subjected to seismic loads. Two types of failure are commonly observed; in-plane failure indicated by a diagonal crack pattern, and out-of-plane failure when cracks are formed along the mortar bed joints. The observed failure in the URM buildings was quite complex depending on several aspects such as boundary conditions, different length-to-height ratios of the walls, types of floor diaphragm, initial compressive stress, mechanical of material properties etc. In the following paragraphs each type of the URM wall failures will be discussed in more detail.

2.3.2. In-Plane Failure of URM Walls

Various in-plane examples of unreinforced masonry walls subjected to seismic lateral loads can be seen in several text books (e.g. Paulay and Priestley, 1992). The in-plane capacity of the wall depended on the relative strength of the masonry and the mortar. Figure 2.5 show the in-plane failure mechanism of unreinforced masonry wall when subjected to lateral load.

The level of the axial load significantly controls the type of failure. There are several failure conditions for in-plane URM walls due to the form of construction and the combine effects of axial load and bending, as follows (Tomaževič, 1999) :

- Sliding shear failure, along head or bed joint because of low normal stresses and/or low friction coefficients, which may be due to poor quality of the mortar
- Shear failure, takes place where the principal tensile stresses developed in the wall under a combination of vertical and horizontal loads, exceeds the tensile strength of masonry materials. The crack propagation either follows the mortar joints or passes through the masonry units, or both. Shear failure should be avoided as it will cause a limited/lower ductility for URM-walls. The strength and stiffness of the URM-wall will degrade rapidly following formation of a diagonal shear crack.

- Flexural failure, crushing of compressed zones at the ends of the URM wall usually takes place, indicating the flexural mode of failure. It happens when the shear resistance still strong enough when compared to the shear demands.

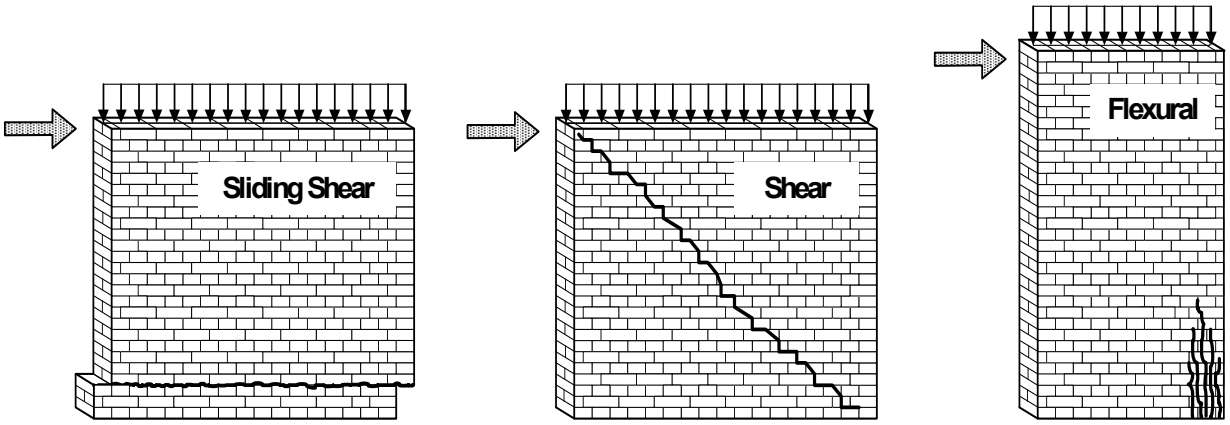

Figure 2.5. Performance of URM walls subjected to in-plane seismic load (Tomaževič, 1999)

The performance of URM wall is linear-elastic before the flexural tension stresses at the wall heel exceed the tensile strengths capacity, or diagonal tension or bed joint shear stresses exceed the shear strength capacities. It is reported the lateral in-plane stiffness of a cantilever URM wall that assumed homogeneous materials, can be calculated using equation :

$$k = \frac{1}{\frac{h^3_{eff}}{3E_m I_g} + \frac{h_{eff}}{A_v G_m}} \quad \text{.....(2.9.)}$$

The lateral in-plane stiffness of a pier between openings with full restraint against rotation at its top and bottom, can be calculated using equation :

$$k = \frac{1}{\frac{h^3_{eff}}{12E_m I_g} + \frac{h_{eff}}{A_v G_m}} \quad \text{..... (2.10.)}$$

URM-wall subjected to seismic loading will progressively degrade with all or some of the failure types occurring as shown in Figure 2.5. In older unreinforced masonry buildings, the joints are the weakest part of the wall. Even in the case of diagonal tension cracking, the failure in most cases occurs by separation of the head joint and slip along the bed joints (i.e.

step cracking). Thus, in both failure modes, a slip occurs along the bed joints and the strength of the bed joint controls the failure pattern.

Abrams and Shah (1992) has reported on a series of unreinforced masonry wall tests. Three walls were built using reclaimed Chicago common bricks from a building that was built in 1917, with different length-to-height aspect ratios. The first wall was stocky with an aspect ratio (width to height) of 2.0 and subjected to a vertical stress of 0.52 MPa. This wall failed in shear (diagonal tension) with no flexural cracking. The second wall had an aspect ratio of 1.5, and was subjected to a stress of 0.34 MPa. This wall, which was subjected to a smaller vertical compressive stress, cracked initially in a toe compression failure. It was classified as a flexure-shear failure. The third wall was a slender wall with aspect ratio of 1.0, and subjected to a stress of 0.34 MPa. The horizontal crack initiated along the bed joint immediately above the bottom course. This wall was clearly a flexural failure. The test result indicates that the type of failure depends on the geometry of the URM-walls and the loading combination. It can also be considered that unreinforced masonry walls are ductile elements capable of dissipating energy through hysteresis. The test results of the hysteresis performance URM walls with different aspect ratio are shown in Figure 2.6.

Calvi et al. (1996) and Costley and Abrams (1995), reported that the flexural tension strength at the wall heel does not limit lateral strength. The limit lateral strength of the wall depends on the diagonal tension, bed-joint sliding, toe crushing or rocking system. Correspondingly, for slender walls that the shear strength capacity will not exceed; the URM wall will start to rock about its toe. The wall can still transfer the shear through the friction at the wall toe and also depends on the axial compressive force. The rocking system can be advantageous system for strengthening an existing URM wall. The rigid body of the wall will rotate about its toe and displace to quite large a drift with limited crack damage and predictable performance.

An initial study of T-section masonry walls was conducted to predict the flexural strength, elastic stiffness after cracking, and ductility capacity of these T-section walls of different flange/web width ratio (Seible and Priestley, 1989). It has concluded that the flexural strength and stiffness are greater when the flange is in tension, but the displacement ductility capacity, is greatly reduced. Clearly the stiffness of such a T-section will depend on the direction of lateral load.

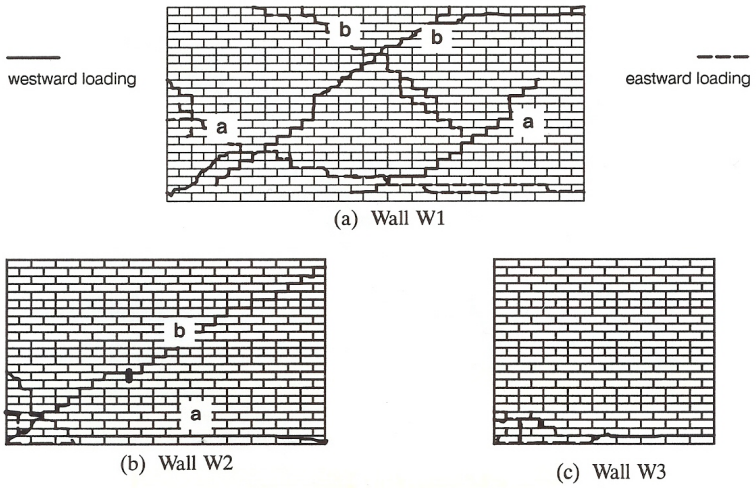

(a) Observed cracked patterns

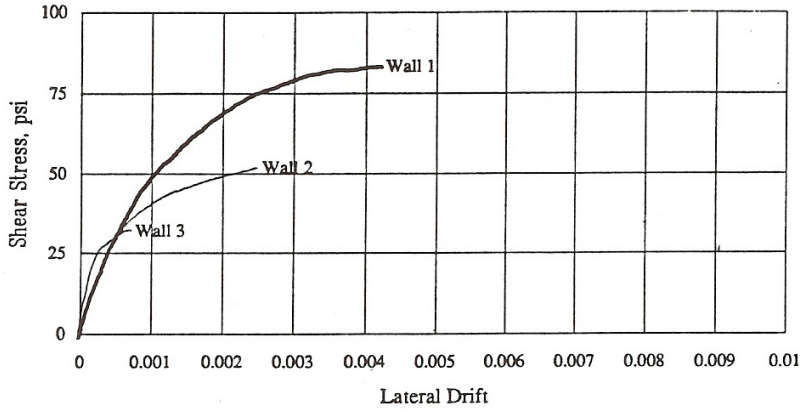

(b) Measured relation between nominal shear stress and lateral drift

Figure 2.6. URM test results with different aspect ratio (Abrams and Shah, 1992)

Lenczer (1972) has reported that the shear strength of a bearing wall, in the case of slip failure mode, can be calculated as

$$\tau_b = \tau_{bo} + \mu\sigma_n \quad \ldots\ldots\ldots\ldots\ldots\ldots\ldots\ldots\ldots\ldots \quad (2.11)$$

where τ_b = shear strength at the shear bond failure; τ_{bo} = shear bond strength at zero normal stress due to the adhesive strength of mortar; μ = coefficient of internal friction between brick and mortar; and σ_n = normal stress.

Anthonie, et al. from Italy (1994) reported the in-plane tests of unreinforced masonry walls with different aspect ratios. The cyclic test result showed that the more slender walls perform

a rocking mechanism while the stockier walls failed by diagonal cracking. The slender walls can fail by diagonal cracking when subjected to larger axial loads.

Bruneau (1995) has reported after 1995 Kobe (Hansin-Awaji) Earthquake that the in-plane behaviour of the few of the building was excellent. It has been concluded, component wise, by Badoux et. al. (2002) that rocking can be a stable non-linear response in slender URM walls providing they have a significant lateral deformation capacity. Doherty (2000) considers that URM buildings may still be satisfactory in medium earthquake risk zones if anchorage and out-of-plane failures of the walls could be prevented. This is because medium levels of earthquakes are not strong enough to cause significant in-plane damage to the building that could jeopardize its stability. In fact, those URM buildings which rocked about their foundation survived during the 15th August 1950 Assam earthquake (Arya, 1992), despite their other weaknesses.

2.3.3. Out-of-Plane Failure at URM Walls

During the seismic loads, the lateral inertia forces will induce both in-plane and out-of-plane forces at the URM walls. These out-of-plane forces can cause the URM buildings to be more unstable and vulnerable to out-of-plane failures. Loading perpendicular to the masonry wall causes bending of the wall and the effect will be determined by the boundary conditions. If the boundary conditions spanned between floor levels or between orthogonal URM walls, the performance of out-of-plane failure can be assumed to act as a one-way slab (see Figure 2.8). In the other case that the boundary conditions are spanned between floor levels and also between orthogonal URM walls, the performance can be assumed to act as a two-way slab.

The capacities of the URM wall to out-of-plane forces depend on the ratio of height of the wall to the thickness, the boundary conditions, types of the floor diaphragm, the compressive stress and the tensile strength of the masonry. The tensile strength of the masonry is low. The performance of the brick wall structure for the out-of-plane action is very brittle and it will crack under light lateral floor response mainly due to lack of adequate wall ties. Several potential URM elements fail due to out-of-plane forces such as parapet walls, veneers, flexibility of the horizontal diaphragm, and unanchored load bearing walls. The out-of-plane failure mechanism can be seen in Figure 2.7.

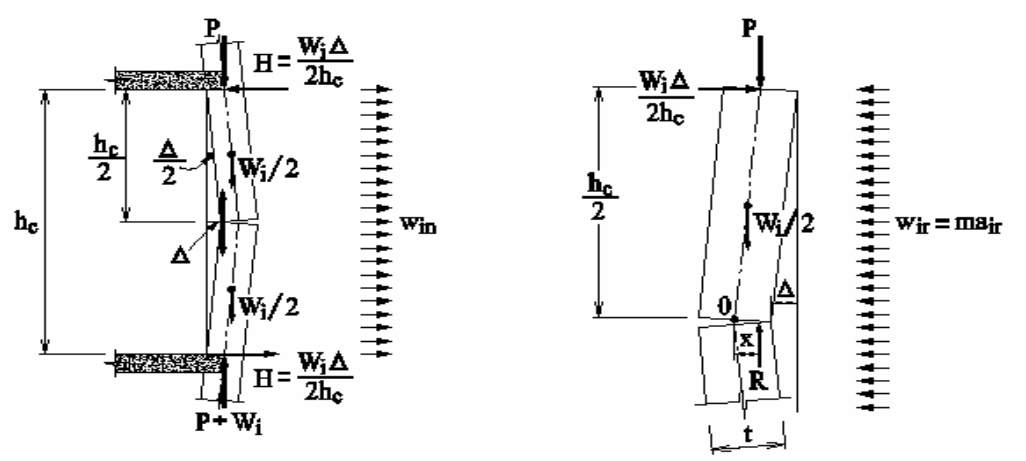

Figure 2.7. Performance of URM walls subjected to out-of-plane load.
(Paulay and Priestley, 1992)

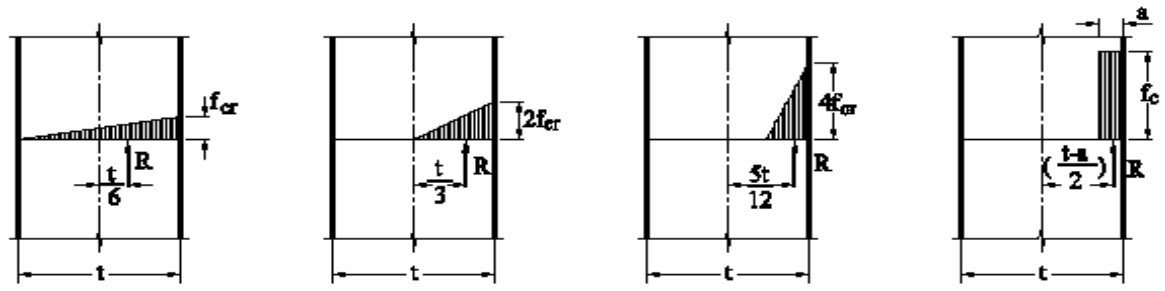

(a) At cracking: $M_{cr} = \frac{Rt}{6}$, $f_{cr} = \frac{2R}{t}$, $\varphi_{cr} = \frac{f_{cr}}{Et}$

(b) Half cracked: $M = \frac{Rt}{3} = 2M_{cr}$, $f_c = \frac{2R}{t/2} = 2f_{cr}$, $\varphi = \frac{2f_{cr}}{Et/2} = 4\varphi_{cr}$

(c) ¾ cracked: $M = \frac{5Rt}{12} = 2.5M_{cr}$, $f_c = \frac{2R}{t/4} = 4f_{cr}$, $\varphi = \frac{4f_{cr}}{Et/4} = 16\varphi_{cr}$

(d) Ultimate: $M = R\left(\frac{t-a}{2}\right) \langle 3M_{cr}$, $f_c = 0.85f'_m$, $\varphi = \frac{\varepsilon_{cu}}{c}$

Figure 2.8. Moments and curvatures at center of face-loaded wall (Paulay and Priestley, 1992)

In the early 70's, Paulay and Priestley of the University of Canterbury carried out some experimental investigations on the unreinforced masonry walls subjected to static cyclic loading concerned particularly with the ductility capability, stiffness degradation and load capacity. Priestley, 1985b, stated that the response of unreinforced masonry walls to out-of-plane (face-load) seismic excitation is one of the most complex and ill-understood area of seismic analysis. In the early 1980s, the ABK Joint Venture in the USA performed most extensive researches on the out-of-plane performances of URM walls. The results still become the main sources for seismic design guidelines of masonry building in the USA.

FEMA – 273 stated that the stiffness of out-of-plane URM walls should be neglected in analytical models of the global structural system if in-plane walls exist. The dynamic stability of the out-of-plane performance also depends on the ratio of height of the wall to the thickness of URM wall and the value of the site spectral acceleration. Bruneau (1994) reported that the out-of-plane collapse of walls could be rapid and explosive in nature. In addition, damage incurred to URM buildings with flexible floor and roof diaphragms can be attributed to their insufficient or total lack of in-plane stiffness and integrity (Fujiwara et al. 1989, NSET 1999, Simsir et al. 2004). The situation is further worsened by inherent weaknesses of the materials and commonly observed bad workmanship in these buildings.

2.4. ENHANCEMENT OR STRENGTHENING SYSTEMS FOR URM WALLS

Masonry structures are seismic prone buildings and it is necessary to improve their performance for the next earthquake. Several methods for seismic rehabilitation of masonry structures were discussed in the United States through their standards such as UCBC (1994), FEMA reports (1992, 1997), NIST GCR 97-724-1 (1997) and others. The United States has a number of databases for seismic rehabilitation of unreinforced masonry buildings which analyse damage data from several previous earthquakes such as the 1933 Long Beach earthquake, the 1971 San Fernando earthquake, the 1987 Whittier earthquake, the 1989 Loma Prieta earthquake, the 1994 Northridge earthquake. Correspondingly, the NZSEE Study Group also released a procedure to improve unreinforced masonry building through the document “Assessment and Improvement of the Structural Performance of Buildings in Earthquake” in June 2006.

Each of the methods mentioned above has its advantages and disadvantages when repairing or strengthening unreinforced masonry wall constructions. Before deciding on the final choice of repair system to be used, it is recommended to make a detailed evaluation of the various systems mentioned above, then make a comparison between one system and another. After the correct repair and strengthening system has been chosen, a final reanalysis will be desirable using an elasticity or inelasticity analysis. The choice of repair system must be adjusted to the local area’s conditions, quality of work force and available funds. This constitutes a very important part in the reanalyzing stages of an old building’s structure and requires considerable experience of the designer.

An initial evaluation method for the analytical assessment of the performance existing URM building was suggested before deciding on the strengthening method. Based on the strength and capacity of the existing wall, the designer can determine the most appropriate strengthening method to comply with recent building codes. The method for strengthening and increasing rigidity of URM walls usually carried out can be categorized into 9 categories as shown at Table 2.4. and explained more detail at Figure 2.9. to Figure 2.17. (NIST GCR 97-724-1, 1997)

Many researches on retrofit techniques for URM walls were conducted. In 1984 Hutchison et al., tested six masonry wall panels and strengthened URM wall models by various methods such as concrete and ferrocement coating to one side of the wall, glass-fiber reinforced concrete on both surfaces, steel-fiber reinforced coating on two surfaces and externally prestressing. The specimens were subjected to in-plane reversed cyclic loading. This strengthening technique resulted in remarkably stable hysteresis loops. It was observed that walls strengthened with sprayed concrete, glass fiber reinforced concrete and steel fiber reinforcement concrete were the most advantageous methods for improving in-plane strength of URM walls when compared to other methods.

Binda et al. (1987, 1990, 1993), Tomaževič & Apih (1993), Calvi & Magenes (1994b) and Manzouri et al. (1996) investigated the effectiveness of injection methods for enhancing the masonry wall. Grout material (i.e. cementitious or epoxy resin) is injected into internal voids and cracks in the unreinforced masonry walls. The injection technique was effective for restoring or improving the original in-plane shear strength and stiffness of damaged URM walls. It was reported; the apparent stiffness of the repaired walls was increased by 80% to 120% when compared to the original walls. Cementitious grout was suitable for filling wider cracks, while the epoxy resin was found to be more effective for the narrower cracks in the masonry walls. Manzouri et al. (1996) used the results from the previous tests to extent the analysis using the finite element method. It was shown the FEM can be used as viable tools for analyzing masonry structures.

Table 2.4. Enhancement of seismic performance of URM buildings

(NIST GCR 97-724-1, 1997) :

No	Methods	The purpose is to increase :
1.	Grout and epoxy injections	• Flexural strength for walls subjected to face loadings • Shear strength for walls subjected to in-plane-loadings
2.	Surface coatings	• Flexural strength for walls subjected to face loadings • Flexural strength for walls subjected to in-plane loadings • Shear strength for walls subjected to in-plane-loadings • Inelastic deformation capacity for walls subject to in-plane loadings • Vertical compressive strength
3.	Adhered fabrics	• Flexural strength for walls subjected to face loadings • Flexural strength for walls subjected to in-plane loadings • Shear strength for walls subjected to in-plane-loadings • Inelastic deformation capacity for walls subject to in-plane loadings
4.	Shotcrete overlays	• Flexural strength for walls subjected to face loadings • Flexural strength for walls subjected to in-plane loadings • Shear strength for walls subjected to in-plane-loadings • Inelastic deformation capacity for walls subject to in-plane loadings
5.	Reinforce cores	• Flexural strength for walls subjected to face loadings • Flexural strength for walls subjected to in-plane loadings • Shear strength for walls subjected to in-plane-loadings • Inelastic deformation capacity for walls subject to in-plane loadings
6.	Post-tensioned masonry	• Flexural strength for walls subjected to face loadings • Flexural strength for walls subjected to in-plane loadings • Shear strength for walls subjected to in-plane-loadings • Inelastic deformation capacity for walls subject to in-plane loadings
7.	Infilled openings	• Flexural strength for walls subjected to face loadings • Shear strength for walls subjected to in-plane-loadings • Vertical compressive strength
8.	Enlarged openings	• Alter the behaviour of a pier from a shear controlled mode to a rocking mode (lateral in-plane strength will be reduced, but deformation capacity will be increased)
9.	Steel bracing	• Lateral strength and deformation capacity of the structural system

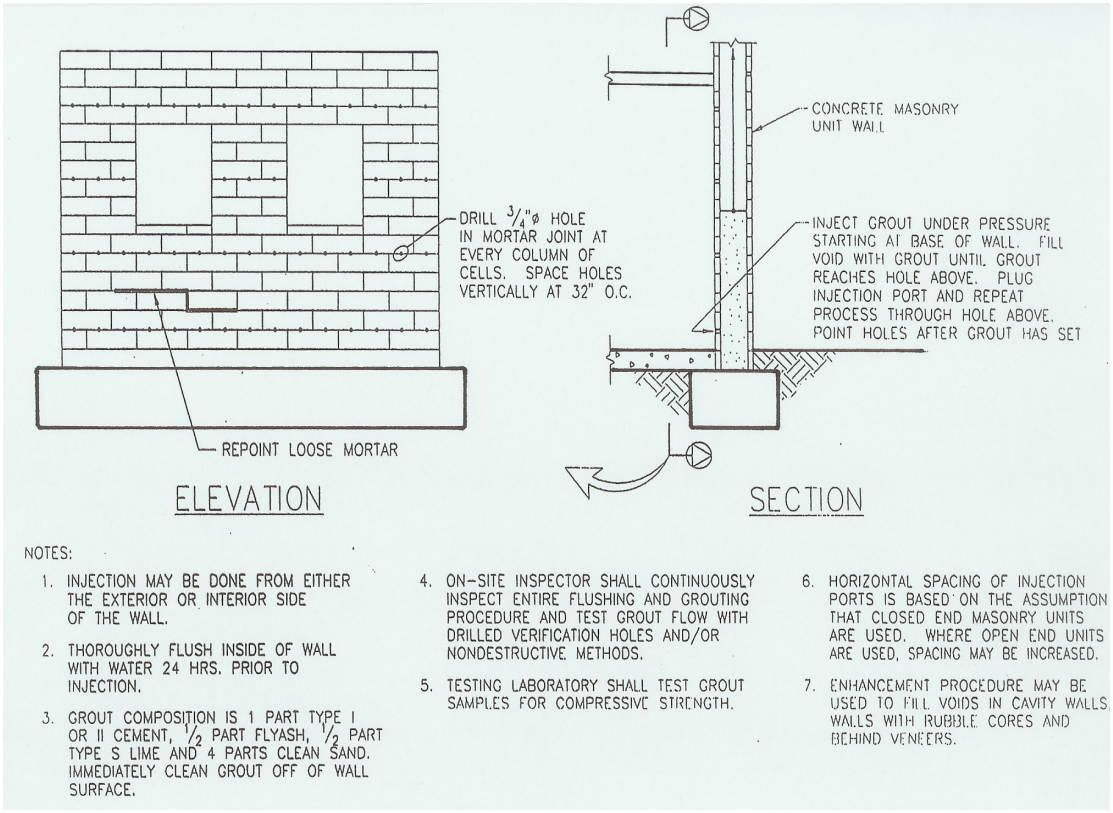

Figure 2.9. Seismic enhancement of URM buildings with Grout and Epoxy Injection (NIST, 1997)

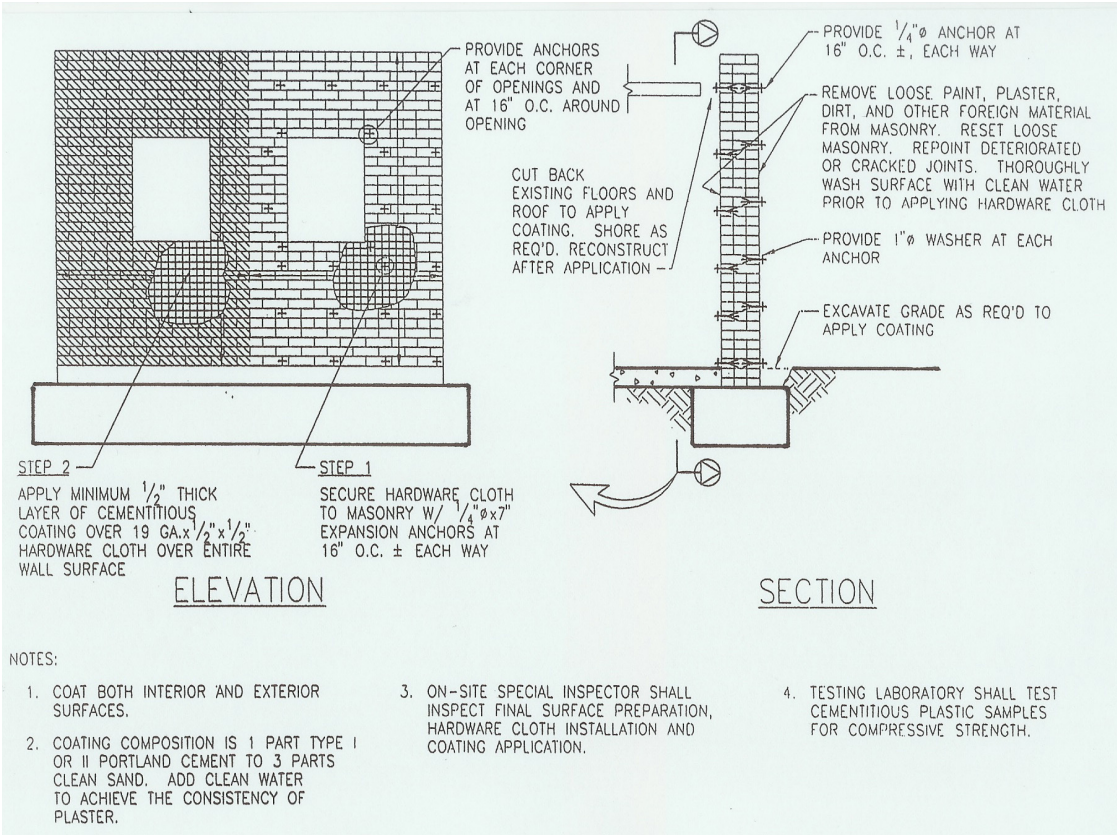

Figure 2.10. Seismic enhancement of URM buildings with Surface Coatings (NIST, 1997)

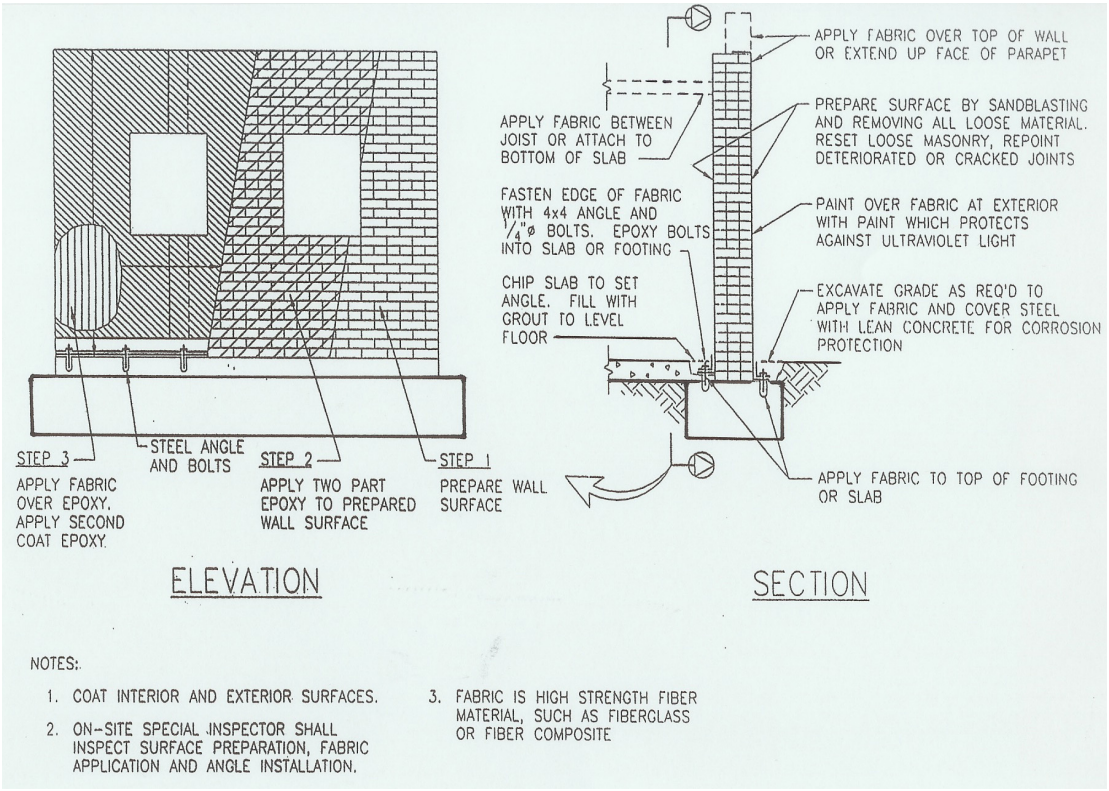

Figure 2.11. Seismic enhancement of URM buildings with Adhered Fabrics (NIST, 1997)

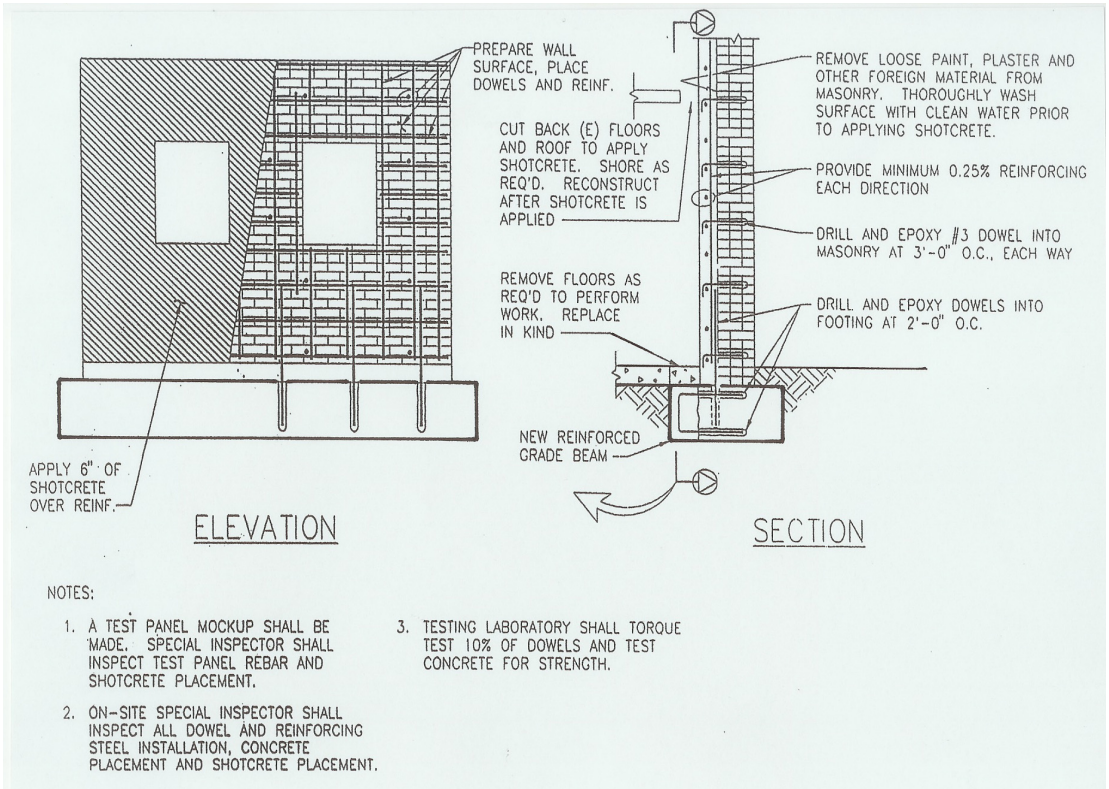

Figure 2.12. Seismic enhancement of URM buildings with Shotcrete Overlay (NIST, 1997)

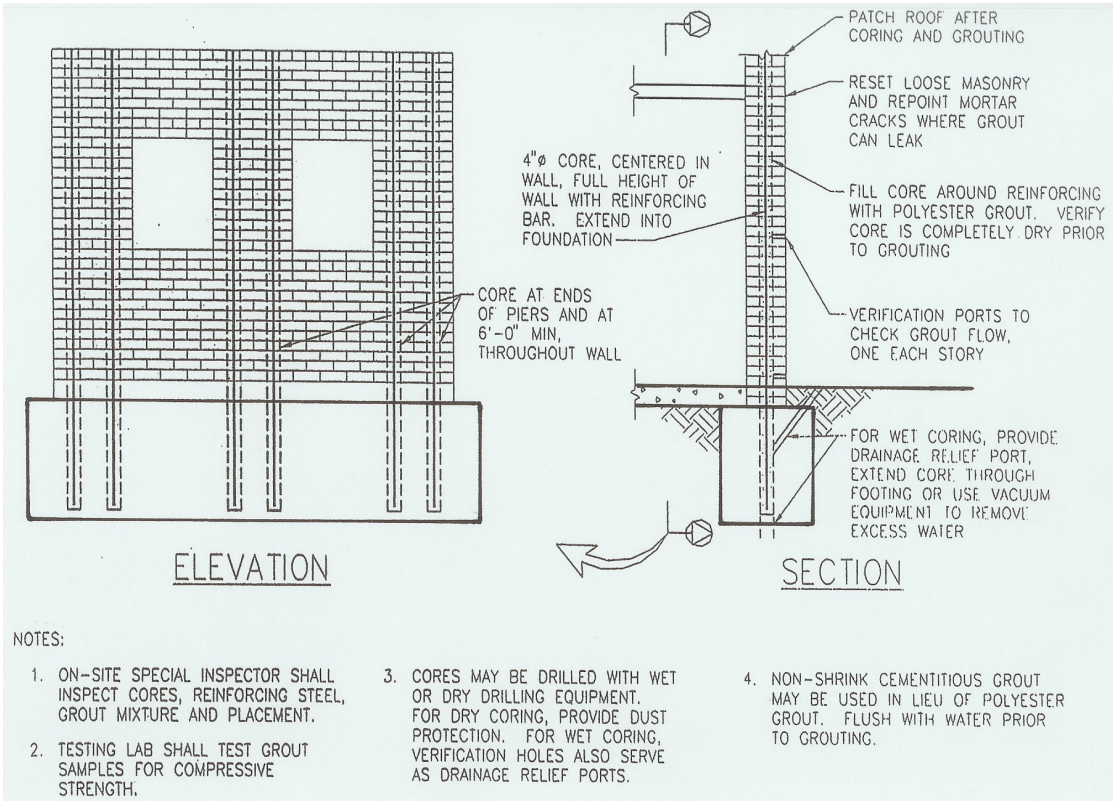

Figure 2.13. Seismic enhancement of URM buildings with Reinforced Cores (NIST, 1997)

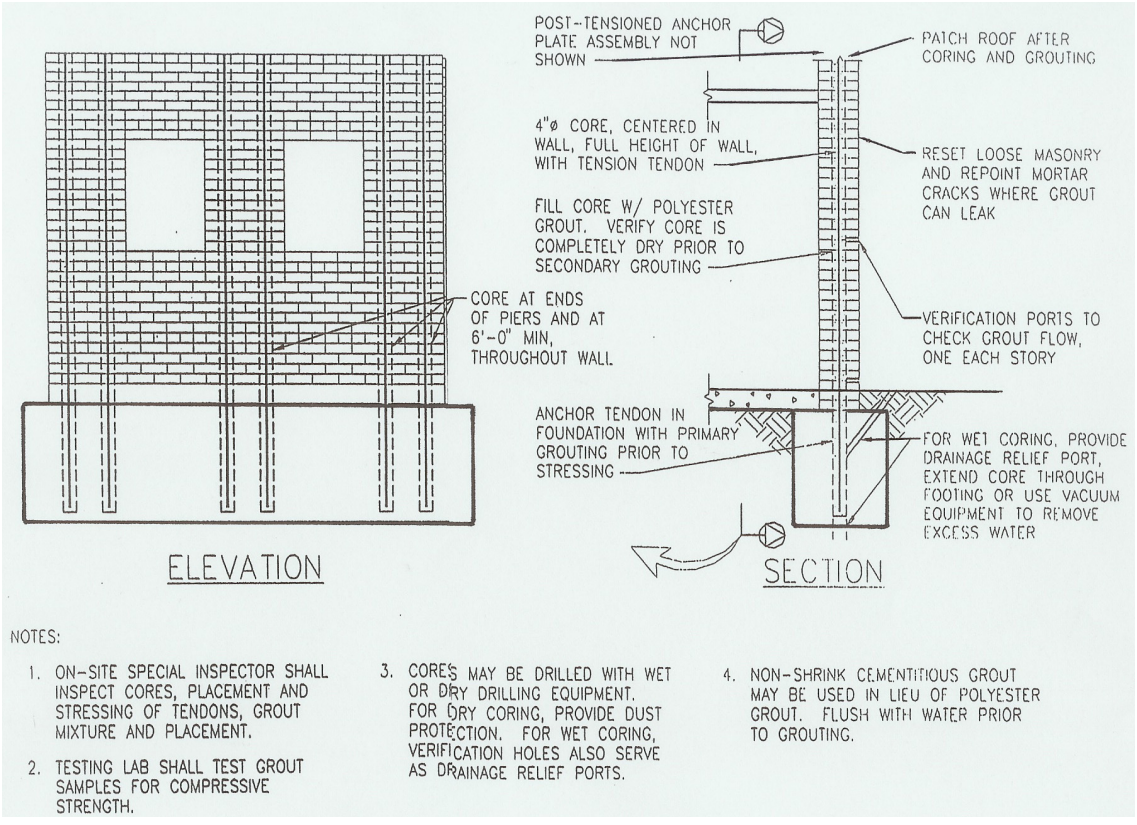

Figure 2.14. Seismic enhancement of URM buildings with Post-Tensioned Masonry (NIST, 1997)

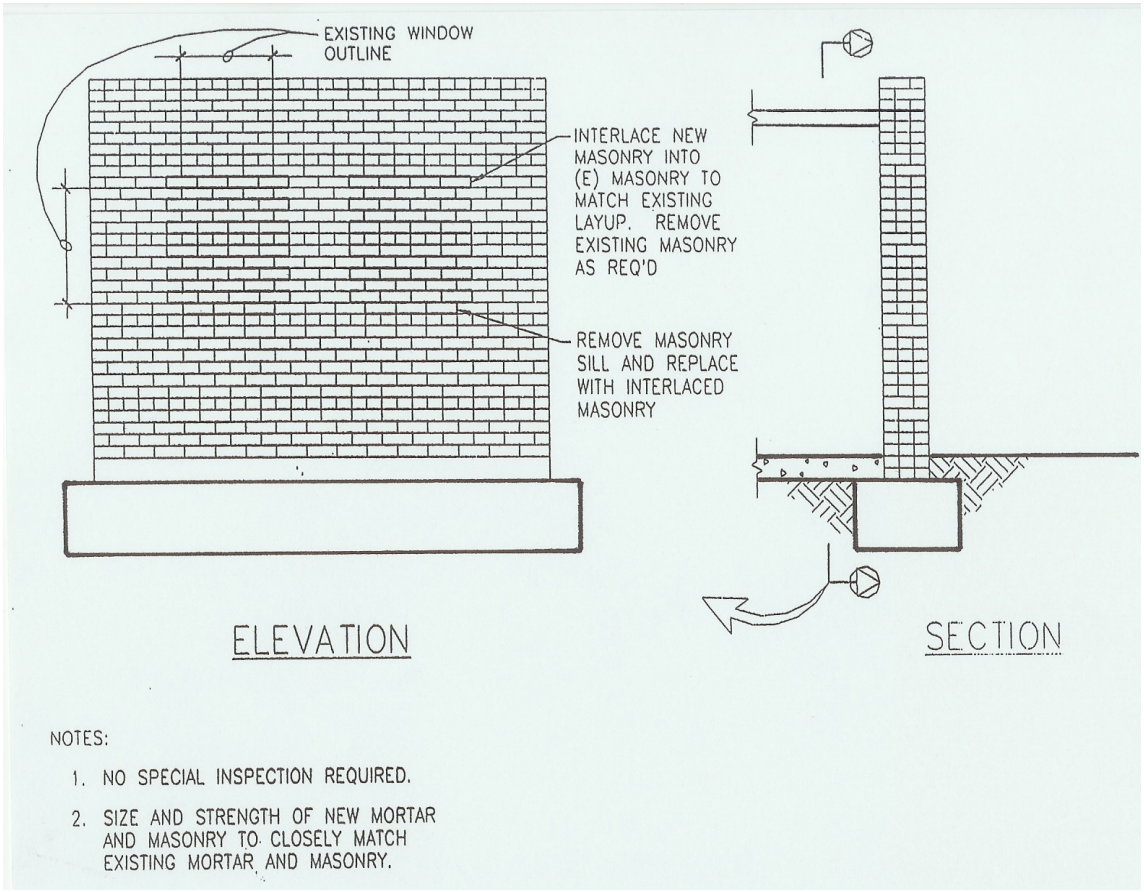

Figure 2.15. Seismic enhancement of URM buildings with Infilled Openings (NIST, 1997)

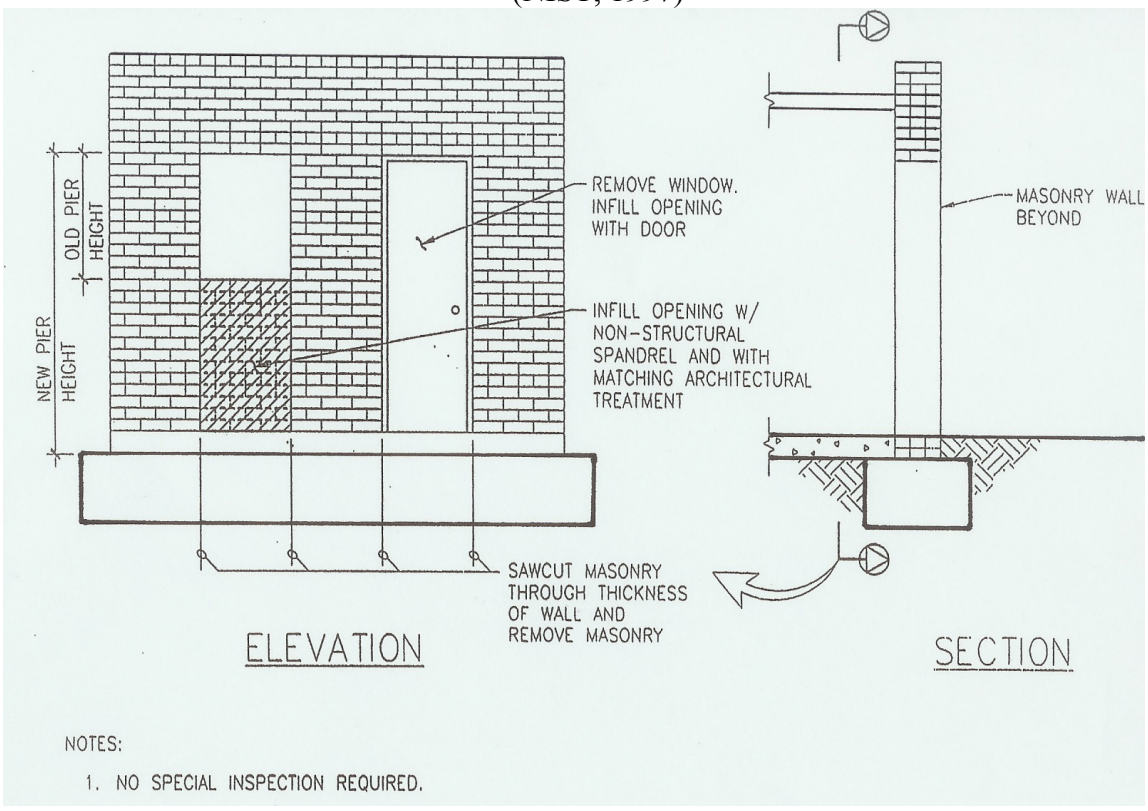

Figure 2.16. Seismic enhancement of URM buildings with Enlarged Openings (NIST, 1997)

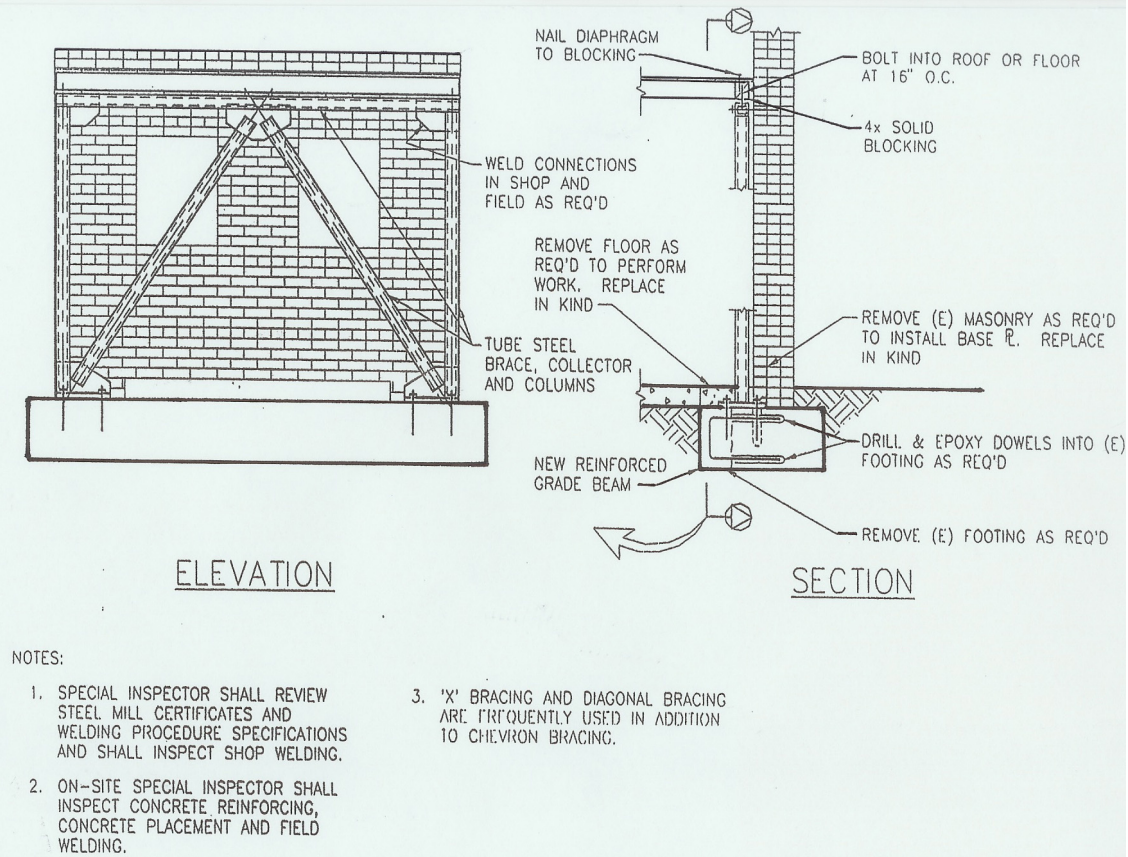

Figure 2.17. Seismic enhancement of URM buildings with Steel Bracings (NIST, 1997)

Research was done by Prawel et al. (1985, 1988, 1990) who investigated the strengthening of masonry walls with a thin ferrocement layers and reinforced with layers of fine steel wire mesh on one or both sides of unreinforced masonry walls. Several URM walls were tested and strengthened with a 13 mm thick coating of ferrocement with varying amount of galvanized welded wire fabric. The load carrying capacity of all strengthened specimens was two or three times that of the un-strengthened specimens. Kahn (1984), investigated the effectiveness of application a layer of reinforced shotcrete of 90 mm thickness to fifteen unreinforced masonry panels. It was shown significant increases in strength and ductility when compared to the uncovered panels.

Ehsani et al. (1996, 1997, 1999) tested many specimens and investigated the effectiveness of surface coatings for improving the seismic resistance of URM walls. Composite materials such as fiber composites (e.g., glass, graphite, Kevlar) with different strength or densities have been used for the seismic rehabilitation of URM walls. These materials have a low weight to strength ratio, immunity to corrosion, fatigue resistance and their ease of

application. The composites were externally attached to both sides of masonry walls using epoxy to increase the members' flexural and shear capacity. The effectiveness of composite retrofit also depends on the orientation of the fibers and from the test result a $\pm 45^0$ layout is the most effective layout when compared to $\pm 0^0/90^0$ layout in carrying shear forces in a shear wall. The test results have shown that flexural, shear strength, and ductility can be increased significantly and the failure mode was governed by the strength of the composite material. It was also suggested that the shear stress at the shear bond failure of a wall retrofitted with FRP can be modified as follows :

$$\tau_b = \tau_{bo} + \mu\sigma_y + \tau_{FRP} \quad \ldots\ldots\ldots\ldots\ldots\ldots\ldots\ldots\ldots\ldots\ldots\ldots \quad (2.12)$$

where, τ_{FRP} = contribution of the FRP laminate in resisting shear.

Seible et. al. (1990), successfully repaired a five story building model using carbon fiber composite materials. The dynamic characteristics of masonry bearing walls have been analyzed experimentally by Al-Chaar & Hassan (1999). Those techniques enhanced the lateral shear strength and provided substantial inelastic deformation capacity. Triantafillou (1998) and Marshall et al. (1999) reported their experimental and analytical studies of the performance of unreinforced masonry walls strengthened with glass and carbon composites. In each of these studies, considerable strength was gained using Fiber-Reinforced Polymer (FRP).

Weng et al. (2004) did the experimental study on URM walls strengthened with low/high strength Glass Fiber Reinforced Polymer (GFRP) and steel-mesh reinforced cement layer. GFRP sheet is suitable material for strengthening URM wall structures in China due to high mechanical property and inexpensive in price. Two types of GFRP tensile strength (98.4 MPa and 2040 MPa) were used in their experiment. It was concluded that high strength GFRP is better than low-strength GFRP and instead of enhance the integrity of URM walls also could enhance the shear capacity and energy dissipating capacity of the URM wall specimens. The similar advantages also obtained when using steel-mesh reinforced cement mortar for the strengthening material of URM wall.

Elgawady et al. (2004) reported the preliminary in-plane performance of URM walls strengthen with GFRP under both dynamic using synthetic earthquakes and static cyclic tests. It was shown that the GFRP could improve the cracking and ultimate load of the retrofitted specimens by a factor of 3 and 2.6 respectively. This strengthening system could create a

rocking mechanism that could be a stable in the non-linear response and provided a significant lateral deformation capacity. The method of testing had insignificant effect on the initial stiffness but the lateral resistance of the specimen under the static cyclic test was 1.2 times more than the dynamic test result.

New material like polymer grids was also used to strengthen the URM wall performances. Juhásová et al. (2004) and Sofronie (2004) reported the performance of masonry wall strengthened with polymer grids. This polypropylene reinforcement was embedded in plaster masonry wall and inserted in the grid of bed layers. The tensile strength of the polymer grid material can be four times higher than the steel tensile strength. Reinforcing masonry with polymer grids proved to be very effective strengthening systems and could increased the dynamic resistance, ductility and contributes to the structure integrity.

Centre core strengthening systems are quite similar with post tensioned strengthening systems, the difference only in using reinforcing bars and prestress tendons respectively. Breiholz (1992) investigated the centre core strengthening systems of unreinforced masonry walls. The reinforcing bars are bonded within a core. It was shown the in-plane shear capacity and out-of-plane bending capacity was enhanced. Ganz (1993a, 1993b) used post-tensioning systems to upgrade unreinforced masonry buildings in USA, Switzerland and Australia. This system can improve shear or flexural capacities both in-plane and out-of-plane actions in unreinforced masonry walls

Rai, et. al. (1994) investigated the use of steel bracing for in-plane strengthening unreinforced masonry buildings. A half-scale model of unreinforced brick masonry walls was strengthening with steel bracing and tested subjected to reversals of lateral loads. The steel bracing members behaved independently of the masonry element. In 1996, Rai investigated the effectiveness of a surrounding steel unbraced frame for improving the rocking behaved of unreinforced masonry piers. Two specimens were subjected to in-plane lateral forces, the first specimen was centrally located in the steel frame to simulate an interior pier and the other was located asymmetrically to simulate an exterior pier. Both specimens showed that the flexural capacity and pier rocking can be enhanced.

2.5. CONCLUSIONS

1. The factor of cost constitutes the main factor in determining the method of repairing or rehabilitating old buildings. Optimalizing the rehabilitation costs definitely does not reduce the requirements of meeting the factors of strength, rigidity and stability of the building viewed from the point of existing regulations. With the development of the performance based design methods the project owner can choose the level of building performance in the event of earthquake, where the choice of level influences the costs of the repair. The choice of building performance level will also influence the amount of insurance premium that will be charged to the building owner. In all stages mentioned above, tight quality control by an experienced engineer is required during the work on site.

2. Proper detailing and appropriate in choosing the right retrofitting material for increasing the structure resistances are key design. It should consider the material is locally available, the transport systems, less dynamic effects, less long term effects from soil settlements and etc.

3. The Mohr Coulomb failure hypothesis (Timoshenko, Strength of Material, 1955) can be used to predict the diagonal cracking strength and failure occurred when both principal stress components in the plane of the wall reach a critical value. This hypothesis is valid for the elastic condition and can predict diagonal cracking when brick failure is brittle and diagonal cracking is initiated at or near the neutral axis of the pier.

CHAPTER 3 :
PROPERTIES OF CONSTRUCTION MATERIALS

3.1 INTRODUCTION

This section will investigate the properties of Indonesian masonry units and other materials that used in this research. The solid brick is made from clay, moulded and burned to harden its structure. The masonry unit has a rectangular prism shape and the production location and resources of the clay-brick which is used in the experimental work is at Cikarang, near the city of Jakarta, operated as traditionally home industry and are known as “HSG” bricks.

As in other countries, masonry structures have been known in Indonesia since as far back as the time of the Indonesian kingdoms, the Dutch colony and today is used in construction in small towns as well as large cities. Masonry is the most dominant element in the construction of buildings and houses in Indonesia. There is hardly any building that does not utilize this material. In the beginning bricks were made of clay material burned in the traditional way and are today still produced in the same manner. Therefore the quality and grade of clay bricks depends very much on the clay soil used for their production, the mixture, production method, and the burning system. The various regions in Indonesia each have their distinct quality of clay brick with a variation in size as well. Research conducted by United Nations Industrial Development Organization (UNIDO) in conjunction with the Indonesian government in the 1980-s for the purpose of establishing a standardization of the clay brick production in Indonesia encountered many obstacles and as a result this program does not run as may be expected.

The Indonesian standard of masonry still does not cover all property tests; it only covers the compressive strength of masonry, dimensions of masonry units and the compressive strength of mortars. Other property tests were conducted using American Society for Testing and Materials (ASTM) or British standard and should be adjusted to the laboratory facilities.

3.2 PROPERTIES OF MASONRY UNITS

3.2.1 General

Clay bricks are made of clay as its main raw material, moulded either manually or by machine. Water, which is used to soften the clay and rice hulls, which are to be mixed is another component. The individual clay bricks were dried in the shade in order to prevent cracking due to drying shrinkage. Afterwards the clay bricks are burned at fireplaces using fire logs that give variants in clay-brick colour and strength. During the burning process the water will evaporate and the clay particles will become soft and will blend. Then the *vitrification* process (change of the material into a kind of glass) will occur and the temperature must be watched for some time. The process will last from 40 to 150 hours, depending on the size and volume of the bricks as well as the burning system. The cooling process further influences the quality of the bricks. A too rapid cooling will cause brittleness of the clay brick units. Therefore avoiding abrupt cooling of the bricks must be avoided.

3.2.2 Clay Bricks

According to the Indonesian Industry Standard, stated as standard clay bricks are solid clay bricks produced from clay and burned to a level where it will not crumble when soaked in water, and with holes over less than 15% of its flat surface. The shape is a "rectangular prism", with angular and sharp sides, smooth flat surfaces and without cracks and classified according to their strength as discussed at Chapter 2.

3.2.3 Dimensional Property

At least 20 tests of masonry unit samples were randomly selected and will be used to measure the length, width and thickness of clay bricks (SNI 15-2094-1991). Each measuring of length, width and thickness of those spots will be carried out at least 3 times, as shown in Figure 3.1. Spots for measuring were indicated by a dashed line.

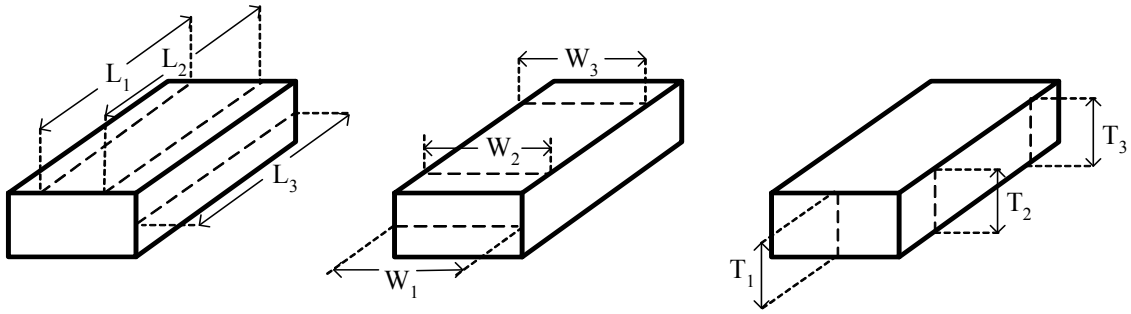

Figure 3.1. Measuring of length, width and thickness of clay brick based on SNI 15-2094-1991 method

The results of these tests indicate that the shape and colour of the bricks vary greatly, and the HSG-brick average dimension is 189 mm length x 90 mm width x 47 mm thick, with coefficient of variation 1.36 %, 2.02 % and 3.07 % respectively. This average masonry unit dimension confirm to the 75% scale compare to original clay brick dimension that is used in the original building. The original clay brick average dimension is 256 mm length x 121 mm width x 53 mm thick. Figure 3.2. is shown the picture of the original clay brick that was used in the existing buildings and HSG clay brick.

(a) Old clay-brick (b) "HSG" clay-bricks

Figure 3.2. Comparison between old clay-brick and "HSG" clay-bricks

The average weight from ten samples of clay-brick is 1326.3 gr with coefficient of variation 5.47% and the average density of clay-brick, which is the average weight divided by the average volume is 16.284 kN/m^3.

3.2.4 Absorption of Masonry Units

The absorption is the amount of water, which is taken up from the mortar to fill pores in the clay brick. An absorption test was conducted on the "HSG" brick units based on Indonesian standard, which is similar to the British Code (BS 5628-1992 or BS 3921-1992).

Twenty specimens of masonry units were tested and the absorption is defined as the amount of water absorbed by a dry masonry unit when partially immersed in water for a given period of one minute. More detailed results from the tests are shown in Table 3.1 and Table 3.2. The result of the IRA value is 48.72 g/minute/dm^2 and the coefficient of variation 30.50 %. This value was higher than the limit IRA value for Indonesia clay brick, which is 20 g/minute/dm^2

(UNIDO, 1978a). It is recommended to soak the clay brick units for approximately 5 to 8 minutes in a container, before placing the mortar.

Table 3.1.a. Absorption Test On Clay Brick

Tested on : 02-09-2002

No	Dim (mm)	Brick Weight (gram), after soaked in minutes									
	L / W / T	0	0,5	1	2	3	5	8	10	12	15
1	190/92/47	1364	1419	1449	1473	1494	1516	1534	1546	1548	1559
2	194/90/47	1369	1429	1469	1495	1520	1541	1559	1559	1565	1567
3	191/92/45	1369	1411	1439	1458	1475	1494	1512	1513	1522	1535
4	191/90/48	1395	1440	1469	1495	1513	1531	1552	1563	1576	1586
5	190/91/47	1414	1456	1481	1501	1517	1526	1541	1547	1554	1561
6	185/89/46	1336	1370	1394	1414	1427	1436	1451	1458	1467	1474
7	188/87/47	1257	1304	1334	1353	1376	1389	1403	1413	1421	1425
8	187/89/48	1363	1394	1416	1431	1448	1459	1471	1482	1491	1499
9	187/90/47	1357	1408	1440	1457	1478	1491	1503	1513	1521	1526
10	188/93/46	1363	1409	1441	1468	1488	1517	1535	1549	1561	1572
11	186/88/43	1223	1260	1284	1297	1310	1323	1332	1337	1343	1350
12	194/94/48	1445	1521	1566	1595	1619	1646	1662	1671	1679	1683
13	187/89/44	1273	1311	1337	1354	1377	1394	1402	1410	1418	1426
14	189/92/45	1334	1428	1483	1511	1535	1545	1547	1547	1547	1548
15	188/88/46	1144	1225	1240	1263	1273	1277	1281	1282	1285	1144
16	194/90/47	1333	1408	1472	1505	1524	1548	1563	1567	1571	1573
17	188/91/47	1261	1295	1329	1353	1372	1394	1414	1426	1439	1453
18	189/91/47	1370	1407	1440	1459	1472	1489	1502	1510	1519	1531
19	190/90/49	1244	1281	1302	1323	1346	1361	1384	1394	1408	1418
20	189/88/47	1312	1380	1410	1435	1460	1469	1477	1481	1483	1483

Table 3.1.b. Absorption Test On Clay Brick

Tested on : 02-09-2002

No	Dim (mm)	Water Absorption Capacity of Clay Brick (in %), after minutes :								
	L / W / T	0.5	1	2	3	5	8	10	12	15
1	190/92/47	4.03	6.23	7.99	9.53	11.10	12.50	13.30	13.50	14.30
2	194/90/47	4.38	7.30	9.20	11.00	12.60	13.90	13.90	14.30	14.50
3	191/92/45	3.07	5.11	6.50	7.74	9.13	10.50	10.50	11.20	12.10
4	191/90/48	3.23	5.30	7.24	8.46	9.75	11.30	12.00	13.00	13.70
5	190/91/47	2.97	4.74	6.15	7.28	7.92	8.89	9.41	9.90	10.40
6	185/89/46	2.54	4.34	5.84	6.81	7.49	8.61	9.13	9.81	10.30
7	188/87/47	3.74	6.13	7.64	9.47	10.50	11.60	12.40	13.10	13.40
8	187/89/48	2.27	3.89	4.99	6.24	7.04	7.92	8.73	9.39	9.89
9	187/90/47	3.76	6.12	7.37	8.92	9.87	10.80	11.50	12.10	12.50
10	188/93/46	3.37	5.72	7.70	9.17	11.30	12.60	13.60	14.50	15.30
11	186/88/43	3.02	4.99	6.05	7.11	8.18	8.91	9.32	9.81	10.40
12	194/94/48	5.26	8.37	10.40	12.00	13.90	15.00	15.60	16.20	16.50
13	187/89/44	2.99	5.03	6.36	8.17	9.51	10.10	10.80	11.40	12.00
14	189/92/45	7.07	11.20	13.30	15.10	15.80	16.00	16.00	16.00	16.00
15	188/88/46	4.55	7.08	8.39	10.40	11.30	11.60	12.00	12.10	12.30
16	194/90/47	5.63	10.40	12.90	14.30	16.10	17.30	17.60	18.00	17.80
17	188/91/47	2.70	5.39	7.30	8.80	10.60	12.10	13.10	14.10	15.20
18	189/91/47	2.70	5.11	6.50	7.45	8.69	9.64	10.20	10.90	11.80
19	190/90/49	2.97	4.66	6.35	8.20	9.41	11.20	12.10	13.20	14.00
20	189/88/47	5.18	7.47	9.38	11.30	12.00	12.60	12.90	13.00	13.00
Mn(mm)	189/90/47	3.77	6.23	7.88	9.37	10.61	11.65	12.20	12.78	13.27
SD(mm)	2.57/1.82/1.43	1.24	1.94	2.22	2.38	2.52	2.48	2.40	2.33	2.21
COV(%)	1.36/2.02/3.08	32.79	31.07	28.18	25.43	23.73	21.29	19.67	18.27	16.68

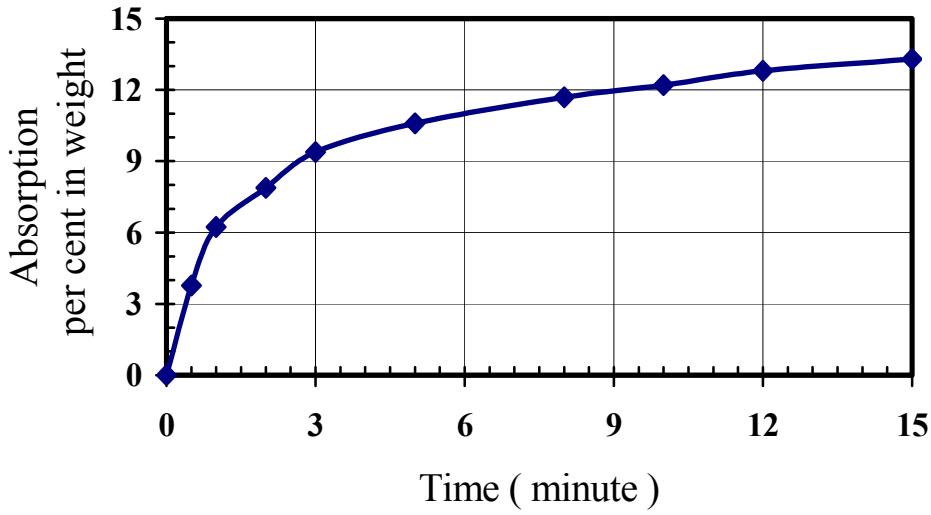

Figure 3.3. Absorption % in weight versus time

Table 3.2 . Test Result of "IRA" Values

No	Dimension (mm)			Brick Weight (gram)		Area (C)	(B-A)	(B-A)/C
	length	width	thickness	Original (A)	After soaking (B)	dm^2	gr	gr/dm2/min.
1	190	92	47	1364	1449	1.75	85	48.6
2	194	90	47	1369	1469	1.75	100	57.3
3	191	92	45	1369	1439	1.76	70	39.8
4	191	90	48	1395	1469	1.72	74	43.0
5	190	91	47	1414	1481	1.73	67	38.8
6	185	89	46	1336	1394	1.65	58	35.2
7	188	87	47	1257	1334	1.64	77	47.1
8	187	89	48	1363	1416	1.66	53	31.8
9	187	90	47	1357	1440	1.68	83	49.3
10	188	93	46	1363	1441	1.75	78	44.6
11	186	88	43	1223	1284	1.64	61	37.3
12	194	94	48	1445	1566	1.82	121	66.4
13	187	89	44	1273	1337	1.66	64	38.5
14	189	92	45	1334	1483	1.74	149	85.7
15	188	88	46	1144	1240	1.65	96	58.0
16	194	90	47	1333	1472	1.75	139	79.6
17	188	91	47	1261	1329	1.71	68	39.7
18	189	91	47	1370	1440	1.72	70	40.7
19	190	90	49	1244	1302	1.71	58	33.9
20	189	88	47	1312	1410	1.66	98	58.9
Mn(mm)	189.25	90.20	46.55	1326.30	1409.75	1.71	83.45	**48.72**
SD(mm)	2.57	1.82	1.43	72.58	81.12	0.05	26.73	14.86
COV(%)	1.36	2.02	3.08	5.47	5.75	2.91	32.03	30.50

3.3 PROPERTIES OF MASONRY MORTARS

3.3.1 Mortars

Mortar is used as a means of sticking or bonding bricks together and to take up all irregularities in the bricks. To do this the mortar must be well workable so that all joints are filled completely. Although mortars form only a small proportion of a masonry wall as a whole, its characteristics have a large influence on the quality of the brickwork. Batching and mixing of the mortar are also essential factors that have great influence on both strength and workability of mortars. The stiffness and plasticity are two things of importance for the workability. The stiffness depends on the quantity of water added to the mortar. The quantity of water to be added depends on the application of the mortar, and does not indicate anything about its quality but it is a characteristic of the condition. Plasticity is a term to describe the ease of forming the mortar. A binder rich mortar has better plasticity than a binder poor mortar. The grading of the aggregate also has a certain influence on the plasticity, the closer the grading is to the ideal curve the better the plasticity. Batching of mortar must be done in proper manner, best by weight, but common practice is measure by volume.

3.3.2 Uniaxial Compressive Strength of Mortar

The measurement of the compressive strength of mortar is conducted based on SNI M-111-1990-03 which was adapted from ASTM C-109 : Test Method for Compressive Strength of Hydraulic Cement Mortars. The samples can be in 50 mm cube specimens or cylinder dimension, which usually with length-diameter ratio equal to 2.0. According to the ASTM C 780, there is a correlation factor should be applied between cylinder samples and cube samples. Curing of mortar cubes test should follow the ASTM C 270.

The mortar is mixed manually; the cementitious material and the aggregate should be mixed dry until a uniform colour is achieved. The water should then be added and shovelled or hoed thoroughly until the mortar is easily workable and the ingredients are thoroughly distributed. The nominal mortar with 1 part of Portland cement to 4 part of sand was used for the mortar joint with thickness of 10 mm. The type of cement used was type I cement in accordance with the ASTM C-150 standard, with a weight density of 3150 kg/m^3. Fine aggregate or sand used is "*Galunggung*" sand (volcanic sand) from "*Tasikmalaya*" which fulfilled the ASTM standard No. C-190 requirements and its properties as shown in Table 3.3.

Batching the mortar was done by volume and used plastic buckets. The results of compressive strength based on cubes of 50 x 50 x 50 mm at 28 days are 10.61 MPa and coefficient of variation 14.23 %. The test results of the compressive strength of mortar specimens are shown in Table 3.4.

Table 3.3. Physical characteristic of fine aggregate

Type of Test	Test Result
Water content (%)	9.69
Mud content (%)	3.58
Water absorption (%)	4.49
Weight Density (gr/cc)	2.52
Weight Content (kg/ltr) - Loose - Solid	 1.439 1.709
Organic substance content (-/+)	
Hardness with *Rudeloff* container Through a 2.0 mm sifter (No. 10) (%)	
Analysis of sifting cumulatively from a sifter (%) 38.0 mm 19.0 mm 9.6 mm 4.8 mm 2.4 mm 1.2 mm 0.6 mm 0.3 mm 0.15 mm pan (base)	 100.0 100.0 90.72 79.21 65.53 51.24 33.06 14.12 5.50 0

3.4 PROPERTIES OF MASONRY

3.4.1 General

Masonry is a non-homogeneous and anisotropic material consisting of clay bricks and mortar as filled joints. This study is mainly focused on the local materials and seismic performance of unreinforced masonry walls commonly used and the brick configuration during the Dutch era in Indonesia.

3.4.2 Compressive Strength of Masonry

Two kinds of compressive strength masonry specimens were tested. The first compressive strength test was conducted according to the Indonesian test standard (SNI 15-2094-1991) and secondly several prismatic-masonry specimens with a total of seven courses were also tested. When loaded in compression, the masonry specimens typically failed by vertical splitting. The mortar being more flexible than the masonry unit expands laterally and induced biaxial transverse tension in the units.

Table 3.4. Test result of compressive strength of mortar specimens

Mortar : 1PC : 4 sand (sieve less than 5 mm)
Tested on : 6th May 2002
Age of specimen = 28 days

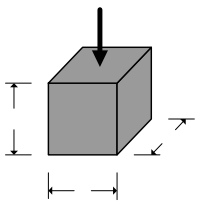

Speci. No.	Dimension (mm)			Weight	Area	Comp. Load (P)		f'_{mortar}
	b	h	t	(gr)	(x 100 mm²)	(kgf)	(N)	(MPa)
M-01	52.71	52.45	51.68	250.15	27.65	3,064	30,058	10.87
M-02	51.82	51.75	49.96	223.10	26.82	2,361	23,161	8.64
M-03	52.12	51.70	52.83	247.44	26.95	3,091	30,323	11.25
M-04	50.50	50.40	50.88	216.02	25.45	2,776	27,233	10.70
M-05	51.80	51.76	51.77	247.23	26.81	3,417	33,521	12.50
M-06	50.65	50.62	50.75	216.14	25.64	2,560	25,114	9.79
M-07	51.64	51.63	52.56	238.36	26.66	3,311	32,481	12.18
M-08	55.51	54.93	54.04	280.38	30.49	3,329	32,657	10.71
M-09	49.15	54.94	51.53	222.20	27.00	2,119	20,787	7.70
M-10	50.52	50.62	51.92	237.33	25.57	3,004	29,469	11.52
M-11	51.91	50.41	52.96	247.09	26.17	3,545	34,776	13.29
M-12	50.83	50.22	50.64	216.15	25.53	2,764	27,115	10.62
M-13	51.26	51.32	51.07	241.98	26.31	3,364	33,001	12.54
M-14	49.37	49.46	51.65	207.88	24.42	2,439	23,927	9.80
M-15	49.32	49.04	51.49	208.10	24.19	2,432	23,858	9.86
M-16	51.99	51.95	51.58	226.78	27.01	2,322	22,779	8.43
M-17	51.67	51.61	50.93	241.07	26.67	2,901	28,459	10.67
M-18	51.93	51.90	52.58	250.74	26.95	2,910	28,547	10.59
M-19	52.51	52.43	50.61	226.97	27.53	2,409	23,632	8.58
M-20	51.88	50.63	54.22	245.65	26.27	3,217	31,559	12.01
					f'm average value from 20 samples	=		**10.61**
					SD	=		**1.51**
					COV	=		**14.23 %**

3.4.2.1. Compressive Strength based on SNI 15-2094-1991

A Brick unit will be cut in half with a saw. Each cut part of the brick will be stacked on the other part and the space between the two cut bricks are to be filled with 6 mm mortar (see Figure 3.4.). Mortar of similar quality will be applied on both the top and bottom surfaces to a thickness of 6 mm. The standard stated that 30 pieces of test items must be produced to determine the compressive strength of clay brick. The test was terminated at the first crack.

Specimens were tested at age 28 days.

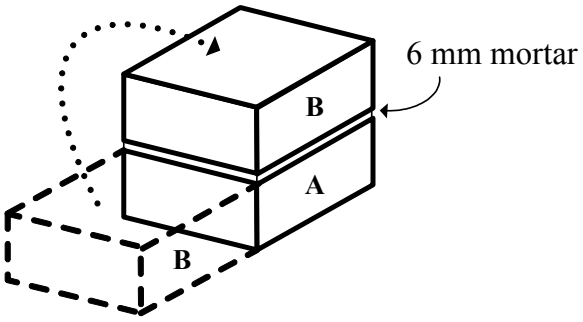

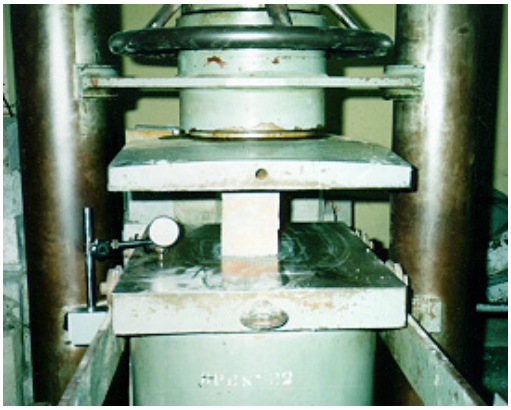

Figure 3.4. Clay brick compression strength test using SNI 15-2094-1991 method

Table 3.5. Test result of clay brick compressive strength based on Indonesian Standard

Clay Brick Type : Cikarang HSG - West Java
Tested on : 05th June -2002
Age of specimen : 28 days

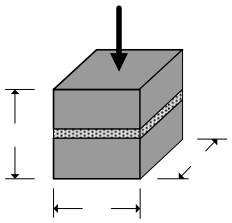

No.	Dimension (mm)			Weight	Density	Comp. Load (P)		Comp.Strength
	h	b	t	(gram)	(kg/m^3)	(tonf)	(kN)	(MPa)
C-B/01	100	93	90	1474	1761	9.00	88.29	10.55
C-B/02	100	91	91	1441	1740	6.04	59.25	7.16
C-B/03	100	91	95	1528	1767	12.46	122.23	14.14
C-B/04	100	90	85	1394	1822	8.11	79.56	10.40
C-B/05	100	94	94	1485	1681	9.68	94.96	10.75
C-B/06	100	89	95	1528	1807	6.36	62.39	7.38
C-B/07	100	87	93	1454	1797	9.76	95.75	11.83
C-B/08	100	91	92	1505	1798	9.19	90.15	10.77
C-B/09	100	93	96	1523	1706	8.84	86.72	9.71
C-B/10	100	95	90	1557	1821	6.89	67.59	7.91
C-B/11	97	94	84	1469	1918	11.30	110.85	14.04
C-B/12	102	91	89	1508	1825	5.58	54.74	6.76
C-B/13	98	90	88	1403	1808	10.97	107.62	13.59
C-B/14	100	90	93	1560	1864	8.38	82.21	9.82
C-B/15	100	90	90	1531	1890	8.19	80.34	9.92
C-B/16	102	88	91	1479	1811	7.56	74.16	9.26
C-B/17	97	90	90	1395	1775	8.67	85.05	10.50
C-B/18	102	90	92	1361	1611	8.38	82.21	9.93
C-B/19	100	92	93	1469	1717	11.41	111.93	13.08
C-B/20	100	90	88	1445	1824	7.42	72.79	9.19
C-B/21	100	90	88	1524	1924	8.38	82.21	10.38
C-B/22	100	93	95	1508	1707	6.76	66.32	7.51
C-B/23	100	94	96	1575	1745	6.18	60.63	6.72
C-B/24	99	90	90	1403	1750	8.20	80.44	9.93
C-B/25	98	91	93	1438	1734	6.21	60.92	7.20
C-B/26	100	95	92	1617	1850	9.91	97.22	11.12
C-B/27	102	93	92	1572	1801	12.83	125.86	14.71
C-B/28	100	92	88	1420	1754	11.03	108.20	13.37
C-B/29	100	91	95	1508	1744	10.71	105.07	12.15
C-B/30	100	92	94	1505	1740	6.37	62.49	7.23
f'm average value from 30 samples =								**10.23**
SD								**2.37**
COV								**23.15 %**

$$f'_m = \frac{F}{A} \quad \ldots\ldots\ldots\ldots\ldots\ldots\ldots\ldots\ldots\ldots\ldots\ldots\ldots \quad (3.1.)$$

Where :

f'_m = compressive strength of masonry (MPa)

F = compressive strength (N)

A = area of longitudinal surface (mm^2)

The warping of the bricks and the cracks has a large influence on the compressive strength of the brick. Results of the compressive strength tests on brickwork specimens indicate that bricks with a deviation in shape will crack easily during loading due to the difference in joint thickness. Not only deviation in size and cracks, but the quality of the brick is also very unequal. The average compression strength of HSG brick based on Indonesian standard is 10.23 MPa with coefficient of variation 23.15%. The average density of clay-brick test result is 17.493 kN/m^3 (1783.14 kg/m^3) and coefficient of variation is 3.86%. These bricks can be categorised as class B according to the Indonesian standard (SNI 15-2094-1991).

3.4.2.2. Compressive Strength based on Prismatic Specimen

Another compressive strength test of a prismatic-masonry was conducted on 20 samples. The samples were assembled by pairing couples of clay brick units and 10 mm mortar thickness for a total of seven courses. The overall size of specimen is around 190 (length) x 190 (width) x 390 (thickness) mm as shown in Figure 3.5. The compressive strength test was conducted after the specimen had reached 28 days age. Four Linear Variable Displacement Transducers (LVDTs) were used for measuring the deformation. A pair LVDTs was mounted on both sides of the prismatic-masonry specimen and opposite each other to measure the vertical deformation. The devices had been connected to the specimen by means of screw bolts glued with epoxy resin on the external part of the brick. Another pair LVDTs was attached at the other sides of the prismatic-masonry at the mid height of the specimen to measure the lateral deformation. In general, this prismatic-masonry were instrumented with four LVDTs and connected to Data Logger TDS 302-10. The data logger was connected to a computer to record the obtained data

The axial force was applied incrementally using a compression test-machine equipped with load controlled. Under compressive loads, the specimens typically failed by in-plane vertical cracking.

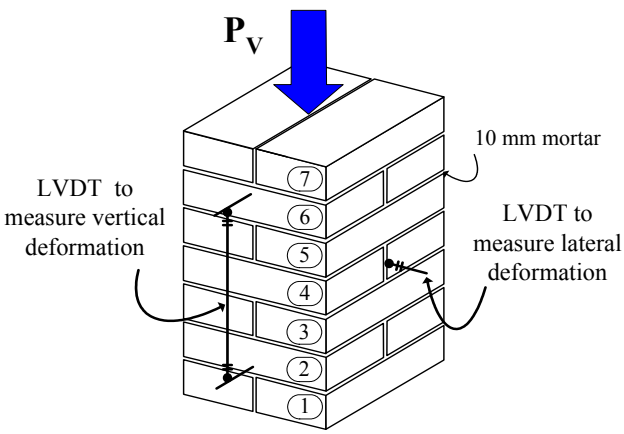

Figure 3.5. Clay brick compression strength tests using prismatic masonry specimen

Table 3.6. Test Result of Axial Compressive Strength at Prismatic Masonry Specimen

Clay Brick Type : Cikarang West Java
Mortar : 1PC : 4 sand (sieve less than 5 mm)

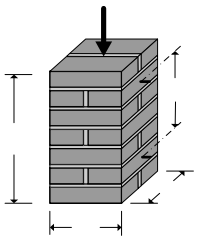

Tested on : 05-06-2002
Age of specimen = 28 days

No.	Unit	Dimension (mm)			Vol.	Weight	Density	$P_{a,m}$	f'_m	Distance Tr (mm)		E_{me}
		b	T	h	(mm^3)	(kg)	(kg/m^3)	(tonf)	(MPa)	j_L	j_R	(MPa)
1	M/01	191	188	391	14040028	26.6	1895	42.76	11.68	285	293	6095.2
2	M/02	190	190	387	13970700	27.3	1954	46.02	12.51	300	292	5809.6
3	M/03	201	190	379	14474010	26.1	1803	42.07	10.81	287	285	7433.3
4	M/04	187	186	390	13564980	27.2	2005	39.06	11.02	290	290	13911.0
5	M/05	193	190	384	14081280	25.9	1839	41.71	11.16	295	290	2056.4
6	M/09	187	185	389	13457455	26.0	1932	32.05	9.09	270	280	4445.1
7	M/10	193	184	371	13174952	25.6	1943	30.72	8.49	280	280	3370.4
8	M/13	187	191	394	14072498	26.7	1897	32.54	8.94	280	280	2704.9
9	M/14	190	189	384	13789440	26.9	1881	31.16	8.51	285	295	5222.2
10	M/15	190	192	392	14300160	26.8	1874	49.45	13.30	290	280	6526.4
11	M/17	188	185	396	13772880	26.7	1939	32.71	9.23	285	290	7698.1
12	M/18	195	190	380	14079000	26.4	1875	35.48	9.39	290	290	3682.8
13	M/20	195	197	388	14905020	25.3	1697	36.74	9.38	228	235	7620.8
14	M/22	190	191	398	14443420	26.8	1856	39.64	10.72	230	237	6128.8
15	M/24	182	191	389	13522418	25.6	1893	30.15	8.51	240	232	11288.0
16	M/25	189	192	386	14007168	25.1	1792	34.81	9.41	242	233	9303.2
17	M/26	184	190	372	13005120	25.4	1953	37.79	10.60	226	219	5968.3
18	M/28	188	194	391	14260552	25.9	1816	43.66	11.74	230	240	9774.5
19	M/29	189	190	388	13933080	25.6	1837	34.07	9.31	240	230	9260.7
20	M/30	187	195	385	14039025	24.7	1759	38.54	10.37	234	230	3055.2
Average value from 20 Units =									**10.21**			**6567.7**
SD									**1.40**			**3062.37**
COV									**13.68 %**			**46.63%**

The LVDTs readings from the test results showed variations mainly due to the imperfections of the external surface prismatic-masonry specimens, which were slightly wavy. The result of average compressive strength based on maximum axial force divided by the top surface area of the specimen is 10.21 MPa, with coefficient of variation is 13.68 %. This value is quite close to the value obtained from the test result based on Indonesian standard (SNI 15-2094-1991). The average density of prismatic masonry test result is 18.49 kN/m^3 (1875.57 kg/m^3) and coefficient of variation is 4.09%.

3.4.3 Shear Test at Bed Joints

Due to limitations on the laboratory equipment available, a modification of the triplet test was introduced. The samples were assembled by three layered clay brick prisms with 10 mm mortar joint. The shear bond test was conducted after the specimen had reached 28 days age and tested under a combination of direct shear stress and a constant normal stress. A cork sheet of 50 mm layer was used as a capping to ensure a good contact between the surface of the clay brick unit and the platens of test machine. Typical specimens and loading apparatus are shown in Figure 3.6. A series of different average constant normal stress values of 0.01 MPa, 0.19 MPa and 0.24 MPa were given and the lateral force was applied incrementally using compression test-machine equipped with load-cell control. A pair LVDTs was mounted on both sides at the second layer masonry unit to measure the horizontal deformations. Minimum of five triplets were taken for each constant normal stress value. The failure condition is where the triplet is no longer capable to carry an additional lateral force or where the shear strength at the bed joints of the triplet brickwork has been exceeded.

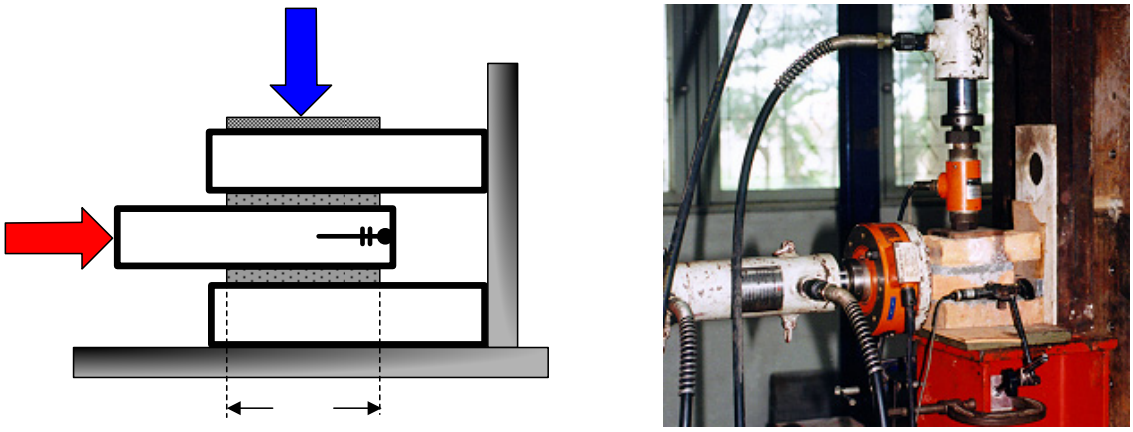

Figure 3.6. Shear strength test on horizontal triplet test

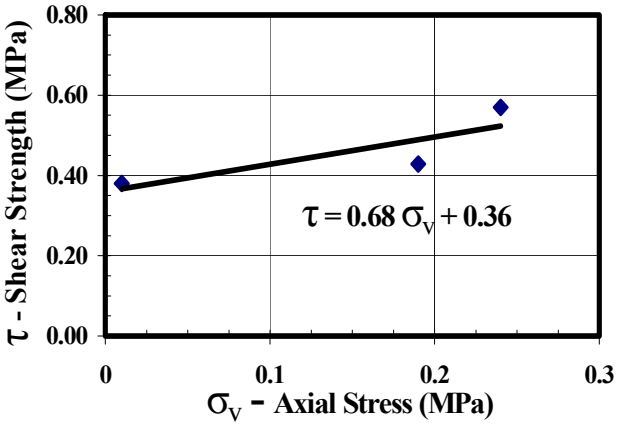

Figure 3.7. Correlation between shear strength and axial stress

Table 3.7. Test result of shear strength on horizontal triplet test

Clay Brick Type : Cikarang West Java
Mortar : 1PC : 4 sand (sieve less than 5 mm)
Tested on : 05-06-2002

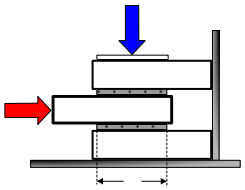

Age of specimen = 28 days

No.	Unit	Dimension (mm)		A	Pv	Axial Strength	P_H	τ
		a	b	(mm^2)	(kg)	σ (MPa)	(kg)	(MPa)
1	S/01	105	92	19320	8	0.010	955	0.48
2	S/03	95	90	17100			687	0.39
3	S/04	95	90	17100			621	0.36
4	S/05	95	90	17100			545	0.31
5	S/09	90	90	16200			578	0.35
					Average shear strength			**0.38**
					SD			**0.07**
					COV			**17.28**
1	S/03	100	90	18000	153	0.19	825	0.45
2	S/04	90	90	16200			692	0.42
3	S/05	84	91	15288			747	0.48
4	S/09	90	90	16200			568	0.34
5	S/10	100	90	18000			829	0.45
					Average shear strength			**0.43**
					SD			**0.05**
					COV			**12.13**
1	S/02	120	90	21600	300	0.24	1250	0.57
2	S/03	125	92	23000			1234	0.53
3	S/04	120	97	23280			1290	0.54
4	S/06	118	90	21240			1338	0.62
5	S/07	120	89	21360			1340	0.62
					Average shear strength			**0.57**
					SD			**0.04**
					COV			**7.23**

The test results of the triplet tests are shown in Table 3.7. The shear strength of the masonry joints has been calculated dividing the ultimate shear load by two times the area of horizontal joint. A regression line was obtained from the graphic plotted average shear strength with respect to the correspondent average normal stress as shown in Figure 3.7. The joint shear strength was expressed as a Mohr-Coulomb type of failure criterion as follows :

$$\tau = 0.68\ \sigma_v + 0.36 \text{ (MPa)} \quad \ldots\ldots\ldots\ldots\ldots\ldots \quad (3.2.)$$

Coefficient 0.36 value indicated the shear bond strength at initial compression equal to zero (cohesion) and 0.68 value indicated friction coefficient (= μ) between mortar and masonry unit which corresponding to a friction angle of 34^0. It is evidently understood that the shear capacities of masonry joints significantly increase as the normal stress level increases.

3.4.4 **Modulus of Elasticity and Poisson's Ratio of Masonry**

There is still no standardized method for evaluating the modulus of elasticity in Indonesia. The elastic modulus of masonry was determined as the relationship between stress-strain diagrams from the compressive strength of prismatic masonry. The average strains obtained by dividing the measured vertical deformations by the corresponding gauge lengths of the recording instruments. Typically, a secant modulus of elasticity, E_{me}, is described by the slope of the line of the stress-strain curve between 5% and 33% of the estimated masonry ultimate compressive stress as shown in Figure 3.8. (FEMA-274, 1997 and NEHRP, 2000). Based on that prismatic masonry test, the average Young's Modulus, $E_{m,}$ of HSG clay-brick is 6567.7 MPa or equivalent to 643.4 f'_m with the coefficient of variation 46.63%. (see Table 3.6). The shear modulus of elasticity, G_m, was taken 0.4 times E_m.

The Poisson's ratio of masonry was evaluated by the ratio of unit lateral contraction and unit axial deformation within the elastic limit. The elastic strain value was described in between 5% and 33% of the masonry ultimate compressive stress. The average vertical strains obtained by dividing measured vertical deformations by the corresponding gauge lengths of the recording instruments. The average lateral strains obtained by dividing the total measured lateral deformations by the corresponding width of the prismatic-masonry specimen. It will be noted that from the 20 prismatic masonry specimens only a few can provide the Poisson's ratio value, because of unrealistic results from the unit lateral contraction and unit axial strain values. Another reason was that the surface of masonry units are not uniform, which means that the LVDTs did not detect the deformation correctly.

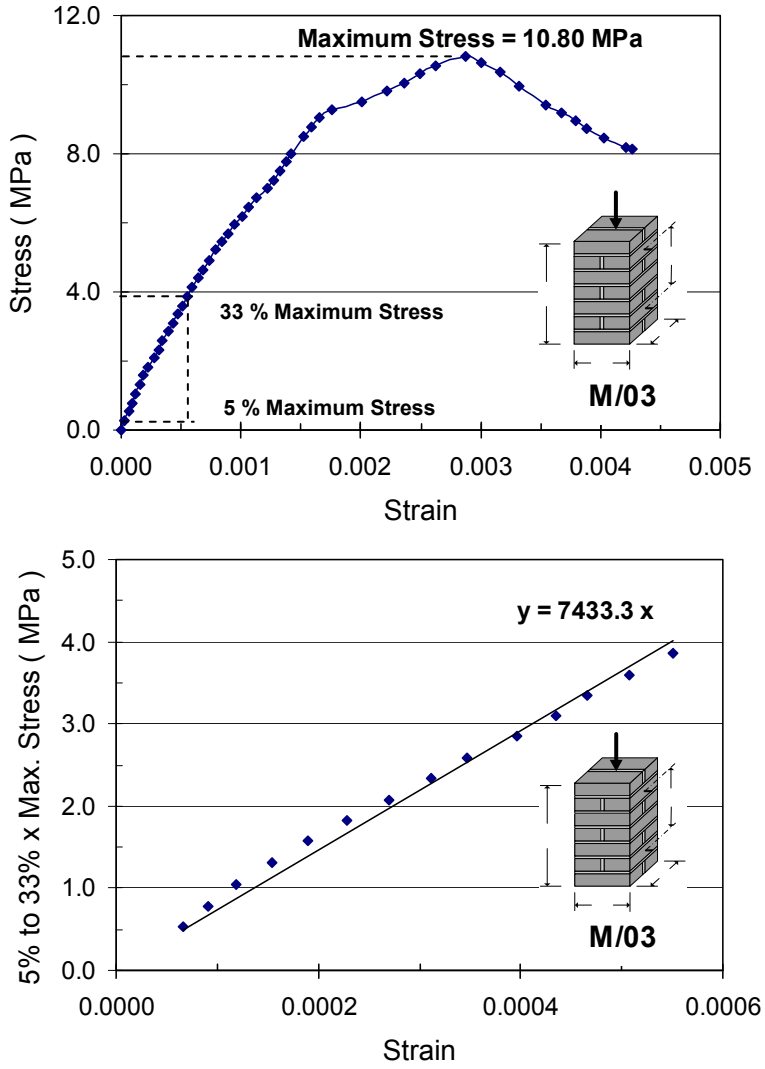

Figure 3.8. Measured Young's Modulus based on FEMA-274, 1997

Test Poisson's ratio results from several prismatic-masonry specimens gave a range value in between 0.25 – 0.46. Hilsdorf (1967) found the Poisson's ratio of brick prisms about 0.2 at the initial loading stage and increased to about 0.35 before the ultimate load was reached. In this research the Poisson's ratio value was taken 0.25.

3.5 PROPERTIES OF STONE FOUNDATION

3.5.1 General

The shallow system foundation, using stone material stacked in a manner resembling a prism, is usually found in old masonry buildings. The stone material is bound together with the use

of mortar. In the standard material regulation in Indonesia what is meant by the stone foundation criteria are natural stones in the shape of natural blocks or cut into blocks large enough to be used for the construction of the base construction of a building.

3.5.2 Compressive Strength of Stone Foundation

There is no reference in Indonesia to specifically determine the Compressive strength of a stone foundation. To obtain the compressive strength of stone foundation material, 7 prismatic samples were made respectively measuring around 400 (length) x 400 (width) x 800 (height) mm. A mortar of 1 part of Portland cement to 4 parts of sand mortar will be applied to bind the stone material units. A compressive strength test was conducted after it has reached 28 days age and the test was terminated at the first crack. Four Linear Variable Displacement Transducers (LVDTs) were used for measuring the deformation. A pair LVDTs was mounted on both sides of the prismatic stone specimen to measure the vertical deformation and another pair LVDTs was attached the other surface of both sides in the mid of specimen height to measure the lateral deformation. The axial force was applied incrementally using compression test-machine equipped with load control. The resulting average compressive strength of stone foundation material is 7.00 MPa with coefficient of variation 9.07%. The average density of stone material, which is the average weight divided by the average volume is 21.307 kN/m^3

3.5.3 Modulus of Elasticity and Poisson's Ratio of Stone Foundation

Typically, a secant modulus of elasticity, E_{stone}, is described by the slope line of the stress-strain curve between 5% and 33% of the estimated stone ultimate compressive strength (FEMA-274, 1997 and NEHRP, 2000). Based on that prismatic stone test, the average Young's Modulus, E_{stone}, of stone specimen is 8168.4 MPa (E_{stone} = 1167 f'm) with coefficient of variation 41.91%. (see Table 3.8). The shear modulus of elasticity, G_{stone}, was taken 0.4 times E_{stone} = 3267 MPa.

It will be noted that from the prismatic stone specimens no one can provide the Poisson's ratio value, because of the unrealistic result from the unit lateral contraction and unit axial strain values. The surfaces of prismatic stone specimens are not uniform, which mean that the LVDTs did not detect the deformation correctly. In this research the Poisson's ratio value of stone foundation material was taken 0.20.

Table 3.8. Test Result of Axial Compressive Strength at Stone Foundation Cube

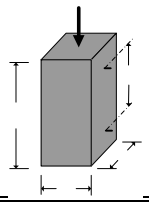

Mortar : 1PC : 4 sand (sieve less than 5 mm)
Tested on : 02-09-2002

No.	Sample	Dimension (mm)			A	Weight	Denstiy	Comp. Load	P_{maks}	f'_{maks}	E_{st}
		B	t	h	(mm^2)	(kg)	(kg/m^3)	(tonf)	(kN)	(MPa)	(N/mm^2)
1	SF-1	397	405	800	160785	277	2156	121.60	1192.90	7.42	11859.0
2	SF-2	400	400	800	160000	276	2160	109.31	1072.33	6.70	6003.0
3	SF-3	385	404	800	155540	271	2175	100.49	985.81	6.34	5567.3
4	SF-4	380	405	800	153900	268	2178	109.71	1076.26	6.99	8916.9
5	SF-5	385	395	800	152075	266	2183	116.21	1140.02	7.50	13483.0
6	SF-6	403	380	815	153140	272	2176	123.40	1210.55	7.91	4259.6
7	SF-7	415	390	800	161850	282	2176	102.12	1001.80	6.19	7089.9
						Average value of Density =	**2172.0**	Average value =		**7.00**	**8168.4**
								SD		**0.64**	**3423.5**
								COV		**9.07%**	**41.91%**

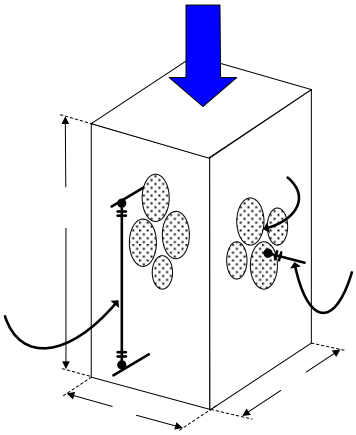

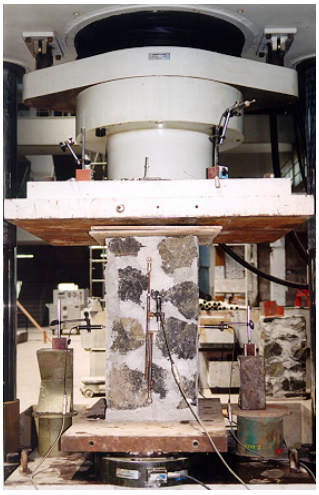

Figure 3.9. Axial compression test on stone material

3.6 BRICKWORK BONDS

3.6.1. Basic Bricklaying

Masonry units can be laid in numerous different ways to make a masonry walls. The basic bricklaying's are shown at Figure 3.10. and 3.11. It is the process of arranging masonry units in courses in order to develop longitudinal and transverse interlocking for individual masonry units. These bond patterns are essential for any wall, which is intended to achieve a united mass, can carry heavy loads, and prevent, as far as possible any structural failure. The method

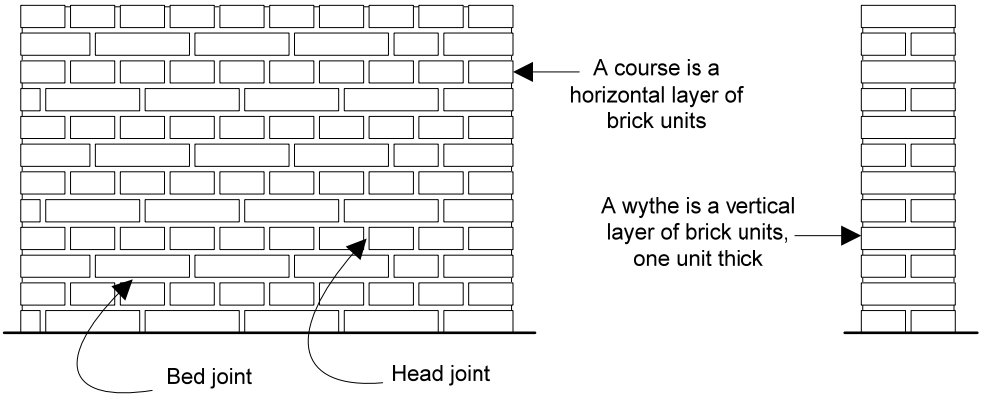

Figure 3.10. Basic brickwork terminology

(a) A stretcher and header

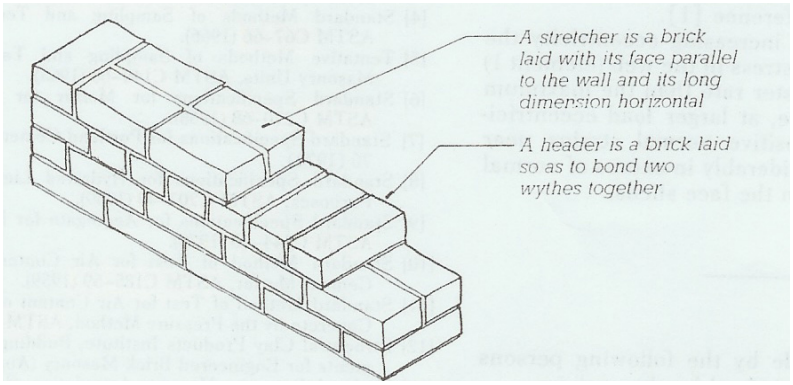

(b) A soldier

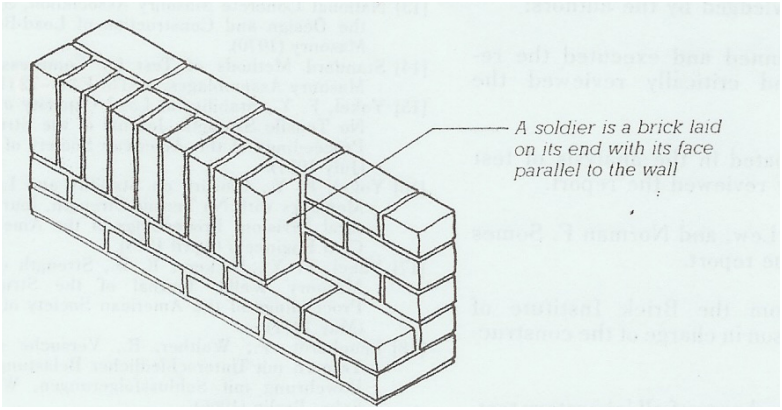

(c) A rowlock

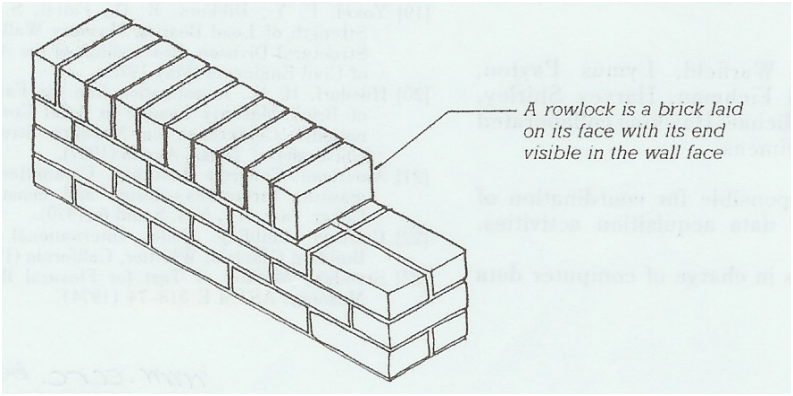

Figure 3.11. Basic Bricklaying (Allen, 1985)

is to ensure that vertical joints do not come in one vertical line over the other so that the vertical load can be distributed over an arc of 45 degrees.

To achieve its effectiveness, the bonding must distribute the loading evenly throughout the length of the wall, so that each part of the wall carries a small amount of the load. If, on the other hand, the load is not distributed but localized to a certain portions of the wall, then this may cause uneven settlement and cracking. In addition to the even distribution of loads throughout the wall, correct bonding at corners, attached piers, junction and separating walls to ensure that they are well tied in together. This will also provide stability.

3.6.2. Types of Bonds

There is an infinite number of possible bonding arrangements of URM walls, but there are five bonding arrangements of the more common ones in general use, as follows :

1. Stretcher bond consists of all bricks laid as stretchers on every course with the courses laid half-bonded to each other. This is affected in a plain wall with stopped ends by introducing a half-bat as the starting brick to alternate courses. Usually only used in walls of a half-brick thickness.
2. Header bond, is satisfactory for walls one brick thick and consisting of all headers, with the bond being formed by three-quarter bats at the quoin (a corner or external angle of a wall), and generally used in footing courses or walling curved on plan. (bats is a portion of an ordinary brick with the cut made across the width of the bricks)
3. English bond consists of alternate courses of headers and stretchers, with a closer placed next to the quoin header to form the lap. There is however, a variation where a closer is not used in the header course, and the lap is formed by staring each stretcher course with a three-quarter bat. Such variation is not very common but occasionally instructions are given on site that no closers are to be used in the work.
4. Flemish bond comprised of alternate headers and stretchers at every course with the headers in one course being placed centrally over the stretcher in the course below. A closer is placed next to the quoin header to form the lap.

(a) Stretcher bond

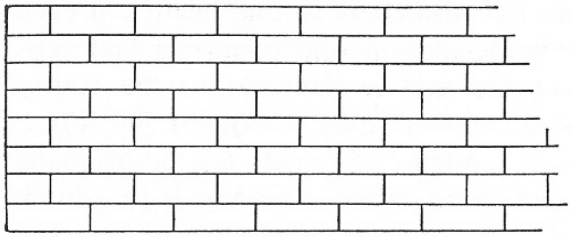

(b) Header bond

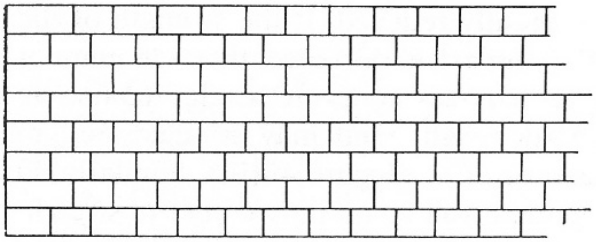

(c) English bond

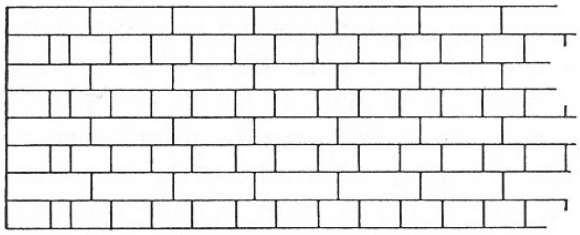

(d) Flemish bond

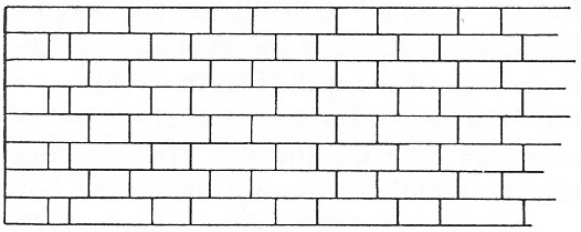

(e) Dutch bond

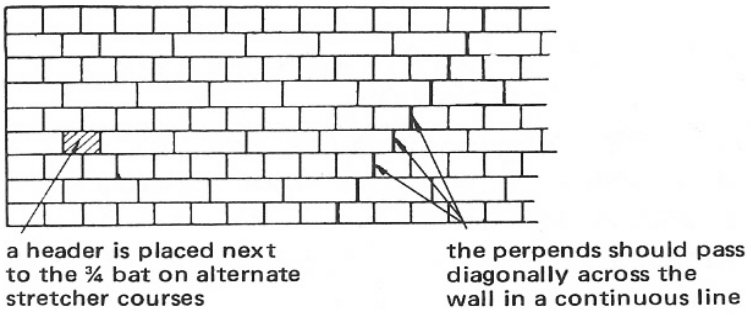

Figure 3.12. Elevation of bonding arrangement for URM walls (Nash, W.G. 2001)

5. Dutch bond is somewhat similar to English bond in that it consists of alternate header and stretcher courses, but there are no closers in the header course, and starting each stretcher course with a three-quarter bat forms the bond. In addition the stretcher courses are laid half-bond to each other; this is affected by placing a header on alternate stretcher courses next to the three-quarter bat. The perpendicular in this bond follows each other diagonally across the wall in an unbroken line.

More detail about the terminology of the five bonding arrangements for URM walls are shown at Figure 3.12.

Unfortunately, the differences of bonding arrangements do not seem to affect the strength of the masonry as reported by Sahlin, 1971. The compressive strength of masonry is strong influenced by the workmanship.

3.7 CONCLUSIONS

1. Clay brick material still represent the most important building material over the whole of the Indonesian region and also around the world. The clay brick quality is very dependent on the condition of the clay soil to be used as the basic raw material, the method of mixtures, the method of moulding as well as the system of burning. It is recommended to carry out the test of material characteristics of masonry wall in each region with local clay brick quality. Therefore the quality of clay brick in Indonesia is very variable and standardization so that test data from groups of clay bricks producing in every region is required.

2. Current local standards still do not cover all mechanical property tests and it seems foreign codes are adapted. More experimental research is needed to provide the variation of masonry units' properties in Indonesia region. The compressive strength of the masonry is depending on many factors such as the mechanical properties of the masonry unit, composition of mortar and workmanship. Compressive strength value can be determined from the Indonesian standard (SNI 15-2094-1991) and compared with the prismatic masonry test. Modulus of elasticity and Poisson ratio calculated from the

prismatic masonry test which equipped with LVTDs and described by the slope of the line of the stress-strain curve between 5% and 33% of the estimated masonry ultimate compressive stress. Shear strength is determined by triplet shear bond testing which can give representative parameters of the shear bond behaviour of the joint.

3. In the absence of test data results, some of the mechanical values of masonry had to be defined from several experimental reports developed by UNIDO, Indonesia researchers and/or foreign literatures such as FEMA, NZS masonry code or others. Although UNIDO test results are already irrelevant with the present condition, but still can be used as good references in Indonesia since the tests were conducted using local materials and local masons.

4. A feature to accommodate the stone foundation in the URM wall test was conducted. The characteristic materials of stone foundation were determined using the similar test for the masonry. Prismatic specimens were conducted to measure the compressive strength, elastic modulus and Poisson ratio.

5. Several Bond types were recognised when dealing with URM buildings, such as Dutch Bond type was used in most existing old URM buildings in Indonesia. More research is necessary to investigate the affect of bond type on the performance of masonry walls, especially at the intersection between orthogonal URM walls.

CHAPTER 4 :
TEST PROGRAMME ON UNREINFORCED MASONRY WALL

4.1 INTRODUCTION

Many considerations have been given to concerns about the assessment and strengthening of unreinforced masonry (URM) walls in existing construction in seismic prone countries. The behaviour of URM-walls are much influenced by the quality of the raw material used in the manufacture of the clay-bricks, the aggregate quality of the mortar composition, the stacking of clay-bricks and, the dominating influence of the quality of the local mason's workmanship. To have a test result that will be able to represent the local conditions where the URM-buildings of interest in this thesis will be located, experiments will be conducted in Indonesia using local materials and labour. An old building of three storeys constructed in 1902 was used as a prototype model as many similar buildings are still found in the big cities in Indonesia that used to be governmental centres during the Dutch colonial period.

The building has an L-shaped plan and popularly known by the name of "*Gedung Lawang Sewu*" (The Building of Thousand Doors) and is located in the centre of Semarang, the capital city of Central Java. The building was constructed in 1902 by the Dutch government and used as the state railway headquarters in 1907. During the Japanese occupation (1942-1945) the building was used as an army headquarters until the 1980's. In 1996 an Indonesian private investor became interested to change the function of the building into a five-star hotel, while still preserving the existing building structure. This project idea was cancelled after the 1997 economic crisis occurred in the Southeast Asian regions, particularly in Indonesia.

The building consists of 2 main floors and one attic-room directly under the steel roof truss of double-steel angles. The heights of the first floor, second floor and the attic are 5.440 m, 5.096 m and 7.000 m to the roof peak respectively. The L-shaped floor plan as shown in Figure 4.1 has lengths of 73.20 m at its longest leg and 52.00 m at its shortest leg while the building's width is 23.10 m. The area per floor is thus approximately 2400 m². The grand-

staircase is found at the main entrance area, with a wide floor opening, connecting the first and second floors. The URM walls are continuous from the ground floor straight up to the attic with a consistent thickness, i.e.. 300 mm, 420 mm, 500 mm and 650 m and placed crosswise make a “box-type” structural system. The 650 mm thickness walls were located at one bay of each edge of L-shaped and provided resistance torsional effect. Conforming to its name, door openings can be found in almost every wall of the building. These openings provide natural light and also cause the surrounding URM walls to function as piers.

The floor slabs, which are functioning as horizontal diaphragms consist of bricks stacked in an arch resting along steel I-beams, 600 to 1000 mm centre to centre. A layer of cement mortar is found on top of the bricks. The total thickness of the slabs near the support is approximately 300 mm. The floor finishing on the first and second floors are ceramic tiles while the attic room is finished with only cement mortar. The foundation of the building is strip footing made of stone filled with cement mortar to a height of 1000 mm to 1500 mm and a width of base foundation is 1500 mm. The ground floor consists of masonry arches spanning between steel I-beam which form the crawling-height space underneath. The soil underneath consists of clay layers where the hard soil layer is found at a depth of around 40 metres from the existing ground floor. The roof frames, which were made of double angle steel trusses with a span of around 20 metres, are simply supported directly on top of the perimeter URM walls at 3 metres centres. The roof materials made of clay-tiles.

The building is still in good condition and by changing the function of the building into a five-star hotel, while still preserving the existing building structure, becomes the theme of this research. The objective of the research will be explained more detail at the next paragraph.

4.2 OBJECTIVES OF THE TEST PROGRAMME

With the current development of seismic regulations all over the world, URM-wall construction is no longer recommended for construction in seismic prone areas. Problems have occurred with regard to old existing buildings constructed with URM-walls and not designed against seismic inertia forces. To retrofit such buildings, it will be necessary to know beforehand the capacity existing strength of the building. By knowing the capacity strength we will be able to evaluate whether the building is either strong enough, or not, given the

prevailing seismic coefficient in the area where the building stands. There are many literatures and researches available concerning URM-wall construction in seismic prone areas in other parts of the world, but very little for URM structures in Indonesia.

The in-plane tests of an URM wall test has not been conducted in Indonesia until this research. These studies are fundamental to understanding the performance of in-plane masonry walls under combination of gravity load and lateral load in Indonesia. The existing URM-buildings are usually constructed in varying wall thicknesses of single-wythe or more than one wythe clay-brick walls. One and half wythe of URM wall in Dutch bond configuration will be used for the test. Studies have also been undertaken to analyze the in-plane response of plain URM wall using current seismic rehabilitation guidelines (FEMA 306, 1999) and the Finite Element Method (FEM).

4.3 TEST UNITS

4.3.1 Design Considerations

Two specimens of unreinforced masonry (URM) walls were made, which represent the interior load bearing walls with a door opening in the centre part of the "*Gedung Lawang Sewu*". The URM wall represents the wall part on the first storey of a three-storey building and constructed on top of a stone foundation usually found in such old URM buildings. Figure 4.1. shows the architectural floor plan and also the picture of front view which was taken in 1910. Figure 4.1.c shows the location of the part of the URM-wall which will be tested. The experimental work was conducted in the Research Institute for Human Settlements (RIHS) laboratory in Bandung-Indonesia. Since the maximum height of the concrete reaction wall is only 10 meters and the maximum steel frame available is 6.5 meters in that laboratory, a simplified model was required. Therefore, the URM-wall models were reduced to 75 % of full scale.

Two URM-walls at 75% scale were erected in the laboratory with a masonry wall thickness of a 1½-wythe clay-bricks and arranged in Dutch bond configuration, generally used at the time of construction of the prototype is shown in Figure 4.2. Since the load bearing walls

(a) Front view of "*Gedung Lawang Sewu*" in Year 1910

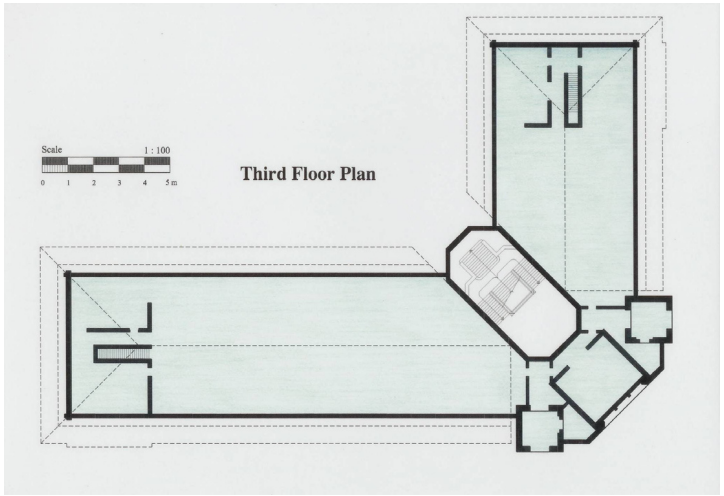

(b) Third Floor Plan

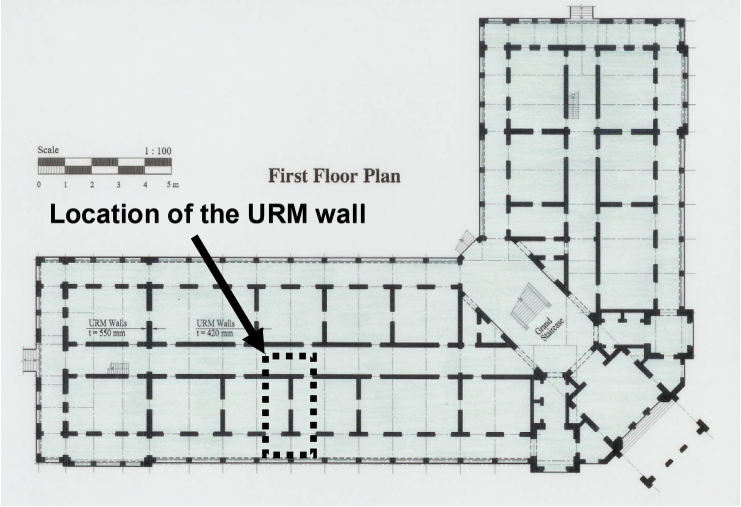

(c) First Floor Plan

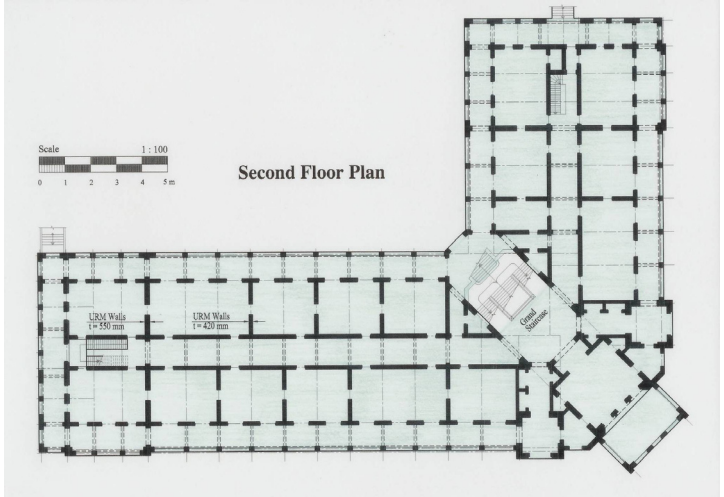

(d) Second Floor Plan

Figure 4.1. Front view and floor plans of "*Gedung Lawang Sewu*"

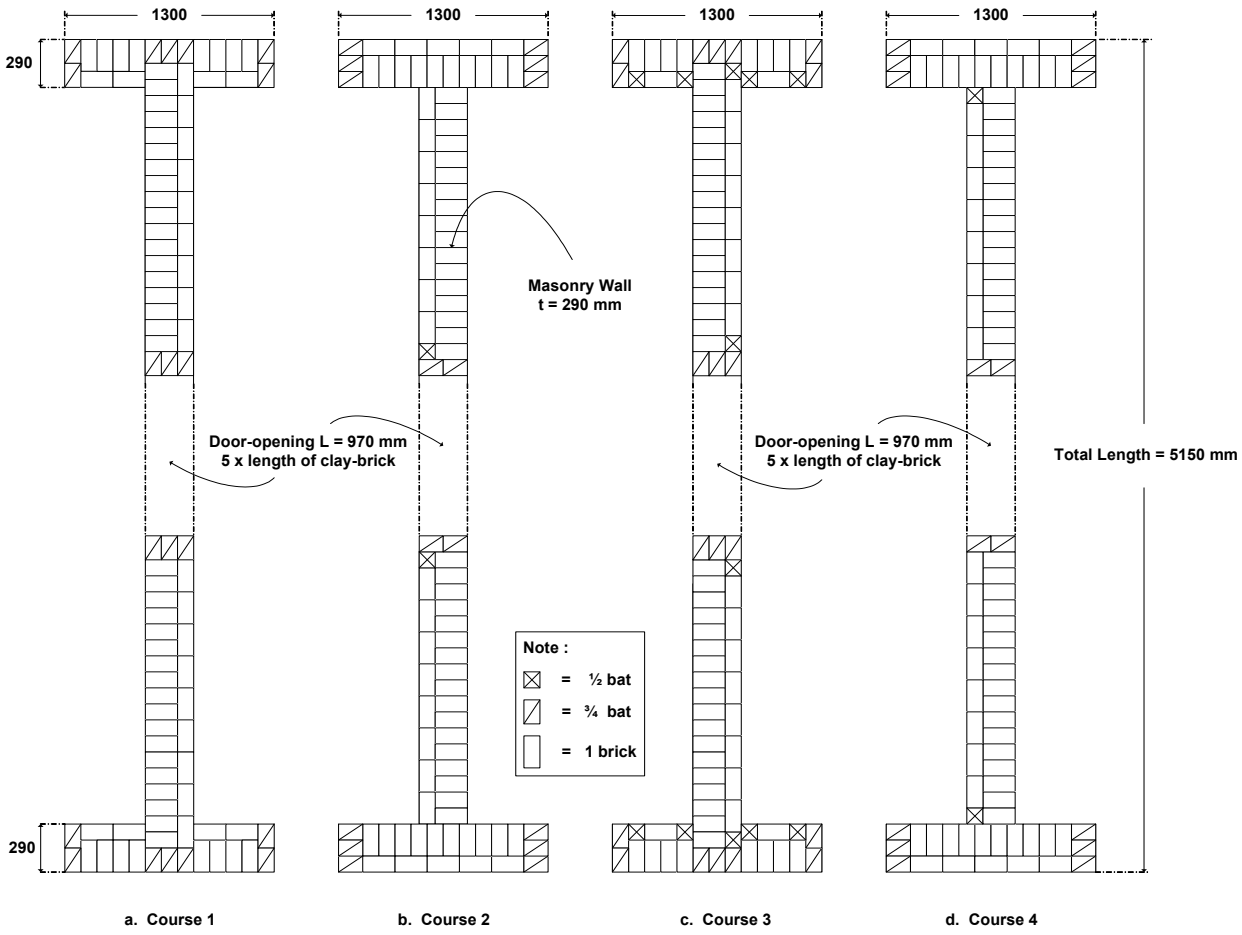

Figure 4.2. Plans of a 1½-wythe URM-wall in Dutch Bond configuration and showing the bonding to each set of four courses

configuration in the building plan like a box system (composed of transverse and longitudinal masonry walls and connecting with brick arch spanning between steel I-beams floor slab), a part of the intersecting walls can be taken into account to increase the main URM wall stiffness and strength. The effective width of the flanges at both sides was 1300 mm. This 75% test model was also made to conform with the dimension of the new clay-brick units currently available in the market i.e. 189 mm x 90 mm x 47 mm compared to the old clay-bricks of 256 mm x 121 mm x 53 mm.

Test Unit-1 was an URM-wall representing an existing structural condition and test Unit-2 was strengthened by high performance aramid fibre containing Kevlar material produced by Fosroc- Indonesia. Both models were tested until failure under quasi-static-reversed cyclic lateral loading. In order to be able to represent a condition closely resembling the existing building, both model units were constructed on top of a stone foundation.

4.3.2 **Description of Test Units**

The walls were built on the one meter thick laboratory structural concrete strong-floor with the following sequence: Firstly, a concrete bottom beam of 250 mm thickness with a concrete quality of f'_c = 20 MPa and reinforced by two layers of D16 mm-diameter bar at 200 mm centre in both directions. Secondly, a strip-footing made of stone filled with cement mortar (1 cement : 4 sand) to a height of 350 mm. Thirdly, an unreinforced clay-brick wall was constructed with a thickness of 290 mm (1½-wythe clay-brick) to a height of 4078 mm and total length including the edge flanges on both sides of 5150 mm. The total width of the flanged wall at both ends is 1300 mm. At the center part of the wall is a door opening, 970 mm wide and 2540 mm high. Fourthly, a concrete beam 400 mm thick with a thickening of 120 mm in its center part with a concrete quality f'_c = 20 MPa and similar reinforcement to that of the concrete bottom beam. For more details see Figures 4.3. to 4.6.

4.3.2.1 Test Unit-1

Unit-1 models the existing load bearing wall as shown in Figure 4.3. The aims of the test are:

1. Find the behaviour of URM-wall with a door opening in the centre when subjected to gravity and lateral load
2. Find the behaviour of the spandrel which connected both pier walls
3. Find the interaction between the URM-wall and the stone foundation in the joint area
4. Find the in-plane strength of the URM-wall

4.3.2.2 Test Unit-2

Walls of similar configuration and dimension as Unit-1 but strengthened with Kevlar on both sides as shown in Figure 4.4. The aims of this test are :

1. Find the behaviour of URM-wall with a door opening in the centre after reinforcement with Kevlar material
2. Find the interaction between the URM-wall and the stone foundation in the joint area
3. Find the advantages of using Kevlar for strengthening URM-wall

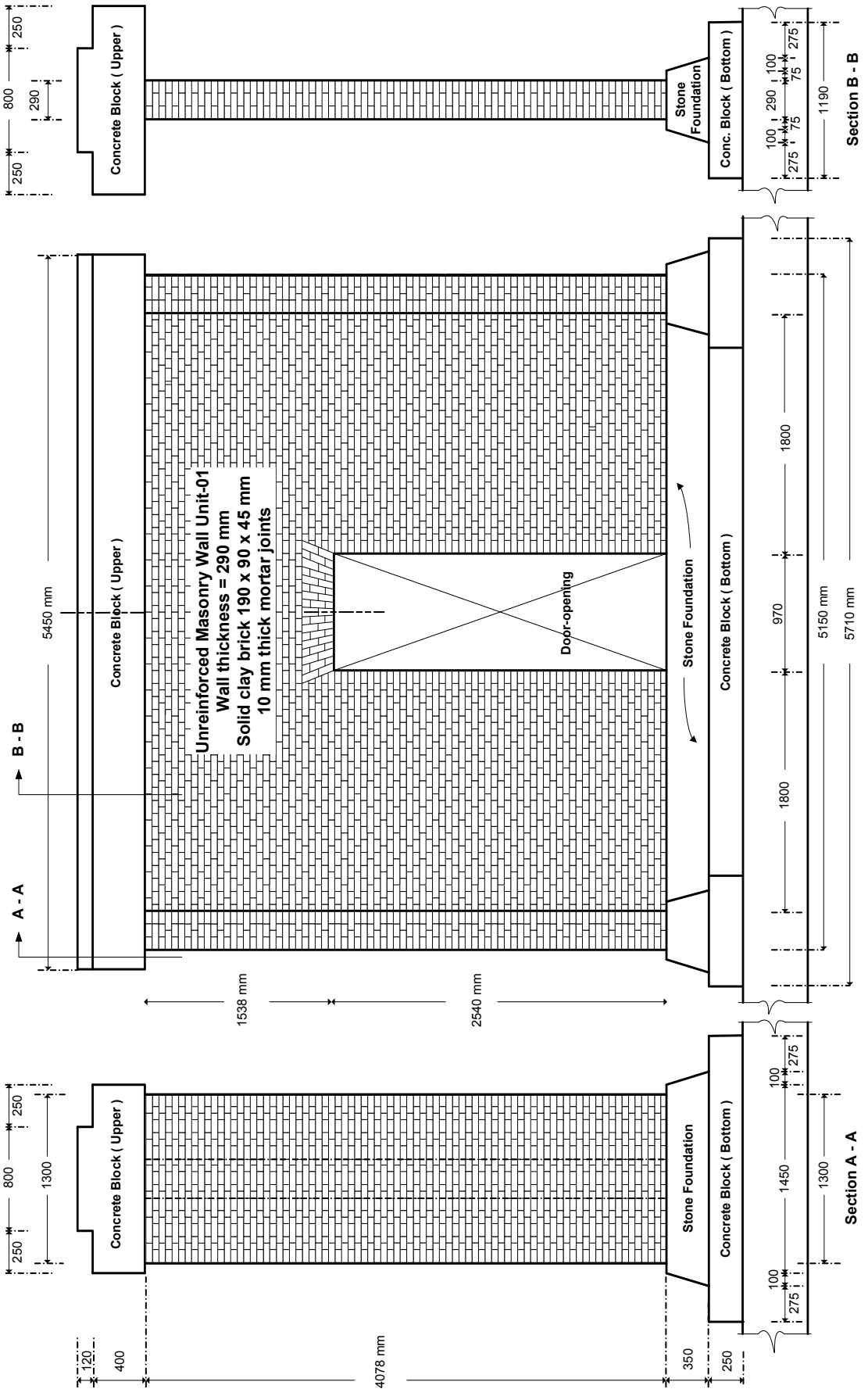

Figure 4.3. Section of URM Wall Unit-1

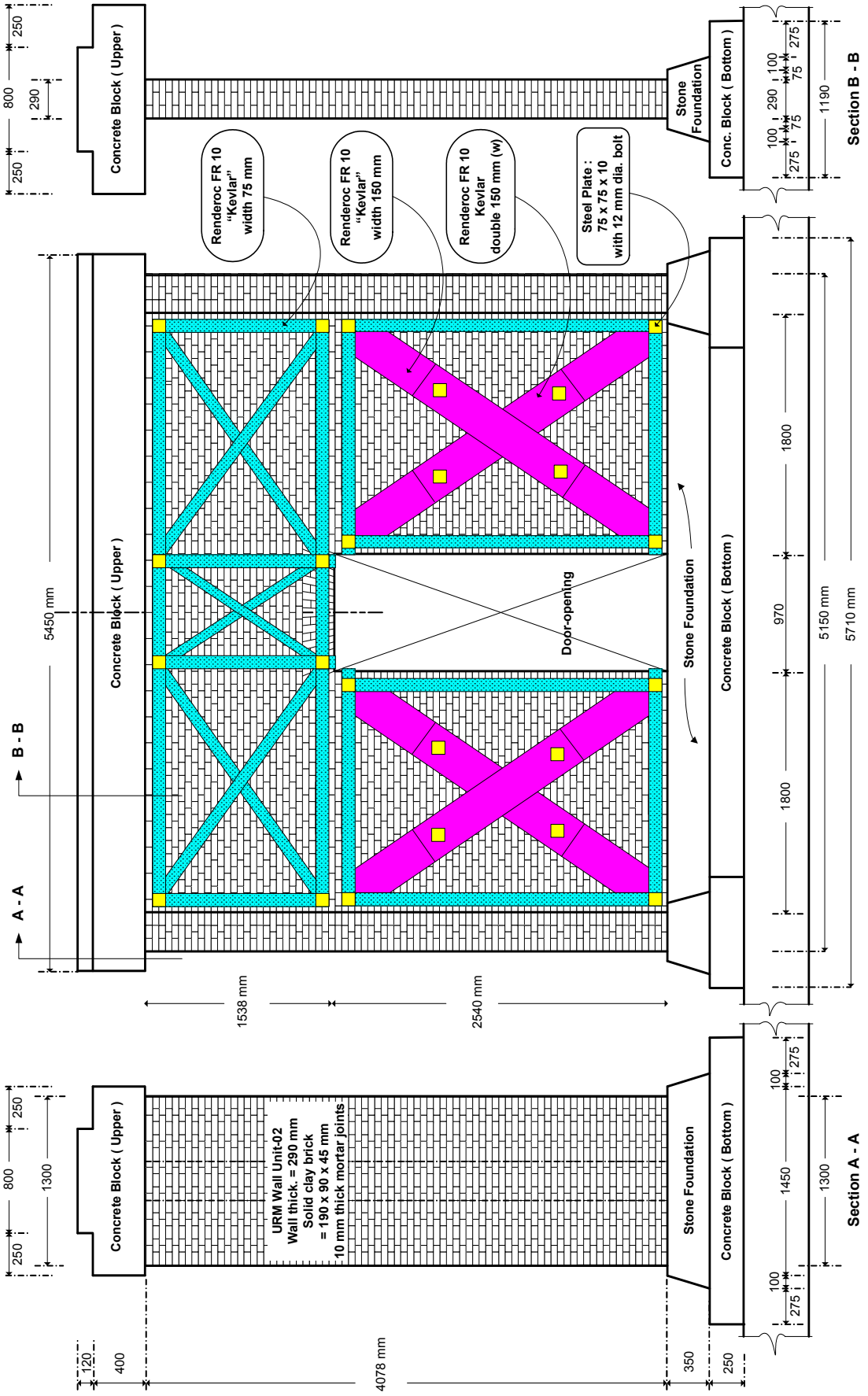

Figure 4.4. Section of URM Wall Unit-2

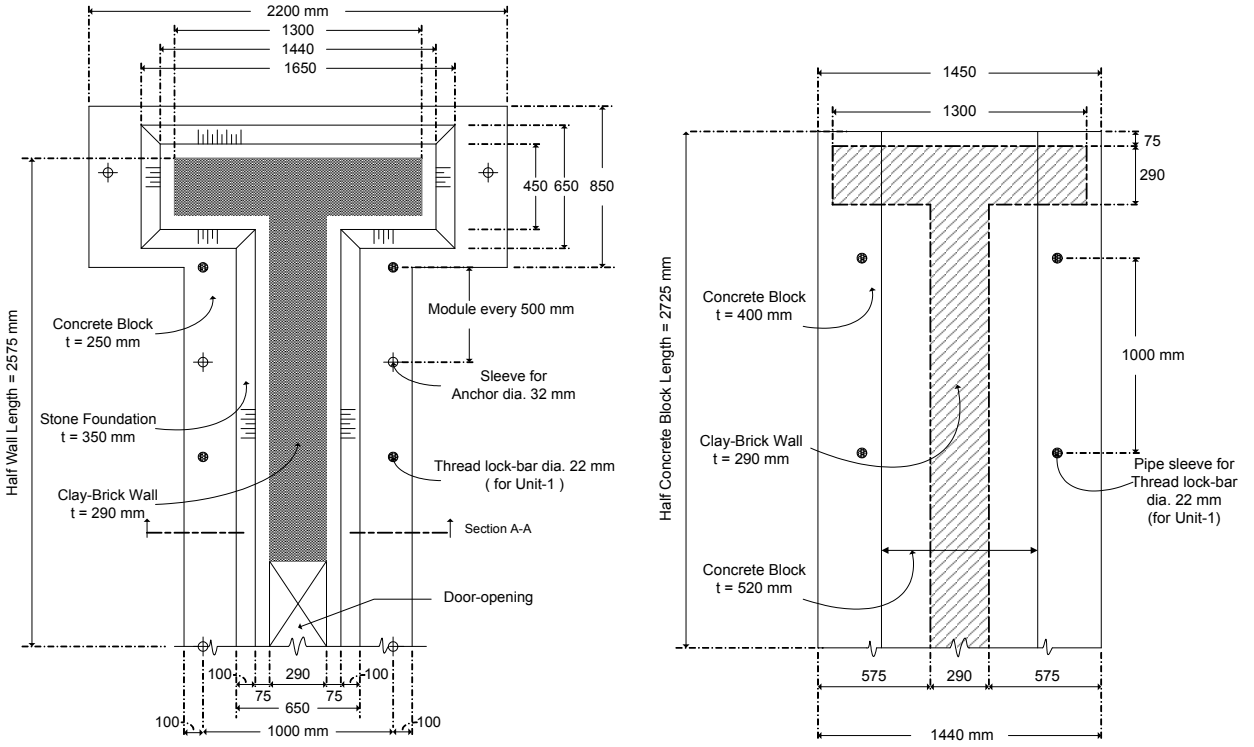

(a) bottom part (b) upper part

Figure 4.5. Detail of bottom part and upper part from the unit models

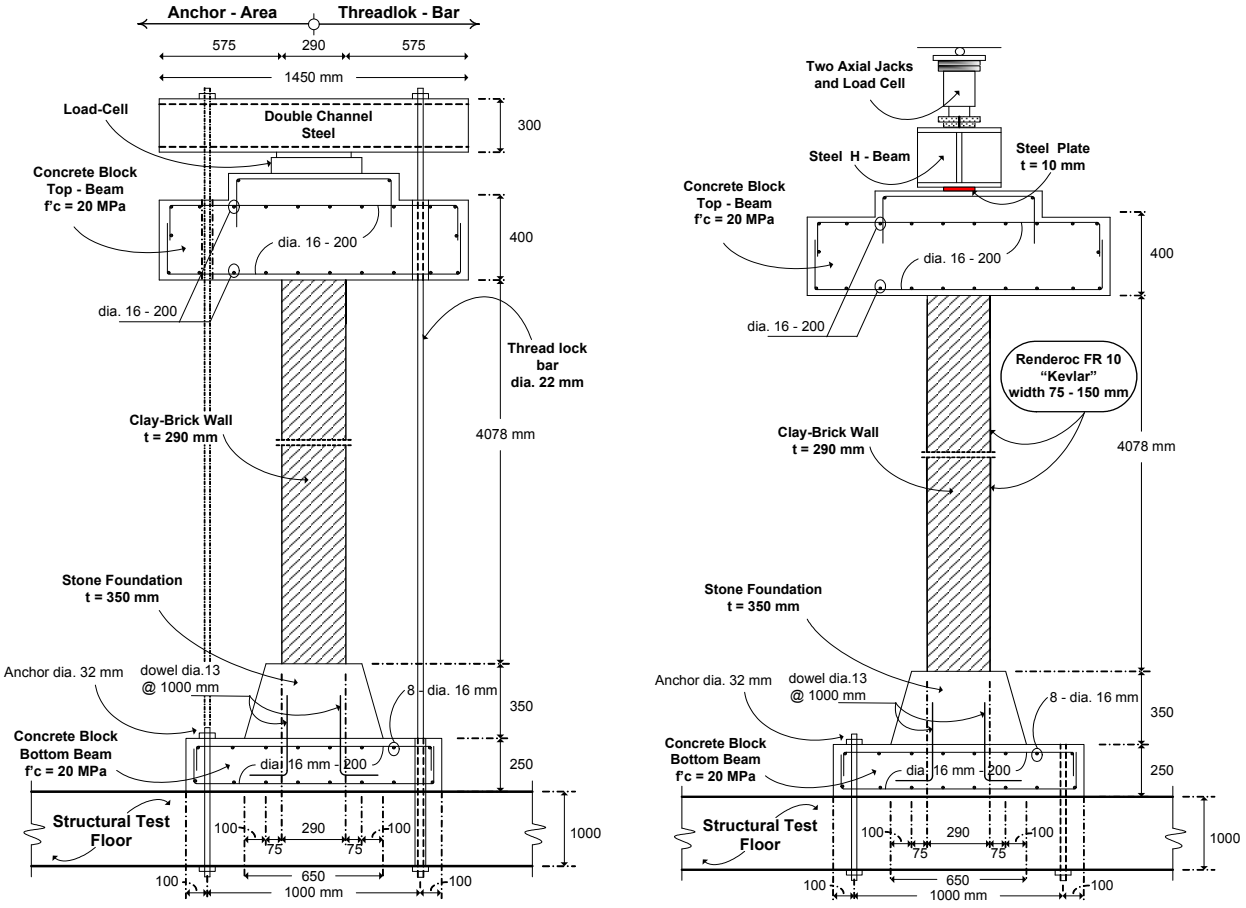

Figure 4.6. Transversal section of Unit-1 (left) and Unit-2 (right)

4.4 CONSTRUCTION OF TEST SPECIMENS

The work was started by setting of the formwork of the bottom concrete block to a height of 250 mm above the laboratory strong floor and the construction of timber form-work at the perimeter of the concrete block. This was followed by the arranging of the bottom concrete block reinforcement consisting of a grid of D16-200 bars, f'_y = 400 MPa, each way top and bottom. On a grid of 500 x 750 mm a 50 mm diameter pvc sleeve pipes are attached to facilitate the anchoring of the concrete block to the strong floor underneath as well as the anchoring of four pairs of VSL thread lock bars (f'_y = 720 MPa) on Unit-1. Concrete placing was carried out using ready-mix concrete of f'_c = 20 MPa quality. To reduce the cost of the concrete from the ready-mix supplier, the placing of the concrete blocks for the two models was carried out simultaneously. ASTM C-192 (Standard Practice for Making and Curing of Concrete), has set the conditions to be maintained during the curing of the concrete by means of covering with wet sacks for 7 days

Three concrete cylinders of 150 mm diameter and 300 mm height were taken during the concrete placing process for the purpose of a concrete quality check at 28 days age. The concrete cylinder was released from its mould after 20 hours to be further curing by submerging in a water tank for compressive testing. Testing of the compressive strength of concrete capacity from the test cylinder was carried out by the Universal Testing Machine (UTM). It is a static monotonic type test which is by adding a relative constant load at an average rate of loading. The compressive strength test of concrete is based on the ASTM C-39 standard (Standard Test Method for Compressive Strength of Cylinder Concrete Specimen). To obtain an even contact field, the surface of the test item is covered with a special layer (capping) to a thickness of 1.5 to 3.0 mm, which does not obstruct the data reading. Loading was carried out until the test item crushed, which was at the moment of maximum load that the test cylinder could bear.

After one-week following the construction of the bottom concrete block a stone foundation was built on top of it. To preserve the monolithic connection between the bottom of stone foundation and concrete block D13-200 dowels are provided at 1 m centres. Because of the limited height of the test model with a steel frame such as available at the laboratory, the maximum height of the stone foundation was only 350 mm. The longitudinal section of the stone foundation is in the form of a prism with a slope conforming to the existing foundation. The slabs of stones measuring approximately 100 mm to 150 mm were put in place with

mortar of 1 part of Portland cement to 4 parts of sand. Before putting the stones in place, these were dumped in a water tank to cleanse them from the existing dust and to make the stones waterlogged. The stones were placed one by one with mortar fillings in such a way as to leave no cavities. The next phase was the erection of the URM-wall.

The laying of the clay-bricks was started by making a sample piling of 4 courses without the use of mortar. This was done to allow the local professional masons to become familiar with the Dutch Bond and 1½-wythe clay brick system to be used. These four courses will be the standard method, which was of upwards-repetitive character. To better clarify the operation, each mason was provided with a Dutch bond configuration drawing as shown in Figure 4.2. The four masons were divided into two groups to build the masonry wall of model unit-1. The first group erected the wing on the left hand side of the door opening and the other group on the right hand side of the door opening. Two assistants carried out mortar mixing. Mortar consists of 1 part of Portland cement to 4 parts of sand, and measuring of the composition was done by volume. All clay-brick units were first soaked for 5 to 8 minutes in a water tank. Thickness of the bed joint and header joint was controlled at an average of around 10 mm. The technique for maintaining the straightness of the masonry wall and plumbness, a set of guide timber trusses were made around the concrete block and a string was placed at each layer of clay-brick to control the thickness of bed joints (see Figure 4.7.b. and 4.7.d.)

The Dutch bond configuration required a variety of clay-brick lengths such as ½ bat and ¼ bat. The clay-bricks were cut with an electric steel saw and water was added to prevent the bricks from breaking during the process. The spandrel above the door opening (a jack arch or also called a flat arch) required special attention during the erection of the clay-brick walls. A soffit board was placed on the floor on which the dimension of the brick spandrel was drawn; afterwards the clay-brick was arranged on the soffit board. To cut the clay-brick units following the shape of the flat arch requires expertise. When these match the required flat arch, they are then laid in the exact position with the temporary assistance of timber formwork below the spandrel beam. Erection was continued until the URM wall reached 4078 mm in height or equal to 73 courses of clay-bricks. The erection of the clay-brick walls of Unit-1 took 15 days. The same procedure also applied to model Unit-2.

A concrete block to a height of 400 mm was poured above the clay-brick wall and the centre was thickened by 120 mm. Reinforcing bars D16-200 each way, top and bottom was used and

in the centre part 6 pvc-sleeves of 2-inches diameter were placed horizontally to a length of 5450 mm. These pvc-sleeves were used to connect the steel base-plate on the front part of the hydraulic jack with the steel base-plate on the other end. This was carried out to ensure that the lateral distributed load worked evenly on the whole longitudinal upper surface of the masonry wall from the concrete block above the wall when a push-pull hydraulic jack was applied. A pvc-sleeve of 2-inches diameter in the vertical direction was made available for the installation of four pairs of VSL thread-lock bars. The upper concrete block for the two unit-models were placed simultaneously with ready mix concrete grade f'_c = 20 MPa. Timber formwork was used to support the concrete block during placing of the concrete. Three concrete cylinders of 150 mm diameter and 300 mm height were taken during placing for testing of the concrete at 28 days age. Some pictures taken during the erection stages of the URM Wall Unit-1 and Unit-2 were shown on Figure 4.7.

The next phase focused on model Unit-1 for in-plane testing purposes as it represent the URM-wall of the existing building. After the specimen had been placed on the test frame, the whole surface of the specimen was painted with water based white paint and on the observed face of the specimen a black vertical and horizontal line was drawn for the purpose of observation and to outline the cracking which occurred during the testing process. The in-plane test for Unit-1 was conducted until failure following with a detail evaluation before continuing with the in-plane test for Unit-2.

URM wall Unit-2 was strengthened diagonally with a thin layer (0.193 mm) of the high tensile capacity “Kevlar” material. The testing was conducted after completion of the unit-1 test results and detail evaluation, so that the reinforcing method applied to Unit-2 would be more beneficial. Kevlar is very expensive material and special attention should be considered to decide on the correct application. Kevlar was applied diagonally on both sides of the unreinforced masonry walls and tightened together with anchor bolts on the edge sides. The unreinforced masonry wall is divided to become three rigid bodies, i.e. the upper part of the door opening and two pier-walls adjacent to the door opening. A rocking mechanism was expected in the piers of both walls.

(a) Instruction on Dutch Bond configuration

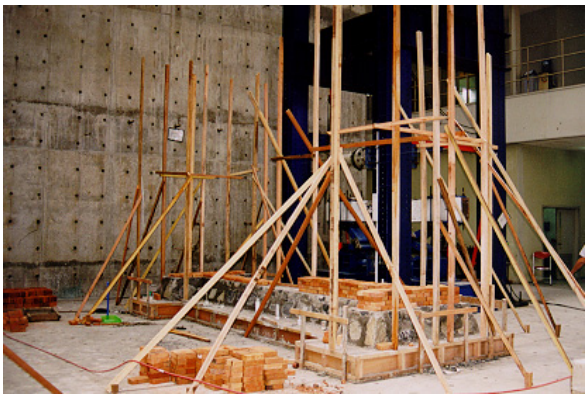

(b) Initial stage of constructing URM Unit-2

(c) Soaked for 5 to 8 minutes in a water tank

(d) Progress on URM Unit-2

(e) Final brick layer for URM Unit-1

(f) spandrel brick above the door opening

(g) Concreting the top beam

(h) Final stage of URM Unit-1 and Unit-2

Figure 4.7. Erection stages of URM wall Unit-1 and Unit-2

The main steps for applying the Kevlar material at Unit-2 as follows :

1. Plot the Kevlar fibre position on both faces of masonry walls
2. Both wall surfaces to be applied by Kevlar sheet were coated with a thin layer of two-component epoxy (Nitobond-EP10P). This coating will function as priming surfaces where the Kevlar sheet is to be applied. The area coated with Nitobond-EP10P was left to dry for at least three days.
3. The area where Kevlar sheet would be applied at masonry wall surfaces was leveling by grinding. Any dust and loose particles were removed with high air pressure.
4. Kevlar fibre was cut according to requirement dimensions (75 mm width and 150 mm width). Steel scissors were used since the Kevlar sheet is very strong.
5. The Kevlar sheet was applied on the areas to be strengthened with the assistance of Nitobond-EC. Nitobond-EC is a two-part epoxy-resin compound of low viscosity and has a specifically formulated epoxy resin adhesive for bonding between Nitobond-EP10P and Kevlar sheet. The Nitobond-EC is applied into the existing Nitobond-EP10P surface using a roller and followed with the pasting of Kevlar sheet on its surface. A second coating of Nitobond-EC was applied on the outside Kevlar surfaces for impregnation.
6. To ensure the Kevlar sheet on both surfaces work together, steel bolts diameter 12 mm were drilled to the masonry walls and used to anchor both Kevlar sheet configurations at every corner.

Figure 4.8. was shown the strengthening material. Figure 4.9. and 4.10. were shown the installation progress of strengthening materials at URM Wall Unit-2.

Figure 4.8. Strengthening materials : Kevlar-fibre, Nitobond-EP10P and Nitobond-EC

(a) Installation of Nitobond-EP10P as priming surfaces

(b) surfaces levelling by grinding prior installation of Kevlar fibre

(c) Installation of Kevlar fibre

Figure 4.9. The installation of strengthening materials at URM Wall Unit-2

Figure 4.10. Progress of primary surfaces and installation of Kevlar fibre at URM Wall Unit-2

The whole surface of the URM wall Unit-2 was also painted with water based white paint as was URM wall Unit-1 and on the observed face of the specimen a black vertical and horizontal line was drawn for the purpose of observation and to outline the cracking that occurred during the testing process. The test on model Unit-2 was conducted one-week after the Kevlar was installed.

4.5 MATERIAL PROPERTIES

4.5.1 Clay-brick Units

It was decided to use the new clay-brick units currently available in the market and was produced at "Cikarang – West Java", i.e. HSG brick. The shape and the colour of bricks are very unequal due to the firing system. The average HSG brick dimension is 189 mm lengths x 90 mm widths x 47 mm thick and the average density is 16.284 kN/m^3. To get good bond strength with compatible mortar for the masonry wall construction, each clay-brick unit was soaked beforehand in a water container for 5 to 8 minutes. The result of the absorption test of the clay-brick used in the experiment can be seen in the Chapter 3.

4.5.2 Mortar

The mortar is mixed manually; the cementitious material and the aggregate were being mixed dry until a uniform colour is achieved. The water was then be added and shovelled or hoed thoroughly until the mortar was easily workable and the ingredients were thoroughly distributed. The nominal mortar with 1 part of Portland cement to 4 parts of sand (in accordance with current Indonesia clay brick code) was used for the mortar joints with an average thickness of 10 mm. Batching the mortar was done by volume, using plastic buckets. The results of the compressive strength, f'_{mc}, based on cubes of 50 x 50 x 50 mm in 28 days are 10.61 MPa. Test results for the mortar strength are shown in Chapter 3.

4.5.3 Masonry

The results of the compressive strength taken from tests based on the Indonesian standard (SNI 15-2094-1991) and other standards are summarized in Chapter 3. The average compression strength for 30 specimens of HSG brick based on Indonesian standard (two courses of half brick with 6 mm mortar) is 10.23 MPa. The other result of average compressive strength of prismatic samples of 20 specimens of 190 (l) x 190 (w) x 390 (h) mm is 10.21 MPa. Both results were pretty close and a masonry compressive strength, f'_m, of 10.20 MPa was used for the finite element analyses. The average density of masonry prismatic from the available data is 18.481 kN/m^3. Based on that masonry prismatic test, the

average Young's Modulus, E_m, of HSG clay-brick is 6567.7 MPa. The shear modulus, G_m, was taken as 0.4 E_m = 2627 MPa.

4.5.4 **Stone Foundation**

To obtain the compressive strength of stone foundation material, 7 samples were made respectively measuring 400 mm (l) x 400 mm (w) x 800 mm (h). Compressive strength test was conducted after the specimens have reached 28 days age. The result of average compressive strength, f'_s, of stone foundation is 7.00 MPa. Based on that prismatic stone test, the average Young's Modulus, E_s, of stone specimen is 8168.4 MPa and the shear modulus, G_s, was taken as 0.4 E_s = 3267 MPa. The average density of stone material is 21.307 kN/m^3.

4.5.5 **Kevlar Aramid Fibre**

High performance aramid fibre containing Kevlar was applied as strengthening material of the URM walls. Kevlar is sold in Indonesia under the market name of Renderoc FR10 and manufactured by PT. Fosroc Indonesia. This material is lighter, stronger and also has high impact resistant compared with other materials such as aluminium, glass or carbon fibre. Tensile strength of Renderoc FR10 is about 5 times that of steel, 3 times that of nylon, 2.5 times that of polyester and also higher compared to glass fibre and carbon fibre (see Figure 4.11.). This material is already used for strengthening of highway bridges, columns and beams of buildings and also masonry wall lighthouses in Japan (according to the Fosroc brochure).

Physical properties of the Kevlar material type AK40 according to manufacture's data as follows:

Breaking strength	= 400 kN/m	
Fibre quantity	= 280 gram/m^2	
Thickness	= 0.193 mm	
Design value of tensile strength	= 2,100 N/mm^2	= 2,100 MPa
Design value of elastic modulus	= 120,000 N/mm^2	= 120 GPa
Design value of maximum strain	= 1.8 %	

Note : Design value means guarantee value

Nitobond-EP10P and Nitobond-EC were used when applying the Kevlar material to the masonry walls. Nitobond-EP10P is effective for priming all masonry wall surfaces where Kevlar sheet will be applied, and has the following specification :

Adhesion Strength	: 8.5 N/mm²
Compressive Strength	: 80 N/mm²
Tensile Strength	: 15 N/mm²
Modulus Elasticity	: 16 kN/ mm²
Shrinkage	: less than 0.1 % linear

Nitobond-EC is an adhesive compound and has a specifically formulated epoxy resin adhesive for bonding between Nitobond-EP10P and Kevlar sheet.

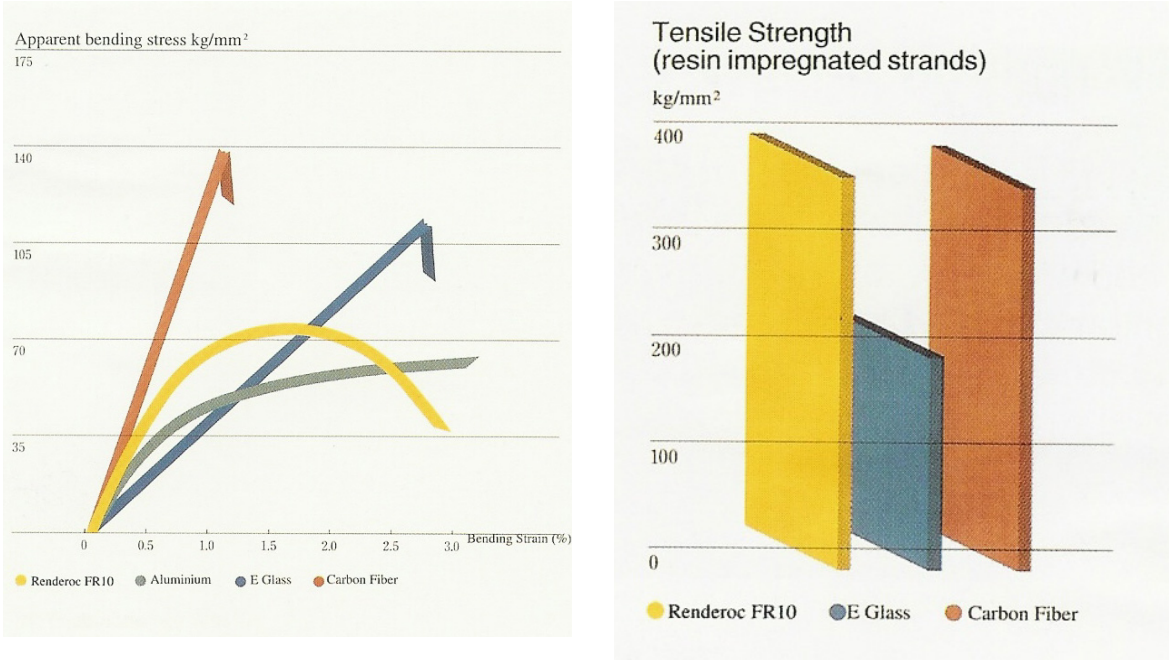

Figure 4.11. Comparison of bending stress and tensile strength between Renderoc FR10 with other materials (reference : Renderoc FR10 brochure)

4.6 DISCUSSION OF THE LOADING SYSTEM

When the structural system specimen to be tested, a set-up on the reaction frame is carried out, complete with loading equipment and internal and external measuring instruments as well as a data-recording instrument. The simulation gravitation load in accordance with the load force as in the existing building were provided by the self weight of top concrete beam plus pretension forces through four pairs of VSL thread lock bars diameter of 22 mm that connected between concrete strong floors to the top of a 400 mm thick concrete beam for Unit-1. The forces in each pair of VSL thread lock bars were measured using load cells. These will give a constant axial forces corresponding to vertical stresses of approximately 0.25 MPa above the unreinforced masonry wall. A pair of axial jacks on top of load cell was utilized for Unit-2 and replaced the previous VSL thread lock bars that used in Unit-1 test. The loading of the axial jack was controlled automatically by hydraulic pump for the purpose of providing vertical stresses plus the additional weight of top concrete beam of approximately 0.25 MPa. This axial jack was connected to a single hydraulic pump unit to ensure constant axial load at all times until the testing is completed. In real field conditions, these simulation normal stresses are provided by the weight of the upper URM wall, other superimposed dead load and live load that applied from the upper floor plan that may be present.

The lateral load had been put on in the form of quasi-static reverse cyclic loading by a 100-tonf actuator, which is an incremental static loading for reverse loading and unloading. This lateral force was measured using load cells. Data obtained from the load cells as well as from the LVDTs are recorded via a data logger. It was necessary to provide lateral stability at the level of lateral load application and ensure the free movement in the plane of URM-wall specimens. Two steel transverse rollers were applied at each side of top concrete beam above the URM-wall and parallel with the lateral load axis. The transverse roller reacted against the steel portal frame, which stands above the strong floor. This steel portal frames also providing the safety precaution if the URM-wall failed in the out-of-plane direction.

The loading history of testing the URM-unit model was carried in a series of cyclic load reversals of increasing the top displacement of the URM-wall. At each peak of loading cycle a crack observation was made, after which the crack was drawn on the location where the crack occurred. Documentation was maintained of the specimen’s condition each time a change in its form occurred by photographs and video.

4.7 INSTRUMENTATION AND OTHER EQUIPMENTS

Various measuring equipment were used for the tests of both URM wall specimen as shown in Figure 4.12. The equipment was calibrated and adjustments to the correction factors were made. The following measuring equipment was used:

4.7.1 Linear Variable Displacement Transducers (LVDTs) and Wire Gauges to measure vertical/horizontal displacements and deformations occurring on the unreinforced masonry wall. LVDTs were placed at those spots to be monitored. The varieties of LVDTs were Tokyo Sokki Kenkyujo Co types: VDP-5, CDP-25, CDP-50, CDP-100 and SDP-200D with maximum measurement 5 mm, 25 mm, 50 mm, 100 and 200 mm respectively.

4.7.2 Two hydraulic pumps, Yamamoto Kosyuki Co. Ltd, type L-3-7 and type A85.8.3 with a pressure capacity of 700 kg/cm^2 were used to give forces to the actuator and a pair of axial jack.

4.7.3 Actuator (push-pull hydraulic jack, type JTC-10, Yamamoto Kosyuki Co. Ltd) with a capacity of 100 tonf for the quasi-static horizontal load in two directions. This was connected to a data logger through a switch box.

4.7.4 A pair of axial jacks on top of load cells was used on top of URM-unit 2 to give a constant vertical load and was controlled by a hydraulic pump.

4.7.5 Two hydraulic hand pumps with a pressure capacity of 700 kg/cm^2 were used to give forces to the two Center Hole Jacks.

4.7.6 Two Center Hole Jacks type JTC-50, Yamamoto Kojyuki Co. Ltd., each with capacity of 50 tonf. These jacks were used to give lateral horizontal loads on both sides of the bottom concrete beam to restraint the URM wall specimen at a steady position under the actuator loads.

4.7.7 Load Measuring Equipments (load cell, Tokyo Sokki Kenkyujo Co, type TCLM-50S and type TCLM-100S) were used to obtain the load bearing capacity during movement. The equipments can measures the load capacity up to 50 tonf and 100 tonf.

4.7.8 Data Logger TDS 302-10 plus external switching box (100 channels) were used to record data (tension and compression) provided by the LVDTs (movement on the masonry wall) as well as load capacity measured by load cells. Data loggers were connected to a computer with monitor to record and display the obtained data.

4.7.9 The simulated gravitation load accompanying the lateral load force as in the existing building was applied using four pairs of VSL thread lock bars (f'_y = 720 MPa) with a diameter of 22 mm (7/8 inch) and length of 3600 mm. Every two thread lock bars was connected with continuously threaded couplers (total length = 100 mm) so that the total length becomes 7200 mm, to be connected between the concrete strong floor to the top of the 400 mm thick concrete beam for Unit-1. A pair of axial jacks on top of load cell was utilized for Unit-2 replaced the VSL thread lock bars that used for Unit-1.

4.7.10 The computer is used to automatically record tension, movement and load data that had been recorded by the data logger. It is also able to show the hysteresis loops of the structure's performance at one of the spots being watched during the testing process. The hysteresis loops represent the correlation between top displacement of the URM wall specimen and lateral load from the actuator.

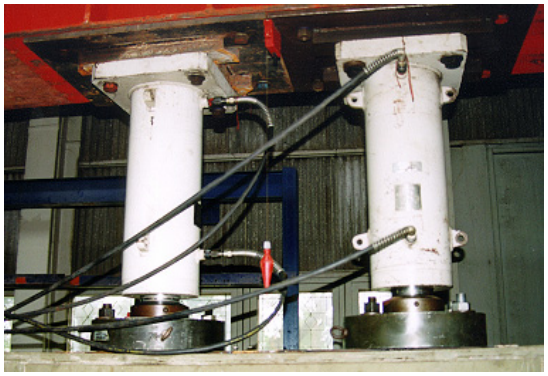

(a) Two axial jack with load cells

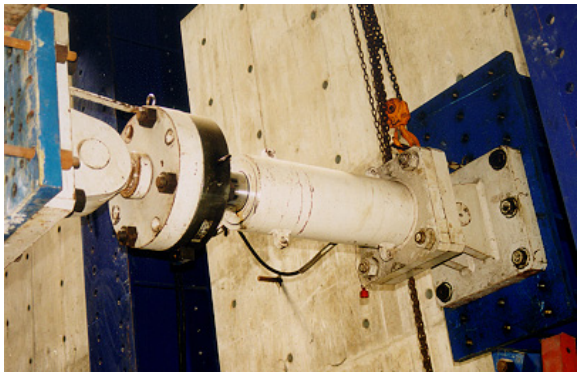

(b) 100 tonf - hydraulic jack and load cell

(c) Hydraulic pump unit type L-3-7

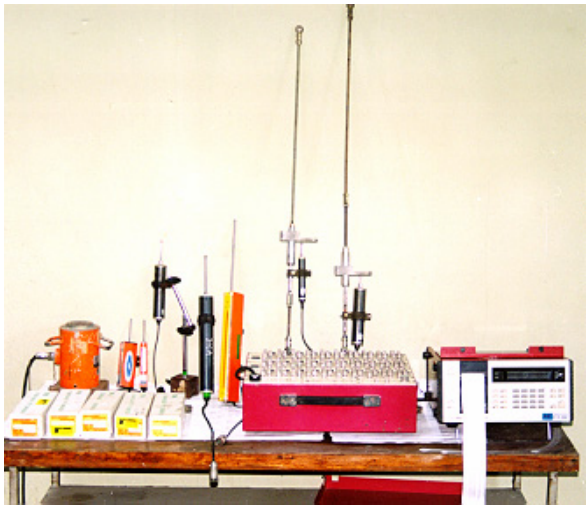

(d) LVDTs, load-cell, data logger, switch box etc.

(e) Diagonal transducers (LVDTs)

Figure 4.12. Various test equipments

The arrangements of LVDTs are shown in Figure 4.14. and Figure 4.16. for Unit-1 and Unit-2 respectively. A total of forty one LVDTs were used to monitor the in-plane displacements, and diagonal deformations of the Unit-1 at several locations through out the masonry walls as follows :

a. Top of concrete beams
b. Left and right on top part of URM wall
c. Left and right on the parallel of upper part door opening
d. Left and right on the stone foundation
e. Left and right on the bottom concrete beam

   The LVDTs at item d. and e. measured any lateral displacement at the bottom part of the URM wall units. To minimize this lateral displacement, two Center Hole Jacks were used to give a constant lateral horizontal load on both sides of bottom concrete beam. Both jack restrained the URM wall specimen at a steady position under the actuator loads. Any value in these LVDTs could affect the real lateral displacement of the URM wall and a correction can be applied to the lateral displacement of LVDTs that were applied to the wall.
f. Four pairs of LVDTs were applied at the bottom of each pier to measure any gap opening that will occur at the heel and the toe of both piers.
g. Ten diagonal LVDTs were mounted on the wall surface to detect local shear and flexural strains. The wall was divided into five rigid bodies: two piers adjacent the door opening and three parts at the spandrel above the door opening. Five sets of diagonal LVDTs were applied at every rigid body to measured global shear distortions of each rigid body.
h. Two vertical LVDTs were installed at the middle upper part of both piers and one vertical LVDT installed at the outer face of left flanged wall. These LVDTs measured any compression strain during the test.

Load cells were provided at the actuator push-pull jack and below each of the double C-channel on top of the upper concrete beam to control the axial force from VSL thread lock bars for Unit-1. The load cells were connected to the Data Logger TDS 302-10 to measure and monitor the loads that were applied.

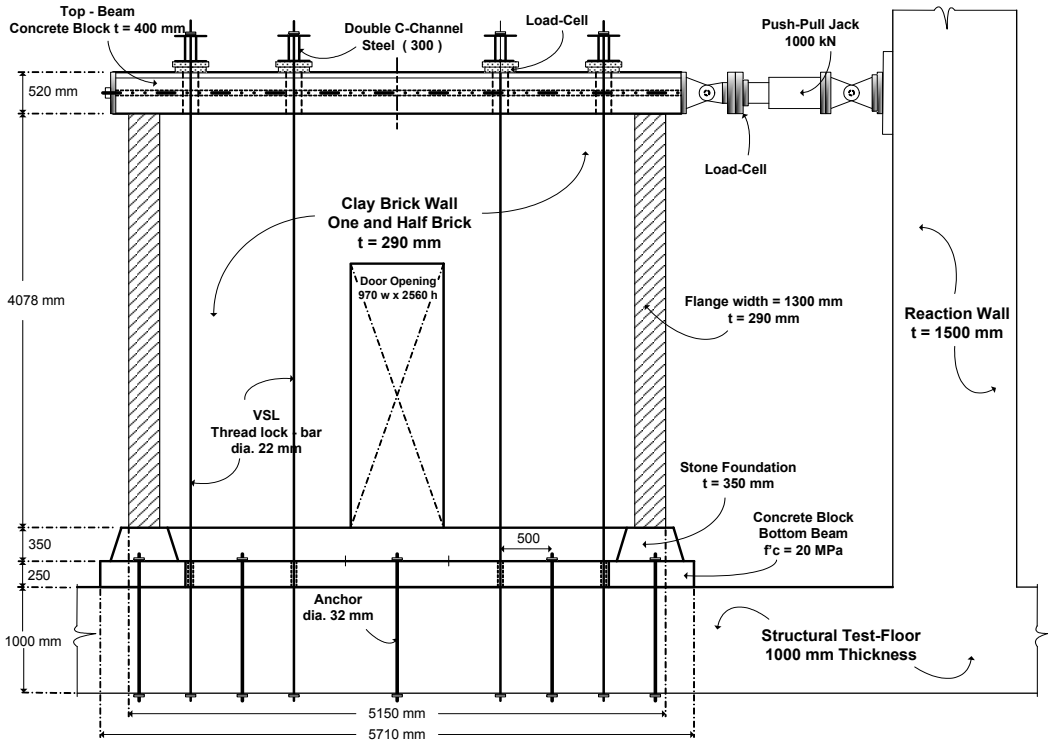

Figure 4.13. Detail section of URM Wall Unit-1

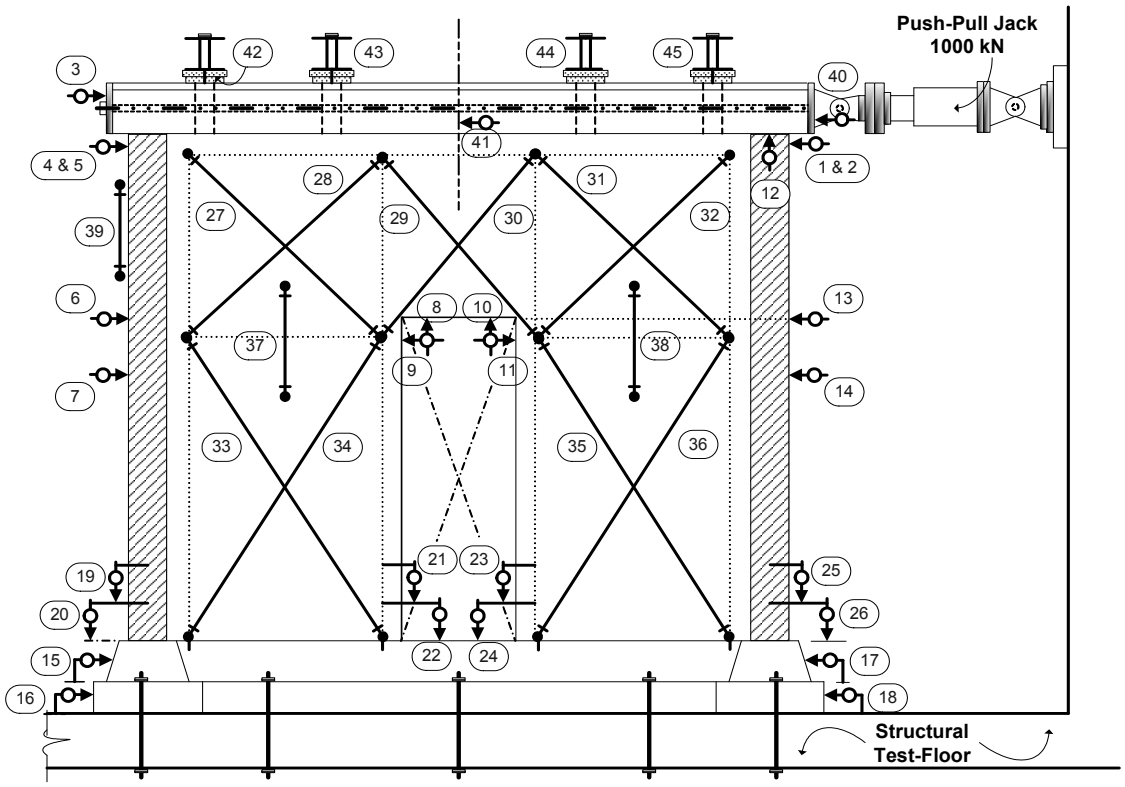

Figure 4.14. : Position of displacement transducers (LVDTs) at URM Wall Unit-1

Fifty one LVDTs were used to monitor the in-plane displacements, and diagonal deformations of the Unit-2 at several locations through out the masonry walls as follows :

a. Top of concrete beams
b. Left and right on top part of URM wall
c. Left and right on the parallel of upper part door opening
d. Left and right on the stone foundation
e. Left and right on the bottom concrete beam

   The LVDTs at item d. and e. measured any lateral displacement at the bottom part of the URM wall units. To minimize this lateral displacement, two Center Hole Jacks were used to give constant lateral horizontal loads on both sides of bottom concrete beam. Both jack restrained the URM wall specimen at a steady position under the actuator loads. Any value in these LVDTs could affect the real lateral displacement of the URM wall and a correction can be applied to the lateral displacement of LVDTs that were applied to the wall.
f. Four pairs of LVDTs were applied at the bottom of each pier to measure any gap opening that will occur at the heel and the toe of both piers.
g. Ten diagonal LVDTs were mounted on the wall surface to detect local shear and flexural strains. The wall was divided into five rigid bodies: two piers adjacent the door opening and three parts at the spandrel above the door opening. Five sets of diagonal LVDTs were attached to the diagonal Kevlar layer at every rigid body to measured global shear distortions of each rigid body.
h. The second diagonal LVDTs were attached to the diagonal Kevlar layer at both piers of Unit-2 since there were two types of strengthened Kevlar layer, one layer and double layers were used.

Load cells were provided at the actuator push-pull jack and at the two axial jacks for Unit-2. The load cells were connected to the Data Logger TDS 302-10 to measure and monitor the loads that were applied.

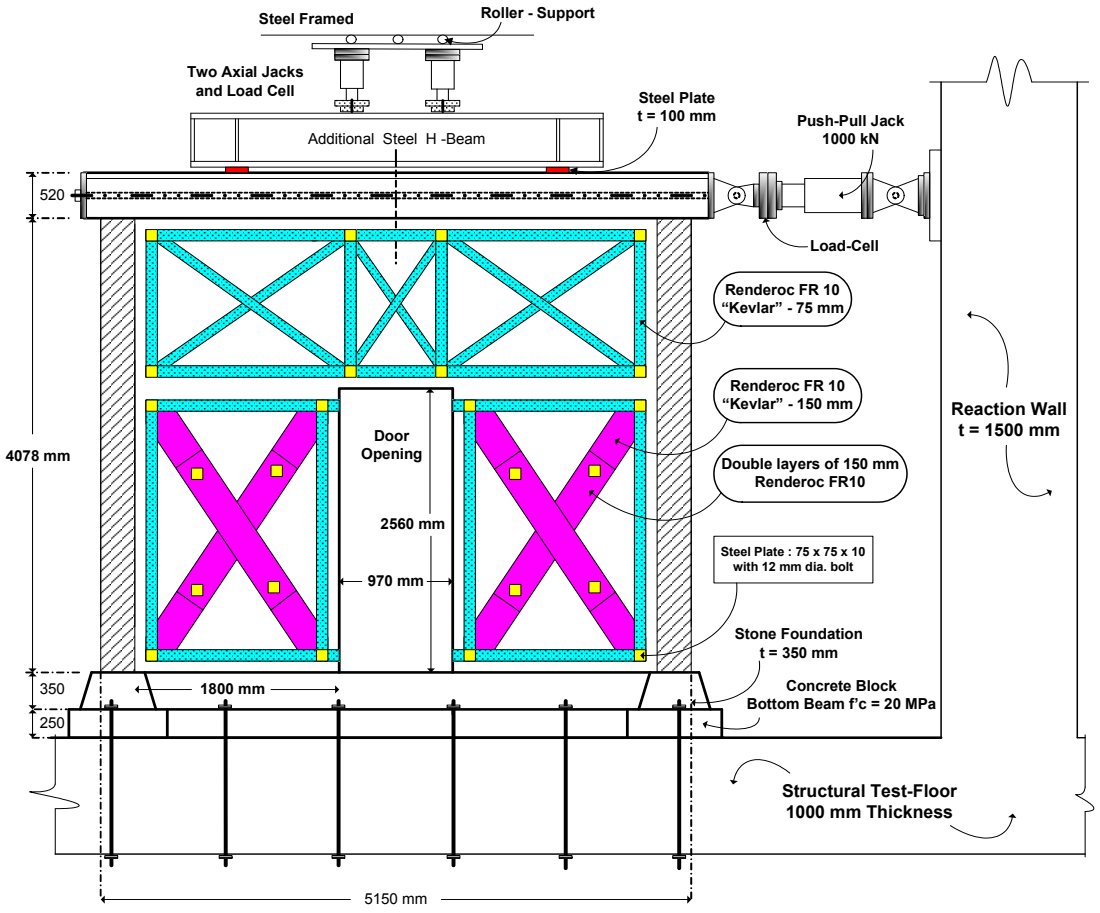

Figure 4.15. Detail section of URM Unit-2

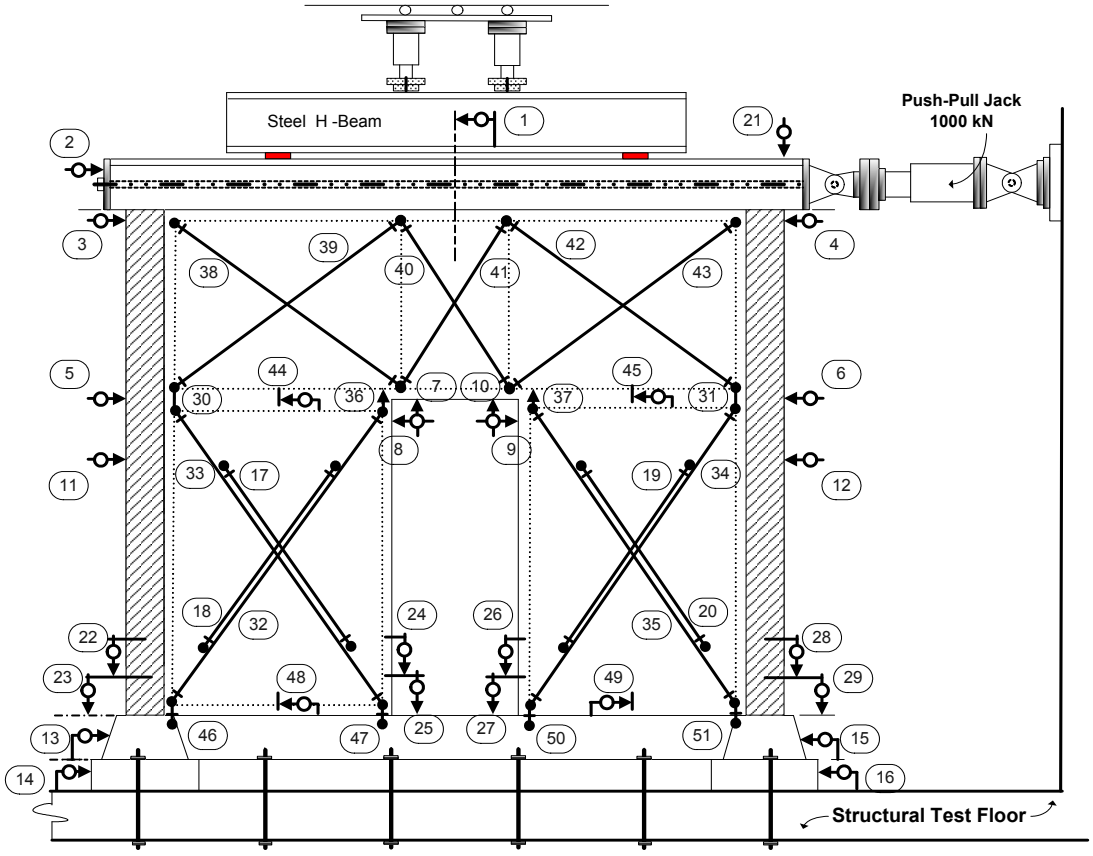

Figure 4.16. Position of displacement transducers (LVDTs) at URM Unit-2

4.8 DESIGN LOAD HISTORY

Two types of design load were applied for both URM wall units. Firstly, vertical load which simulated the gravitation load from the existing building and secondly, the lateral load that represent the lateral earthquake load. The simulated gravitation load through four pairs of VSL thread lock bars plus the weight of the top concrete beam was applied up to the designed value of 0.25 MPa at the top surface of URM wall Unit-1. Each pair of VSL thread lock bars will provide 11.1 tonf pretension forces and it will measure with load cell. This vertical load was kept as constant load during the test. A pair of axial jacks on top of each load cell was utilized for Unit-2 and replaced the four pairs of VSL thread lock bars that used in Unit-1 test. These axial jacks and load cells were applied on top of the top concrete beam through very stiff steel beams that will give a uniform stress at the top surface of URM wall Unit-2. These axial jacks were connected to a single hydraulic pump unit to ensure a constant load at all times until the testing is completed. The reason of using a pair of axial jack at the Unit-2 to get a better constant normal stress compare to the previous system.

The lateral loading history of testing the URM wall unit was carried in a series of cyclic lateral load reversals of increasing the top displacement of the URM-wall. The first cycles of lateral loading history were applied in each direction with force control. The lateral force was increased gradually with increment of approximately 5 tonf for each loading step until reaching the maximum top displacement of 1 mm for positive direction and continues to other reversal direction and following with the displacement control for the next cycles. Two complete cycles of lateral loading were applied at every escalation of the top lateral displacement of the URM wall specimen. A series of top displacement values are providing at Table 4.1. Test Sequence of cyclic load for Unit-1 and Unit-2 were shown at Figures 4.17. and 4.18. respectively. The loading was carried out until the specimen unit failure, which means that the specimen cannot carry the lateral load. From these cycles, it was used to determine the elastic response, the first yield, the maximum capacity, and the collapse position.

Table 4.1. Top Lateral Displacement of URM Wall Specimen for Each Cycle :

Cycle	URM Unit-1		URM Unit-2	
	Top Displ. (mm)	Drift (%)	Top Displ. (mm)	Drift (%)
1 – 2	± 1.0	0.025	± 1.0	0.025
3 – 4	± 1.4	0.034	± 1.4	0.034
5 – 6	± 2.0	0.049	± 2.0	0.049
7 – 8	± 3.0	0.074	± 3.0	0.074
9 – 10	± 4.5	0.110	± 4.5	0.110
11 – 12	± 7.0	0.172	± 7.0	0.172
13 – 14	± 10.0	0.245	± 10.0	0.245
15 – 16	± 15.0	0.368	± 15.0	0.368
17 – 18	± 21.0	0.515	± 21.0	0.515
19 – 20			± 27.0	0.662
21			± 33.0	0.809

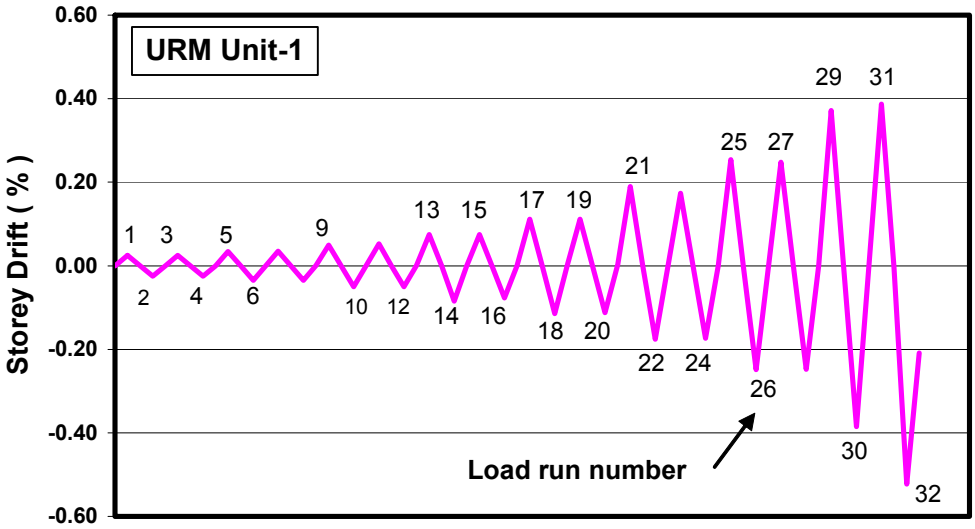

Figure 4.17. Test sequence of cyclic load for Unit-1

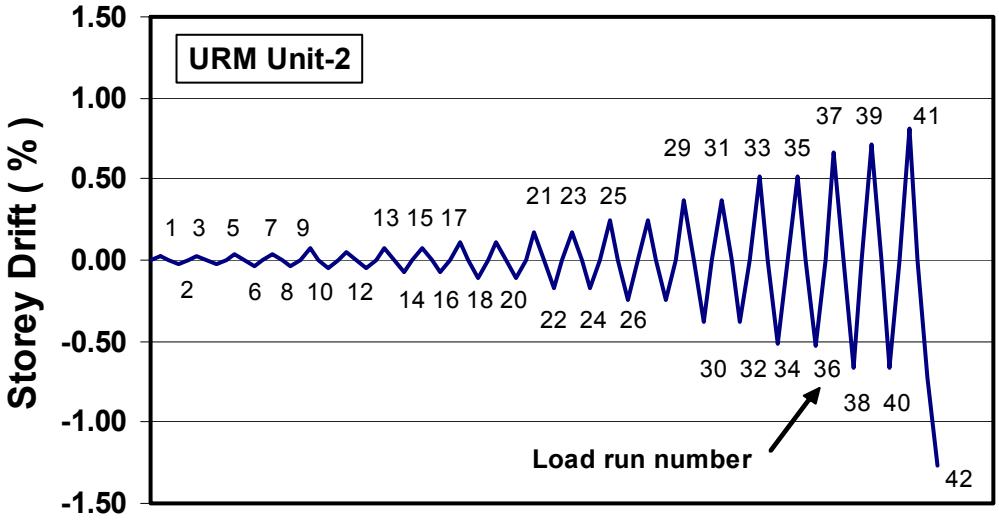

Figure 4.18. Test sequence of cyclic load for Unit-2

4.9 CONCLUSIONS

1. The construction of two URM wall specimens, material properties and testing procedure for in-plane forces were discussed in this chapter. Due to the limitation of laboratory facilities and also the availability of clay-brick dimensions, the specimen unit was constructed to a reduced scale of 75%. This 75% scale test model was confirmed with the dimension of the new clay-brick units currently available in the market i.e. 189 mm x 90 mm x 47 mm compared to the old clay-bricks of 256 mm x 121 mm x 53 mm.

2. The URM wall specimens perforated with door opening in the middle were represented the first storey from a three-storey existing URM building. The URM wall configuration in the existing building like a box-type structural system and the influence of flanged wall section was accommodated in the specimen. Another feature is accommodating the stone foundation in the URM wall specimens.

3. The combination of constant axial forces corresponding to the vertical stresses of approximately 0.25 MPa above the unreinforced masonry wall and a series of cyclic lateral load reversals of increasing the top displacement of the URM-wall were carried out for both units. The first cycles of lateral loading history were force control until

reaching the maximum top displacement of $\pm$ 1 mm and following with the displacement control for the next cycles. Two complete cycles of lateral loading were applied at every escalation of the top lateral displacement of the URM wall specimen.

4. Verification of the in-plane performances of the URM wall Unit-1 result will determine the arrangements of the application of Kevlar fibre material as an improvement or strengthening system for the Unit-2 specimen. Kevlar fibre material offers important advantages in strengthening technique, such as :
   - Higher tension capacity,
   - The small weight of a thin layer of Kevlar fibre (0.193 mm) does not change the axial gravity load significantly, does not effect the long-term settlement to the existing soil layer under the building and also does not effect the inertial forces due to the seismic loading,
   - Easy to install and reduces construction time when compared to other conventional retrofitting methods such as Ferro-cement coating, shotcrete etc.

   From the architectural point of view, very thin Kevlar fibres do not reduce the architectural space. Kevlar material is more expensive when compared to other fabrics such as glass-fibre and carbon-fibre but it should be applied in limited volumes and so essential locations that can increase the in-plane URM wall capacity economically.

CHAPTER 5 :
TEST RESULTS OF URM WALL UNIT-1

5.1 INTRODUCTION

As described earlier in Chapter 4, the Unit-1 model was constructed to represent an URM-wall at 75% scale with wall thickness of 1½-wythe clay bricks arranged in Dutch bond configuration. The wall was perforated with a door opening and 1300 mm length of flanged walls on both edges. The URM-wall was constructed above the stone foundation. Figure 5.1 shows the test arrangement of URM-wall Unit-1 at the laboratory.

The applied loading history was described in detail in Section 4.8 of Chapter 4. The test results are reported in this Chapter, including its crack pattern, lateral force-displacement response, pier behavior, and the estimated energy dissipation.

Figure 5.1. Test arrangement of URM wall Unit-1

5.2 GENERAL BEHAVIOUR OF URM-WALL UNIT-1

5.2.1 Crack Pattern Histories

The test result of URM-wall Unit-1, which represents the existing building, was very satisfactory. An overview of the crack histories is given in Table 5.1. and the final crack pattern after the test was shown at Figure 5.2. This final crack pattern was shown at the back side from LVDTs position as shown in Figure 4.14. The first cracking happened at a + 1 mm lateral displacement at the top of the URM-wall (storey drift = + 0.025%). A small crack started at the header joint between the flat arch brick and the horizontal brick course was observed at the left side of the spandrel above the door opening. The left flanged wall contributes additional stiffness in tension and a small horizontal crack at the bed joint appeared at the one fourth from the pier height. The crack at the left side of the spandrel extended at the next stage of positive lateral displacement in the joint between the flat arch brick above the door opening. In the reverse lateral displacement, a bed joint crack also appeared at one course below the right of the spandrel above the door opening. It was indicated that flexural behaviour still dominated and the spandrel behaved as a coupled beam. As shear cracks developed in the joint between the spandrel and both piers, the pier capacity was decreased.

A bed joint crack appeared at the one fourth from the bottom of the left web pier when the top lateral displacement reached + 3 mm. Bed joint cracks at the left side of spandrel also extended. In the reverse lateral displacement, a bed joint crack appeared at the one fourth from the bottom of the right flanged pier. The crack at the right side of the spandrel was extended.

Bed joint cracks on the one fourth from the bottom part of the left flanged pier wall and the upper part of the left pier were extended when the top lateral displacement was + 4.5 mm. Splitting Cracks also appeared at the bottom part of the web left pier adjacent the door opening and propagated to the stone foundation. Many cracks occurred during the test run at the top lateral displacement of - 4.5 mm. Shears cracking started to occur on the left pier-wall. A new shear crack appeared on the upper part of the right pier-wall extended to the right flanged wall in the bed joint. This new crack connected to the previous bed joint crack near the right part of bottom level of the door opening. Upon the reversed lateral loading, the shear

crack at the left pier-wall fully closed. Shear cracking occurred in the right pier wall at a top lateral displacement of + 7 mm. The shear crack width at both piers became larger with the increase in the value of lateral displacement.

The maximum positive lateral load was recorded at 416 kN (42.41 tonf) and occurred at + 7.695 mm top lateral displacement (0.189 % storey drift). In the next cycles, the capacity of the unreinforced masonry wall was decreased gradually. It was also noted that the diagonal shear cracking in both pier walls only happened in one diagonal direction for each pier. At the top lateral displacement of + 10.0 mm, the shear crack of the right pier widened and crushing of the brick units and mortar at the right pier-wall was observed. The width of the shear crack at the middle of the right pier-wall was up to 6.45 mm wide. The bottom part of the flanged wall at the left pier-wall was displaced to the right side by approximately 6.82 mm. This displacement influenced the lateral load value which was lower than that of the previous cycle. At this step, some LVDTs were removed to avoid any possible damage. In the reverse lateral displacement, a big shear crack was also observed at the middle of the left pier-wall. In the next cycle, when the top lateral displacement was + 10.0 mm, the width of the diagonal shear crack on the right pier-wall reached 10.59 mm. On the other hand, the shear crack on the left pier-wall was not fully closed.

The final stage of the test occurred at the pull lateral load cycle 32. The maximum top lateral displacement was recorded at - 21.26 mm and the lateral load was -333 kN (-33.39 tonf). The shear failure at the web of left pier wall was sudden, cracking sounds were heard and involved a big shear crack. Cracks also happened at the right spandrel above the right pier wall and continued to the flanged wall. At this final stage, the shear crack on the right pier-wall was not closed anymore. The test was discontinued because of the instability of the URM-wall and retrofitting could not be carried out for this specimen.

Some photos related to crack pattern during the test and after the test were shown at Figure 5.3. to Figure 5.6. The recorded responses of all transducers and diagrams of lateral load vs. lateral displacement or strain value are shown in Appendix A.

Table 5.1. Crack histories for URM wall Unit-1

Crack Histories	Load Run Number	Top Displacement (mm)	Drift (%)
The first minor cracking appeared on the left side of the upper part of door opening and also horizontal crack on the outside flanged wall (side A and left pier) between the 15th and 16th course	1	+ 1.0	+ 0.025
The crack at the upper part of door opening extended following the mortar joint between flat arch brick and horizontal brick	5	+ 1.4	+ 0.034
Horizontal crack was appeared on the right side of the upper part of door opening	6	- 1.4	- 0.034
The horizontal crack on the outside flanged wall (side A) between the 15th and 16th course extended along the flanged wall	9	+ 2.0	+ 0.049
The horizontal crack start appeared on the outside flanged wall (side B) between the 13th and 14th course	10	- 2.0	- 0.049
Horizontal cracks appeared on the bottom part of the left pier and the upper part of the left pier (in line with top of flat arch brick level)	13	+ 3.0	+ 0.074
Horizontal cracks also appeared on the bottom part of the right pier between the 13th and 14th course and continue with the previous crack at cycle 10. Crack at the upper part of the right pier was extended (slightly lower than bottom level of door opening)	14	- 3.0	- 0.074
Horizontal cracks on the bottom part of the left pier and the upper part of the left pier were extended. Cracking appeared at the bottom part of the left pier near the door opening and propagated to stone foundation	17	+ 4.5	+ 0.110
Horizontal cracks on the bottom part of the right pier and the upper part of the right pier were extended. Cracking appeared at the bottom part of the right pier near the door opening and propagated to stone foundation. Diagonal crack was appeared on the left pier.	18	- 4.5	- 0.110
Diagonal crack appeared on the right pier and the diagonal crack at the left pier-wall was fully closed	21	+ 7.0	+ 0.172
The left pier-wall a slightly sliding from the stone foundation	24	- 7.0	- 0.172
Widening the diagonal crack and crushing to the brick units or mortar on the right pier-wall was observed. The width of the diagonal crack on the right pier-wall was 6.45 mm. The bottom part of flanged wall at the left pier-wall was displaced around 6.82 mm. At this step, some LVDTs were removed prior to avoid possible damage	25	+ 10.0	+0.245
The width of the diagonal crack on the right pier-wall reached 10.59 mm. The diagonal crack on the left pier-wall was not closed anymore.	27	+ 10.0	+0.245
The failure were sudden, involving a large diagonal crack	32	- 21.17	-0.519

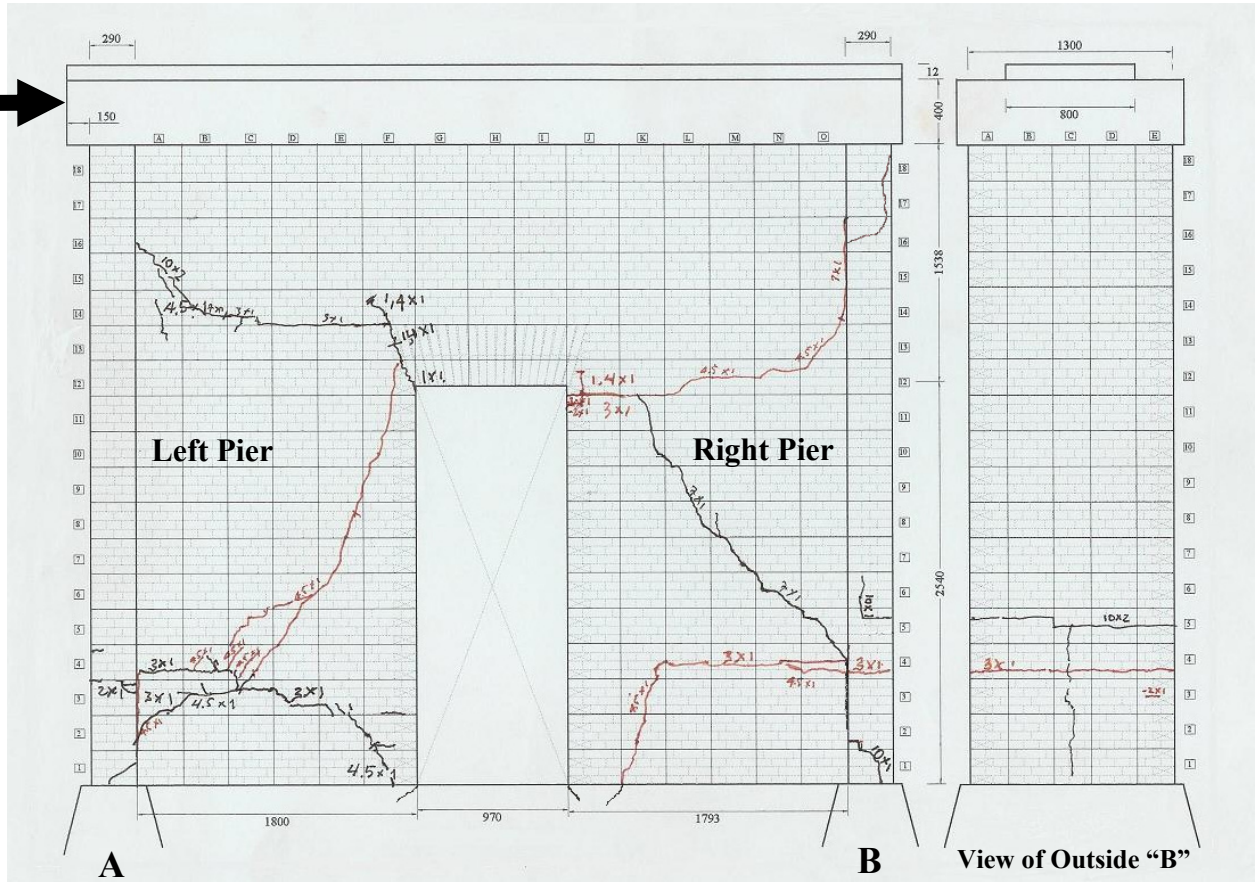

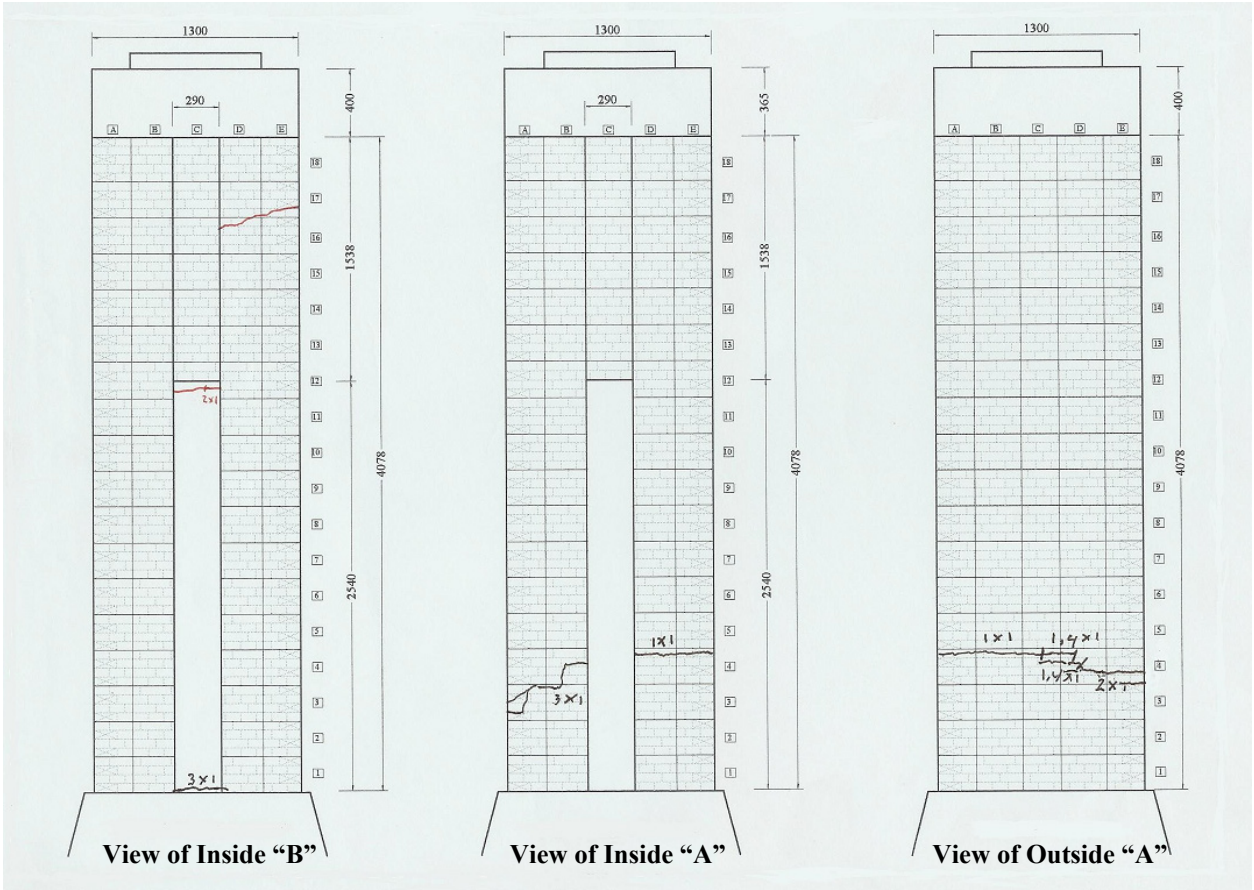

Figure 5.2. Final crack pattern for URM wall Unit-1

(a) Lateral displacement = + 1.0 mm

(b) Lateral displacement = + 1.4 mm

(c) Lateral displacement = + 10 mm

(d) Lateral displacement = + 15 mm

(e) At the end of the test

Figure 5.3. Crack pattern above door opening at flat arch for URM wall Unit-1

Figure 5.4. Top lateral displacement + 3 mm

(left pier crack penetrate at both sides of URM wall Unit-1)

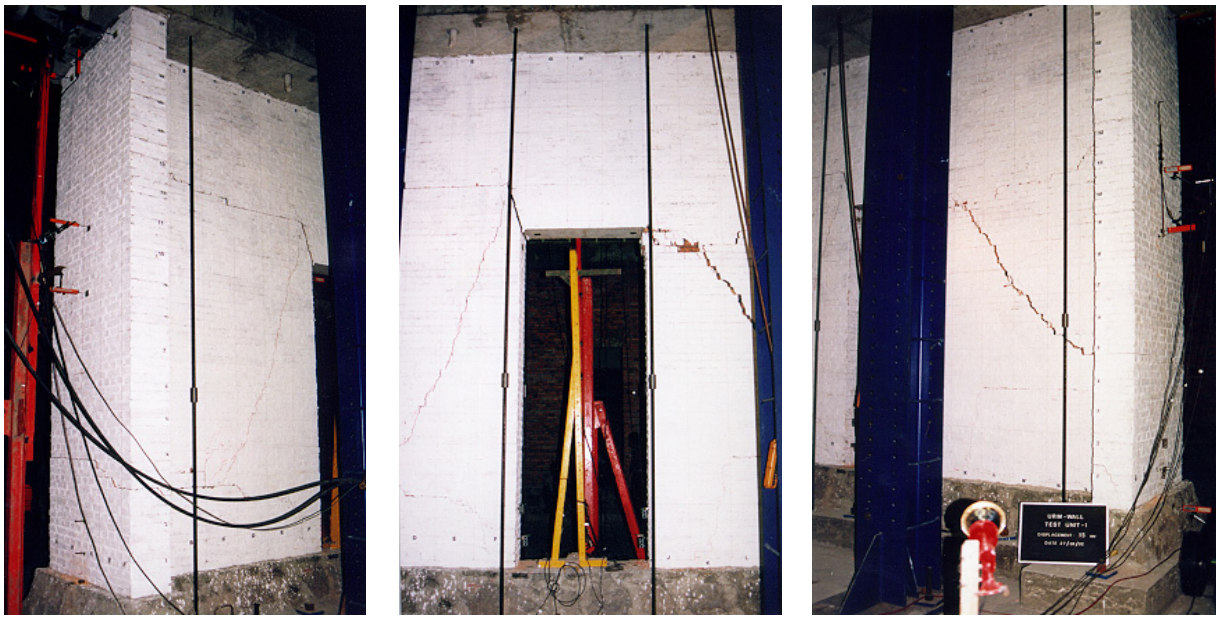

Figure 5.5. Top lateral displacement + 15 mm
(crack through top left pier to the right bottom pier)

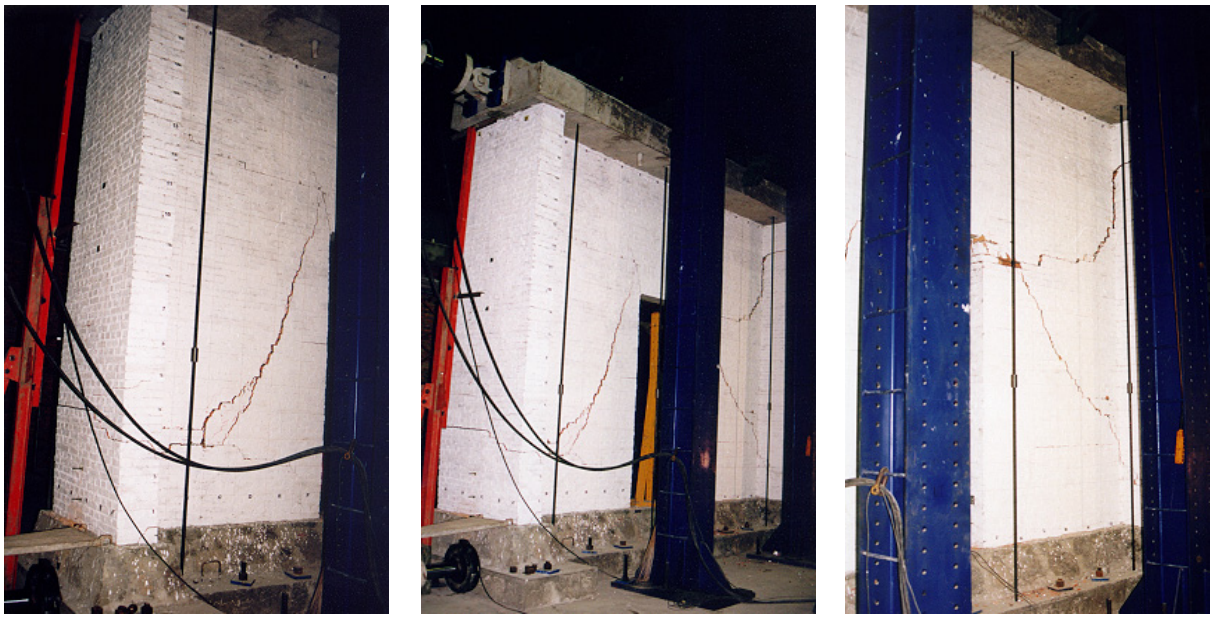

Figure 5.6. Top lateral displacement – 21.26 mm (end of the test)

5.2.2 Lateral Force-Displacement Response

The overall response of the URM-wall Unit-1 is summarized in the hysteresis loop for lateral force versus top displacement or storey drift value is shown in Figure 5.7. It is of interest to note that the wall responded linearly with a high stiffness for the first stage at lower storey drift. After reaching a new maximum deflection, the URM-wall responded in the next cycle for the same storey drift value with a reduced stiffness. Subsequent cycles indicated that some strength loss might have taken place. The positive maximum lateral force was recorded 416 kN (42.41 tonf) at cycle number 11 with +7.695 mm top lateral displacement (0.189 % storey drift). In the reversed direction of loading, the maximum lateral force was recorded 369 kN (37.57 tonf) at cycle number 11 with -7.135 mm top lateral displacement (0.175 % storey drift).

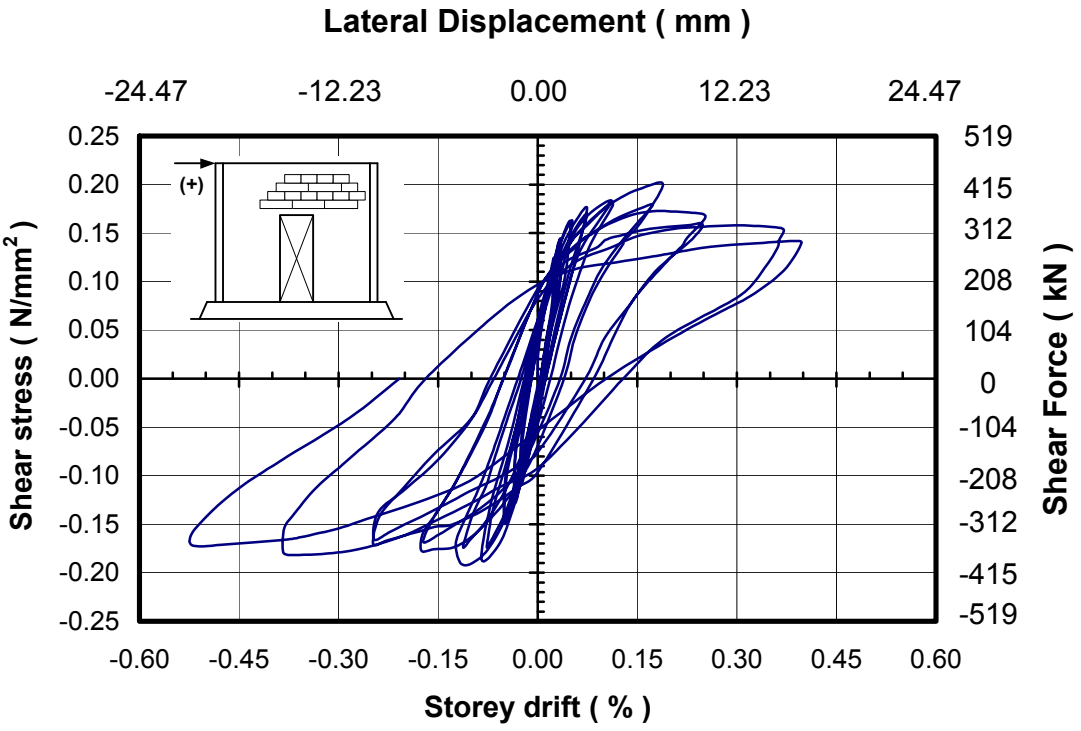

Figure 5.7. Overall Response of URM-wall Unit-1 hysteresis loop

Propagation of cracks during the cyclic loading causes the strength and stiffness degradation of the URM-wall unit-1. It was also observed when the cycle repeated for the same storey drift value. The cyclic secant stiffness is defined as the slope of the line joining the origin and the peak value of the respective cycle. The secant stiffness degradation of every cycle can be plotted as shown in Fig. 5.8. The ordinate represents the ratio between the stiffness at

particular cycle with respect to the first cycle. The secant stiffness reduction between the initial storey drift values ranging from 13% to 40% respectively.

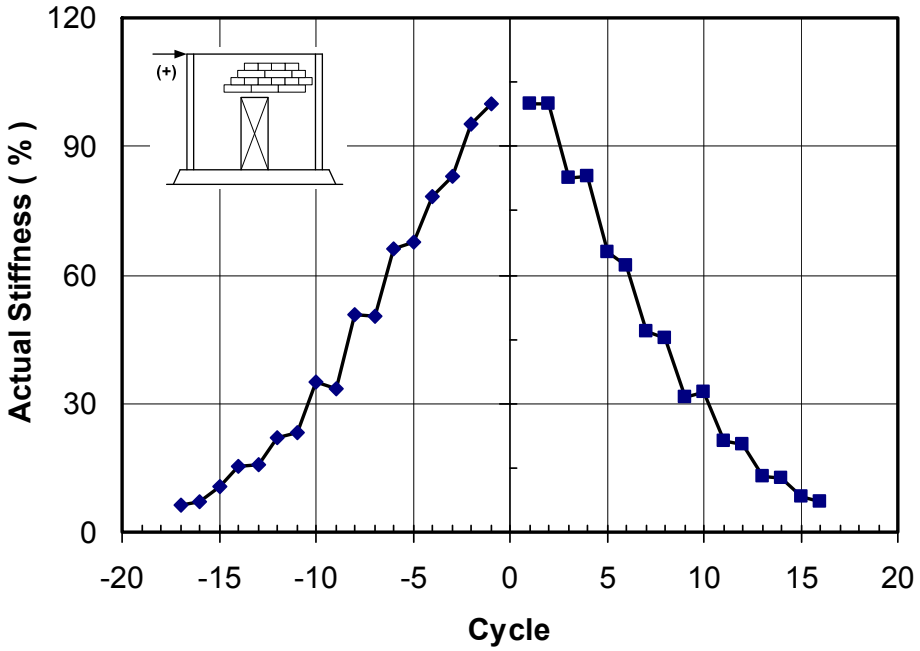

Figure 5.8. Secant stiffness degradation of URM wall Unit-1

A backbone curve from quasi-static reversed cyclic loading was shown at the following Figure 5.9.

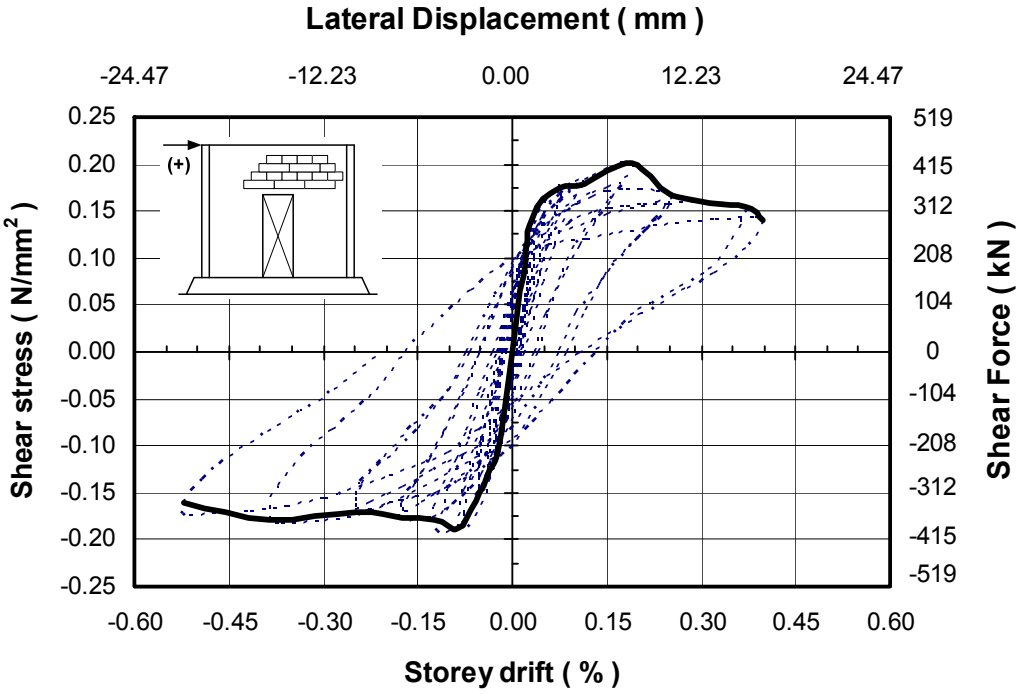

Figure 5.9. Hysteresis Envelope of URM wall Unit-1

After the completion of the test unit-1 model, the strengthening of the wall could not be carried out considering that the shear cracks were significantly larger and the URM wall vertical orientation was offset and too dangerous. It may be concluded from this test that a building of unreinforced masonry wall, when affected by a strong earthquake where its capacity strength has been exceeded, will experience significant damage and it can be taken for certain that it would almost be impossible to do the retrofitting follow the earthquake.

5.2.3 **Pier Behaviour**

Both piers adjacent the door opening was connected with a masonry spandrel and at initial stages coupling effects were provided. The bending tensile stresses caused a flexural crack at the lower mortar layer and also at the corner of the door opening. This crack gradually became longer and wider with the increases of lateral load. As the flexural crack stopped propagating, it was continued with a shear crack at both piers. After the diagonal crack formed, the stiffness of the masonry wall was reduced and the lateral displacement at top of masonry wall was increased subsequently. When the lateral load was reversed, the initial shear diagonal crack at the left pier relatively closed and another diagonal was appeared at the right pier. In-plane performance shows that the shear failure mechanism is much more dominant than the rocking failure mechanism and both piers relatively weaker than the spandrel as shown in Figure 5.10.

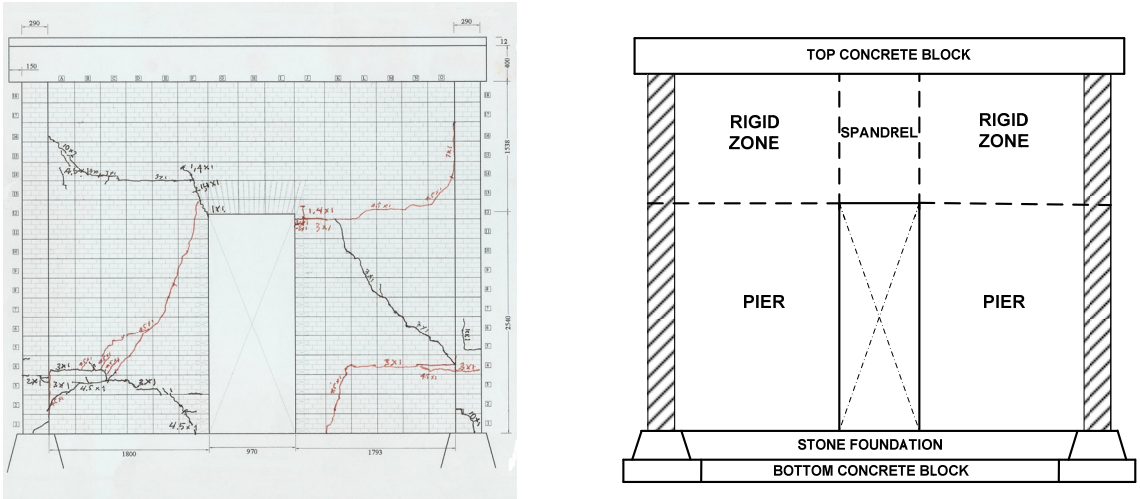

Figure 5.10. Crack pattern at both piers and rigid zones represent the performance of weak pier and strong spandrel

The ultimate strength has been governed by shear cracking and failure at both piers. The hysteresis loops for lateral force versus diagonal displacement transducer (LVDTs No. 33, 34, 35 and 36) were shown in Figure 5.11. Those LVDTs measured the sliding of the bed joints, separation of head joints due to shear, and as well as the splitting of the clay brick unit. The result of LVDT 33 and LVDT 36 have similar trends to the tensile resistance for each pier. The value of shear forces resisted by each pier was not equal. When the lateral force resulted in increasing axial compression, a pier deformed with a greater amount of inelasticity than when axial tension due to overturning was applied (see LVDTs No. 33 and 34, LVDTs 35 and 36). Lateral resistance of the apparently symmetrical structure was asymmetrical because of the variation in axial force applied to each pier.

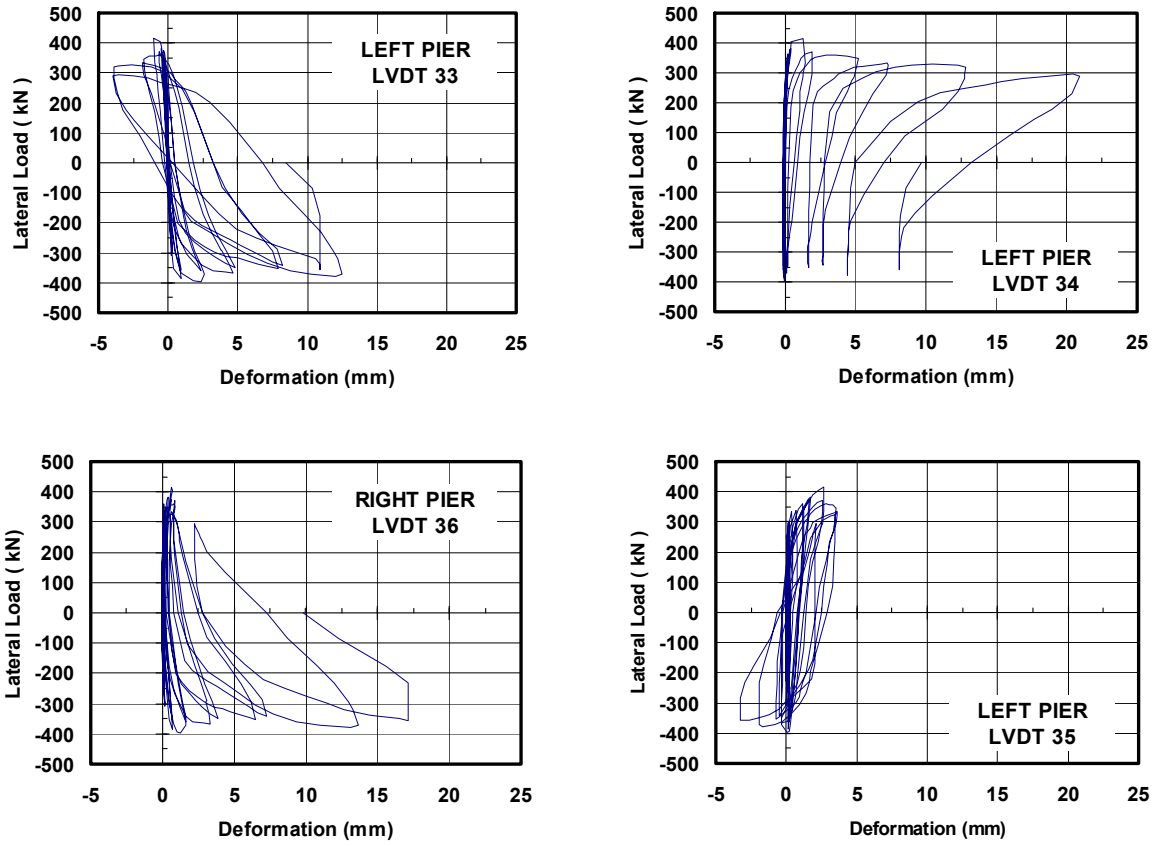

Figure 5.11. Diagonal deformation of left and right pier at URM wall Unit-1

It was noted at Figure 5.12. the lateral displacement that measured at the top left flanged wall and the top door opening level for top lateral displacement values from $\pm$ 4.5 mm to $\pm$ 15 mm. The lateral displacement that was measured at the top right flanged wall and the top door opening level for top lateral displacement values from $\pm$ 4.5 mm to $\pm$ 15 mm are shown in Figure 5.13.

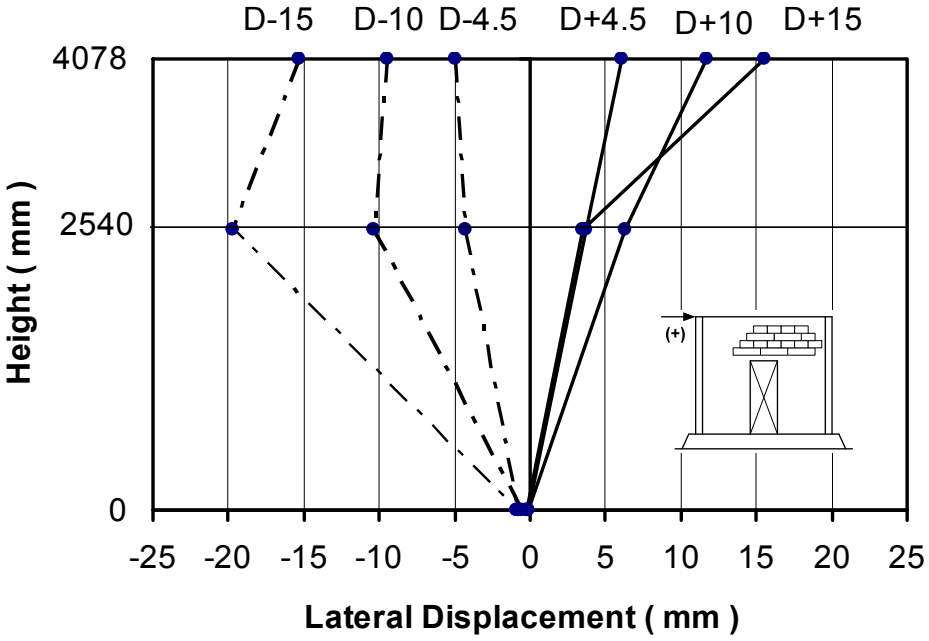

Figure 5.12. Measured Lateral Displacement at Left Flanged Wall for top displacement values from ± 4.5 mm to ± 15 mm

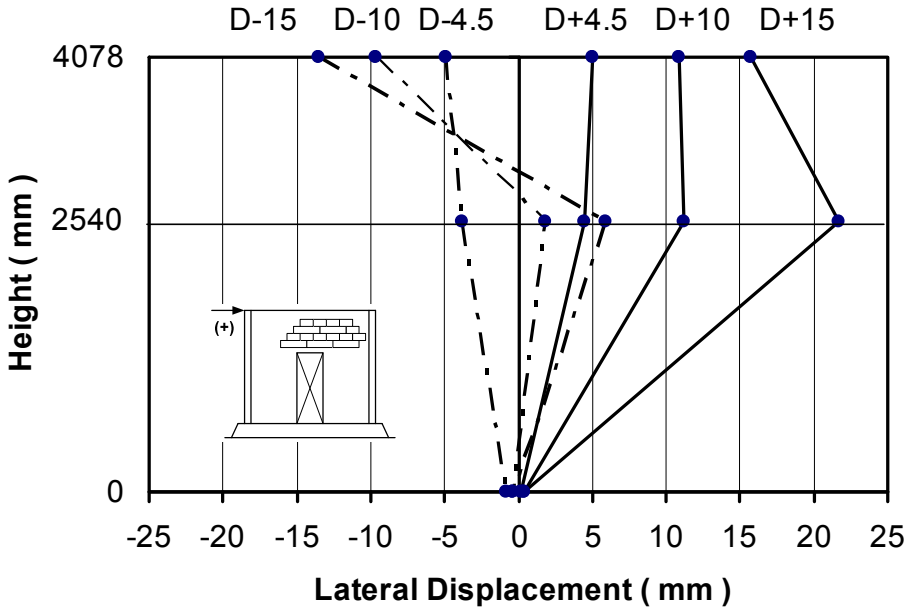

Figure 5.13. Measured Lateral Displacement at Right Flanged Wall for top displacement values from ± 4.5 mm to ± 15 mm

5.2.4 **Energy Dissipation**

The work done in each cycle is stored as strain energy and will be released in the unloading process. Energy dissipated per cycle, E_D, was measured from the area in one cycle (as shown in Figure 5.14.a) and the absorbed strain energy, E_A, (as shown in Figure 5.14.b) in half cycle as follow :

$$E_A = \frac{K.\Delta_m^2}{2} \quad \text{.............................. (5.1.)}$$

Where K is the secant stiffness of the structural system and Δ_m is the total displacement of cycle. The damping can be derived using (Clough, 1993) :

$$\xi = \frac{E_D}{4.\pi.E_A} \quad \text{.......................... (5.2.)}$$

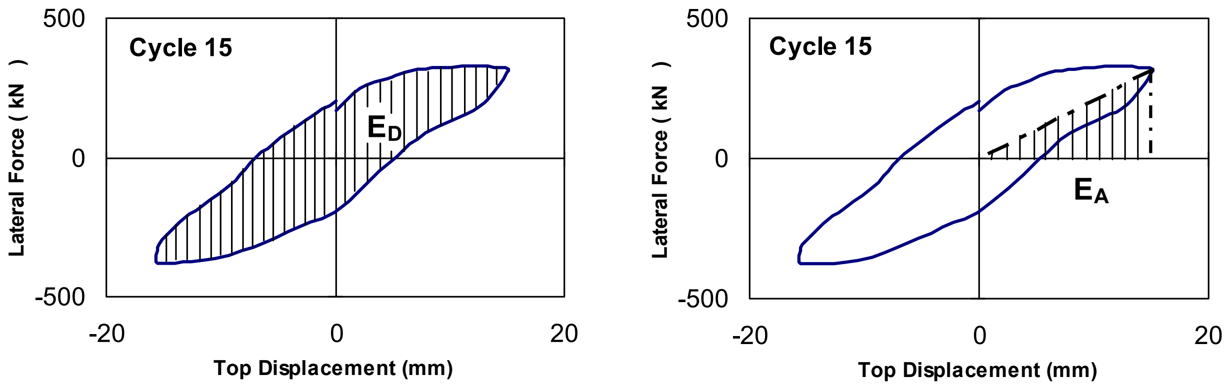

(a) Dissipated energy

(b) Absorbed strain energy in linear equivalent system

Figure 5.14. Evaluation of dissipated energy

The ratio between E_A/E_D and the equivalent damping were evaluated using Eq. 5.1. and 5.2., and are plotted in Figure 5.15. and Figure 5.16 respectively. The area of E_A and E_D were calculated using AutoCAD-2007 program. It was noted that the value of ratio E_A/E_D increased at every new escalation of the top lateral displacement of the URM wall up to cycle 10 (drift value 0.110%) and decreased for the next cycle. It was indicated that the URM wall can dissipate much energy before reaching the ultimate value. The damping ratio was measured from 8.73% to 25.77%.

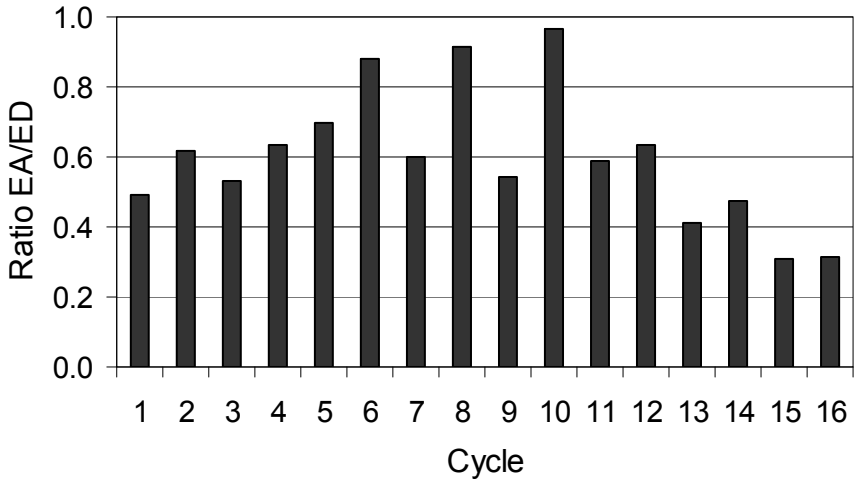

Figure 5.15. Measured of the ratio EA/ED values of URM Unit-1

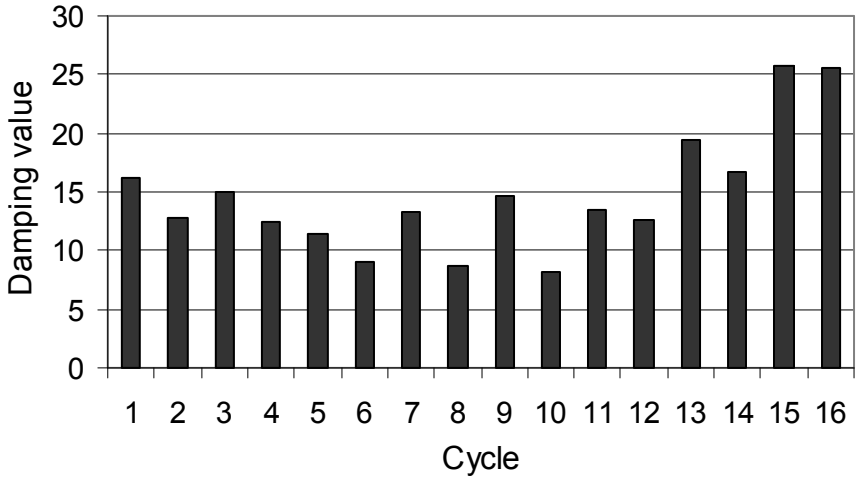

Figure 5.16. Measured of the damping values of URM Unit-1

5.3 CONCLUSIONS

1. The overall in-plane performance of URM wall the Unit 1 that represents the existing masonry building with a perforated door opening was very good. At the initial stage, flexural cracking was observed and overturning effects were resisted by axial vertical forces in each pier. The large relative depth of the spandrel beam above the door opening certainly acted as a coupling beam for both piers. The crack pattern at the URM wall unit-1 was representing weak piers and strong spandrel which is a common performance observed in older existing URM buildings after an earthquake has occurred. The masonry piers failed in a shearing mode as was evidenced by the shear cracks in both piers.

2. The elastic behaviour from the hysteresis loops was confirmed at the initial stage. It is also consider that URM wall has a post-elastic behaviour in terms of "ductility" value of around 8 to 10. The positive maximum lateral force was recorded at 416 kN with + 7.695 mm top lateral displacement (0.189 % storey drift). In the reverse direction, the maximum lateral force was recorded -369 kN with -7.135 mm top lateral displacement (0.175 % storey drift). The final stage of the test occurred at the pull lateral load of - 333 kN with a maximum lateral displacement of - 21.26 mm or equivalent to 0.52% storey drift value.

3. As predicted, to be masonry material is variable and non homogeneous, which caused the hysteresis loop non symmetrical between push and pull lateral loads. Some simplification is necessary for numerical analysis.

4. The effectiveness of the flanged wall was to increase the stiffness and the strength of each pier especially when the flanged wall is in the tensile condition. It was noted by the bed joint crack started at both flanged pier walls from between the 15^{th} - 16^{th} course and between the 13^{th} - 14^{th} course for the left pier flanged wall and the right pier flanged wall respectively. These courses are around one fourth of the pier height.

5. It may be concluded from this test result that if an existing URM building located in a seismic prone area is hit by a strong ground excitation it might experience a significant damage which would almost be impossible to be repaired. Therefore its seismic resistance needs to be assessed as to whether it would still behave elastically during a certain level of ground excitation. Improvement or strengthening is mandatory, if the seismic demand exceeds its elastic capacity.

CHAPTER 6 :
TEST RESULTS OF URM WALL UNIT-2

6.1 INTRODUCTION

Unreinforced masonry walls have limited capacity to resist shear forces, as described in Chapter 5 regarding the test results of URM wall Unit-1. A classical retrofit system on existing URM buildings was to overlay both faces of the URM-wall with reinforced concrete or shortcrete. Although this alternative approach offers a low cost solution, these strengthening systems will impact on the architectural appearance which is usually not favored by the architects. Besides these systems may also increase the total weight of the structure and in turn it may raise the inertia lateral force during a seismic attack. Along with the development of fiber composite materials, the use these much lighter strengthening supplies become more and more popular.

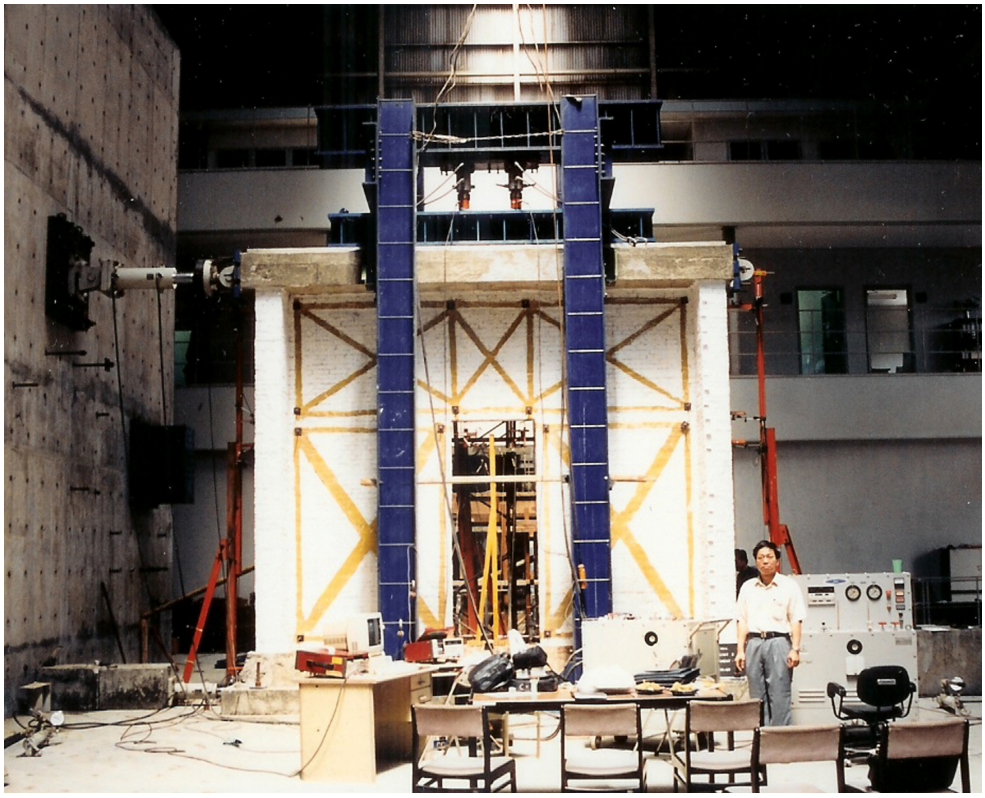

Figure 6.1. Test arrangement of URM Wall Unit-2

In order to obtain a better performance of URM walls, Kevlar fiber composite layers were used in this study for strengthening the URM wall Unit-2. The perforated URM wall Unit-2 with door opening was divided into three rigid bodies, i.e. the upper part of the door opening and two pier-walls adjacent to the door opening. The Kevlar layers were applied diagonally on both sides of the URM wall Unit-2 as shown in Figure 6.1. The same pattern of loading was then applied to this URM wall Unit-2.

The test results of this URM wall Unit-2 model are reported in this chapter including its crack pattern, lateral force-displacement response, pier behavior, and the estimated energy dissipation.

6.2 GENERAL BEHAVIOUR OF URM-WALL UNIT- 2

6.2.1 Crack Pattern Histories

URM wall Unit-2 responded very well during the testing and the influence of the strengthening could be seen fairly clearly by the increased capacity of the unreinforced masonry wall in resisting the lateral shear load. It was clear the performance of URM-Unit 2 during the test was dominated by a rocking mode. A brief description of the test results for URM wall Unit-2 is presented in Table 6.1. It presents a summary of crack histories during the selected test runs, top lateral displacements of the URM wall and drift values. The final crack pattern after the test was shown at Figure 6.2. This final crack pattern is shown on the reversed side from the LVDTs position is shown in Figure 4.16. The results are also discussed in the following paragraph.

At the early loading stages, the flexural cracks were initiated at the bed joints in between the first and the second courses at the lower part of both piers, and also above the pier head below the spandrel beam. Then the cracks spread horizontally along the bed joint and allowed for a rocking motion of both piers.

Flexural cracking started at the top lateral displacement of - 1.40 mm, i.e. cracking start at the bed joint between the first and the second course at the lower part of the right pier and extended to the right flanged wall. Horizontal bed joint cracks were also observed between the first and the second course at the lower part of the left pier and extended to the left flanged

wall at the next cycle where the lateral top displacement was + 2 mm. At the next top lateral movement, bed joint cracking on the lower part of the left pier penetrated to the stone-foundation. These cracks lead to a rocking mechanism, where the bed joint cracks developed along the interface of the bottom and top of both piers. The URM wall Unit-2 was divided into three rigid bodies, i.e. the upper part of the door opening and two piers adjacent to the door opening. These rocking mechanisms occurred continuously following the increasing top lateral displacement.

Cracking of the 'Kevlar' layer started from the weakened area surrounding the bolt anchor placement where the anchor bolts are drilled into the Kevlar sheets and also penetrate the thickness of the URM wall at every corner. It was initially observed at the bottom of the spandrel beam side on top of the right pier. Rocking occurred and the increase of lateral displacement resisted additional vertical load, in the first instance at 44.4 tonf, to reach a maximum of 53.94 tonf. The automatic pump, which regulates a pair of axial jack forces apparently, did not function well. The variety of axial forces during the experiment was shown in Figure B.16. page 188.

The maximum positive lateral force was recorded at 536 kN (54.64 tonf) at load run number 31 with the top lateral displacement was + 33.19 mm (0.816 % storey drift). It was much higher when compared to URM wall Unit-1 which was only 416 kN. The breaking of the left upper part of the 'Kevlar' layer at the left pier-wall from its anchor-bolt caused further cracking (see Figure 6.4.d). The Kevlar layer also delaminated from the surface of the URM wall. The maximum lateral load resistance of URM wall Unit-2 was -699 kN (= - 71.22 tonf) with a maximum lateral displacement - 29.49 mm and then the lateral load decreased to - 168.5 kN but the top lateral displacement increased to - 51.69 mm due to large tensile cracking on the diagonal part of the left pier-wall. The failure was sudden, and the diagonal tension crack in the middle of the left pier was measured at 36 mm width. It was end of the test which was discontinued because of the potential instability of the URM-wall.

Some photos related to crack pattern during the test and after the test were shown at Figure 6.3. to Figure 6.5. The recorded responses of all transducers and diagrams of lateral load vs. lateral displacement or strain value are shown in Appendix B.

Table 6.1. Crack histories for URM wall Unit-2

Crack Histories	Load Run Number	Top Displacement (mm)	Drift (%)
The first crack appeared at the bed joint between the first and the second course at the lower part of the right pier (exactly below the Kevlar layer) and extended to the right flanged wall	6 (55)	- 1.4	- 0.034
Bed joint crack appeared at the upper part of the left pier adjacent to the upper part of the door opening and also at the bed joint between the 1st and the 2nd course at the lower part of the left pier continue to the left flanged wall. The pier-wall displayed a rocking behaviour	9 (83)	+ 2.0	+ 0.049
The crack at the lower part of the right pier was extended to the left side	10 (94)	- 2.0	- 0.049
The crack at the lower part of the right pier was extended to the stone foundation. Other bed joint cracks were appeared at the upper part of the right pier and the bottom part of the left pier.	14 (137)	- 3.0	- 0.074
Crack was observed on the stone foundation below the left side of the right pier	17 (174)	+ 4.5	+ 0.110
The previous bed joint crack at the upper part of the right pier was extended to right side. Crack width $\pm$ 2.8 mm	18 (186)	- 4.5	+ 0.110
Bed joint cracks parallel to the horizontal Kevlar layer above the left pier were indicated. Cracks width was measured around 4.8 mm	21 (233)	+ 7.0	+ 0.174
Horizontal crack in line below the Kevlar layer above the right pier-wall	22 (251)	- 7.0	+ 0.174
Horizontal cracks on the bottom part and the upper part of the left pier were extended.	25 (310)	+ 10.0	+ 0.247
The left pier-wall a rocking slightly and crack extended on the bottom left pier-wall	29 (415)	+ 15.0	+ 0.370
Bed joint crack above the right pier across the whole width and extended to the flanged wall. Bolt joint for Kevlar layer at the upper part of right pier was broken off	30 (439)	- 15.0	+ 0.370
Bed joint crack above the left pier across the whole width and extended to the flanged wall. The wall specimen was divided into three rigid bodies, i.e. Left pier, right pier and spandrel above both piers and door opening	37 (679)	+ 27.0	+ 0.664
The diagonal tension crack on the right pier appeared	39 (770)	+ 27.0	+ 0.664
Diagonal Kevlar at the right pier was delaminated and the clay brick unit was splitting surrounding the epoxy layer.	41 (850)	+ 33.0	+ 0.814
Kevlar joint at the right top of the left pier was torn along with the fiber direction and delaminated. The diagonal tension crack occurred in the left pier with 36 mm crack width. The test was stopped	42	- 33.0	- 0.814

Note : (..) = Number at Figure 6.2. final crack pattern for URM Wall Unit-2

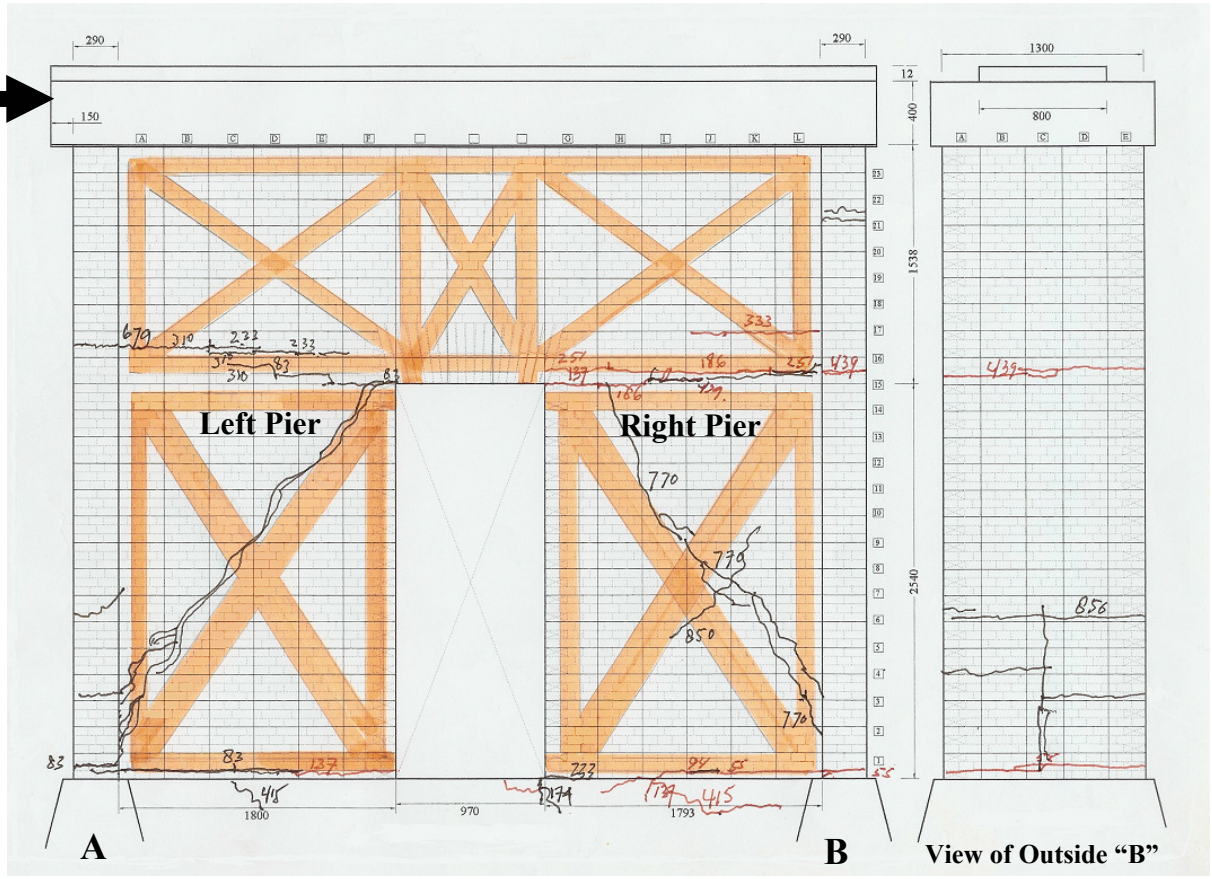

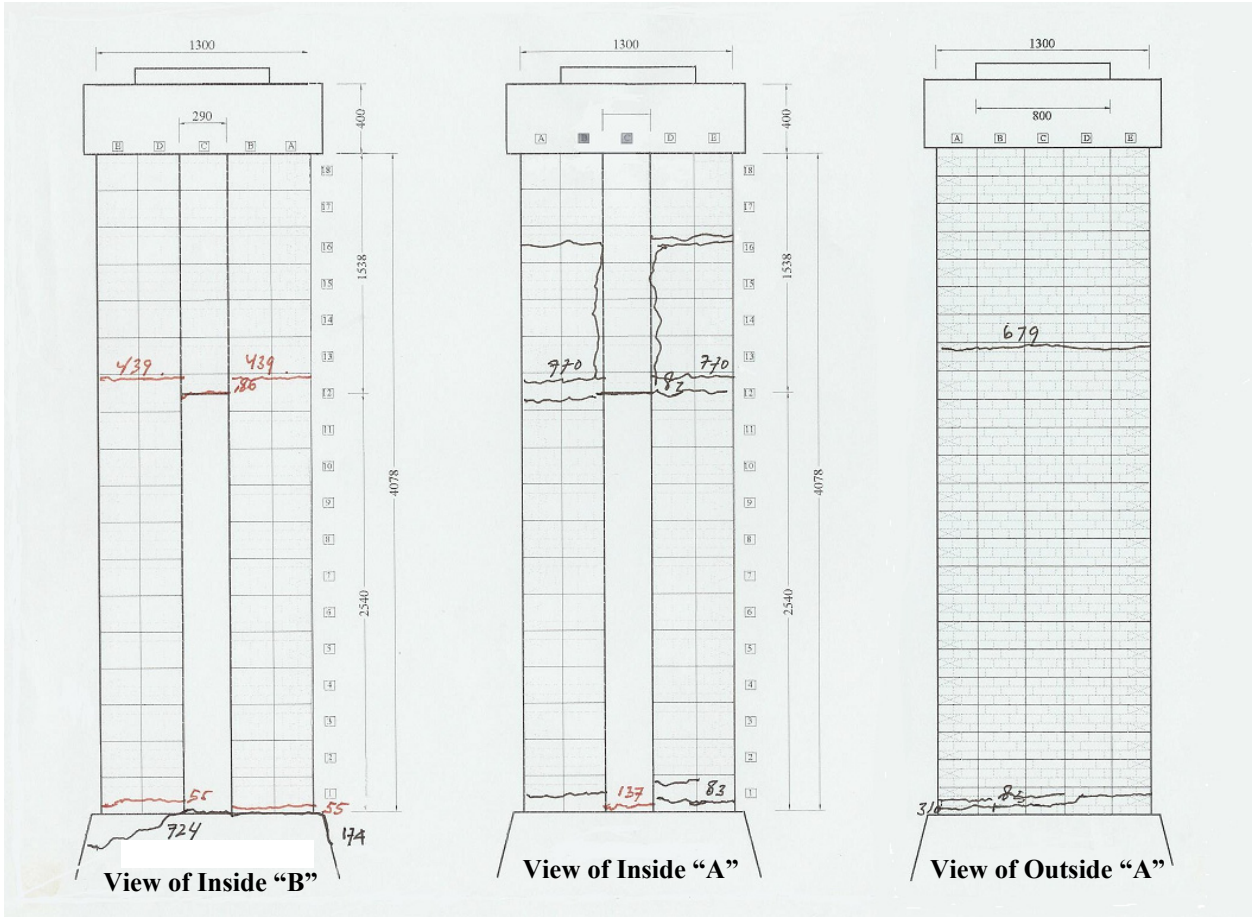

Figure 6.2. Final crack pattern for URM Wall Unit-2

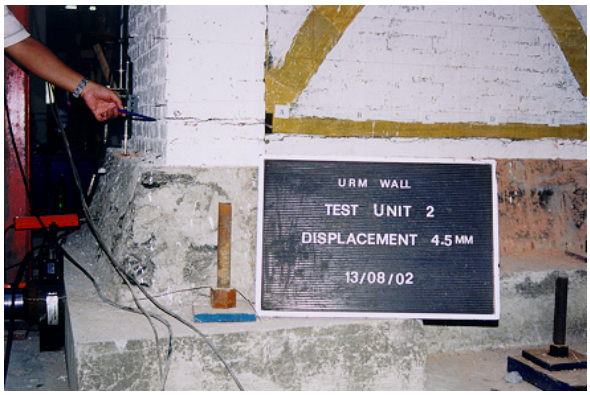

(a) Lateral displacement + 4.5 mm

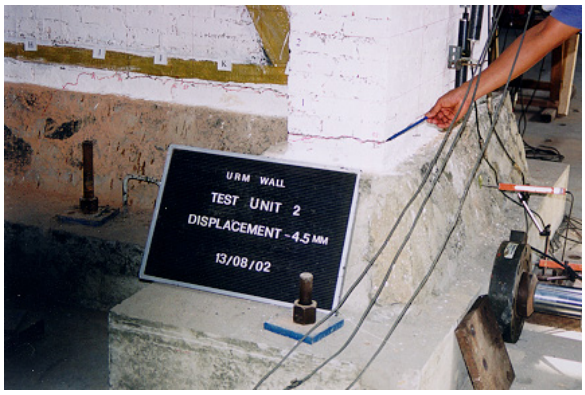

(b) Lateral displacement - 4.5 mm

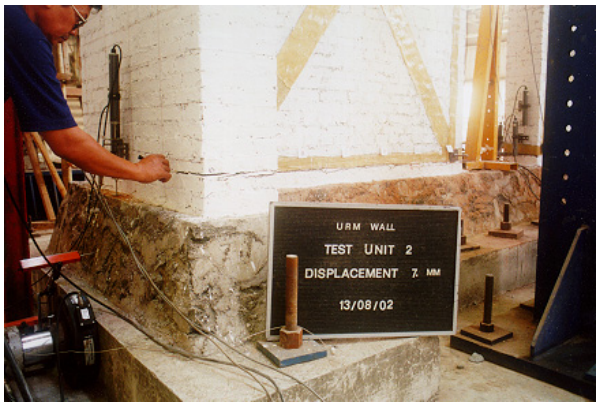

(c) Lateral displacement + 7.0 mm

(d) Lateral displacement - 7.0 mm

(e) Lateral displacement + 21.0 mm

(f) Lateral displacement - 21.0 mm

(g) Lateral displacement - 27.0 mm

Figure 6.3. Cracks on the bottom of both piers of URM Wall Unit-2

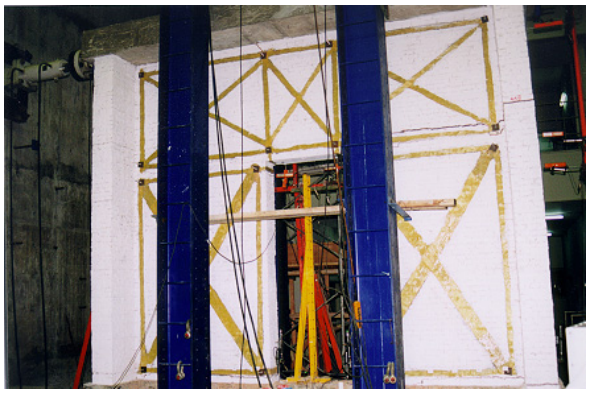

(a) Lateral displacement -27 mm

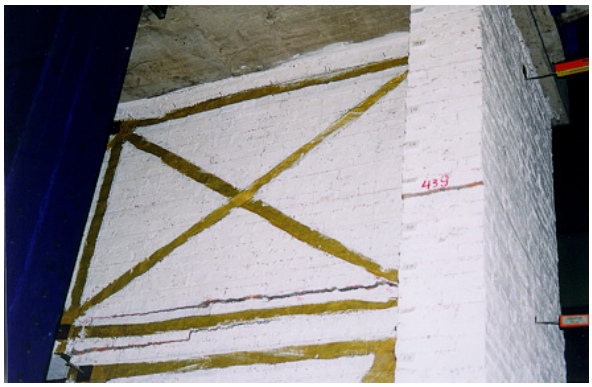

(b) Cracks at cycle 30 (Reading No. 439)

(c) Crack above door opening and Kevlar Fiber was torn along with the fiber direction

(d) Bed joint cracks at upper part and Kevlar fiber delaminated

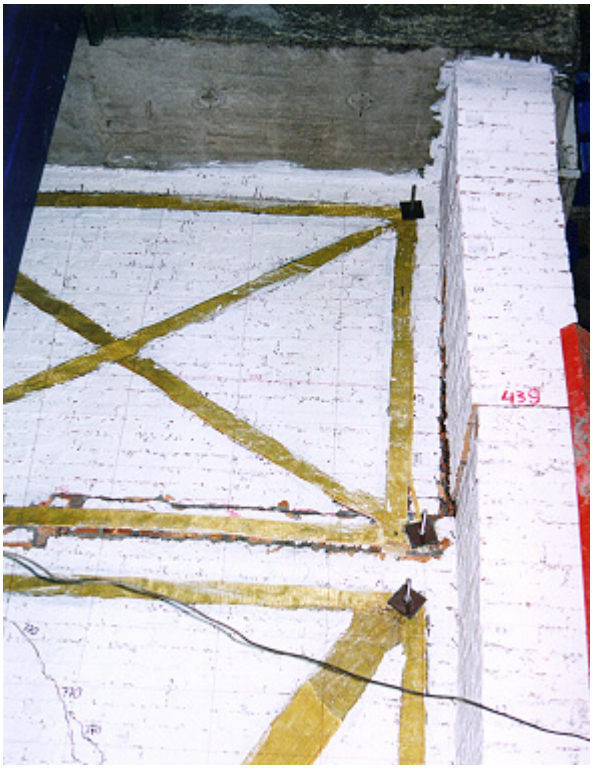

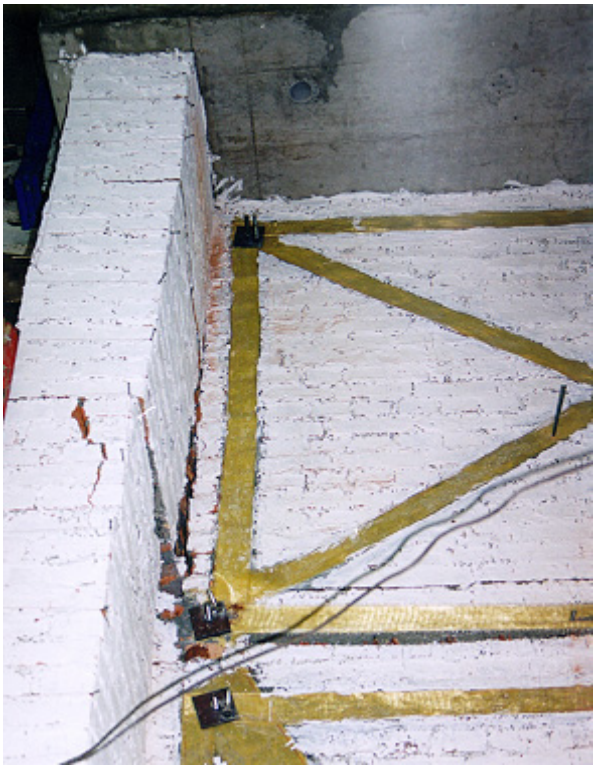

(e) Crack penetrate at both sides along the right upper part wall

Figure 6.4. Cracks due to rocking at upper part for URM Wall Unit-2

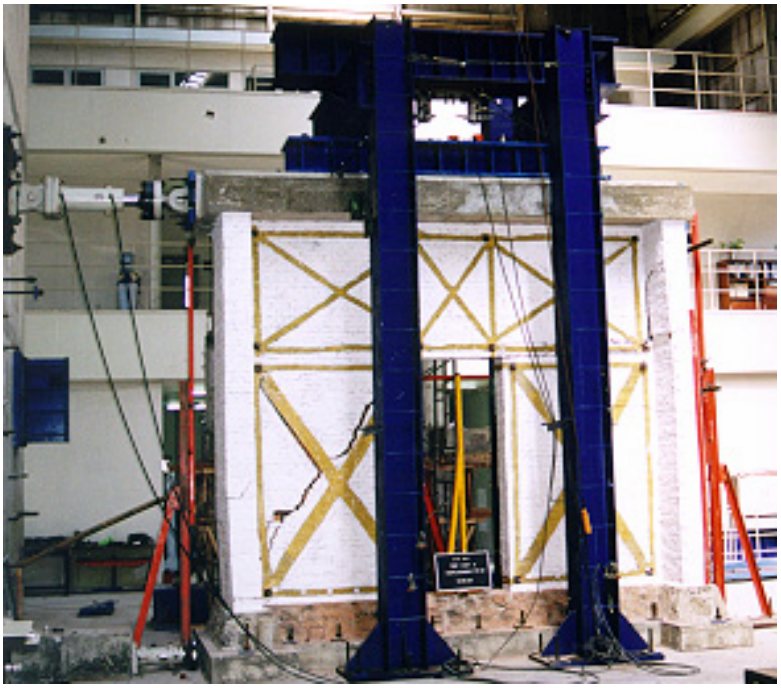

(a) Overall Response for Lateral displacement - 33.0 mm

(b) 36 mm crack width

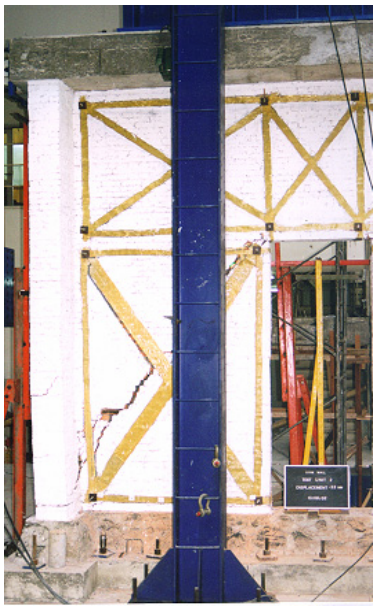

(c) Left pier

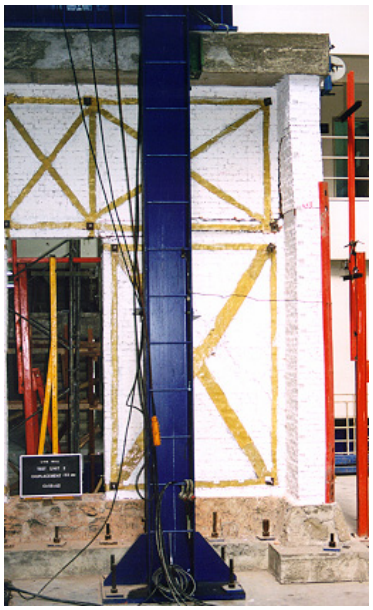

(d) right pier

Figure 6.5. Final failure cracks for URM Wall Unit-2

The above phenomena was exactly as we predicted when rocking would happen but the broken and delaminated Kevlar fiber which started from the weakening bolt joint connection could not resist the diagonal forces any longer. It was observed that the diagonal tension crack occurred in the clay brick at the left pier.

6.2.2 Lateral Force-Displacement Response

The overall response of the URM-wall Unit-2 is summarized in the hysteresis loop for lateral force versus top displacement of the URM wall or storey drift value is shown in Figure 6.6. Shear force vs. storey drift response of URM wall Unit-2 up to load run number 11 that gave storey drift value = $\pm$ 0.11 % or top lateral displacement $\pm$ 4.5 mm was shown in Figure 6.7. It is of interest to note that the stiffness in the positive direction (push lateral load) is much less than the other direction until load run number 17 that top lateral displacement value was + 21 mm (0.517 %). A probable reason is no uniformity of the brick material and also the brick masonry workmanship.

The wall responded linearly with a high stiffness for the first cycle at low storey drift and reduced in stiffness for the next cycle for the same storey drift value. After reaching a new maximum deflection, the URM-wall responded in the next cycle with a reduced stiffness. Subsequent cycles indicated that some strength loss might have taken place. The maximum positive lateral force was recorded 536 kN (54.64 tonf) at load run number 31 with + 33.19 mm top lateral displacement (0.816 % storey drift). The final stage of the test occurred when the negative lateral load cycle was recorded at -699 kN (-71.22 tonf) with a maximum top lateral displacement - 29.49 mm (0.725% storey drift) and measured to - 51.69 mm with negative lateral load decreased to -168.5 kN. Both maximum positive and negative lateral forces where still satisfactory but the Kevlar fiber torn off near the bolt joint triggered the diagonal tension cracks on the clay brick units at both piers and reduced the shear capacity of the pier instantly. The hysteretic curves show a bilinear behaviour with a softening part when the rocking crack is open, the hysteretic loops show noticeable pinching and indicate limited energy dissipation was available. A backbone curve from the quasi static reversed cyclic loading was shown in Figure 6.8.

Propagation of cracks during cyclic loading causes the stiffness degradation of the URM-wall unit-2. It was also occurred when the cycle repeated for the same storey drift value. The cyclic stiffness is defined as the slope of the line joining the origin and the peak value of the respective cycle. The stiffness degradation of every cycle can be plotted as shown in Fig. 6.9. The ordinate represents the ratio between the stiffness at a particular cycle with respect to the first cycle. The stiffness reduction between initial storey drift values ranging from 8% to 40% respectively. The stiffness dropped drastically up to 40% at Cycle + 5 or load run number 9.

The lateral load value was similar with the previous cycle but the top displacement increased significantly from the target displacement + 2 mm to become +2.79 mm. It could be rocking was happening since the bed joint cracks at the bottom and top left pier were extended along the pier-wall length.

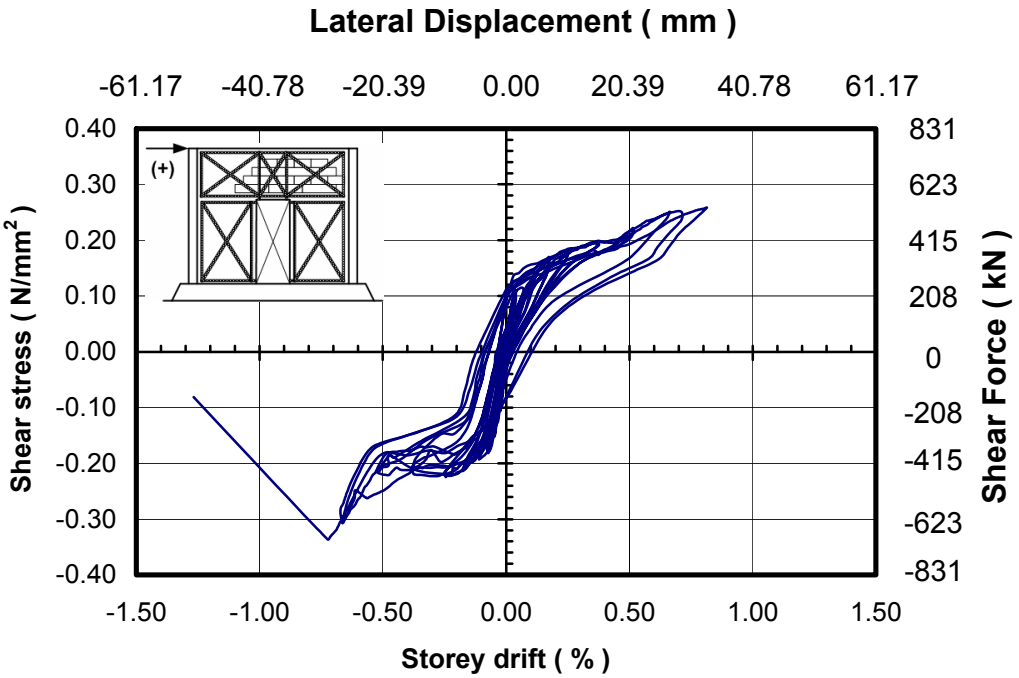

Figure 6.6. Overall response of Unit-2 hysteresis loop

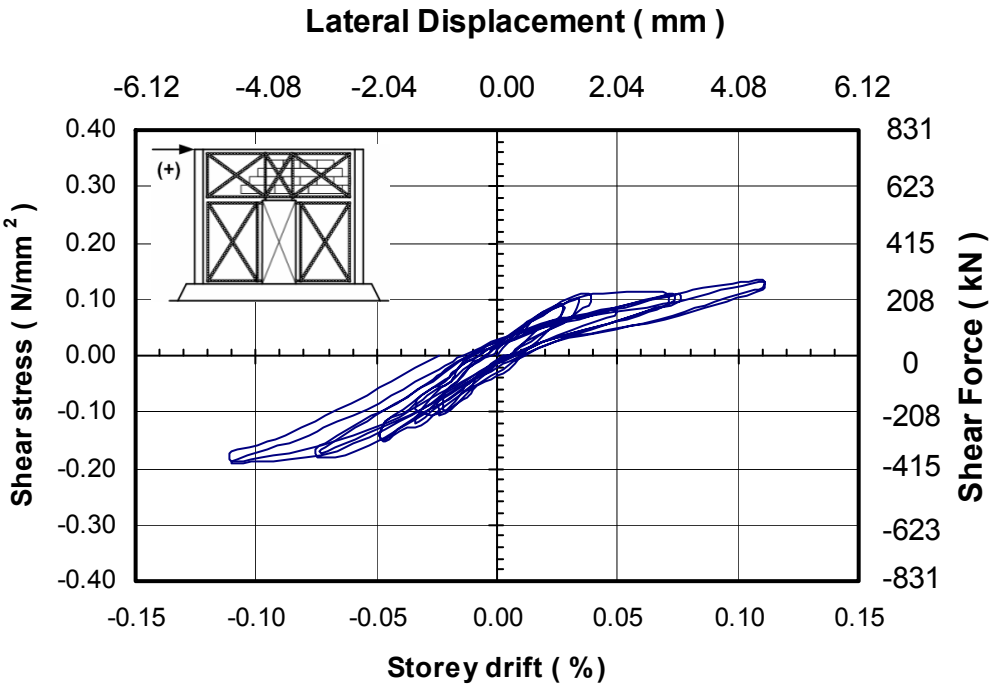

Figure 6.7. Shear force-storey drift response of Unit-2 up to a storey drift = 0.11%

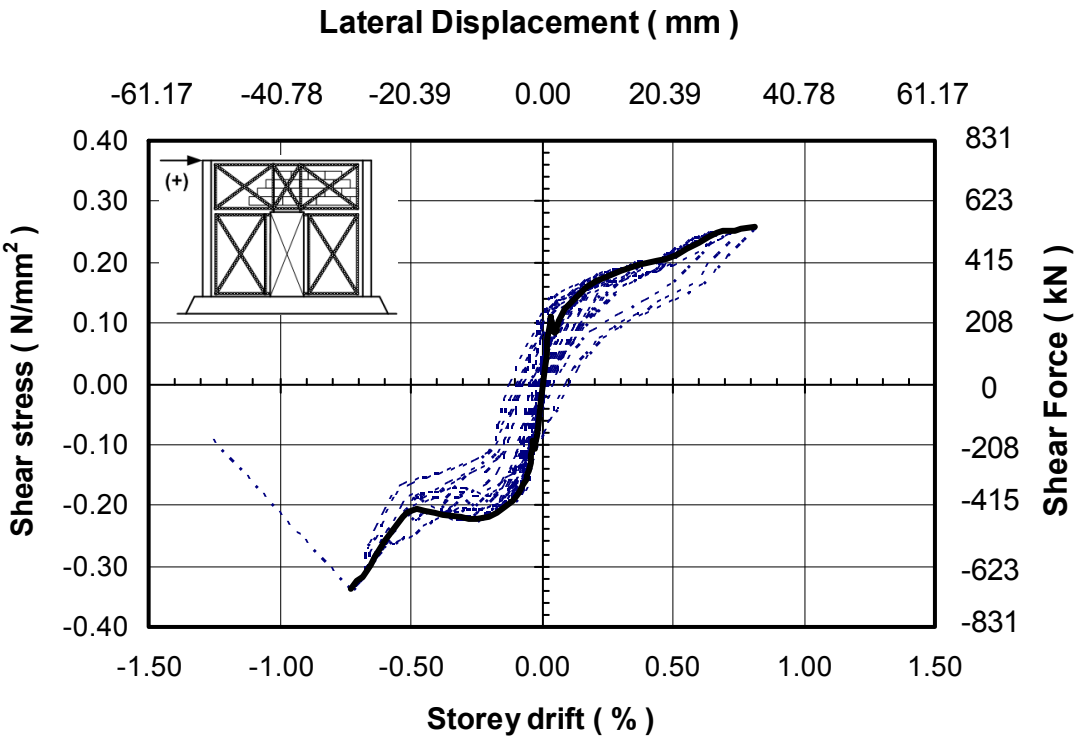

Figure 6.8. Hysteresis envelope of Unit-2

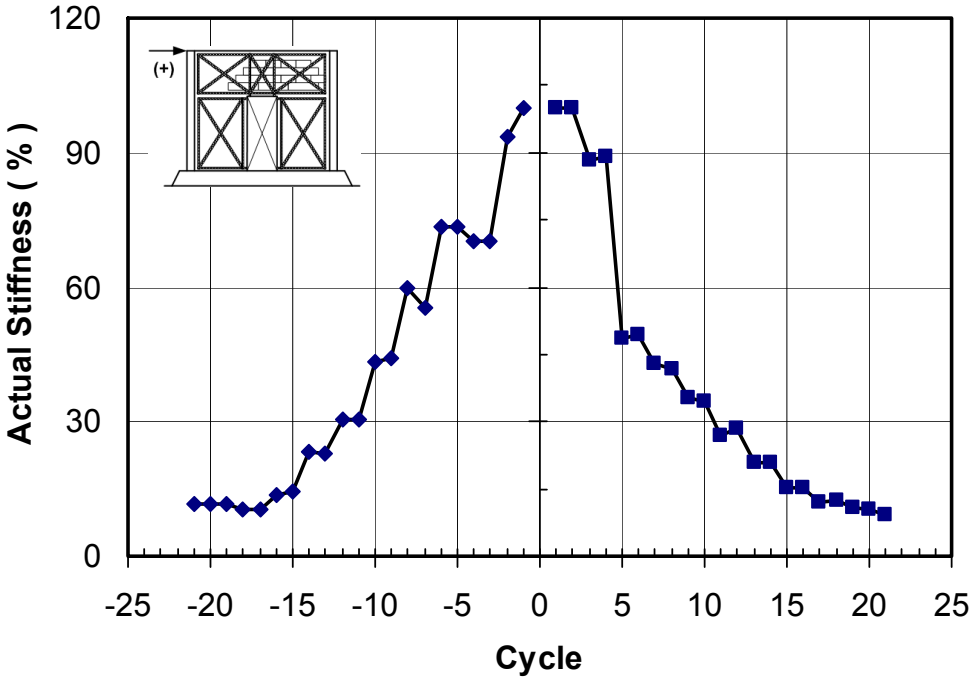

Figure 6.9. Stiffness degradation of Unit-2

6.2.3 Pier Behaviour

Both piers adjacent the door opening are strengthened by diagonal Kevlar on both sides. Another layer of Kevlar fiber was applied in the middle part of their diagonal configuration so that it becomes double layers. The URM wall unit-2 was designed using a pier-based design philosophy, where plastic hinges form at the top and bottom of both piers. It can be assumed as a "strong-spandrel weak-piers" concept that the spandrel acts as a rigid body. After the bed joint cracks appeared at the bottom courses and upper courses of both piers, each pier was clearly performance as rocking pier, it was noted from Figure 6.11. and Figure 6.12. Each pier was sliding and rocking, and the performance of the pier was dependent on its vertical compression load. The vertical stress in the pier changed due to the overturning moment.

The hysteresis loops for the lateral force versus diagonal displacement transducer (LVDTs No. 32, 33, 34 and 35) were shown in Figure 6.10. Those LVDTs reflected the tensile resistance for each pier. In the initially stages, the shear forces are resisted by Kevlar fibre. When the lateral force increased and both piers rocked, both piers deformed a greater amount and some of the Kevlar fibres at the bolt joints were broken. This phenomenon is because the Kevlar fibre cannot resist the diagonal tension anymore and the shear cracks happened in each pier.

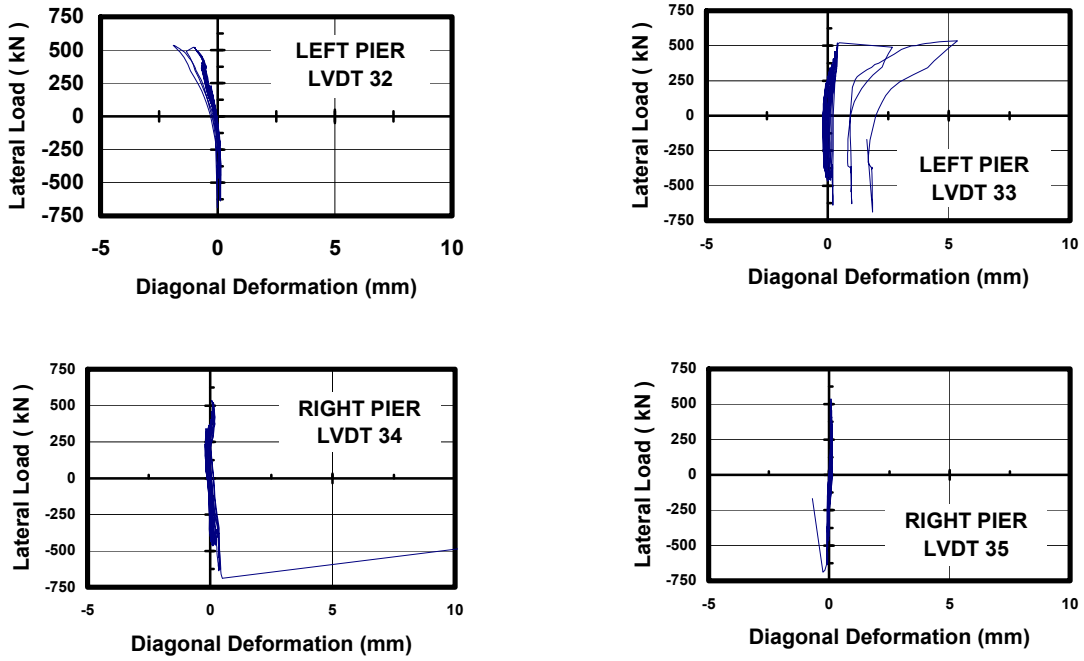

Figure 6.10. Diagonal deformation of the left and the right pier Unit-2

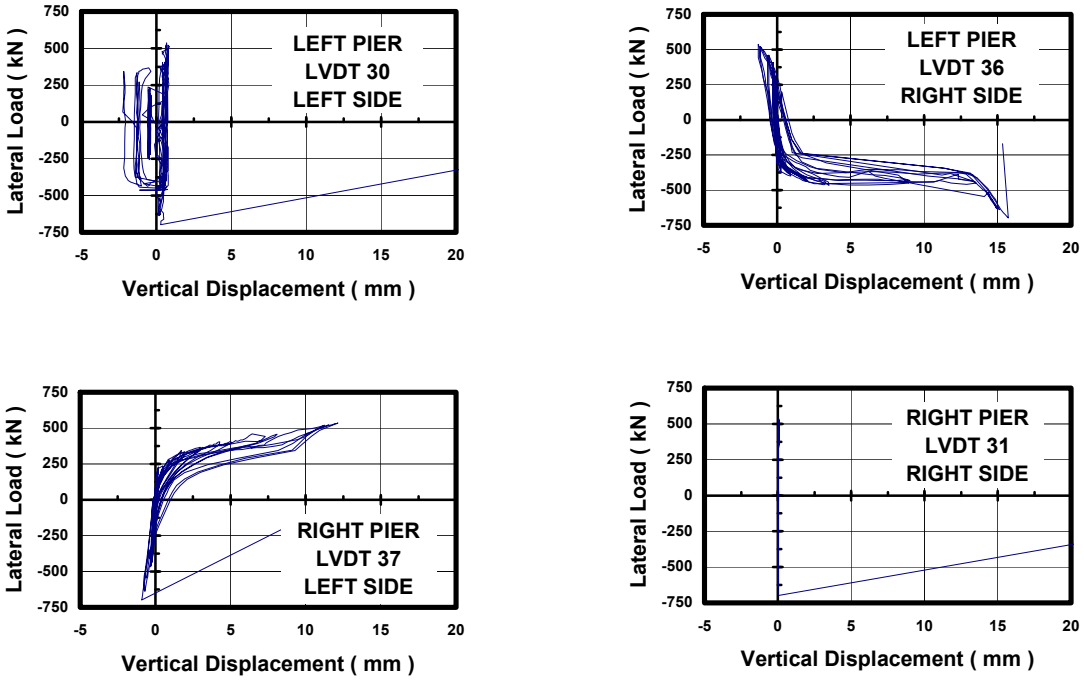

Figure 6.11. Vertical deformation at the top of URM-piers

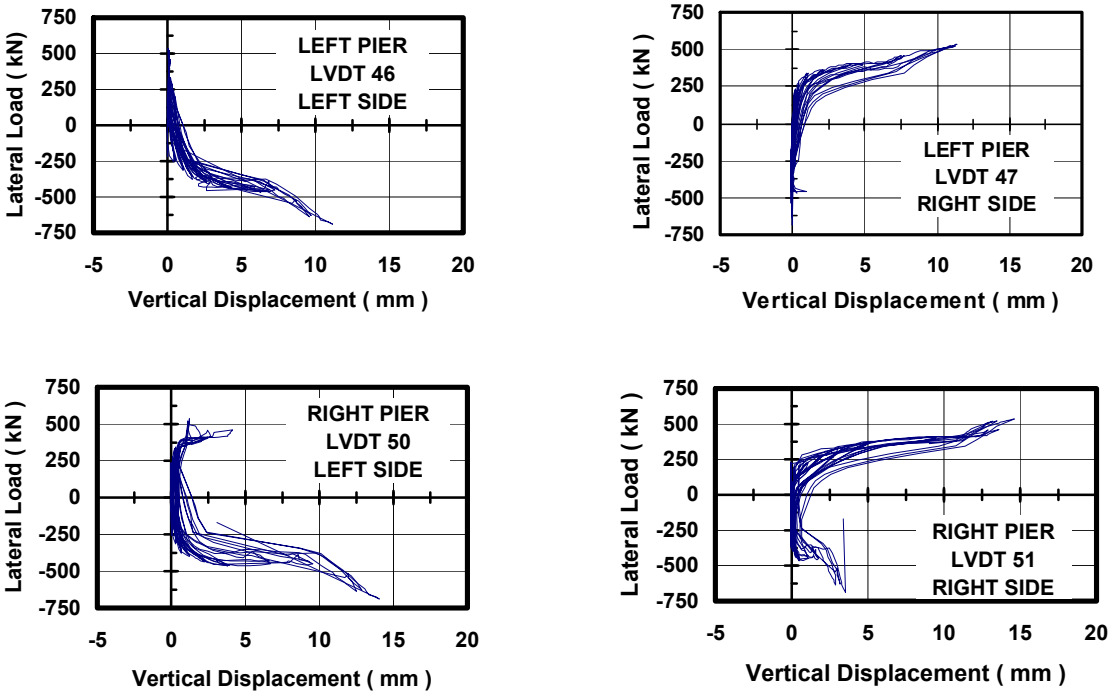

Figure 6.12. Vertical deformation at the base of URM-piers

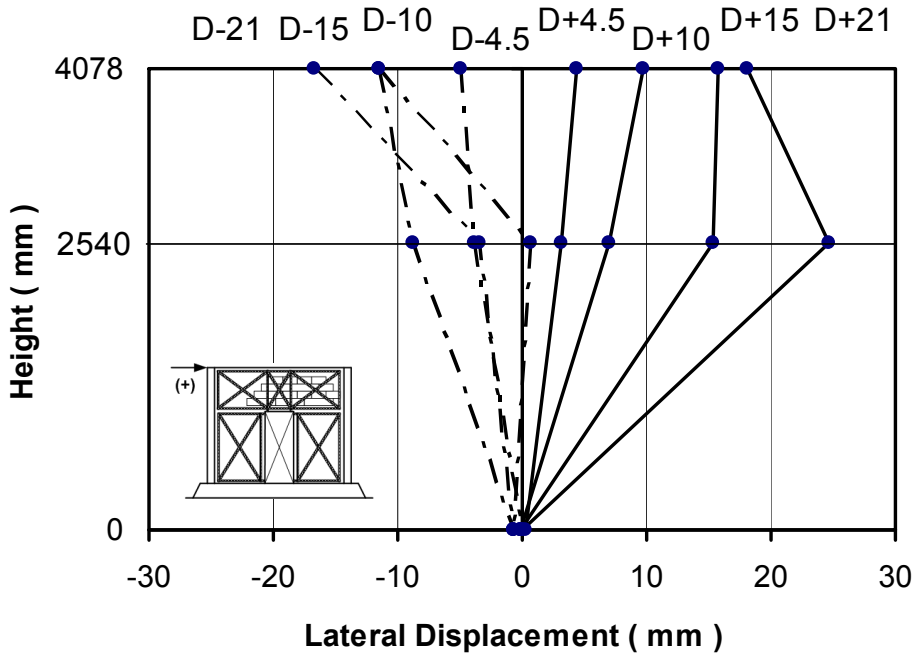

Figure 6.13. Measured Lateral Displacement at Left Flanged Wall for top lateral displacement values from ± 4.5 mm to ± 21 mm

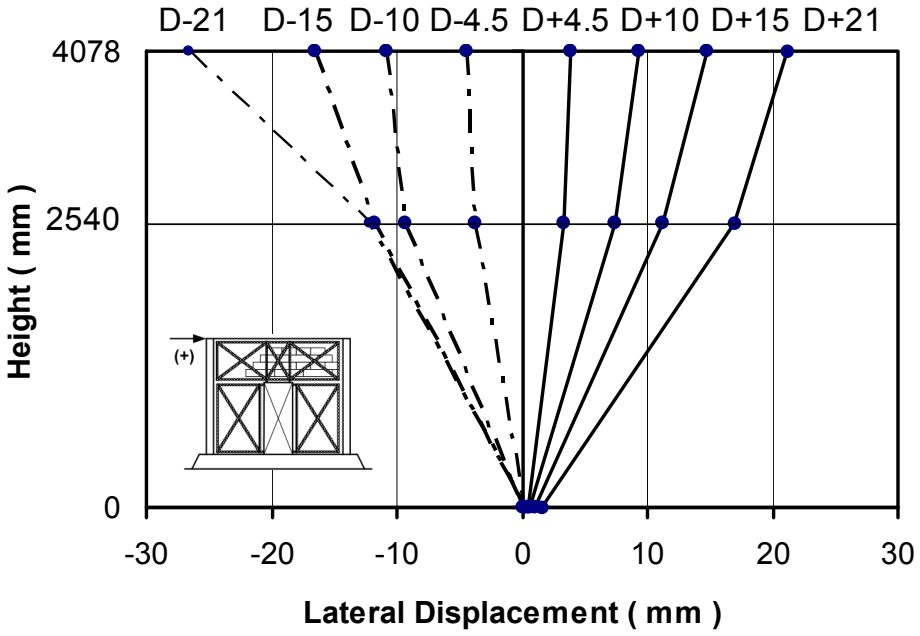

Figure 6.14. Measured Lateral Displacement at Right Flanged Wall for top lateral displacement values from ± 4.5 mm to ± 21 mm

It was noted at Figure 6.13. the lateral displacement that was measured at the top left flanged wall and the top door opening level for top lateral displacement values from ± 4.5 mm to ± 21

mm. The lateral displacement that measured at the top right flanged wall and the top door opening level for top lateral displacement values from ± 4.5 mm to ± 21 mm is shown in Figure 6.14.

6.2.4 Energy Dissipation

The work done in each cycle is stored as strain energy and will be released in the unloading process. Energy dissipated per cycle, E_D, was measured from the area in one cycle (as shown in Figure 6.15.a) and the absorbed strain energy, E_A, (as shown in Figure 6.15.b) in half cycle as follow :

$$E_A = \frac{K.\Delta_m^2}{2} \quad \ldots\ldots\ldots\ldots\ldots\ldots\ldots\ldots\ldots\ldots \quad (6.1.)$$

Where K is the secant stiffness of the structural system and Δ_m is the total displacement of cycle. The damping can be derived using (Clough, 1993) :

$$\xi = \frac{E_D}{4.\pi.E_A} \quad \ldots\ldots\ldots\ldots\ldots\ldots\ldots\ldots\ldots\ldots \quad (6.2.)$$

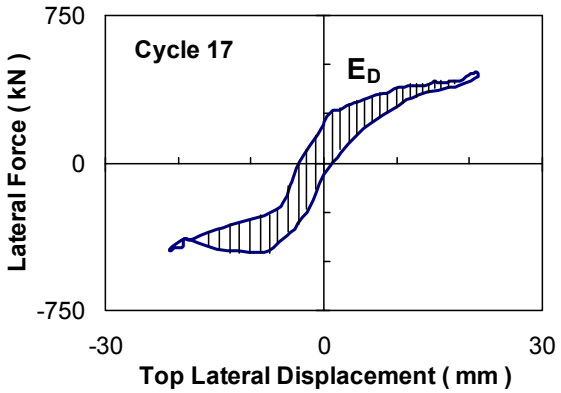

(a) Dissipated energy

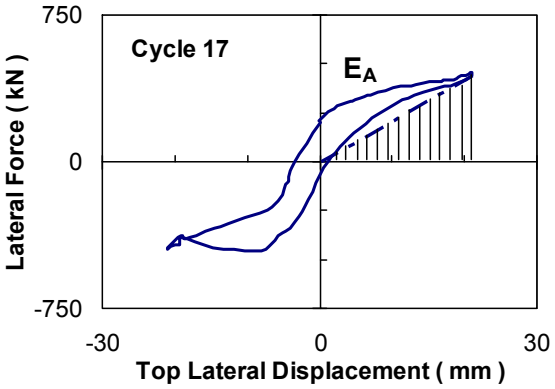

(b) Absorbed strain energy in linear equivalent system

Figure 6.15. Evaluation of dissipated energy

The ratio between E_A/E_D and the equivalent damping were evaluated using Eq. 6.1. and 6.2., and are plotted in Figure 6.16. and Figure 6.17 respectively. The area of E_A and E_D were calculated using AutoCAD-2007 program. It was noted that the value of ratio E_A/E_D more than 50% after the first cycle and almost constant until at the end of the test. The damping ratio was measured from 7.67% to 18.71%.

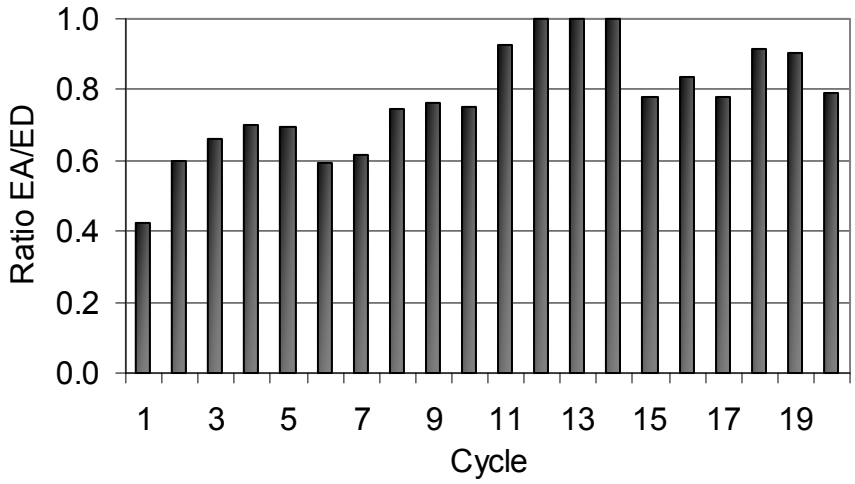

Figure 6.16. Measured of the ratio EA/ED values of URM Unit-2

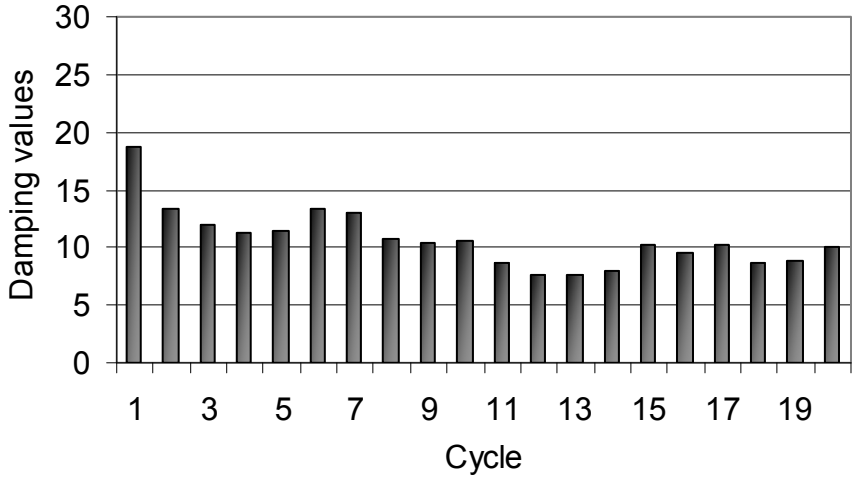

Figure 6.17. Measured of the damping values of URM Unit-2

6.3 CONCLUSIONS

1. The of URM wall Unit-2 has demonstrated a substantial increase in its in-plane capacity by applying externally bonded diagonal Kevlar to both faces of the wall. The lateral resistance of URM wall Unit-2 was enhanced by about 30% in positive direction and 90% in negative direction when compared to Unit-1. The application of Kevlar fiber also has localized and significantly reduced the crack pattern. Bed joint cracks just occur outside the Kevlar application area. It can be summarized that this strengthening technique is promising and with great ease of installation. Kevlar material is more expensive when compare to other fabrics such as glass-fibre and

carbon-fibre so it should be applied in essential locations and in limited volumes so that it can increase the in-plane URM wall capacity economically.

2. The configuration of Kevlar fibre which was applied at the URM wall Unit-2 was confirmed by the test result that showed rocking was happening in both piers after bed joint cracks were occurred at the perimeter of the three rigid bodies. Both piers showed a combined rocking mode and sliding mechanism. These can be a stable non-linear behaviour in URM-walls when an out of plane response does not occur and a slip stopper is provided at the bottom of both pier walls, in order to prevent any sliding of the pier-walls.

3. The maximum positive lateral force was recorded 536 kN (54.64 tonf) at load run number 31 with + 33.19 mm top lateral displacement (0.816 % storey drift). The final stage of the test occurred at the pull lateral load of -699 kN (-71.22 tonf) with a maximum lateral displacement up to - 29.49 mm or equivalent to 0.725% storey drift value. Both maximum lateral push and pull forces still increased but the broken Kevlar fiber at the bolt joints initiated diagonal tension cracks in both piers and reduced the shear capacity of the wall drastically.

4. It was observed from the test result, that the anchorage of the Kevlar layers on both faces at bolted connection becomes a weak point. The Kevlar fibre starts tearing from the existing bolt hole and along the fiber direction at the higher lateral loading and reduced the diagonal tensile capacity of both piers and spandrel beam. A good anchorage system should be arranged to maintain the Kevlar effectiveness.

5. As predicted the masonry material was variable and non homogeneous which caused the hysteresis loop to be non symmetrical between push and pull lateral load directions. Simplification is necessary for numerical analysis.

CHAPTER 7 :
INTERPRETATION OF PERFORMANCE TEST RESULTS

7.1 INTRODUCTION

The general performances between both URM-wall units with flanged walls at both ends and the effectiveness configuration of the Kevlar fibre as retrofit material were presented in Chapters 5 and 6. URM-wall unit 1 represent the existing wall and the URM-wall unit 2 strengthened by applying Kevlar fibre material externally attached to both sides of masonry walls to increase the members' flexural and shear capacity. The hysteretic behaviour including the ultimate strength and strength deterioration stiffness degradation, and energy dissipation for both units have been presented

This Chapter will address some comparisons of the performance of both URM-walls as follows :

a. The relation between in-plane shear stiffness for both units
b. The crack pattern for each perforated URM-wall with door opening, representing the existing wall and the strengthened wall.
c. The pier behaviour for both units

7.2 IN-PLANE SHEAR STIFFNESS

The backbone curves of the hysteresis loops for the URM-wall Unit-1 and Unit-2 are compared in Figure 7.1. The horizontal axis represents the displacement between the top and the bottom of the URM wall unit and the vertical axis represents the horizontal load at the top of the wall. From the hysteresis loops, the initial stiffness in strengthening system at URM Unit-2 was quite similar with URM Unit-1. The hysteresis loops have shown non symmetrical between push and pull lateral load directions especially for URM Unit-2. As predicted, this non symmetrical can cause by several factors such as non homogeneous material and also quality of workmanship.

The maximum lateral load of URM wall Unit 2 was measured by about 30% in positive direction and 90% in negative direction compare to URM wall Unit 1. After Kevlar fibre started delaminating and tearing off near the bolt joints, the lateral resistance of the pier wall URM Unit-2 dropped significantly.

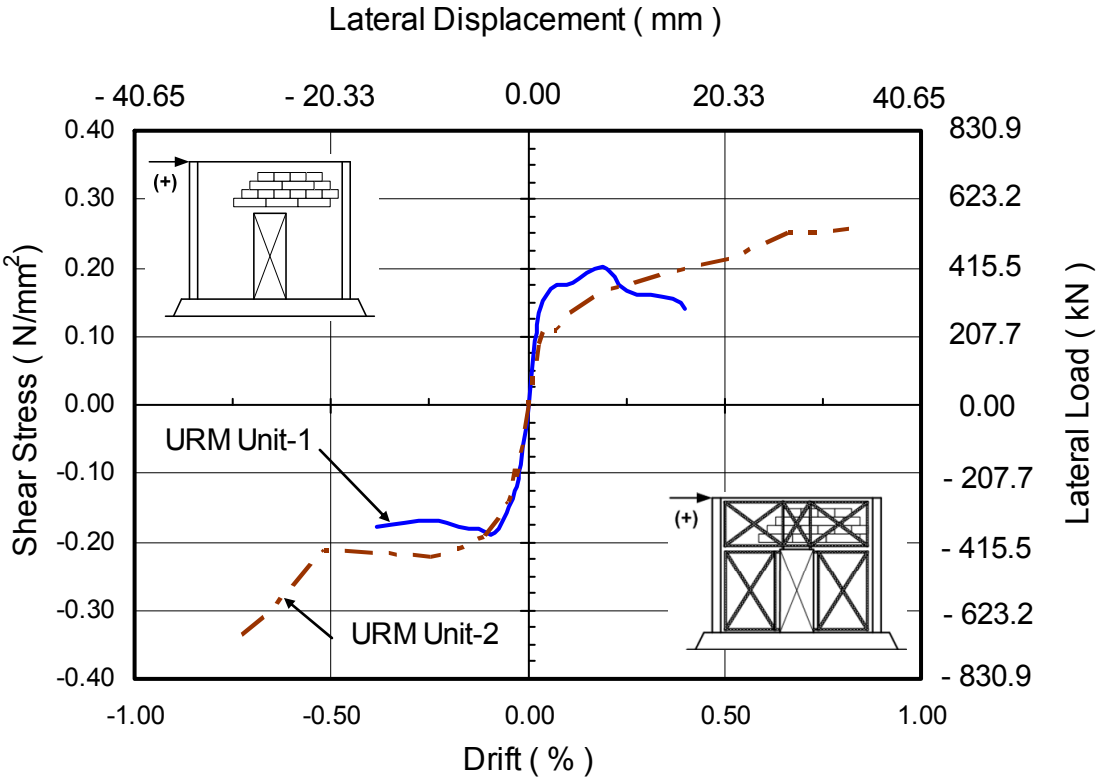

Figure 7.1. Comparison between hysteresis loop envelope of URM-wall Unit-1 and Unit-2

Different lateral stiffness performances were occurred on both URM unit models. Thirty two cycles were applied for Unit-1 compare to forty two cycles for Unit-2 as shown in Table 7.1.

7.3 THE CRACK PATTERNS

The difference in the cracking behaviour for both URM-wall units is shown in Figure 7.2. Shear cracks were observed for both pier walls at URM Unit-1 and the bed joint crack at each flanged wall was started at one fourth to one third of the flanged pier walls height. It was indicated that the flanged wall increased the stiffness and the strength of each pier especially when the flanged wall is in the tensile condition. The crack pattern at the URM wall unit-1

Table 7.1. Comparison top displacement, drift and lateral load values between URM wall Unit-1 and URM wall Unit-2

Load Run Number	URM Wall Unit-1			URM Wall Unit-2		
	Top Disp. (mm)	Drift (%)	Lateral Load (kN)	Top Disp. (mm)	Drift (%)	Lateral Load (kN)
0	0	0	0	0	0	0
1	1.00	0.025	245	1.09	0.027	184
2	-1.02	-0.025	-227	-0.99	-0.024	-219
3	1.01	0.025	259	1.09	0.027	191
4	-1.01	-0.025	-215	-0.89	-0.022	-205
5	1.40	0.034	297	1.49	0.037	231
6	-1.42	-0.035	-264	-1.39	-0.034	-196
7	1.41	0.035	298	1.39	0.034	217
8	-1.41	-0.035	-247	-1.39	-0.034	-251
9	2.01	0.049	336	2.79	0.069	237
10	-2.05	-0.050	-310	-1.89	-0.046	-315
11	2.13	0.052	337	1.99	0.049	172
12	-2.03	-0.050	-300	-1.99	-0.049	-295
13	3.03	0.075	362	2.99	0.074	226
14	-3.44	-0.085	-388	-3.09	-0.076	-344
15	3.02	0.074	351	3.09	0.076	226
16	-3.14	-0.077	-357	-2.99	-0.074	-344
17	4.61	0.113	370	4.49	0.110	278
18	-4.98	-0.123	-373	-4.49	-0.110	-400
19	4.53	0.111	377	4.49	0.110	271
20	-4.58	-0.113	-360	-4.49	-0.110	-391
21	**7.70**	**0.189**	**416**(*)	7.09	0.174	335
22	**-7.14**	**-0.176**	**-369**	-7.09	-0.174	-438
23	7.06	0.174	372	7.09	0.174	353
24	-7.05	-0.173	-350	-7.09	-0.174	-434
25	10.31	0.254	346	10.09	0.248	367
26	-10.10	-0.248	-354	-10.09	-0.248	-462
27	10.12	0.249	325	10.09	0.248	367
28	-10.08	-0.248	-344	-9.99	-0.246	-466
29	15.10	0.371	319	15.09	0.371	404
30	-15.64	-0.385	-372	-15.39	-0.379	-450
31	16.21	0.399	291	15.09	0.371	409
32	-21.26	-0.523	-333	-15.49	-0.381	-431
33				21.09	0.519	443
34				-21.09	-0.519	-441
35				21.09	0.519	458
36				-21.29	-0.524	-441
37				27.09	0.666	520
38				-27.09	-0.666	-638
39				28.89	0.711	522
40				-26.99	-0.664	-630
41				**33.19**	**0.816**	**536**
42				**-29.49**	**-0.725**	**-699**

Note : (*) Maximum value for URM Unit-1

was representing weak piers and strong spandrel mechanism, as shown in Figure 7.2.a. Shear crack was appeared at the web of left pier wall under pull lateral load with the drift value of 0.11%. In the reverse lateral load, a shear crack was also observed at the right pier-wall with the drift value of 0.189%.

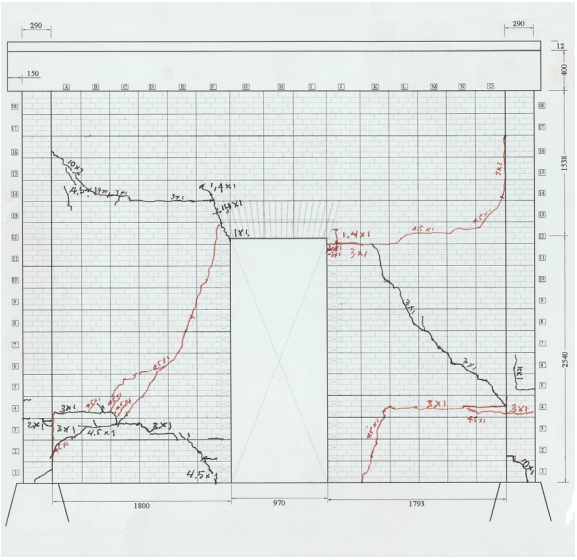

(a) Cracks observed from URM Unit-1

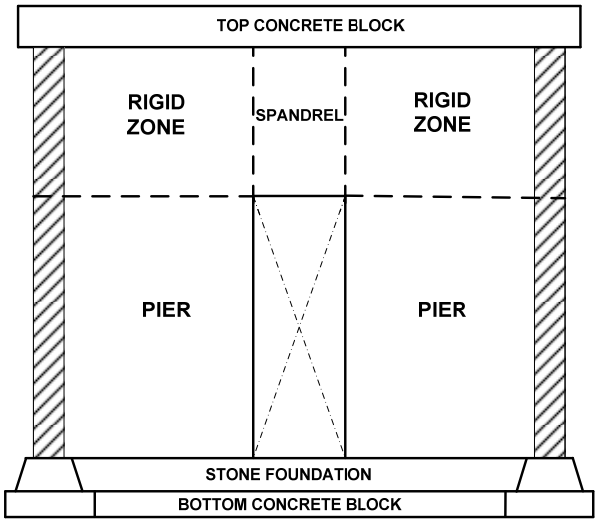

(b) Weak pier – strong spandrel mechanism

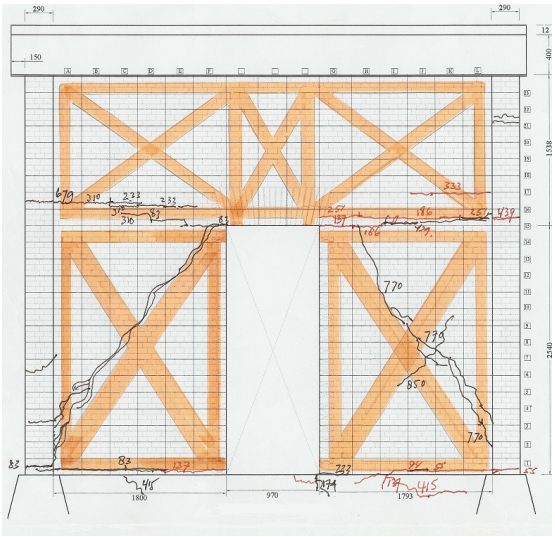

(c) Cracks observed from URM Unit-2

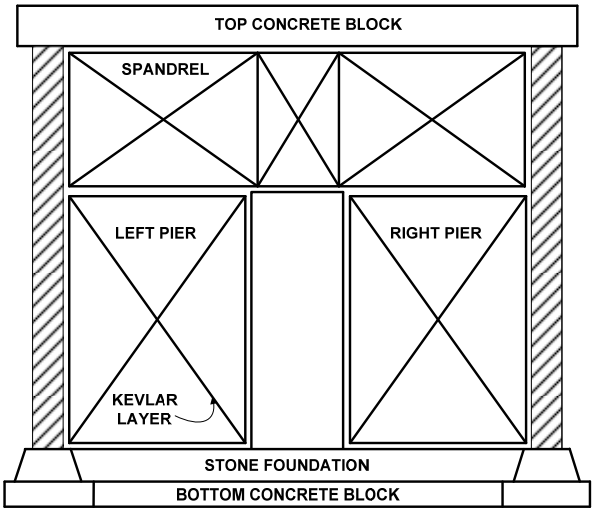

(d) Rocking mechanism

Figure 7.2 . Comparison between crack patterns for both URM walls

The URM-wall unit 2 were designed by applying Kevlar fibre material which externally attached to each side or both sides of masonry walls to increase the members' flexural and shear capacity. It was observed from the test result that both pier walls showed a combined

rocking mode and sliding mechanism. The URM wall Unit-2 divided into the three rigid block walls. No cracks were visually observed inside the Kevlar configurations until drift value reached + 0.370%. Next cycle the bolt joint for Kevlar layer at the upper part of the right pier was started tearing off and shear crack was appeared inside the pier wall parallel to the diagonal Kevlar fibre.

7.4 THE PIER BEHAVIOUR FOR BOTH UNITS

The initial performance of URM wall unit-1 behaved as coupled wall-based design philosophy. The crack started at the header joint between the flat arch brick and the horizontal brick course was observed along the spandrel above the door opening. These cracks change the behaviour of the URM wall become pier-based design philosophy as shown in Figure 7.3. Shear crack was observed at both piers before end of the test.

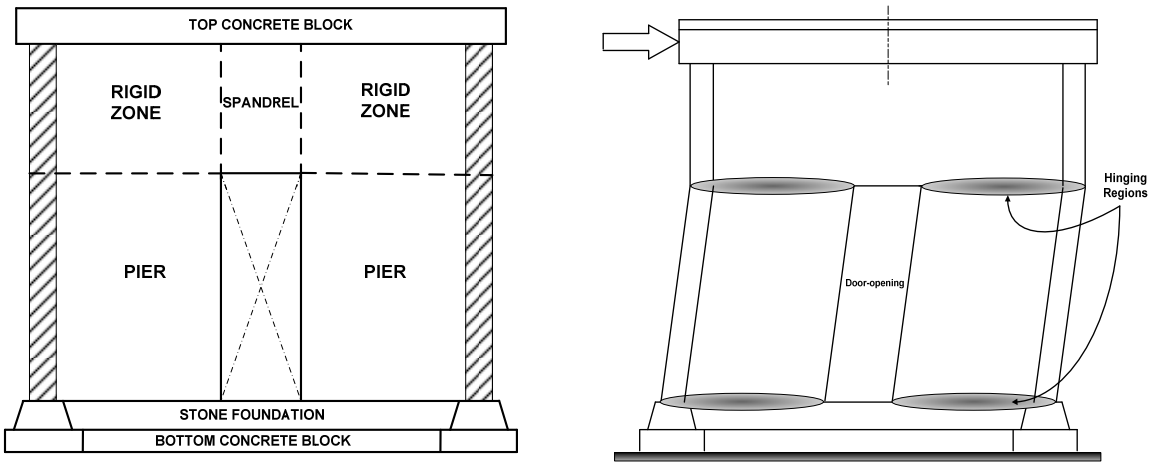

Figure 7.3. Pier-based design philosophy of URM wall Unit-1

The strengthening technique for URM wall unit-2 was design as pier-based design philosophy, which plastic hinges form at the top and bottom of both piers. Both piers were strengthened by Kevlar fibre to resist the diagonal tension as shown in Figure 7.4. Stable rocking mechanism was observed for in-plane loading up to the top displacement value is 27 mm or drift value 0.664%. Next cycle the Kevlar fibre started tearing off at the bolt joints, the lateral resistance dropped significantly and shear cracks were observed at both pier walls. It was indicated that the diagonal Kevlar fibre at the pier wall can not resist the shear forces anymore.

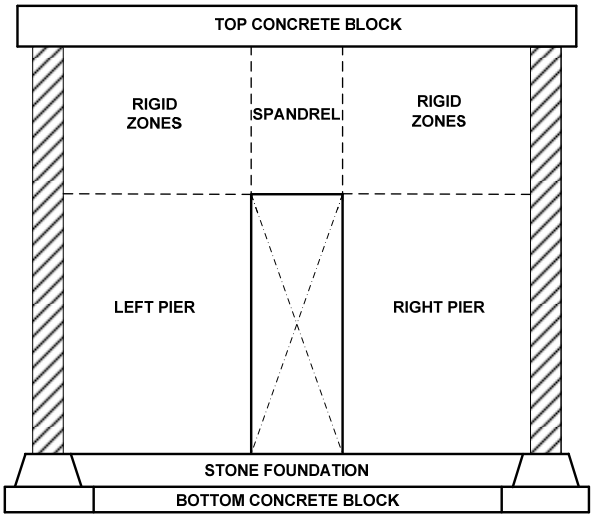

(a) URM- Unit1

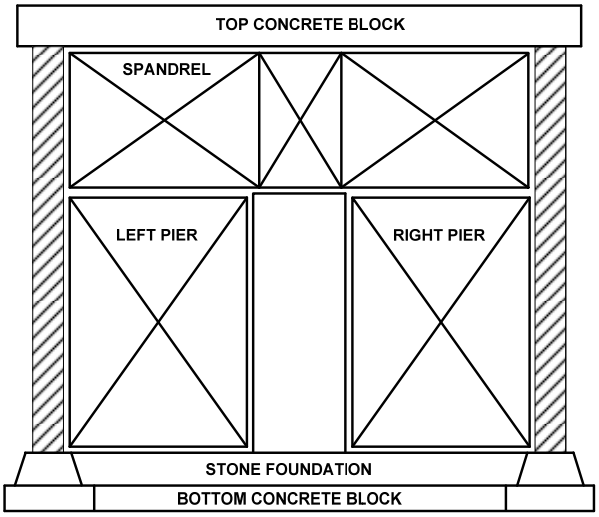

(b) URM-Unit2

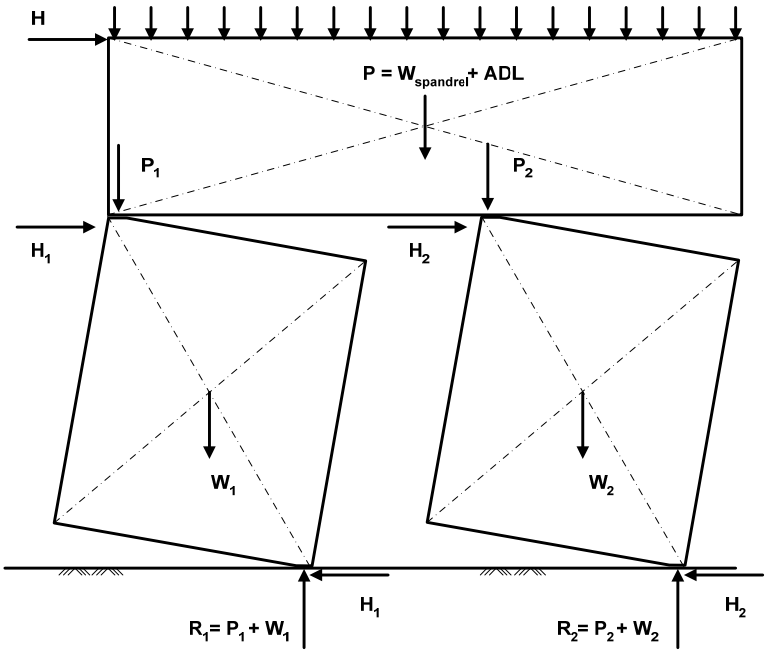

(c) Force flow in URM wall

Figure 7.4 . URM wall Mechanism

The comparison hysteresis loops for cycle number 11 is shown in Figure 7.5. The shape of hysteresis loop URM Unit-1 fatter than hysteresis loop URM Unit-2. URM Unit-2 dissipated less energy compare to URM Unit-1, due to rocking mechanism. The energy absorbed and dissipated in each cycle, E_A and E_D, respectively, was measured by AutoCAD program and illustrated in Figure 7.6. It can be observed that the ratio E_A/E_D for URM Unit-1 was increased at the beginning until reach the maximum lateral load. After the maximum lateral load, the ratio E_A/E_D decreased gradually. The ratio E_A/E_D for URM Unit-2 remained

approximately constant more than 0.5. Figure 7.7. illustrates the variation of the equivalent damping value, which indicate the damping value for URM Unit-1 increased in the final stage of the cycle. The damping value for URM Unit-2 remained approximately constant until the final stage.

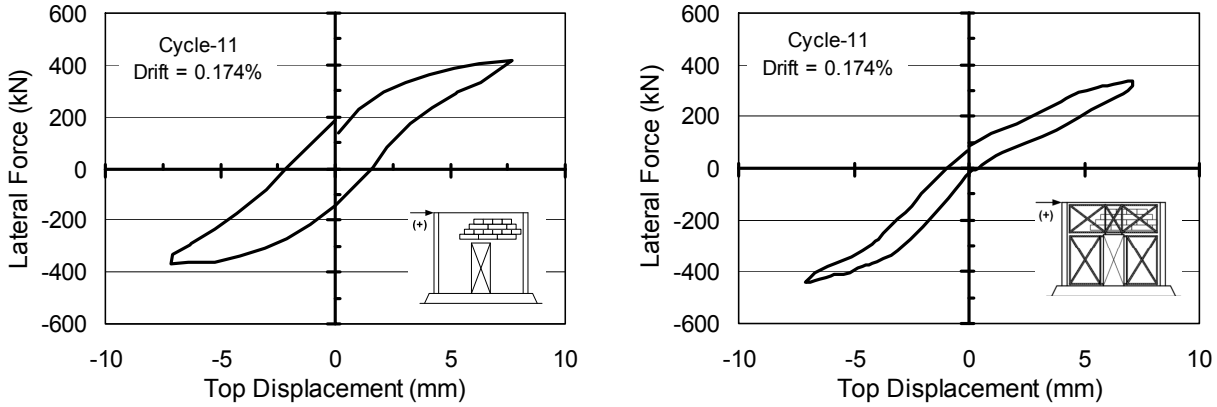

Figure 7.5 . Comparison of the shape of the hysteresis loops cycle number 11 of URM Unit-1 and URM Unit-2

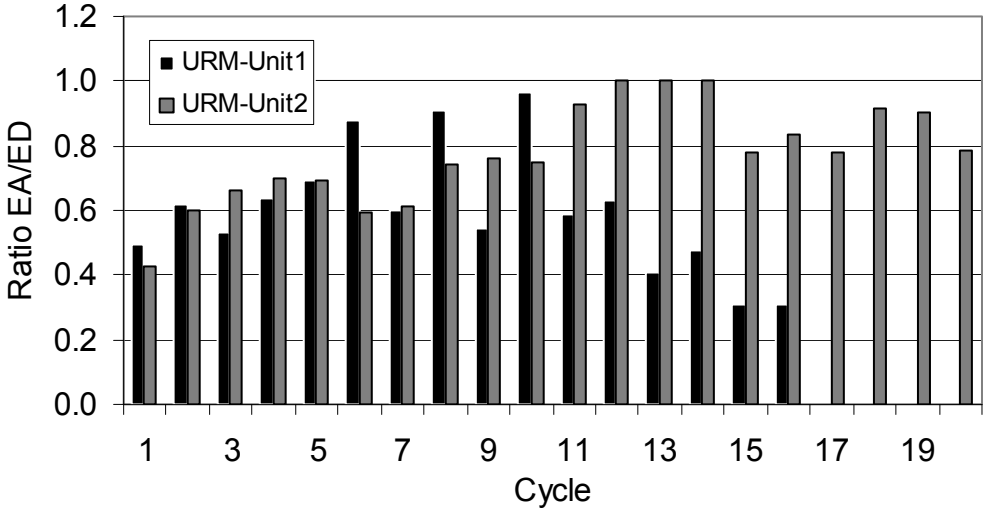

Figure 7.6. Variation of the ratio EA/ED values of URM Unit-1 and URM Unit-2

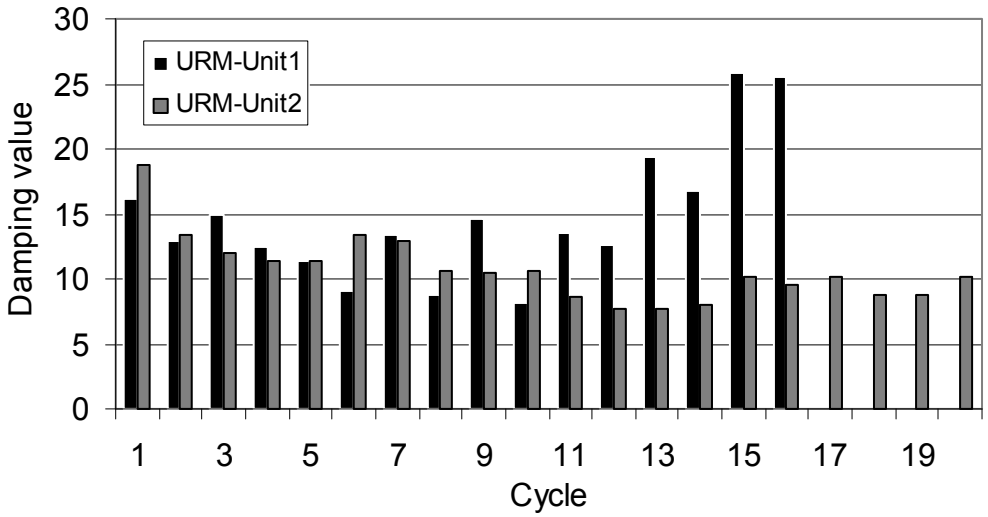

Figure 7.7. Variation of the damping values of URM Unit-1 and URM Unit-2

7.5 CONCLUSIONS

1. The lateral strength capacity of the strengthening URM wall Unit-2 was significantly increased before the Kevlar fibre delaminated and tore off at the bolt joints. Pier rocking at URM wall Unit-2 has been clearly established. It was created the lateral displacement increase significantly and able to withstand after several cycles. The in-plane strength of URM wall Unit-2 was improved by about 30% in positive direction and 90% in negative direction compared to the URM wall Unit-1.

2. Kevlar fibre with its thickness of only 2 mm proved to be a good alternative for retrofitting URM walls against the lateral load. It will not affect the weight of the structure and also the architectural appearance of the existing building. It was observed, the strengthening technique URM wall Unit-2 with Kevlar fibre could localize and significantly reduced the crack pattern compare to the URM wall Unit-1. It can be concluded that any repairs that would have to be carried out after an earthquake would be simpler and cheaper.

3. The strengthening technique for URM wall unit-2 was design as pier-based design philosophy, which plastic hinges form at the top and bottom of both piers. Both piers were strengthened by Kevlar fibre to resist the diagonal tension and stable rocking

mechanism was observed during the test. Therefore, rocking method is a recommended post-cracking behaviour for rehabilitation URM structures in the seismic prone area.

CHAPTER 8 :
ANALYSIS OF UNREINFORCED MASONRY WALLS USING FINITE ELEMENT METHOD AND CURRENT SEISMIC ASSESSMENT STANDARD

8.1 INTRODUCTION

Application of the finite element method (FEM) as a numerical analysis method becomes more popular in solving numerous engineering problems and currently there are available many ranges of commercial finite element software. Based on the concept of piece-wise approximation, and specifically designed for computer applications, this method frees the analysis of complications due to geometry and boundary conditions.

A three dimensional linear finite element model was developed to determine the strength, lateral displacement and stress distribution throughout the URM-wall. Using this model, a series of analyses for both test units were conducted using the computer program ABAQUS which is capable treating material and geometric non-linearity. The masonry wall, stone foundation and concrete block were modeled as macro modeling by using 8-node continuum elements. The Kevlar material in the second URM wall was modeled by truss elements.

8.2 PROCEDURE ANALYSIS OF UNREINFORCED MASONRY WALLS

Masonry itself is a composite material that consists of two materials depending upon the properties of the masonry unit and the mortar. In general, they are two approaches towards its numerical representation and depend on the level of accuracy and simplicity desired. First, it focuses on the masonry as a composite material or non-homogeneous elements or hereby denoted as “micro modeling”. In this approach, brick unit and mortar are represented as separate materials with individual mechanical characteristics. Non-homogeneous finite element models of masonry were implemented by some researches such as Page (1978), Lourenco and Rots (1994), Lotfi and Shing (1994) etc. The most advanced analysis also

introduces the interface parameter between brick unit and mortar using a smeared cracking approach. This model is highly complex analysis, exclusively for detail research purposes and need more CPU time.

Second, it is simplify the micro-modeling problem that assumes the masonry as a homogeneous material that combined characteristics of brick unit and mortar as a composite material or so called “macro-modeling”. The macro-modeling does not make a distinction between individual units and joints but treats masonry as a homogeneous an-isotropic continuum. The composite material parameters can be obtained from sufficiently prismatic masonry tests under homogeneous states of stress. Macro-modeling has been used for practical analysis of URM wall subjected to lateral load in addition to their gravity load and generally similar end result compare to micro modeling analysis. This method has already implemented by some researches, such as Dhanasekar et al. (1984), Brencich and Lagomarsino (1997), Laurenço et al. (1998), Abrams and Calvi (1994) extend this macro modeling idea into dynamic range analyses. Masonry can be assumed to be a homogeneous material if a relationship between average stress and strains in the composite material is established. For the numerical analysis, this method will be compromised between accuracy and efficiency in engineering practice.

In this research, the macro modeling is adopted to model the URM walls in the finite element analysis. The computer software package ‘ABAQUS’ is a superior of finite element analysis with advanced capabilities. The masonry material model is the smeared cracking model that allows the masonry to crack in tension and strain-soften in compression.

8.3 MODELING OF UNREINFORCED MASONRY WALLS WITH THE ABAQUS PROGRAM

Both unit tests will be validated by comparing the ABAQUS analysis results with the experimental observations. The linear finite element model was attempted to form all characteristic physical and material properties data on both URM walls and loaded up to initial crack stage. The URM-walls were discretized into several meshes and a feature of stone foundation was also modeled.

8.3.1 Selection of Element Types

There is a large variety of element type that can be chosen for the FEM analysis, as follows (see Figure 8.1.) :

1. Bar elements : these are only capable of sustaining axial forces and can be used to model reinforcing bars, either individually or as groups
2. Solid elements : These are used to model structures that are essentially monolithic and available in two- and three-dimensional versions. The two-dimensional elements are derived by assuming plane stress, plane strain or axysymetric conditions.
3. Plate elements : These are flat elements, generally triangular or rectangular in shape, which are capable of carrying out-of-plane loads by plate-bending action.

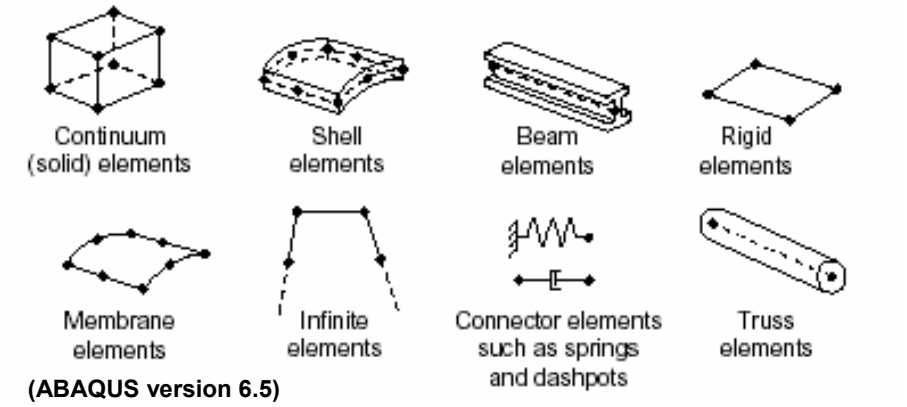

Figure 8.1. Variety of element types that can be chosen for the FEM analysis (Hibbit et al., 2004)

Macro modeling in three dimensional analyses was carried out using the finite element ABAQUS and the 8-node continuum elements was used to model the URM-walls in this thesis. The element has six degrees of freedom at each node. The Kevlar material in the second URM wall was modeled by truss elements. Both element types are shown in Fig. 8.2.

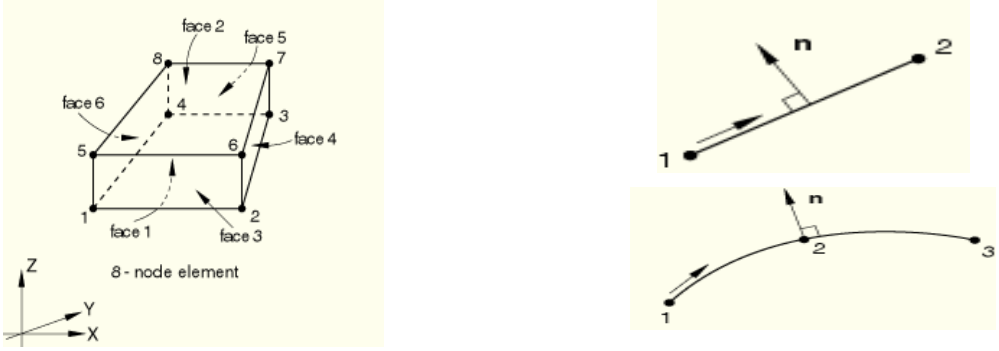

(a) Tetrahedral element faces – 8 nodes (b) Truss elements – 3 dimensional and 2 nodes

Figure 8.2. Continuum element and Truss element (Hibbit et al., 2004)

8.3.2 Boundary Conditions

The base of the bottom concrete block was restrained from all displacements. The masonry wall was idealized in ABAQUS program as shown in Figure 8.3. and Figure 8.4.

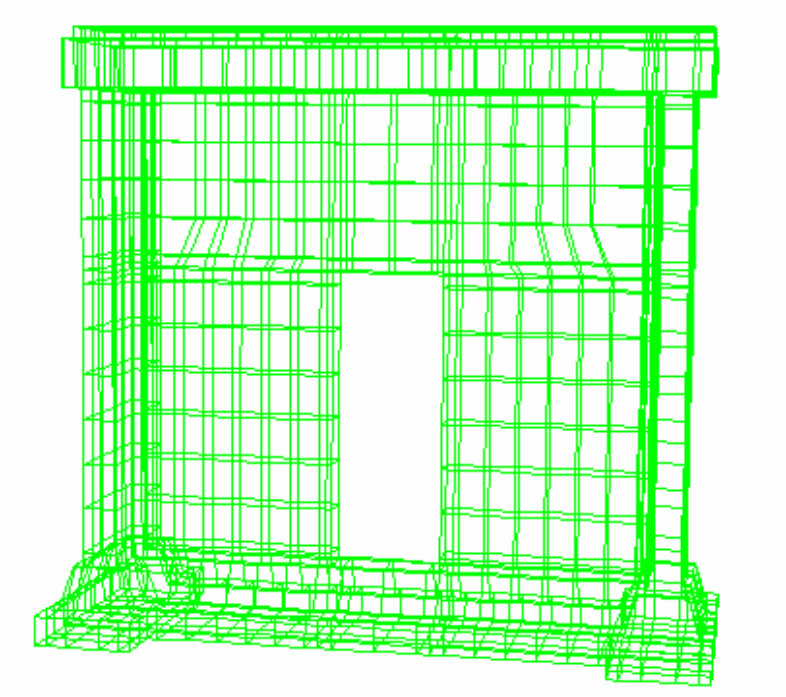

Figure 8.3. Finite Element Model of URM Wall Unit-1

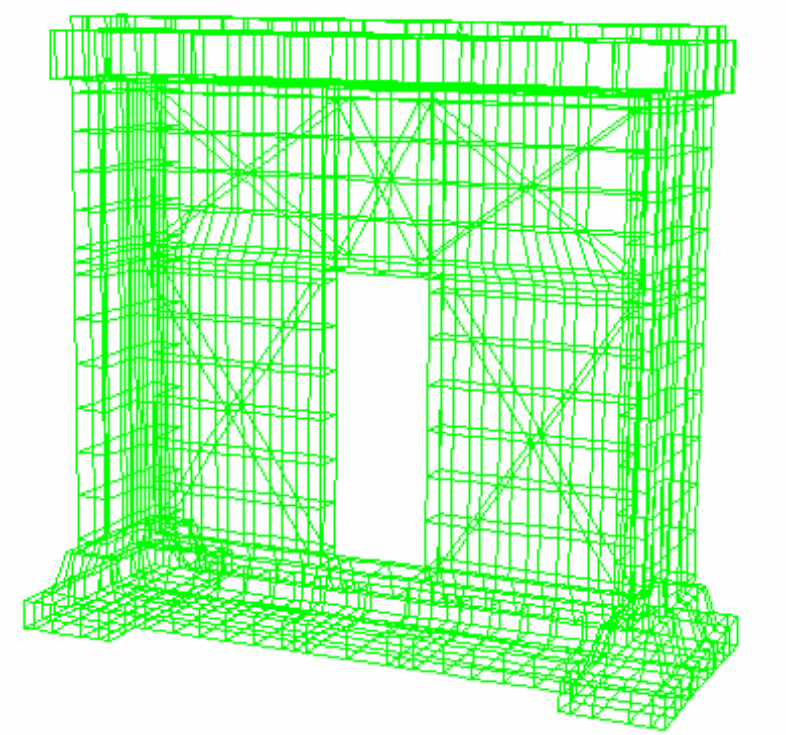

Figure 8.4. Finite Element Model of URM Wall Unit-2

8.3.3. Masonry Properties

The material properties used for the analysis are shown in Table 8.1. which obtained from the material testing program discussed at Chapter 3. The data obtained from the material testing program that conducted by Indonesia laboratory is insufficient, any additional data were considered from other research formula.

In the linear model, the shear modulus value will remain constant until cracking start and it will decrease progressively after cracking. The other way, the damping value will progressively increase after cracking was happen. The parameters of the macro elements need to be considered as representative of an average data which can represent the composite material between masonry unit and mortar.

Table 8.1. Material properties

Material	Properties	Value
1. Masonry	Compression strength, f'_m	10.20 MPa
	Tensile strength, f_t	0.31 MPa $^{(*)}$
	Elastic Young's Modulus, E_m	6567.7 MPa
	Poisson's ratio, υ_m	0.25
	Density	18.481 kN/m^3
2. Stone foundation	Compression strength, f'_s	7.00 MPa
	Elastic Young's Modulus, E_s	8168.4 MPa
	Poisson's ratio, υ_s	0.20
	Density	21.307 kN/m^3
3. Kevlar fibre material Type - AK40 Thickness = 0.193 mm	Breaking strength	400 kN/m
	Fibre quantity	280gram/m2
	Tensile strength (Design), f_{tkv}	2,100 MPa
	Elastic Young's Modulus, E_{kf}	120,000 MPa

Note : $^{(*)}$ Tensile strength, f_t assume = 3% f'_m

8.3.4 Non-Linear Modeling

Non-linear models of masonry walls can allow for the effects of cracking and crushing of masonry as unit or homogeneous elements. The smeared crack concrete model was used to represent the behaviour of masonry wall. Masonry in compression was modeled as an elastic-plastic material with strain softening is shown in Fig. 8.5. The stress-strain behavior of concrete in compression was assumed to be linier elastic up to 0.33 f'_m. Beyond this point, it was in the plastic regions in which plastic strain was input to define the stress-strain relationship in the finite element model.

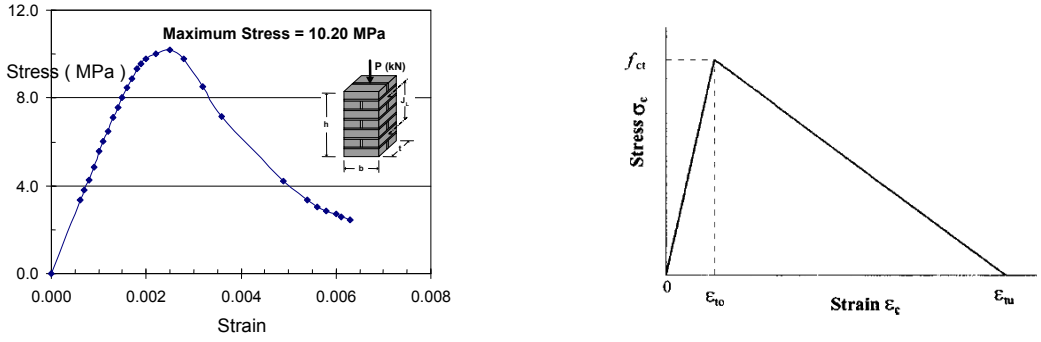

(a) in compression (b) in tension

Figure 8.5. Stress-Strain curve for smeared crack of masonry model

In the present study, some difficulties were come up to run ABAQUS analyses remotely from Indonesia and Auckland. A further research should be conducted to do the non-linear analysis.

8.4. WALL BEHAVIOUR ANALYSIS

8.4.1. Flow of Stress and Top Lateral Displacement

Finite element analysis using ABAQUS program was conducted for URM wall Unit-1 with the drift value is 0.05%. It was observed from contour plot is shown in Figure 8.6. that the tension level stress increase at the corner between the spandrel, at the toe of left pier and the toe of the right flanged pier wall. It is well predicted that initial cracking takes place in this points. As lateral load increases, compression stress started to concentrate in the pier diagonal.

The same analysis was also conducted for URM wall Unit-2. It was observed from contour plot is shown in Figure 8.7. there is no increase stress concentrated inside the Kevlar fibre configuration. It is consistent with the test result that crack was appeared outside the Kevlar fibre configuration only.

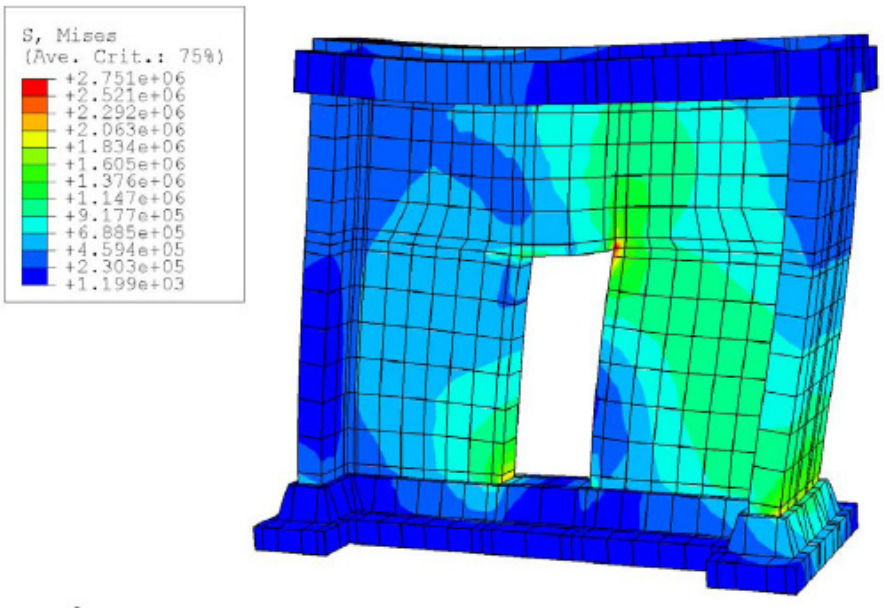

Figure 8.6. Stress contour plot of URM Wall Unit-1

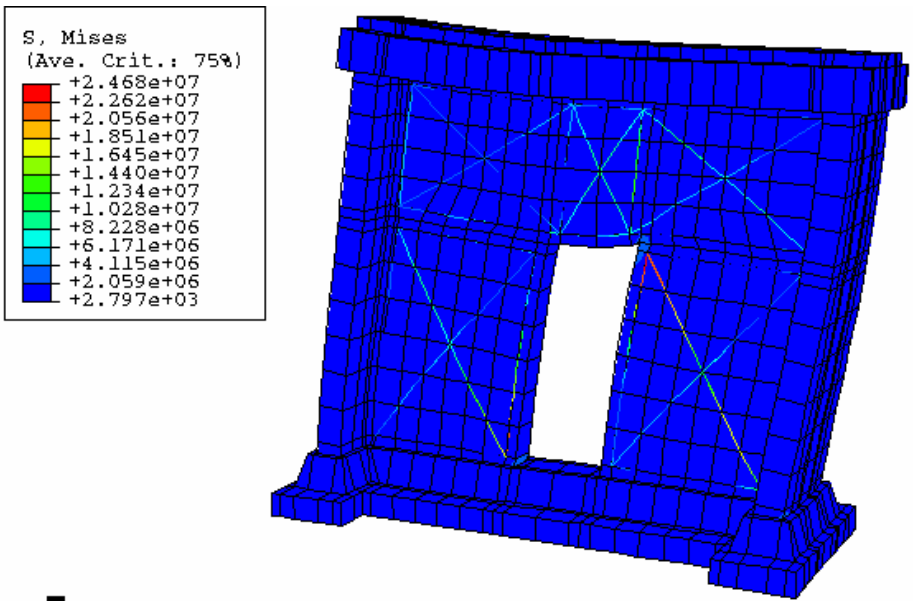

Figure 8.7. Stress contour plot of URM Wall Unit-2

A series of elastic analysis was conducted using ABAQUS and ETABS program which is common program in Indonesia. A reduction in E_m value (E_m = 6567.7 MPa) was applied to match the analysis and experiment result. The variety of E_m value from 20 samples give the coefficient of variation is 46.63% (E_m minimum = 2056.4 MPa and E_m maximum = 13911.0 MPa). Close correlation of the lateral top displacement between experiment and analysis was reported in Table 8.2. and shown in Figure 8.8.

Table 8.2. Comparison lateral top displacement between experiment and elastic analysis

Lateral Load (ton)	Lateral Disp. (mm)	ABAQUS v. 6.5 Lateral Displ.(mm) (E = 6567.7 MPa)		ETABS v. 9.11 Lateral Displ.(mm) (E = 6567.7 MPa)		Lateral Displ.(mm) (E' = 80% E)		Lateral Disp.(mm) (E = 60% E)	
0	0	0	(*)	0	(*)	0	(*)	0	(*)
24.96	1	0.632	(37%)	0.653	(35%)	0.800	(20%)	1.017	(2%)
26.36	1.01	0.666	(34%)	0.6897	(32%)	0.844	(16%)	1.073	(6%)
30.25	1.4	0.762	(46%)	0.7917	(43%)	0.965	(31%)	1.227	(12%)
30.42	1.405	0.766	(45%)	0.7961	(43%)	0.971	(31%)	1.234	(12%)
34.22	2.005	0.86	(57%)	0.8957	(55%)	1.089	(46%)	1.385	(31%)
34.38	2.125	0.864	(59%)	0.8999	(58%)	1.094	(48%)	1.391	(35%)
35.75	3.02	0.897	(70%)	0.9358	(69%)	1.137	(62%)	1.446	(52%)
36.91	3.03	0.925	(69%)	0.9662	(68%)	1.174	(61%)	1.492	(51%)
37.71	4.605	0.945	(79%)	0.9872	(79%)	1.199	(74%)	1.524	(67%)
38.38	4.53	0.962	(79%)	1.0219	(77%)	1.219	(73%)	1.550	(66%)
42.41	7.695	1.06	(86%)	1.1104	(86%)	1.345	(83%)	1.711	(78%)

Note : (*) percentage difference of lateral displacement between computer analysis and experiment

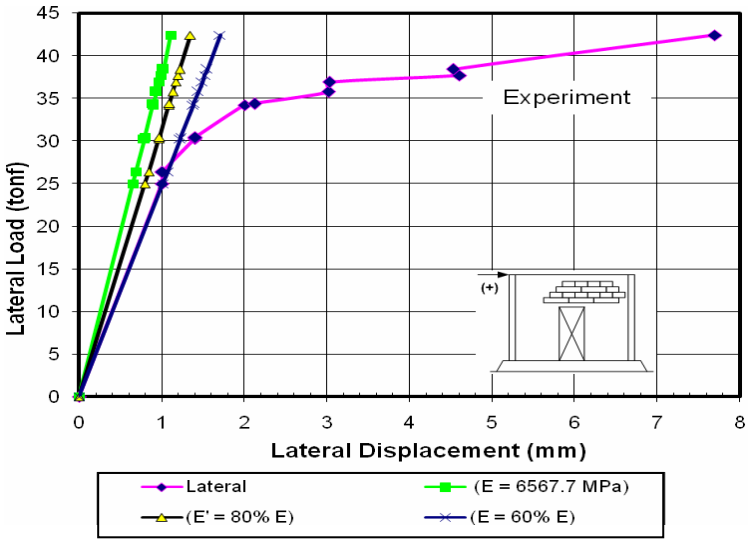

Figure 8.8. Comparison lateral top displacement between experiment and ETABS elastic analysis

8.5. RESPONSE CALCULATED OF URM WALL WITH CURRENT SEISMIC ASSESSMENT STANDARD

A structural analysis model was developed to calculate the strength and the performance of URM Wall Unit-1. The method was referred to FEMA 306, 1999, for the seismic assessment analysis of unreinforced masonry wall. It was used to determine the lateral resistance of URM Wall Unit-1 and compared to the test result. It was observed from the test result that the spandrel is not damaged; therefore the URM wall unit-1 was representing weak piers and strong spandrel. Evaluation procedures for in-plane behaviour of piers in walls with weak pier – strong spandrel mechanism referred to FEMA 306, 1999 in three-step process as follows :

Step 1 : Calculate capacities for individual behaviour modes

a. Rocking (V_r):

$$V_r = 0.9\ \alpha\ P_{CE}\ (l_w/h_{eff}) \quad \text{..... (8.1)}$$

Where α factor equal to 0.5 for fixed-free cantilever wall, or equal to 1.0 for a fixed-fixed pier wall. P_{CE} is expected vertical axial compressive force per load combination in FEMA 273 (ATC,1997a).

b. Bed joint sliding with bond plus friction (V_{bjs1}) :

$$V_{bjs1} = \nu_{me}\ A_n \quad \text{..... (8.2)}$$

Bed joint sliding with friction only (V_{bjs2}) :

$$V_{bjs2} = \nu_{friction}\ A_n \quad \text{..... (8.3)}$$

$$V_{bjs2} = [0.75(P_{CE}/A_n)/1.5][A_n] = 0.5\ P_{CE} \quad \text{..... (8.4)}$$

c. Diagonal tension (V_{dt})

$$V_{dt} = f'_{dt} A_n (\beta)(1+f_{ae}/f'_{dt})^{1/2} \quad \text{..... (8.5)}$$

Where β factor equal to 0.67 for $l/h_{eff} < 0.67$, 1.0 for $l/h_{eff} > 1.0$ and interpolation β value when $0.67 \leq l/h_{eff} \leq 1.0$

d. Toe crushing (V_{dt})

$$V_{tc} = \alpha\ P_{CE}\ (l_w/h_{eff})\ (1-f_{ae}/0.7f'_{me}) \quad \text{..... (8.6)}$$

Step 2 : Determine predicted behaviour mode and capacity

The pier aspect ratio of URM wall Unit-1 is 0.71 which is lower than 1.25 and the lowest capacity of the pier wall between V_r, V_{bjs1}, V_{dt} and V_{tc} will be predicted the damage of the pier wall. The lowest value is V_{dt} and conclude the behaviour of URM wall Unit-1 preemptive diagonal tension.

Table 8.3. Predicted pier capacity of URM wall Unit-1 based on FEMA 273, 1997

No	Individual Behaviour Modes	Predicted Pier Capacity	Value in kN
1	Rocking (V_r)	$V_r = 0.9\ \alpha\ P_{CE}\ (l_w / h_{eff})$	214
2	Bed joint sliding with bond plus friction (V_{bjs1})	$V_{bjs1} = \nu_{me}\ A_n$	351
	Bed joint sliding with friction only (V_{bjs2})	$V_{bjs2} = \nu_{friction}\ A_n$ $V_{bjs2} = [0.75(P_{CE}/A_n)/1.5][A_n]$ $= 0.5\ P_{CE}$	145
3	Diagonal tension (V_{dt})	$V_{dt} = f'_{dt} A_n (\beta)(1+f_{ae}/f'_{dt})^{1/2}$	196
4	Toe crushing (V_{tc})	$V_{tc} = \alpha\ P_{CE}\ (l_w / h_{eff})\ (1-f_{ae}/0.7f'_{me})$	227

Step 3 : Compare predicted mode with observed field damage

The predicted diagonal tension crack from step 2 was consistent with the crack pattern of URM wall Unit-1 result.

8.6. CONCLUSIONS

1. The elastic analysis of the ABAQUS program and also ETABS program were performed by comparison between the numerical prediction results with the experimental performances from URM wall unit-1 and unit-2. The parameter data for masonry was taken from a series of tests conducted at the Bandung laboratory that explained in Chapter 3. The initial elastic top lateral displacement analysis of Unit-1 and Unit-2 can be predicted well enough after E_m value calibrated with 60% scale factor. Lateral loading in the computer analysis was based on the force-deformation curves for monotonic loading that represents the envelope curve that obtained for quasi-static reverse cyclic loadings, neglecting the hysteretic loops. Furthermore the stress contours obtained from a series elastic analysis in the ABAQUS results for URM wall unit-1 and unit-2 give an early indication that the maximum stress flows quite similar with crack propagation. It can be seen that cracks started from the corners of the door opening and propagated diagonally.

2. Finite element models to simulate the elastic structural performance of URM walls have been described and compared with the test results. These include the maximum top lateral displacements and von-Mises stress curves. The material model in the FEM model is assumed as isotropic one, while in the reality masonry wall are contained masonry units and mortar (anisotropic). Nevertheless, that inhomogeneous of materials had no significant effect on FEM analysis. Both units were validated using macro modeling. The results from the finite element analyses show that the finite element model has now reached a state where it is possible to obtain a realistic result.

3. The quality of the finite element analysis not always depend on the model assumptions but also associated with the accuracy of getting the material properties of the masonry that used. It was studied that FEMA 306, 1999, can be used as an initial prediction of the URM wall performance. This basic procedure is quite simple and quite accurate.

CHAPTER 9 :
CONCLUSIONS AND RECOMMENDATIONS

9.1 CONCLUSIONS

Many considerations have been given to answer the concerns about the assessment, improvement and strengthening of URM walls at existing buildings located in seismic prone areas. The behaviour of URM-walls is highly influenced by the quality of the local raw material used in the manufacturing of the clay-bricks, the aggregate quality of the mortar composition, the stacking of clay-bricks and, the dominating influence of the quality of the local mason's workmanship. To obtain a test result that will be able to represent the local conditions where the URM-buildings of interest in this thesis, experiments have been conducted in Indonesia using local materials and local labours. An old Dutch building of three storeys constructed in 1902 was used as a model representing many similar existing buildings which are still found in many big cities in Indonesia and all over the world.

Two 75%-scale URM walls were constructed and subjected to combinations of gravity and lateral loads. Test Unit-1 was a URM-wall representing an existing structural condition and Test Unit-2 was the similar URM wall strengthened by Kevlar fibre. Both URM walls were subjected to combinations of constant axial forces and a series of cyclic lateral load reversals of increasing the top displacement of the URM-wall. Both were tested until failure under in-plane condition. Each of the URM wall specimens was perforated with a door opening representing typical URM walls of many aged masonry buildings in Indonesia. The specimens were constructed with a one and half wythe of Dutch bond configuration. Two features were taken into account. First, it accommodated the influence of flanged wall and second, the URM wall was built on the stone foundation.

These specimens seem to be the largest of its kind which have ever been tested to study the behaviour of traditional masonry walls with a door opening. A series of comprehensive analytical studies using the ABAQUS computer program were also carried out to back up the experimental work. The modeling of these masonry walls was a very important learning

process which would definitely give a significant contribution to many practicing engineers dealing with masonry walls.

Some conclusions can be drawn based on these test results and the outcome of analytical studies carried out to accompany the experiments. The concluding remarks are as follows:

1. It was clearly from the performance of the test results that the URM wall Unit-1 did not behave as a brittle structure. It could dissipate energy without loss of strength even after both pier walls failed in a shearing mode. The apparently ductile performance of the URM wall Unit-1 had a post-elastic behaviour in terms of "overall displacement ductility" value of around 8 to 10 with the maximum drift up to 0.52% measured at the final cycle. As predicted, the masonry material was variable and non homogeneous which caused the hysteresis loop to be non symmetrical between push and pull lateral load directions. Simplification is necessary for numerical analysis.

2. The effectiveness of the flanged wall increased the stiffness and the flexural strength of each pier especially when the flanged wall is in the tensile condition. It was noted that the bed joint crack started at one fourth to one third of the flanged pier walls height. The crack pattern at the URM wall unit-1 was representing weak piers and strong spandrel which is a common performance observed in aged existing URM buildings after an earthquake has occurred. The masonry piers, with aspect ratio l_w/h_{eff} is 0.71, failed in a shearing mode as was evidenced by the shear cracks in both piers. Evaluation procedures based on FEMA 306-1999 confirmed the performance of the URM Unit-1 as demonstrated by the test result.

3. It can also be concluded from this test, when the demand forces has been exceeded its elastic capacity, the URM wall will experience significant damage and any retrofitting effort would almost be impossible to be done. With regard to the existing URM buildings in the seismic prone areas, assessment and improvement analyses need to be made as to whether the residual strength would still be capable of resisting predicted seismic forces in accordance with the current seismic code. Improvement or strengthening is mandatory, if the demand forces exceed its capacity forces.

4. External application of Kevlar fibre material at both faces of the URM wall Unit-2 has demonstrated :
   - Improved the in-plane capacity of URM wall Unit-2. The lateral resistance was enhanced by about 75% when compared to Unit-1.
   - Localized and significantly reduced crack patterns. Bed joint cracks just occurred outside the Kevlar application area.
   - The maximum drift up to 0.814% was measured at the final cycle
   - The configuration of Kevlar fibre which was applied to the URM wall Unit-2 changed the performance of both piers from a shear mode to a rocking mode before the Kevlar fibre started tearing from the existing bolt holes and along the fibre direction at the higher lateral loading and reduced the diagonal tensile capacity of both piers drastically.

   It can be summarized that Kevlar fibre strengthening technique is promising and with great ease of installation. Although Kevlar material is more expensive when compared to other fabrics as long as it was applied at the essential locations and in limited volumes, it can significantly increase the in-plane URM wall capacity. With appropriate arrangements of Kevlar fibre, a practicing engineer will be able to obtain a desired rocking mechanism in the masonry structure.

5. A series of comprehensive finite element analyses in elastic condition were conducted using the ABAQUS computer programme. For this purpose, a structural modelling incorporating all related properties was set up for representing the masonry walls. The simpler monotonic models still can be considered as tools which can be used for assessment in the current practice. This finding is very useful for practicing engineers in predicting the seismic performance of existing traditional masonry walls, especially those with a door opening.

9.2 RECOMMENDATIONS FOR FURTHER RESEARCH

1. These experiments have only been carried out for an in-plane URM wall under quasi-static-reversed cyclic lateral loading. There is a need for further research of the dynamic

performance of URM walls using local material and local mason. Another consideration should be also conducted to cover the out-of-plane performances.

2. More work needs to be conducted to investigate in more detail the effect of total lateral displacements, i.e. flexure, shear, sliding and rocking displacements by putting more transducers along the URM wall height.

3. Further study needs to be done to evaluate the effect of different floor systems which are usually used in the existing colonial buildings such as wooden floors, arch clay brick floors, concrete floors, and in particular the connections to the masonry walls in 3-D experiment models and also in the computer modelling.

4. Different Kevlar fibre configurations to get more efficiency in preventing the URM pier walls from forming shear cracks under rocking modes still requires further investigation. It was observed from the test results, that the anchorage of the Kevlar layers on both faces at bolted connection becomes a weak point, see chapter 6.2.1. A kind of anchorage system should be studied to avoid any tear off along the fibre direction at the higher lateral force and also a slip stopper needs to be provided at the bottom of both pier walls, in order to prevent any sliding of the pier-walls

5. Further non-linear analysis needs to be conducted for both models and also study the right model of the interface surface joint between Kevlar fibre and masonry element in the Finite element analysis, see chapter 8.3.4.

6. The occurrence of earthquakes in several areas of Indonesia recently has raised some questions regarding the safety and reliability of all URM building stocks in Indonesia. This phenomenon has initiated to prepare the basic procedure in assessment the existing URM building stock with local experiments that represents the region.

REFERENCES

[A1] Abrams, D.P. and Shah, N., 1992, Cyclic Load Testing of Unreinforced Masonry Walls, *Advanced Construction Technology Center Report #92-26-10*, College of Engineering, University of Illinois at Urbana-Champaign, USA, 45 p.

[A2] Abrams, D.P. and Calvi, G.M., 1994, Proceedings of the US-Italy Workshop on Guidelines for Seismic Evaluation and Rehabilitation of Unreinforced Masonry Buildings, *National Center for Earthquake Engineering Research, Technical Report NCEER-94-0021*, State University of New York at Buffalo.

[A3] Al-Chaar, G.K., and Hasan, H.A., 1999, Seismic Testing and Dynamic Analysis of Masonry Bearing and Shear Walls Retrofitted with overlay Composite, *ICE '99*, Cincinnati, May 10-12,1999

[A4] Alcocer, S.M. and Klinger, R.E., 1994, Masonry Research in the Americas, *Masonry in the Americas*, American Concrete Institute, SP-147, pp. 127-169

[A5] Allen, E., 1985, Fundamental of Building Construction – Material and Method, *John Willey and Sons*, pp. 242-317

[A6] Ambrose, J., 1991, Simplified Design of Masonry Structures, *John Wiley & Sons, Inc*. 201 pp.

[A7] Anand, S.C. and Rahman, M.A., 1994, Accurate Estimation of Interface Shear Stresses in Composite Masonry Walls, *Journal of Structural Engineering*, ASCE, Vol. 120, No. 3, pp. 998-1015

[A8] Anand, C. and Rahman, M.A., 1991, Numerical Modeling of Creep in Composite Masonry W*all*, *Journal of Structural Engineering***,** Vol. 177, No. 7, pp. 2149 - 2165

[A9] Andreaus, U., 1996, Failure Criteria for Masonry Panels Under In-Plane Loading, *Journal of Structural Engineering*, ASCE, Vol. 122, No. 1, pp. 37-46

[A10] Anthonie, A., Magenes, G and Magonette, G., 1994, Shear-Compression Testing and Analysis of Brick Masonry Walls, *Procccedings of The 10th European Conference on Earthquake Engineering*, Vienna – Austria

[A11] Aprile, A., Benedetti, A. and Grassucci, F., 2001, Assessment of Cracking And Collapse for Old Brick Masonry Columns, *Journal of Structural Engineering*, ASCE, Vol. 127, No. 12, pp. 1427-1435

[A12] Ali, S. and Page, A.W., 1988, Concentrated Loads on Solid Masonry Wall-a Parametric Study and Design Recommendations, *Proceeding Institution of Civil Engineers*, Part 2, pp. 271–289

[A13] ASTM (American Society for Testing and Materials), 1996, Test Method for Compressive Strength of Cylindrical Concrete Specimens, ASTM C39-1996, West Conshohocken, Pa.

[A14] ASTM, 1998, Standard Terminology Relating to Lime and Limestone, ASTM C51-1998, West Conshohocken, Pa.

[A15] ASTM, 1998, Standard Test Methods of Sampling and Testing Brick and Structural Clay Tile, ASTM C67-1998, West Conshohocken, Pa.

[A16] ASTM, 1988, Compressive Strength of Hydraulic Cement Mortars, ASTM C109-1988, West Conshohocken, Pa.

[A17] ASTM, 1989, Specification for Aggregate for Masonry Mortar, ASTM C114-1989, West Conshohocken, Pa.

[A18] ASTM, 1997, Specification for Portland Cement, ASTM C150-1997, West Conshohocken, Pa.

[A19] ASTM, 1999, Specification for Hydrated Lime for Masonry Purposes, ASTM C207-1999, West Conshohocken, Pa.

[A20] ASTM, 1999, Specification for Mortar for Unit Masonry, ASTM C270-1999, West Conshohocken, Pa.

[A21] ASTM, 1997, Standard Specification for Moist Cabinets, Moist Rooms, and Water Storage Tanks Used in the Testing of Hydraulic Cements and Concretes, ASTM C511-1997, West Conshohocken, Pa.

[A22] ASTM, 1997, Practice for Preparing Precision Statements for Test Methods for Construction Materials, ASTM C670-1997, West Conshohocken, Pa.

[A23] ASTM, 1996, Methods for Preconstruction and Construction Evaluation of Mortars for Masonry, ASTM C780-1996, West Conshohocken, Pa.

[A24] ASTM, 1997, Standard Practice for Petrographic Examination of Hardened Concrete, ASTM C856-1997, West Conshohocken, Pa.

[A25] ASTM, 1986, Test Methods for Bond Strength of Mortars to Masonry Units, ASTM C952-1986, West Conshohocken, Pa.

[A26] ASTM, 1984, Standard Test Method for Splitting Tensile Strength of Masonry Units , ASTM C1006-1984, West Conshohocken, Pa.

[A27] ASTM, 2000, Standard Test Method for Measurement of Masonry Flexural Bond Strength, ASTM C1072-2000, West Conshohocken, Pa.

[A28] ASTM, 1996, Standard Test Method for Portland-Cement Content of Hardened Hydraulic-Cement Concrete, ASTM C1084-1996, West Conshohocken, Pa.

[A29] ASTM, 1997, Terminology of Mortar for Unit Masonry, ASTM C1180-1997, West Conshohocken, Pa.

[A30] ASTM, 1998, Standard Method for Constructing and Testing Masonry Prisms Used to Determine Compliance with Specified Compressive Strength of Masonry, ASTM C1314-1998, West Conshohocken, Pa.

[A31] ASTM, 1997, Specification for Wire-Cloth Sieves for Testing Purposes, ASTM E11-1997, West Conshohocken, Pa.

[A32] ASTM, 1997, Test Method for Young's Modulus, Tangent Modulus, and Chord Modulus, ASTM E111-1997, West Conshohocken, Pa.

[A33] ASTM, 2002, Standard Test Measures for Flexural Bond Strength of Masonry, ASTM E518-2002, West Conshohocken, Pa.

[A34] ACI 530/ASCE5/TMS 402-02, Building Code Requirements for Masonry Structures, Masonry Standards Joint Committee, *American Concrete Institute, American Society of Civil Engineers and The Masonry Society*, Detroit, New York and Colorado, 2002

[A35] Arya, A.S., 1988, Repair and Strengthening of Damaged Stone Houses After Dhamar Earthquake of Dec. 1982, *Proceedings of Ninth World Conference on Earthquake Engineering*, Tokyo-Kyoto, Japan (Vol. VIII), pp. 1141–1146.

[A36] Arya, A. S., 1992, *Masonry and Timber Structures including Earthquake Resistant design*, Nem Chand & Bros., Roorkee, India.

[B1] Badoux, M., Elgwady, M. A., Lestuzzi, P., 2002, Earthquake Simulator Tests on Unreinforced Masonry Walls before and after Upgrading with Composites, *Proceedings of 12th European Conference on Earthquake Engineering*, Paper Ref. 862, Elsevier Science Ltd.

[B2] Basoenondo, E.A., L., Thambiratman, D.P. and Purnomo, H., 2003, Study on The Effect of Surface Mortared Confinement to The Improvement of Lateral Stiffness of Masonry Wall Panels Under Lateral Loading, *Proceedings of the Ninth North American Masonry Conference,* Clemson, South Carolina USA, pp. 370-380.

[B3] Binda, L., Baronio, G., Fontana, A. and Frigerio, G., 1987, Experimental Study on Decayed Brick-Masonry Strengthened by Grouting, *Evaluation and Retrofit of Masonry Structures, Joint USA-Italy Workshop,* pp. 111-122.

[B4] Binda, L., Baronio, G. and Fontana, A., 1990, Strengthening and Durability of Decayed Brick-Masonry Repaired by Injections, *Proceedings of the Fifth North American Masonry Conference,* University of Illinois at Urbana-Champaign, Vol. 2, pp. 839-852.

[B5] Binda, L., Modena, C. and Baronio, G., 1993, Strengthening of Masonries by Injection Technique, *Proceedings of the Sixth North American Masonry Conference,* Drexel University, Philadelphia, Vol. 1, pp. 1-14.

[B6] Beca Carter, 1981, Masonry Testing, *Indonesian Earthquake Study*, Volume 7, November 1981.

[B7] Benedetti, D., Carydis, P. and Pezzoli, P., 1998, Shaking Table Tests on 24 Simple Masonry Buildings, *Earthquake Engineering and Structural Dynamics*, Vol. 27, pp. 67-90.

[B8] Bonneville, D.R. and Cocke, D.W., 1991, Effectiveness of Limited Seismic Strengthening Of Unreinforced Masonry Buildings, *Proceedings 60th Annual Convention Structural Engineers Association of California*, Palm Springs, California.

[B9] Breiholz, D.C., 1992, Centre Core Seismic Hazard Reduction Systems for URM Buildings, *Proceedings of the Tenth World Conference on Earthquake Engineering*, Vol. 9, pp. 5395-5399.

[B10] Brencich, A. and Lagomarsino, S., 1997, A Macroelement Dynamic Model for Masonry Shear Walls, *Proceedings of the Fourth International Symposium on Computer Methods in Structural Masonry*, Florence, Italy.

[B11] British Standards Institution, 1992, BS-3921 : Specifications for Clay Bricks, *BSI*, London

[B12] British Standards Institution, 1992, BS-5628 : Code of Practice for Use of Masonry; Part 1 : Structural Use of Unreinforced Masonry, *BSI*, London

[B13] Bruneau, M., 1994, State-of-The-Art Report on Seimic Performance of Unreinforced Masonry Buildings, *Journal of Structural Engineering*, Vol. 120, No 1, pp. 230-251.

[B14] Bruneau , M. and Saatcioglu, M., 1994, Behavior of Unreinforced Masonry Structures During the 1992 Erzincan, Turkey Earthquake, *Fifth US National Conference on Earthquake Engineering Proceeding,* Volume III, pp. 409-418.

[B15] Bruneau, M., 1995, Damage to Masonry Buildings from the 1995 Hansin-Awaji Earthquake-Preliminary Report, *Proceedings of the Seventh Canadian Masonry Symposium*, Vol.1, pp 84-95.

[C1] Calvi, G.M. and Magenes, G., 1994a, Experimental Research on Response of URM Building System*, Proceedings of the U.S.-Italy Workshop on Guidelines for Seismic Evaluation and Rehabilitation of URM Buildings*, Pavia, Technical Report NCEER-94-0021, National Centre for Earthquake Engineering, Buffalo, pp 3.41-3.57.

[C2] Calvi, G.M. and Magenes, G., 1994b, Experimental Results on Unreinforced Masonry Shear Walls Damaged and Repaired*, Proceedings of the Tenth International Brick and Block Masonry Conference*, Vol. 2, pp 509-518.

[C3] Calvi, G.M., Kingsley, G.R. and Magenes, G., 1996, Testing of Masonry Structures for Seismic Assessment*, Journal of Earthquake Spectra*, Volume 12, No. 1, pp. 145-162.

[C4] Corrêa, M.R.S. and Page, A.W., 2003, Experimental Study of Masonry Walls With Opening, *Proceedings of the Ninth North American Masonry Conference,* Clemson, South Carolina USA, pp. 896-907.

[C5] Costley, A.C. and Abrams, D.P., 1995, Dynamic Response of Unreinforced Masonry Buildings with Flexible Diaphragms, *Structural Research Series Report No. 605*, Department of Civil Engineering, University of Illinois at Urbana-Champaign, October 1995, 281 p.

[C6] Crisafulli, F.J., Carr, A.J. and Park, R., 1995, Shear Strength of Unreinforced Masonry Panels, *Proceedings of The Pacific Conference on Earthquake Engineering, Volume 3,* Melbourne, Australia, pp 77-86

[C7] Crisafulli, F.J., 1997, Seismic Behaviour of Reinforced Concrete Structures with Masonry Infills, *PhD thesis*, Department of Civil Engineering, University of Canterbury, New Zealand, 404 p

[D1] Dhanasekar, M., Page, A.W., and Kleeman, P.W., 1984, A Finite Element Model for The Inplane Behaviour of Brick Masonry, *9th Australasian Conference Mechanic of Structures and Materials*, Sydney, August 1984, pp 262-267

[D2] Dhanasekar, M., Kleeman, P.W. and Page, W., 1985, Biaxial Stress-Strain Relations for Brick Masonry, *Journal of Structural Engineering*, Vol. 111, No. 5, pp. 1085–1100

[D3] Doherty, K. T., 2000, An Investigation of the Weaklinks in the Seismic Load Path of Unreinforced Masonry Buildings*, PhD Thesis*, Faculty of Engineering, University of Adelaide, Australia.

[D4] Drysdale, R.G., Hamid, A.A., and Baker, L.R., 1994, Masonry Structures, Behavior and Design, *Prentice Hall Inc.*, Englewood Cliffs, 784 p.

[E1] Ehsani, M.R. and Saadatmanesh, H., 1996, Seismic Retrofitting of URM Walls with Fiber Composites, *The Masonry Society Journal*, pp. 63–72.

[E2] Ehsani, M.R., Saadatmanesh, H. and Al-Saidy, A., 1997, Shear Behaviour of URM Retrofitted With FRP Overlays, *Journal of Composites for Construction*, ASCE, 1 (1), pp. 17–26

[E3] Ehsani, M.R., Saadatmanesh, H., & Velazquez-Dimas, J.I., 1999, Behavior of Retrofitted URM Walls Under Earthquake Loading, *Journal of Composites for Construction*, ASCE, pp. 134–142

[E4] Elgawady, M., Lestuzzi, P., & Badoux, M., 2004, Dynamic Versus Static Cyclic Tests of Masonry Walls Before and After Retrofitting With GFRP, *Proceedings of the 13th World Conference on Earthquake Engineering*, Vancouver – Canada, Paper N0. 2913.

[F1] Fattal, S.G., and Cattaneo, L.E., 1977, Evaluation of Structural Properties of Masonry in Existing Buildings, *National Bureau of Standards*, Department of Commerce, Washington.

[F2] Fattal, S.G., 1994, The Capacity of Unreinforced Masonry Shear Walls Under Membrane Loads, *5th US National Conference on Earthquake Engineering Proceeding*, Volume III.

[F3] Federal Emergency Management Agency, 1992, Handbook of Techniques for the Seismic Rehabilitation of Existing Buildings, *FEMA-172*, Building Seismic Safety Council, Washington, DC

[F4] Federal Emergency Management Agency, 1992, NEHRP Handbook for the Seismic Evaluation of Existing Buildings, *FEMA-178*, Building Seismic Safety Council, Washington, DC

[F5] Federal Emergency Management Agency, 1997, NEHRP Guidelines for The Seismic Rehabilitation of Buildings, *FEMA Publication 273*, Washington D.C.

[F6] Federal Emergency Management Agency, 1997, NEHRP Commentary on the Guidelines for The Seismic Rehabilitation of Buildings, *FEMA Publication 274*, Washington D.C.

[F7] Federal Emergency Management Agency, 1999, Evaluation of Earthquake Damaged Concrete and Masonry Wall Buildings, Basic Procedures Manual, *FEMA Publication 306*, Washington D.C.

[F8] Federal Emergency Management Agency, 1999, Evaluation of Earthquake Damaged Concrete and Masonry Wall Buildings, Technical Resources, *FEMA Publication 307*, Washington D.C.

[F9] Federal Emergency Management Agency, 1999, Repair of Earthquake Damaged Concrete and Masonry Wall Buildings, *FEMA Publication 308*, Washington D.C.

[F10] Fujiwara, T., Sato, T., Kubo, T., Murakami, H. O., 1989, *Reconnaissance Report on the 21 August 1988 Earthquake in The Nepal-India Border Region*, Japanese Ministry of Education, Science and Culture (Grant No. 63115017), Japanese Group for the Study of Natural Disaster Science.

[G1] Gambarotta, L., Lagomarsino, S. and Morbiducci, R., 1994, Brittle-Ductile Response of In-plane Loaded Brick Masonry Walls, *Proceedings of the 10th European Conference on Earthquake Engineering*, Vienna Austria, Volume 3, pp. 1663 – 1668

[G2] Gambarotta, L. and Lagomarsino, S., 1997, Damage Models for The Seismic Response of Brick Masonry Shear Walls. Part I : The Mortar Joint Model and Its Applications, *Earthquake Engineering and Structural Dynamics*, Vol. 26, by John Wiley & Sons, Ltd., pp. 423 – 439

[G3] Gambarotta, L. and Lagomarsino, S., 1997, Damage Models for The Seismic Response of Brick Masonry Shear Walls. Part II : The Continuum Model and Its Applications, *Earthquake Engineering and Structural Dynamics*, Vol. 26, pp. 441 – 462

[G4] Ganz, H.R., 1993a, Strengthening of Masonry Structures with Post-Tensioning, *Proceedings of the Sixth North American Masonry Conference*, Philadelphia, pp. 645-655.

[G5] Ganz, H.R., 1993b, Recent Experience with Post-Tensioned Masonry in Switzerland, *Proceedings of the Sixth North American Masonry Conference*, Philadelphia, pp. 657-667.

[G6] Gavarini, C., 1988, An Attempt for a New Definition of Seismic Vulnerability of Masonry Buildings, *Proceedings of Ninth World Conference on Earthquake Engineering*, Tokyo-Kyoto, Japan (Vol. VIII), pp. 1147–1152

[G7] Gurley, C.R. and Nicholls, J.S.F., 1982, Earthquake Strengthening of Old Masonry with Reference to the Auckland Ferry Building, *Bulletin of The New Zealand National Society for Earthquake Engineering*, Vol. 15, No 4, pp. 199-215

[H1] Hamid, A.A., Drysdale, R.G., and Heidebrecht, A.C., 1979, Shear Strength of Concrete Masonry Joins, *Journal of Structural Engineering*, Vol. 105, No. ST7, pp. 1227–1241

[H2] Hart, G.C., Holmes, W.T. and Poland, C.D., 1994, Typical Costs of Seismic Rehabilitation of Building, *Proceeding of 5th US National Conference on Earthquake Engineering,* Volume III, pp. 881-891

[H3] Hart, G.C. and Elhassan, R.M., 1994, Base Isolation a Tall Historic Unreinforced Masonry Building, *Proceeding of 5th US National Conference on Earthquake Engineering*, Volume III, pp 931-940

[H4] Hendry, A.W., Sinha, B.P and Davies, S.R., 1997, Design of Masonry Structures, *Third Edition of Load Bearing Brickwork Design*, E&FN Spoon, UK

[H5] Hibbit, Karlsson and Sorensen, Inc., 2004, ABAQUS/Standard User's and Theory Manuals, *Ver. 6.5*, USA

[H6] Hilsdorf, H.K., 1967, Investigation Into the Failure Mechanism of Brick Masonry Loaded in Axial Compression*, International Conference on Masonry Structural Systems,* University of Texas, Austin.

[H7] Holberg, A.M., and Hamilton, H.R., 2002, Strengthening URM with GFRP Composites and Ductile Connections*, Journal of Earthquake Spectra*, Volume 18, No. 1, pp. 63-84.

[H8] Hopkins, D.C. and Robertson, T.W., 1981, Earthquake Risk Buildings - Lessons from Experience, *Bulletin of NZNSEE*, Vol. 14, No 2

[H9] Hutchison, D.L., Yong, P.M.F. and McKenzie, G.H.F., 1984, Laboratory Testing of a Variety of Strengthening Solutions for Brick Masonry Walls, *Proceedings of the Eighth World Conference on Earthquake Engineering*, Vol. 1, pp 575-582.

[I1] International Conference of Building Officials (ICBO), 1997, "Uniform Building Code Chapter 21 Masonry", *California Building Standards Commission*, Whittier, California

[I2] International Code Council (ICC), 2003, "International Building Code (UBC) Chapter 21 Masonry", *International Code Council Inc.*, Falls Church, Virginia

[J1] Jain, L.C. and Koopmans, A., 1979, Some Observations on Brick and Tile Industry Near Jakarta*, Technical Paper No. 48*, United Nations Indonesia, Bandung, 17 p

[J2] Jain, L.C., 1979, Problems of Brick And Tile Industry In Indonesia, *Technical Paper No. 50*, United Nations Indonesia, Bandung, 21 p

[J3] Juhásová, E., Labák, P. and Juhás, P. , 2004, The Masonry in Areas of Moderate Seismicity, *Proceedings of the 13th World Conference on Earthquake Engineering*, Vancouver – Canada, Paper N0. 2548.

[K1] Kahn, L.F., 1984, Shotcrete Retrofit for Unreinforced Brick Masonry, *Proceedings of the 8th World Conference on Earthquake Engineering*, Volume 1, pp. 583 – 590

[K2] Kapos, A.J., Penelis, G.G. and Drakopoulos C.G., 2002, Evaluation of Simplified Models for Lateral Load Analysis of Unreinforced Masonry Buildings, *Journal of Structural Engineering*, Vol. 128, No. 7, pp. 890 – 897

[K3] Karantoni, F.V. and Fardis, M.N., 1992, Computed Versus Observed Seismic Response and Damage of Masonry Buildings, *Journal of Structural Engineering*, Vol. 118, No. 7, pp. 1804 – 1821

[K4] König, G., Mann, W. and Ötes, A., 1988, Experimental Investigations on The Behaviour of Unreinforced Masonry Walls Under Seismically Induced Loads and Lessons Derived, *Proceedings of Ninth World Conference on Earthquake Engineering*, Tokyo-Kyoto, Japan (Vol. VIII), pp. 1117–1122

[L1] Lam, N.T.K., Wilson, J.L. and Hutchinson, G.L., 1995, The Seismic Resistance of Unreinforced Masonry Cantilever Walls in Low Seismicity Areas, *Bulletin of The New Zealand National Society for Earthquake Engineering*, Volume 28, No. 3

[L2] Laurenço, P.B., Rots, J.G. and Blaaauwendraad, J., 1998, Continuum Model For Masonry : Parameter Estimation and Validation, *Journal of Structural Engineering*, June 1998, pp. 642-652

[L3] Lenczner, D., 1972, Element of Load Bearing Brickwork, *Pergamon Ltd.*, Oxford, England

[L4] Livesley, R.K., 1992, A Computational Model for The Limit Analysis of Three-Dimensional Masonry Structures, *Masonry Construction, Structural Mechanics and Other Aspects*, Maccanica, Volume 27, No. 3, pp. 161–172

[L5] Lotfi, H.R., and Shing, B., 1994, Interface Model Applied to Fracture of Masonry Structures, *Journal of Structural Engineering*, January 1994, Vol. 120, No. 1, pp. 63-80

[M1] Magenes, G. and Calvi, G.M., 1997, In-Plane Seismic Response of Brick Masonry Walls, *Earthquake Engineering Structural Dynamics*, Volume 26, pp. 1091–1112

[M2] Mann, W. and Mûller, H., 1982, Failure of Shear-Stressed Masonry An Enlarge Theory, Tests and Application to Shear Walls, *Proceedings – British Ceramic Society*, pp. 223-235

[M3] Manzouri, T., Schuller, M.P., Shing, P.B. and Amadei B., 1996, Repair and Retrofit of Masonry Structures, *Journal of Earthquake Spectra*, Volume 12, No. 4, pp. 903-921

[M4] Marshall, O.S., Sweeney, S.C. and Trovillion, J.C., 1999, Seismic Rehabilitation of Unreinforced Masonry Walls, *Fourth International Symposium on Fiber Reinforced Polymer Reinforcement for Reinforced Concrete Structures*, Baltimore.

[M5] Mendola, L.L. and Papia, M., 1993, Stability of Masonry Piers Under Their Own Weight and Eccentric Load, *Journal of Structural Engineering*, Volume 119, No. 6, pp. 1678–1693

[N1] Nagel, R.B. and Yong, P.M.F., 1984, Masonry Strength Evaluation of Five Existing Buildings Case Studies, *Central Laboratories Report No. 5-84/5*, Ministry of Works and Development, New Zealand, 70 p.

[N2] Naraine, K. and Sinha, S., 1991, Cyclic Behavior of Brick Masonry Under Biaxial Compression, *Journal of Structural Engineering*, Vol. 117, No. 5, pp. 1336–1355

[N3] Nash, W.G., 2001, Brickwork, *Volume 1, 2 and 3*, Nelson Thornes Ltd., United Kingdom

[N4] NEHRP, 2000, Recommended Provisions for Seismic Regulations for New Buildings and Other Structures, 2000 edition

[N5] NIST GCR 97-724-1, 1997, Development of Procedures to Enhance the Performance of Rehabilitated URM Buildings, August

[N6] Noland, J.L., 1988, State-of-the Art Report : Design, Construction and Research in Masonry : Current Status in Selected Regions of The World, *Proceedings of Ninth World Conference on Earthquake Engineering*, Vol. VIII, Japan, pp. 1099-1109

[N7] NSET, 1999, Reconnaissance Report on Chamoli Earthquake of 29 March 1999, India; *A joint study report by National Society for Earthquake Technology-Nepal, and Department of Earthquake Engineering*, University of Roorkee,

[N8] NZSEE Study Group, 2006, Assessment and Improvement of the Structural Performance of Buildings in Earthquakes, *Recommendations of a NZSEE Study Group on Earthquake Risk Buildings*, New Zealand, June 2006

[P1] Page, A.W., 1978, Finite Element Model for Masonry, *Journal of Structural Engineering*, ASCE, Vol. 104, No. 8, pp. 1267-1285

[P2] Page, A.W., 1996, Unreinforced Masonry Structures an Australian Overview, *Bulletin of the New Zealand National Society for Earthquake Engineering*, Vol. 29, No. 4, pp. 242–255

[P3] Pagnoni, T., 1994, Seismic Analysis of Masonry and Brick Structures With The Discrete Element Method, *Proceedings of the 10th European Conference on Earthquake Engineering*, Vienna Austria, Volume 3, pp. 1669 – 1674

[P4] Pandey, B.H. and Meguro, K., Applied Element Simulation of Masonry Wall Behavior Under In-Plane Lateral Loading,

[P5] Pasquale, S.D., 1992, New Trends in The Analysis of Masonry Structures*, Masonry Construction, Structural Mechanics and Other Aspects*, Maccanica, Volume 27, No. 3, pp. 173–184

[P6] Paulay, T. and Priestley, M.J.N., 1992*,* Seismic Design of Reinforced Concrete and Masonry Buildings, *John Wiley & Sons, Inc*., 744 p

[P7] Prawel, S.P. and Reinhorn, A.M., 1985, Seismic Retrofit of Structural Masonry Using a Ferrocement Overlay, *Proceedings of the Third North American Masonry Conference*, pp. 59.1-59.19.

[P8] Prawel, S.P., Reinhorn, A.M. and Qasi, S.A., 1988, Upgrading the Seismic Resistance of Unreinforced Brick Masonry Using Ferrocement Coatings, *Proceedings of the Eighth International Brick/Block Masonry Conference*, Dublin, Ireland, pp. 785-791.

[P9] Prawel, S.P. and Lee, H.H., 1990, The Performance of Upgraded Brick Masonry Piers Subject to In-plane Motion, *Proceedings of the Fourth US National Conference on Earthquake Engineering*, Vol. 3, pp. 273-282.

[P10] Priestley, M.J.N. and Bridgeman, D.O., 1974, Seismic Resistance of Brick Masonry Walls, *Bulletin of the New Zealand National Society for Earthquake Engineering*, Vol. 7, No. 4, pp. 167 – 187

[P11] Priestley, M.J.N., 1980, Seismic Design of Masonry Buildings – Background to the Draft Masonry Design Code DZ4210, *Bulletin of the New Zealand National Society for Earthquake Engineering*, Vol. 13, No. 4, pp. 329 – 346

[P12] Priestley, M.J.N. and Elder, D.M., 1982, Cyclic Loading Tests of Slender Concrete Masonry Shear Walls, *Bulletin of the New Zealand National Society for Earthquake Engineering*, Vol. 15, No. 1, pp. 3 – 21

[P13] Priestley, M.J.N., 1982, Ductility of Confined Concrete Masonry Shear Walls, *Bulletin of the New Zealand National Society for Earthquake Engineering*, Vol. 15, No. 1, pp. 22 – 26

[P14] Priestley, M.J.N. & Elder, D.M., 1983, Stress-Strain Curves for Unconfined and Confined Concrete Masonry, *ACI Journal*, May-June 1983, pp. 192–201

[P15] Priestley, M.J.N., 1985a, Ultimate Strength Design of Masonry Structures – The New Zealand Masonry Design Code, *Proc. 7th International Block Masonry Conferences*, Melbourne, pp. 1 –13

[P16] Priestley, M.J.N., 1985b, Seismic Behaviour of Unreinforced Masonry Walls, *Bulletin of the New Zealand National Society for Earthquake Engineering*, Vol. 18, No. 2, pp. 191 – 205

[P17] Priestley, M.J.N., 1986, Discussion Seismic Behaviour of Unreinforced Masonry Walls, *Bulletin of the New Zealand National Society for Earthquake Engineering*, Vol. 19, No. 1, pp. 65 – 75

[P18] Priestley, M.J.N. and Limin, H., 1990, Seismic Response of T-Section Masonry Shear Walls, *Proceedings of the Fifth North American Masonry Conference*, University of Illinois at Urabana-Champaign, pp. 359-372.

[R1] Rai, D.C., Goel, S.C. and Holmes W.T., 1994, Seismic Strengthening of URM Buildings with Steel Bracing, *Proceedings of the Fifth U.S. National Conference on Earthquake Engineering*, Chicago, Vol. 3, pp. 697-705.

[R2] Rai, D.C., 1996, Hysteresis Behaviour of Unreinforced Masonry Piers Strengthened with Steel Elements, *Proceedings of Eleventh World Conference on Earthquake Engineering*, Acapulco, Elsevier Science Ltd., Paper No. 501.

[R3] Romano, F., Ganduscio, S. and Zingone, G., 1993, Cracked Nonlinear Masonry Stability under Vertical and Lateral Loads, *Journal of Structural Engineering*, Vol. 119, No. 1, pp. 69–87

[R4] Rots, J.G., 1997, Structural Masonry An Experimental/Numerical Basis for Practical Design Rules, *A.A. Balkema*, Rotterdam, 152 p.

[S1] Sahlin, S., 1971, Structural Masonry, *Prentice-Hall Inc*., Englewood Cliffs, New Jersey, 290 p.

[S2] Scrivener, J.C., 1972, Reinforced Masonry – Seismic Behaviour and Design, *Bulletin of the New Zealand National Society for Earthquake Engineering*, Vol. 5, No. 4, pp. 143 – 156

[S3] Seible, F. and Priestley, M.J.N., 1989, Large Scale Structural Testing At the University of California, San Diego, *Proceedings 58th Annual Convention, Structural Engineers Association of California*, San Diego, September 27-30, 1989

[S4] Seible, F., Hegemier, N., Priestley, N., Kingsley, G., Igarashi, A., and Kurkchubasche, A., 1990, Preliminary Results from the TCCMAR 5-story Full-Scale Reinforced Masonry Research Building Test, *The Masonry Society Journal*, 12 (I) : 53-60.

[S5] Seible, F., Priestley, M.J.N., Kingsley, G.R. and Kürkchübasche, A..G., 1994, Seismic Response of Full-Scale Five-Story Reinforced-Masonry Building, *Journal of Structural Engineering*, Vol. 120, No. 3, pp. 925-946

[S6] Seible, F., Hegemier, G.A., Igarashi, A. and Kingsley, G.R., 1994, Simulated Seismic-Load Tests on Full-Scale Five-Story Masonry Building, *Journal of Structural Engineering*, Vol. 120, No. 3, pp. 903-924

[S7] Shing, P.B., Manzouri, T., Atkinson, R.H., Schuller, M.P. and Amadei, B., 1994, Evaluation of Grout Injection Techniques For Unreinforced Masonry Structures, *Proceeding of 5th US National Conference on Earthquake Engineering*, Volume III, pp. 851-860

[S8] Simsir, C.C., aschheim, M.A., Anrams, D.P., 2004, Out-Of-Plane Dynamic Response of Unreinforced Masonry Bearing Walls Attached to Flexible Diaphragms, *Proceedings of the 13th World Conference on Earthquake Engineering*, Vancouver – Canada, Paper N0. 2045.

[S9] SNI 15-2094-1991, Mutu dan Cara Uji - Bata Merah Pejal (in Indonesian), *Departemen Perindustrian*

[S10] SNI M-111-1990-03, Metode Pengujian Kekuatan Mortar Semen Portland Untuk Pekerjaan Sipil (in Indonesian), *Departemen Pekerjaan Umum*

[S11] Sofronie, R.A., 2004, Performances in Seismic Strengthening of Masonry, *Proceedings of the 13th World Conference on Earthquake Engineering*, Vancouver – Canada, Paper N0. 182.

[S12] Spence, R. and Coburn, A., 1992, Strengthening Buildings of Stone Masonry to Resist Earthquakes, *Masonry Construction, Structural Mechanics and Other Aspects*, Maccanica, Volume 27, No. 3, pp. 213–221

[S13] Standard Association of New Zealand, 1963, Clay Building Bricks, *NZS 366-1980*, New Zealand

[S14] Standards Australia/Standard Association of New Zealand, 1997, Masonry Units and Segmental Pavers – Method of Test – Determining Breaking Load of Segmental Paving Units, *AS/NZS 4456.5* , Standards Australia, Sydney

[S15] Standards Australia, 2001, Masonry Code, *AS3700-2001*, Standards Australia, Sydney

[S16] Sucuoğlu, H. and Erberik, A., 1997, Performance Evaluation of a Three-Storey Unreinforced Masonry Building During the 1992 Erzincan Earthquake, *Earthquake Engineering and Structural Dynamics*, Vol. 26, pp. 319–336

[S17] Sugano, S., 1996, State-of-The-Art in Techniques for Rehabilitation of Buildings, *Eleventh World Conference on Earthquake Engineering*, Paper No.2175, Mexico, 16 p.

[T1] Tanrikulu, A.K., Mengi, Y. and McNiven, H.D., 1992, The Non-Linear Response of Unreinforced Masonry Buildings to Earthquake Excitations, *Earthquake Engineering and Structural Dynamics*, Vol. 21, pp. 965–985

[T2] Timoshenko, S., 1955, Strength of Material Part I & II, Elementary Theory and Problems, *Van Nostrand Reinhold*, 3rd edition,

[T3] Tomaževič, M. and Velechovsky, T., 1992, Some Aspects of Testing Small-Scale Masonry Building Models on Simple Earthquake Simulators, *Earthquake Engineering and Structural Dynamics*, Vol. 21, pp. 945-963

[T4] Tomazevic, M. and Apih, V., 1993, The Strengthening of Stone-Masonry Walls by Injecting the Masonry-Friendly Grouts*, Journal of European Earthquake Engineering*, pp. 10-20

[T5] Tomazevic, M., Lutman, M. and Weiss, P., 1996, Seismic Upgrading of Old Brick-Masonry Urban Houses : Tying of Walls with Steel Ties*, Journal of Earthquake Spectra*, Volume 12, No. 3, pp. 599-622

[T6] Tomazevic, M., 1997, Seismic Resistance Verification of Masonry Buildings : Following The New Trends, *Seismic Design Methodologies for the Next Generation of Codes*, Fajfar & Krawinkler (editors), Balkema, pp. 323-334

[T7] Tomazevic, M., 1999, Earthquake-Resistant Design of Masonry Buildings, *Series on Innovation in Structures and Construction,* Volume I, Chapter 3, Masonry Materials and Construction Systems, Imperial College Press

[T8] Tomaževič, M., Klemenc, I. and Lutman, M., 2000, In Situ Tests for the Assessment of Seismic Resistance of Old Stone-Masonry Houses, *Proceeding 12th WCEE*, Auckland

[T9] Triantafillou, T.C., 1998, Strengthening of Masonry Structures Using Epoxy-Bonded FRP Laminates, *Journal of Composites for Construction*, ASCE, 2(2): 96-104

[T10] Tumialan, J.G., Morbin, A., Micelli, F. and Nanni, A. (200 , Flexural Strengthening of URM Walls with FRP Laminates

[U1] Uniform Code for Building Conservative (UCBC), 1994 Edition, *International Conference of Building Officials*, Whittier, California

[U2] United Nations Industrial Development Organization (UNIDO), 1978a, First Progress Report on Improved Brickwork : Mortar And Bricklaying*, Technical Paper No. 11*, Bandung, 43 p

[U3] United Nations Industrial Development Organization (UNIDO), 1978b, Second Progress Report on Improved Brickwork : Testing of Brickwork I*, Technical Paper No. 12*, Bandung, 58 p

[U4] United Nations Industrial Development Organization (UNIDO), 1979, Fourth Progress Report on Improved Brickwork : Testing of Brickwork II*, Technical Paper No. 41*, Bandung, 46 p

[V1] Vasseur, L., 1975, Notes On Masonry*, Working Paper, No. 95/75/21379*, Regional Housing Centre, Bandung, 33 p

[W1] Watanabe, F. and Sumi, A., 1998, Assessment of Seismic Performance and Upgrading of Building Structures, *Proceedings of the XIIIth FIP Congress on Challenges for Concrete in The Next Millennium*, Amsterdam, Netherlands, 13 p.

[W2] Weng, D., Lu, X., Zhou, C., Kubo, T. and Li, K., 2004, Experimental Study on Seismic Retrofitting of Masonry Walls Using GFRP, *Proceedings of the 13th World Conference on Earthquake Engineering*, Vancouver – Canada, Paper N0. 1981.

[W3] Wijanto S. and Andriono T., 1999, Evaluation of The Seismic Performance of A 1907's L-shaped 3Three Storey Unreinforced Masonry Building in Indonesia, *Proceeding of NZSEE Conference*, Rotorua – New Zealand, pp. 103-110

[W4] Wijanto, S., Andriono, T. and Satyarno, I., 2000, Strengthening of a 1902'S L-Shaped Three Storey Unreinforced Masonry Building in Indonesia, *Proceedings of 13th World Conference on Earthquake Engineering*, Auckland – New Zealand

[W5] Wijanto, S., 2002, Performance of Unreinforced Masonry Wall with and without Strengthening Due to Lateral Loads, *Workshop PPAUIR/ITB-NILIM/Jepang: Confined Masonry Behavior and Its Relation to Housing Structure Issues in Indonesia*, Bandung - Indonesia

[W6] Wood, R.H., 1978, Plasticity, Composite Action and Collapse Design of Unreinforced Shear Wall Panels in Frames, *Proceeding of Instn. Civ. Engrs, Part 2*, pp. 381–411

[W7] Wylie, L.A. and Alaluf, R., 1994, The Challenge Of Repairing And Strengthening San Francisco's Historic Ferry Building, *Proceeding of 5th US National Conference on Earthquake Engineering*, Volume III, pp. 575-584

[Z1] Zienkiewics, O.C. and Taylor, R.L., 1989, The Finite Element Method, Volume 1 Basic Formulation and Linear Problems, Fourth Edition, *McGraw-Hill International Editions*, Singapore

[Z2] Zienkiewics, O.C. and Taylor, R.L., 1991, The Finite Element Method, Volume 2 Solid and Fluid Mechanics Dynamics and Non-Linearity, Fourth Edition, *McGraw-Hill International Editions*, Singapore

[Z3] Zhuge, Y., Thambiratman, D. and Corderoy, J., 1998, Non-Linear Dynamic Analysis of Unreinforced Masonry*, Journal of Structural Engineering*, Vol. 124, No 3, pp 270-277

[Z4] Zoutenbier, J, 1986, The Seismic Response of Unreinforced Masonry Buildings, *Master thesis, Department of Civil Engineering, University of Canterbury*, New Zealand, 68 p

APPENDIX A :

LATERAL FORCE AND DISPLACEMENT OR STRAIN OUTPUT DATA FROM URM-WALL UNIT 1

A total of forty one LVDTs were used to monitor the in-plane displacements, and diagonal deformations of the Unit-1. The recorded responses of all transducers and diagrams of lateral load vs. lateral displacement and also strain value are shown on the following pages.

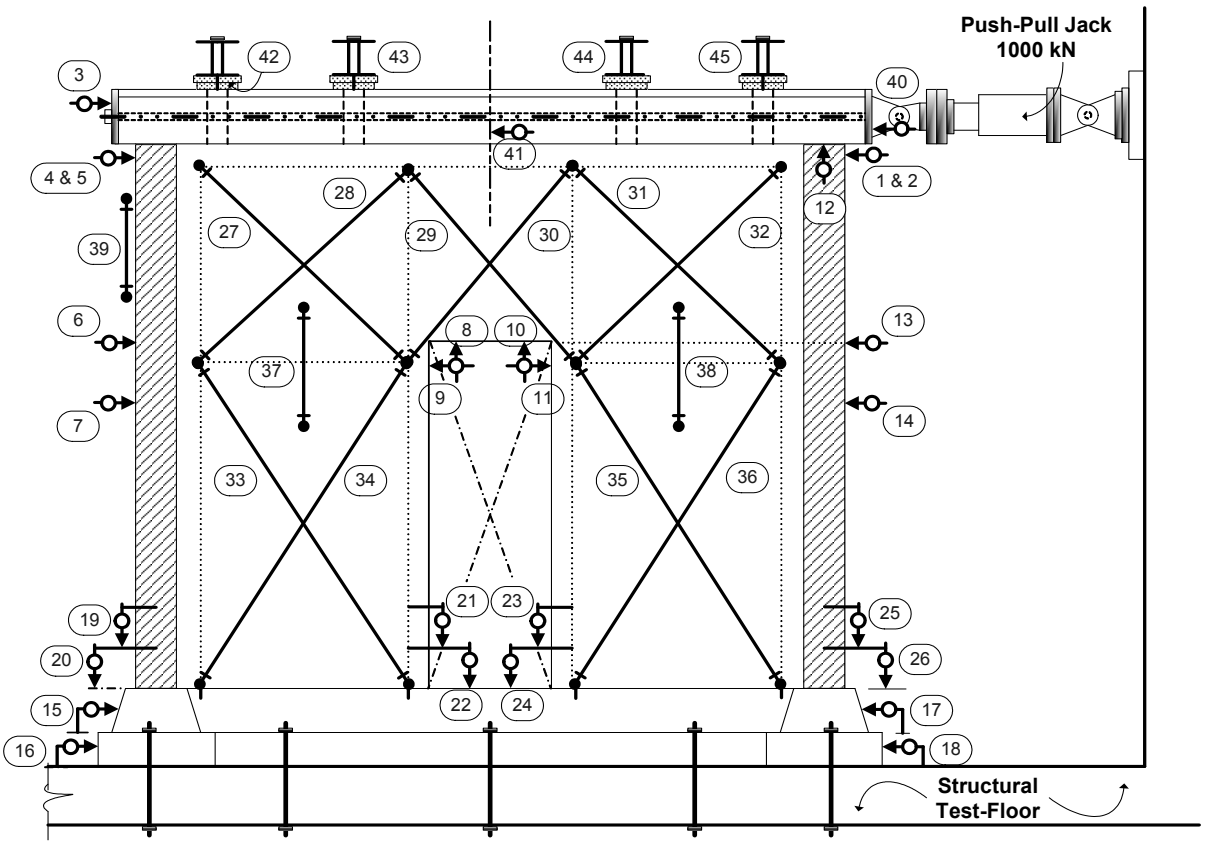

Figure A.1. : Position of displacement transducers (LVDTs) at URM Unit-1

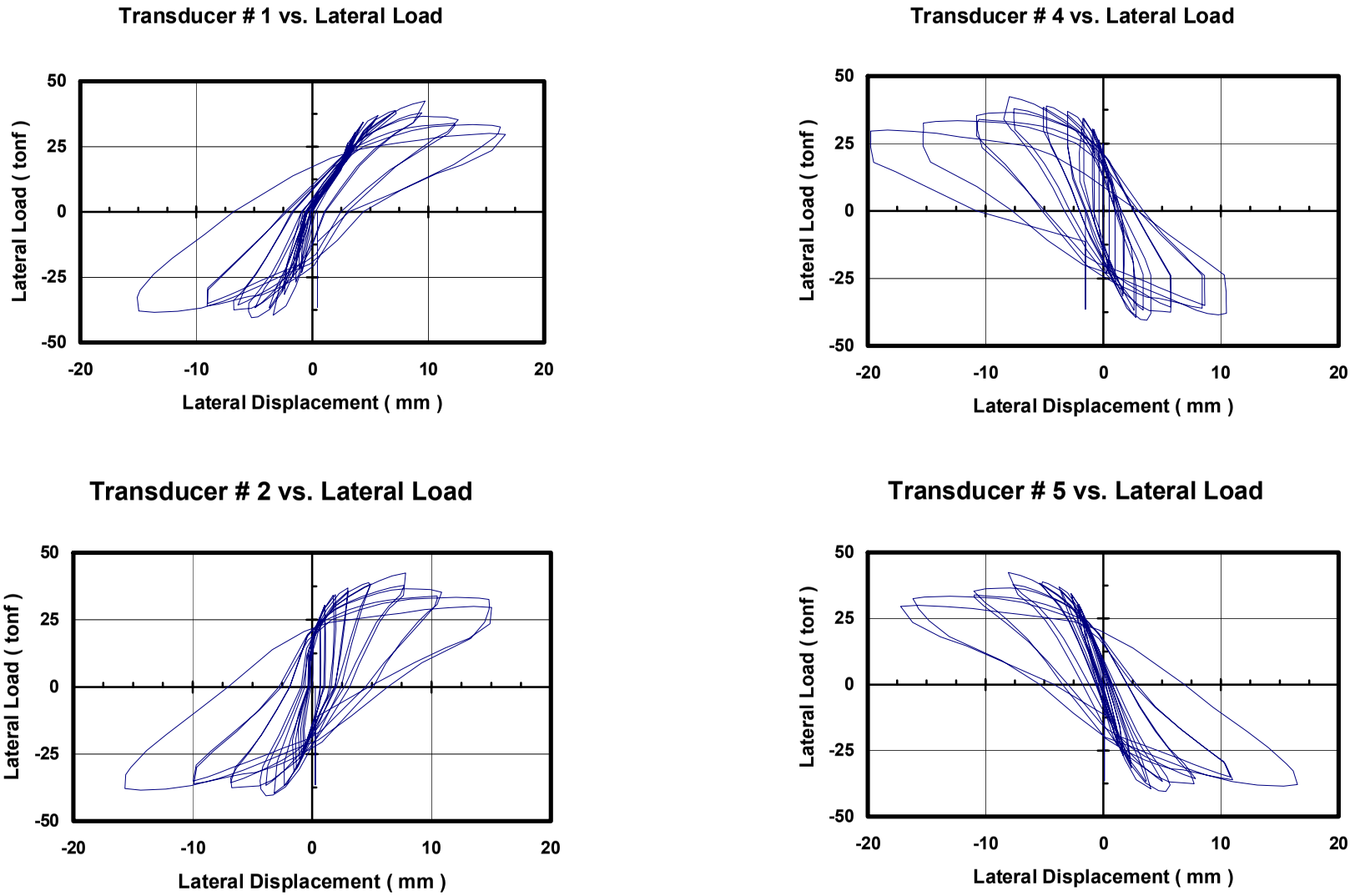

Figure A.2. Lateral force – displacement response of URM-wall Unit-1

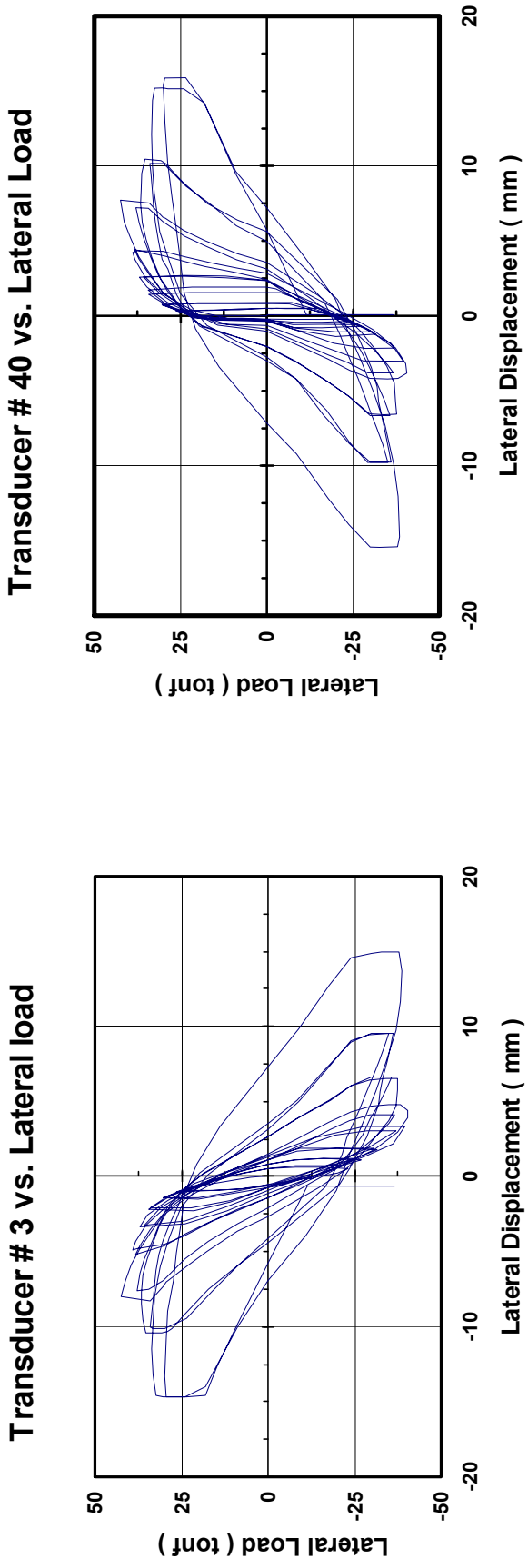

Figure A.3. Lateral force – displacement response of URM-wall Unit-1

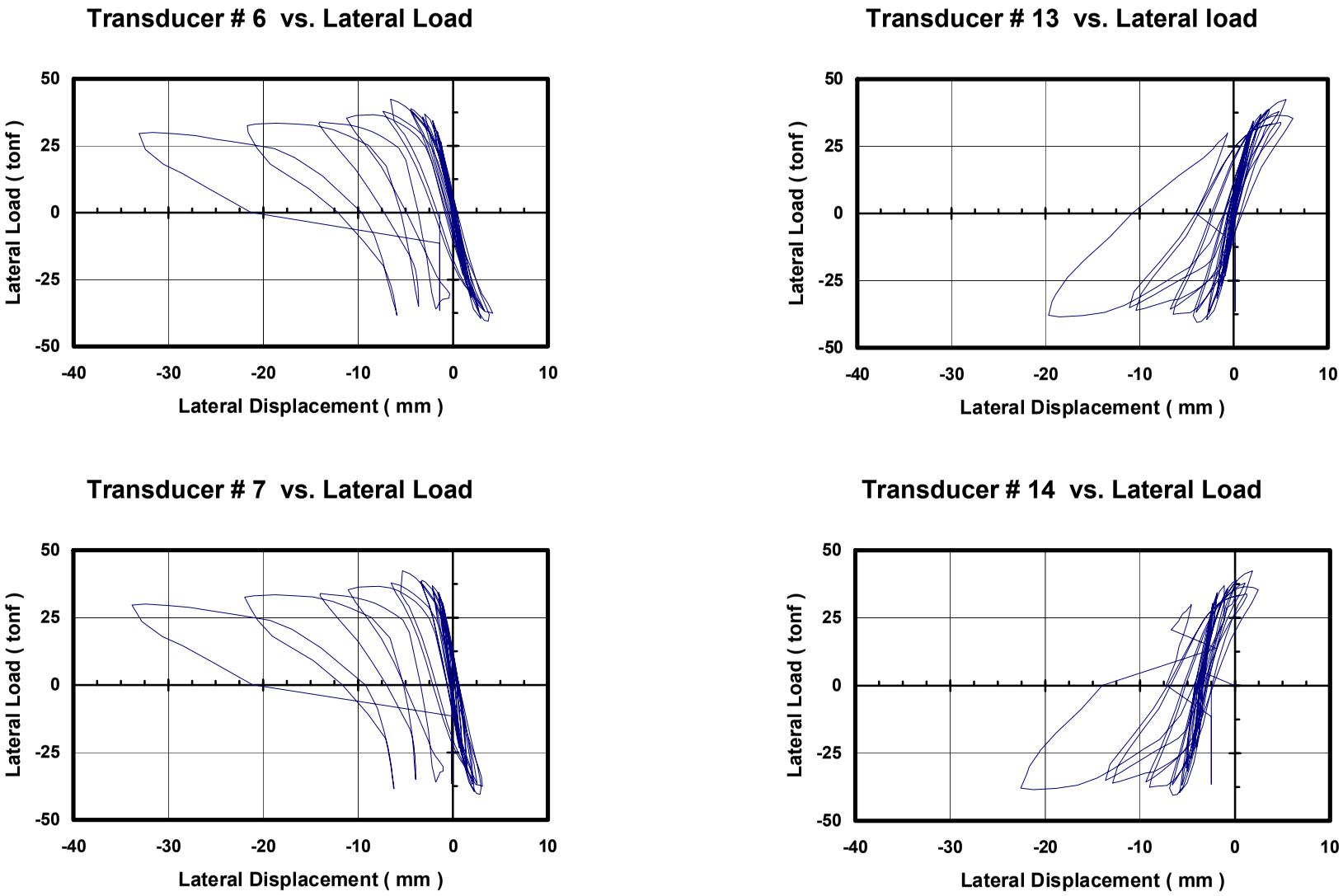

Figure A.4. Lateral force – displacement response of URM-wall Unit-1

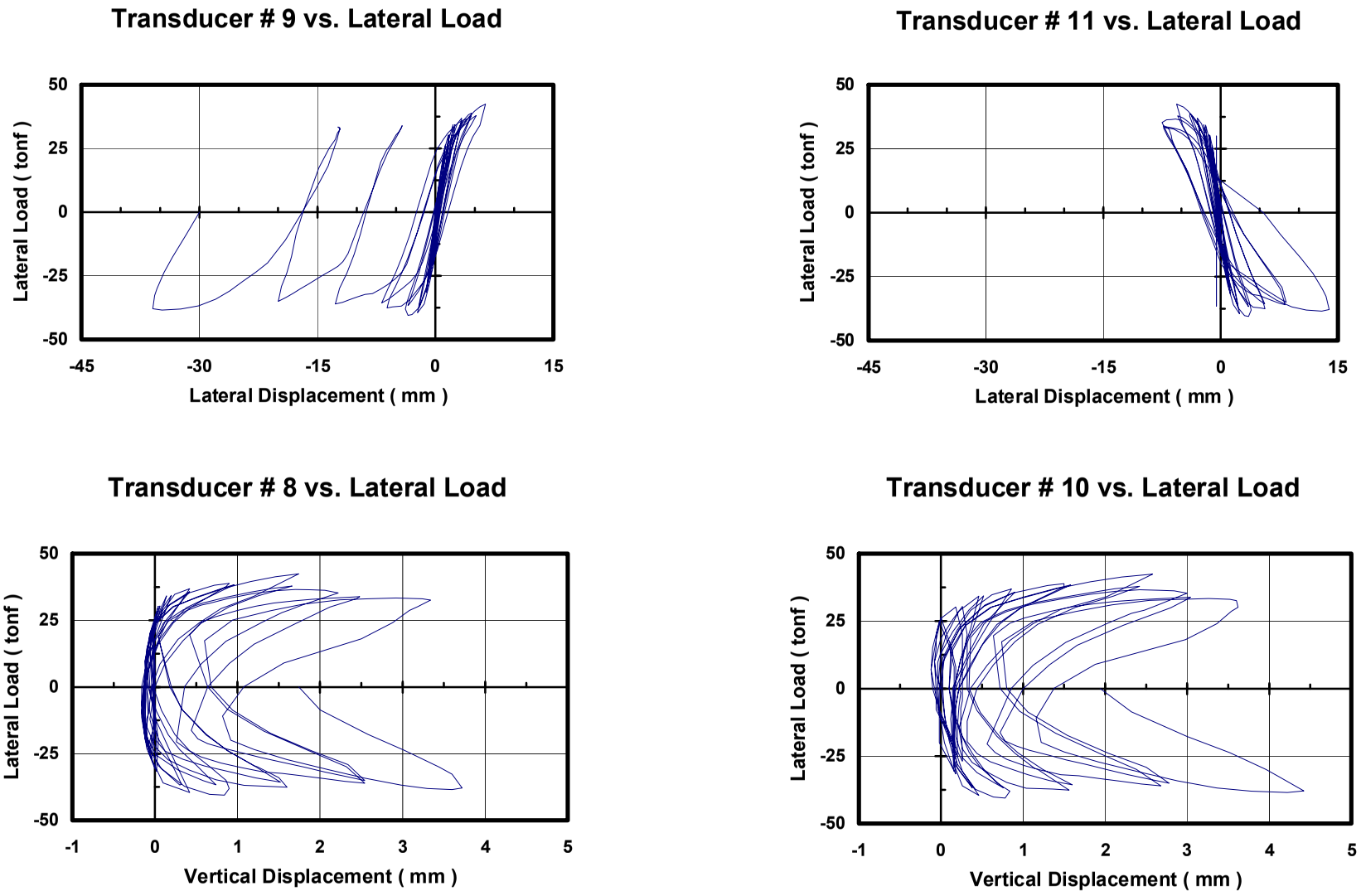

Figure A.5. Lateral force – displacement response of URM-wall Unit-1

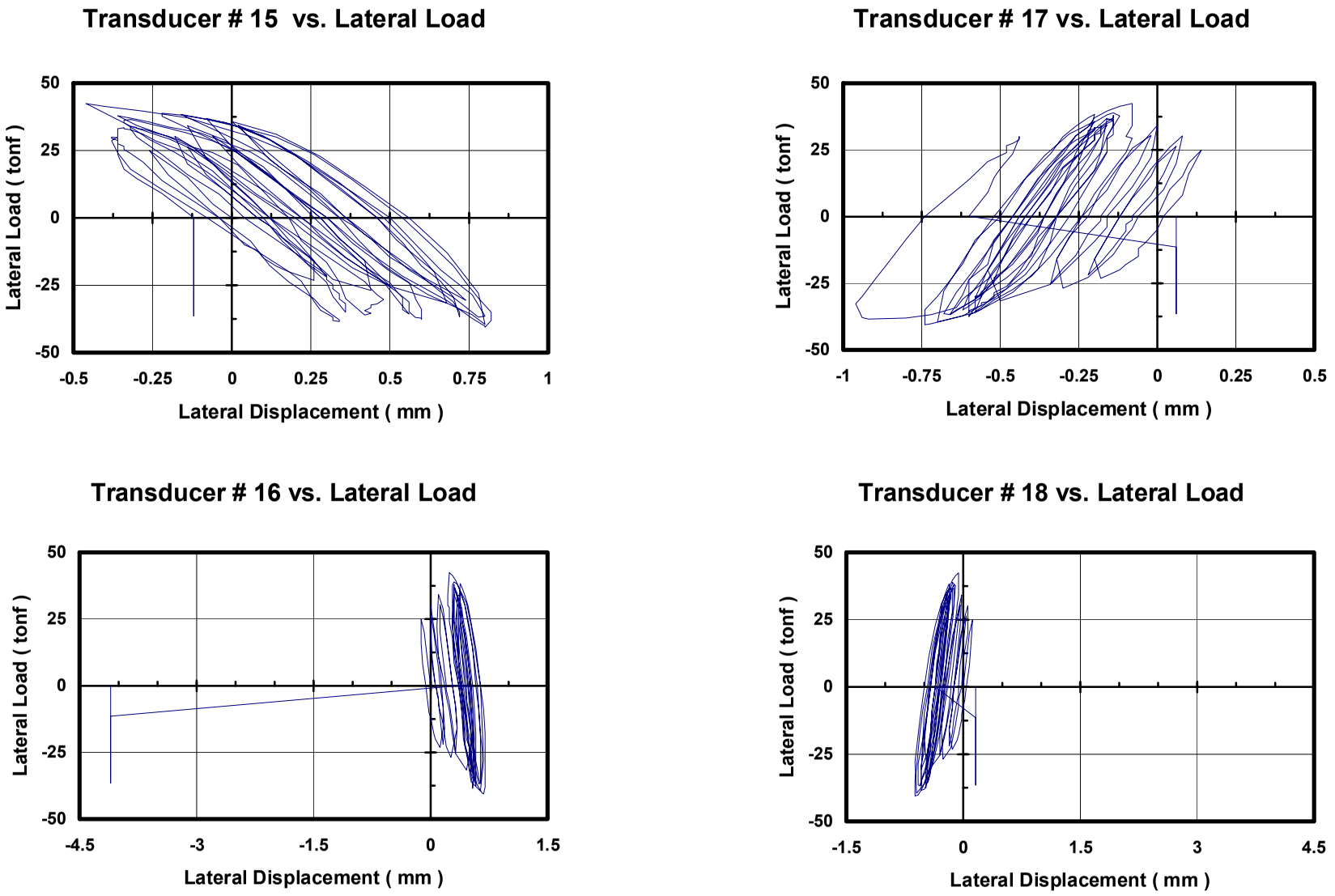

Figure A.6. Lateral force – displacement response of URM-wall Unit-1

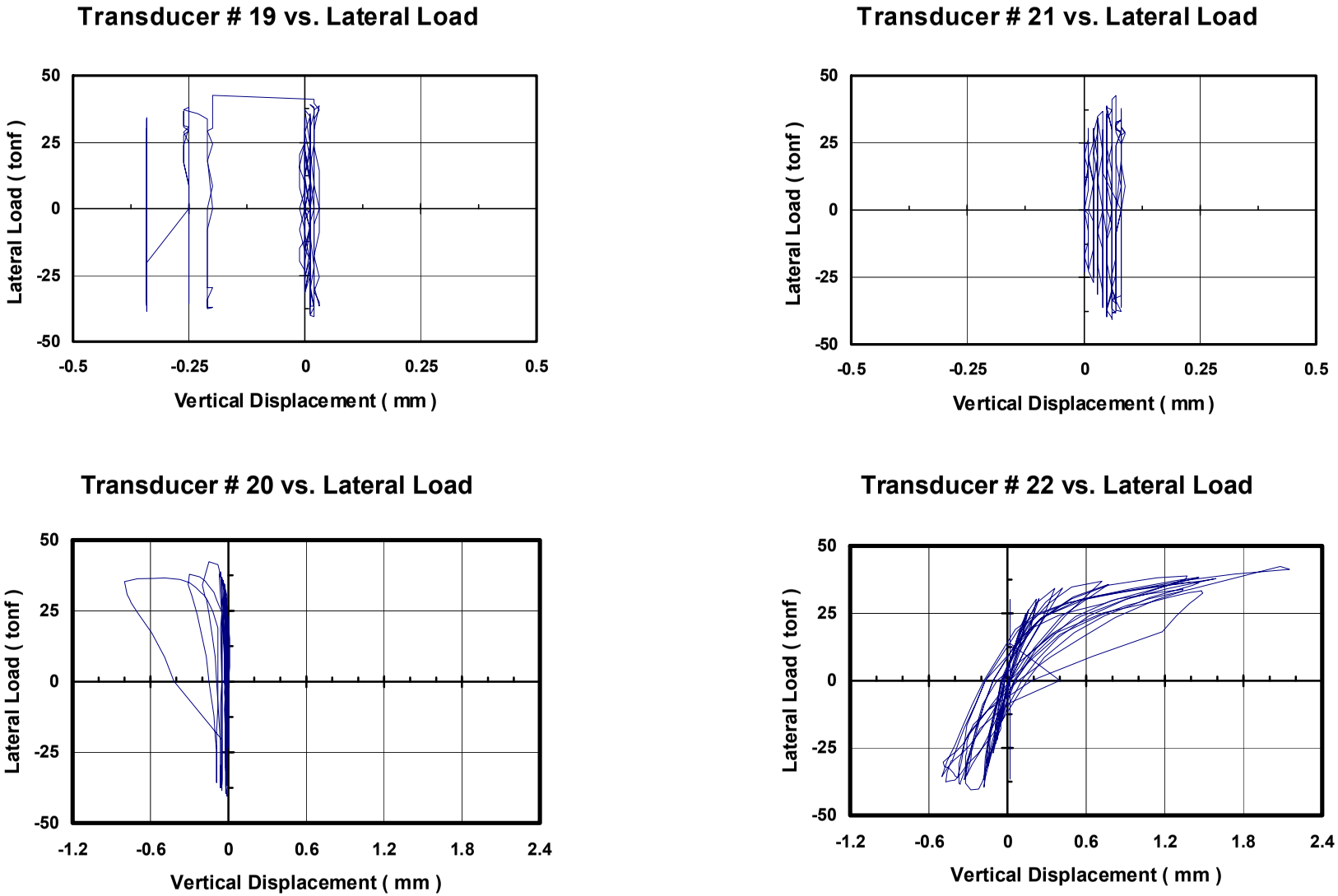

Figure A.7. Lateral force – displacement response of URM-wall Unit-1

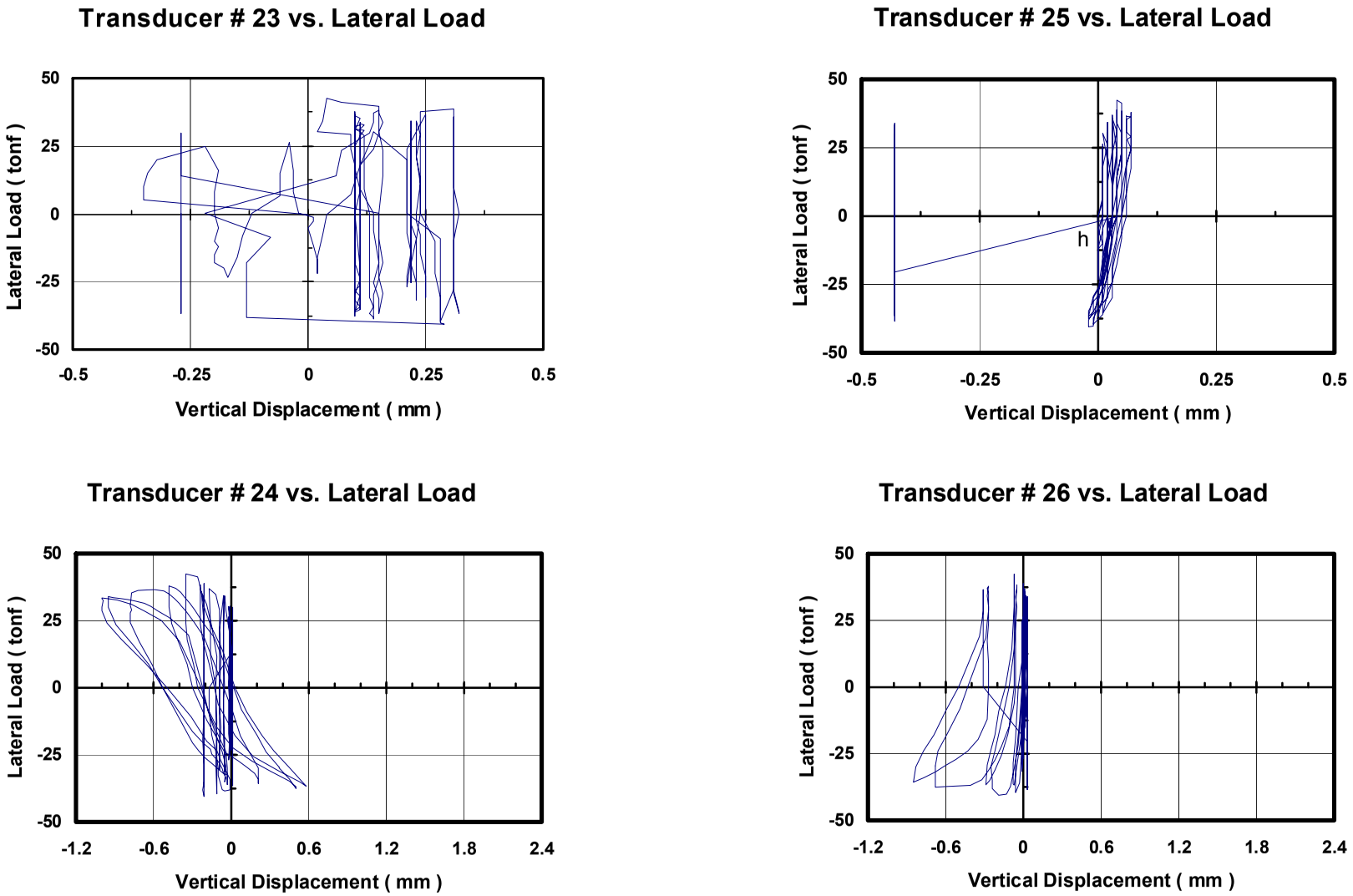

Figure A.8. Lateral force – displacement response of URM-wall Unit-1

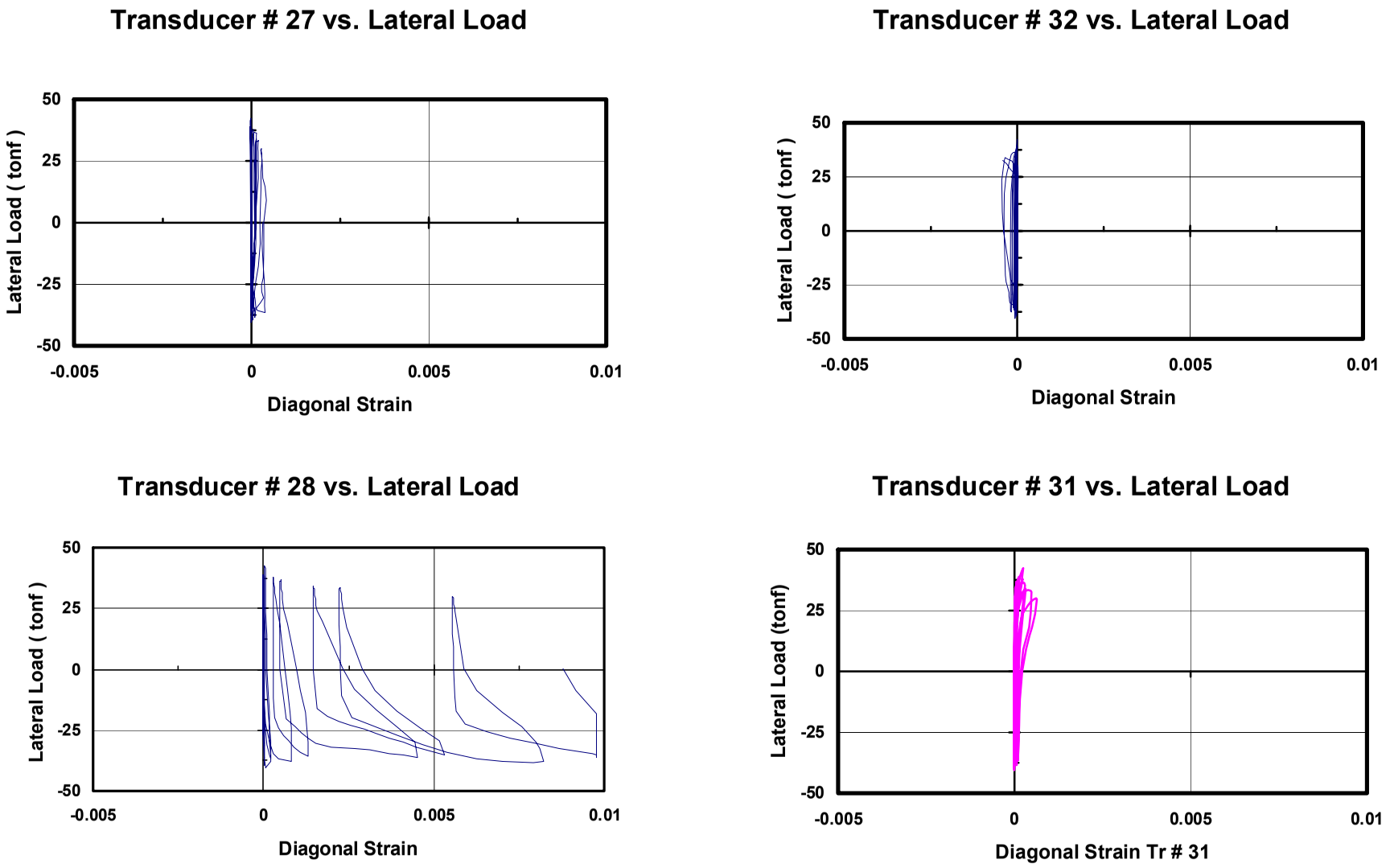

Figure A.9. Lateral force – diagonal strain of URM-wall Unit-1

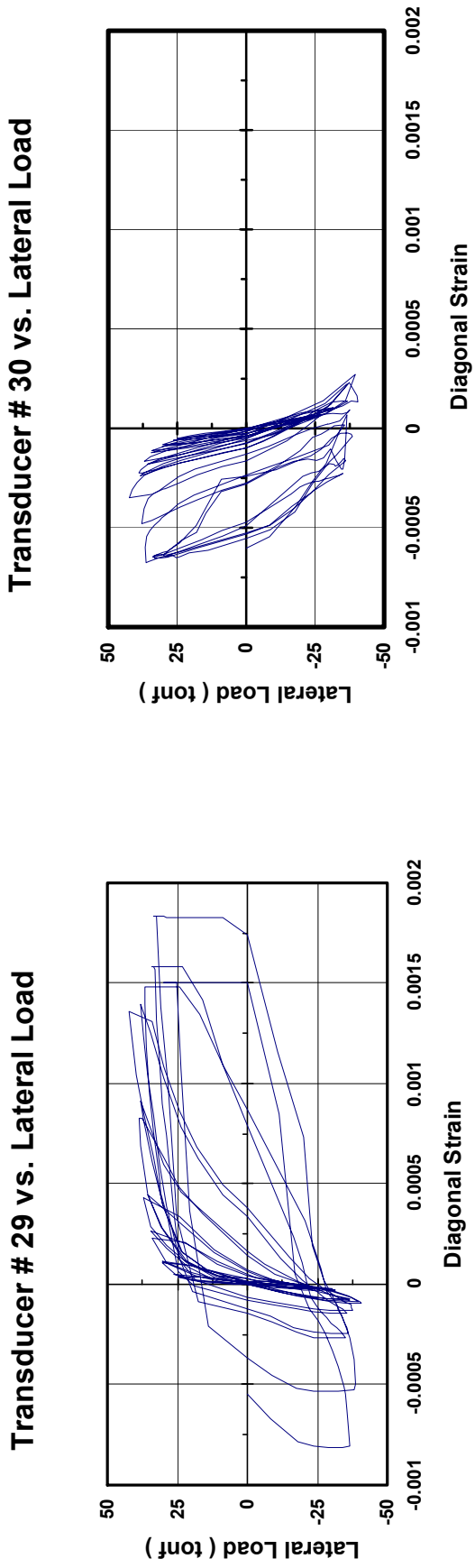

Figure A.10. Lateral force – diagonal strain of URM-wall Unit-1

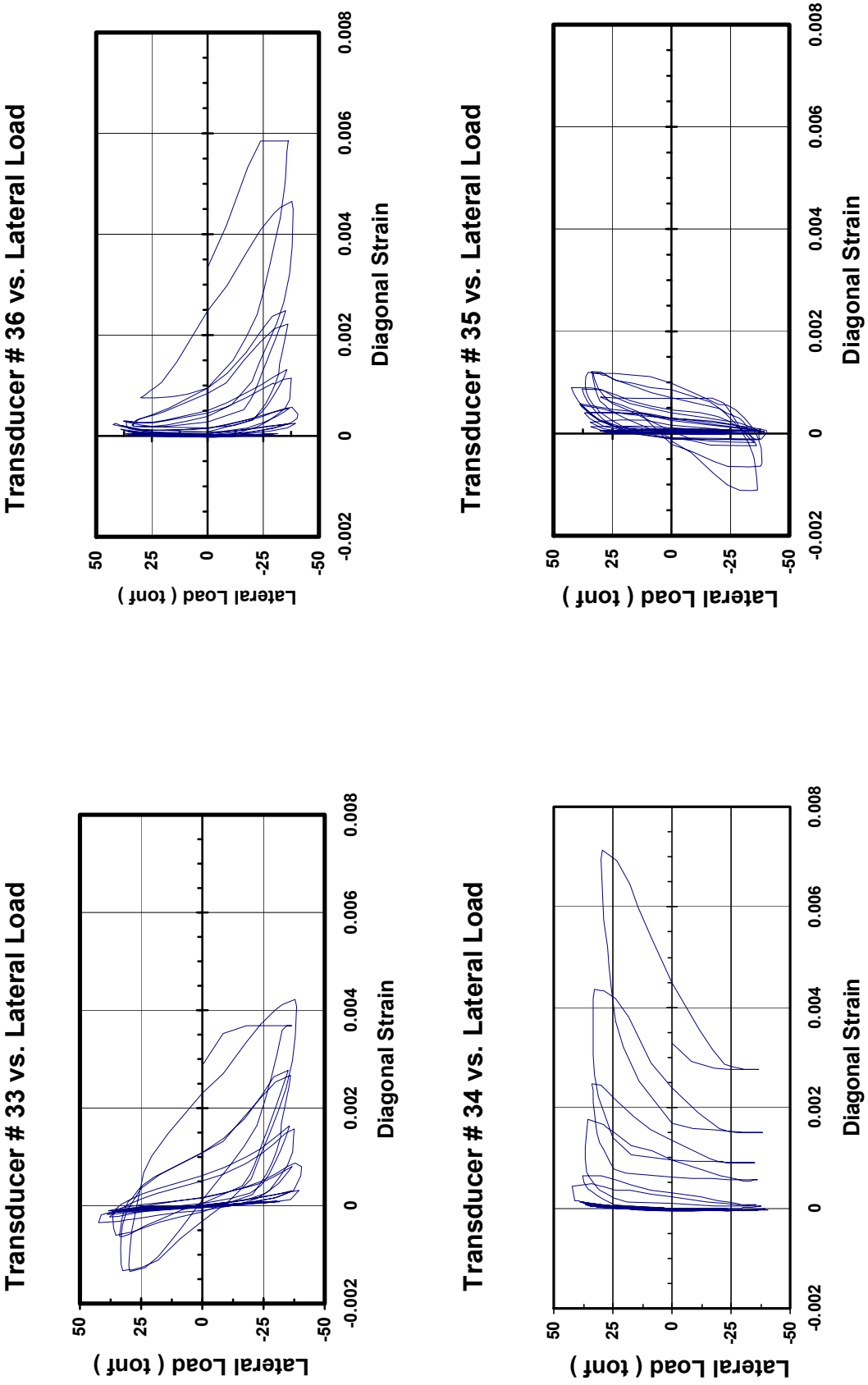

Figure A.11. Lateral force – diagonal strain of URM-wall Unit-1

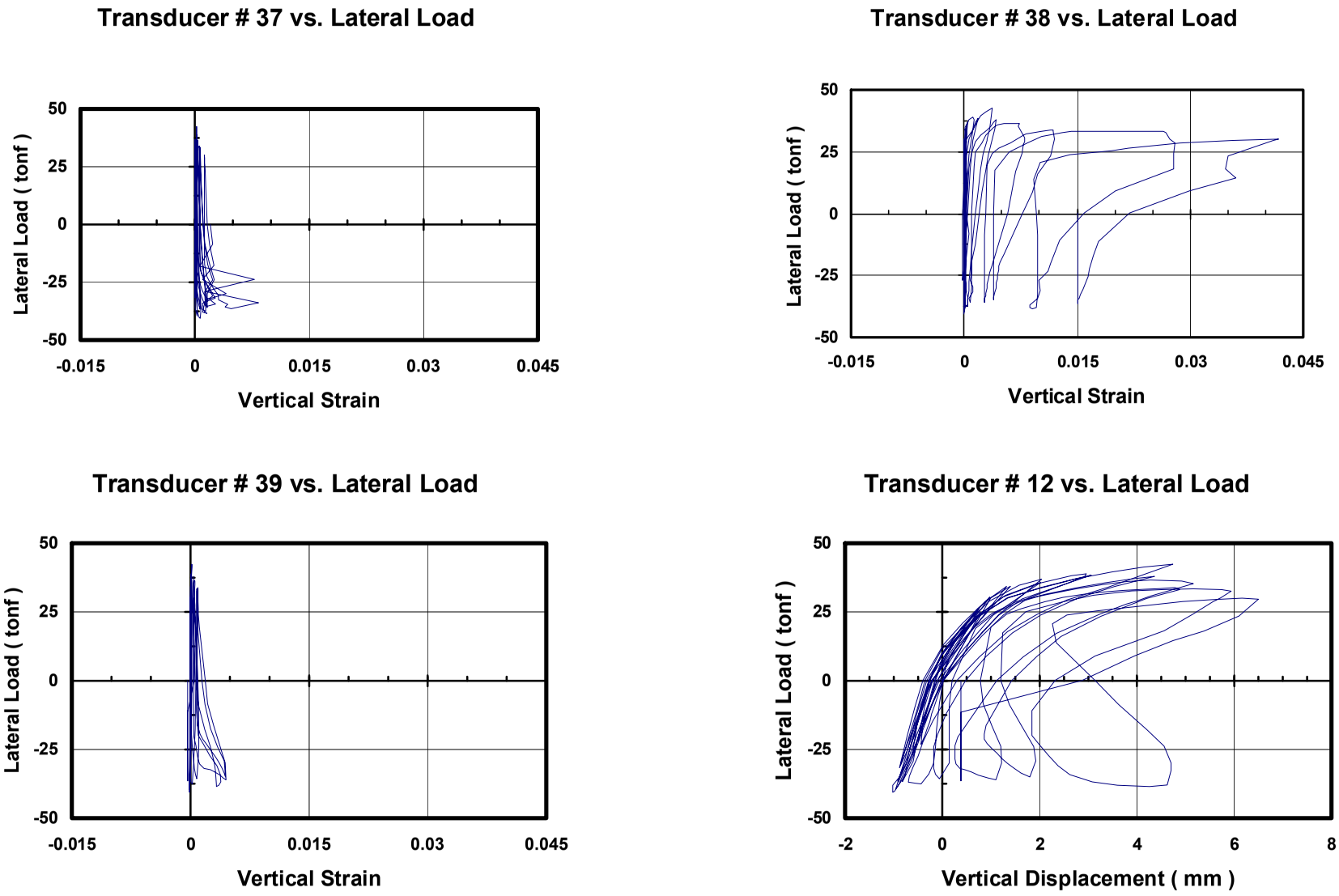

Figure A.12. Lateral force – vertical strain of URM-wall Unit-1

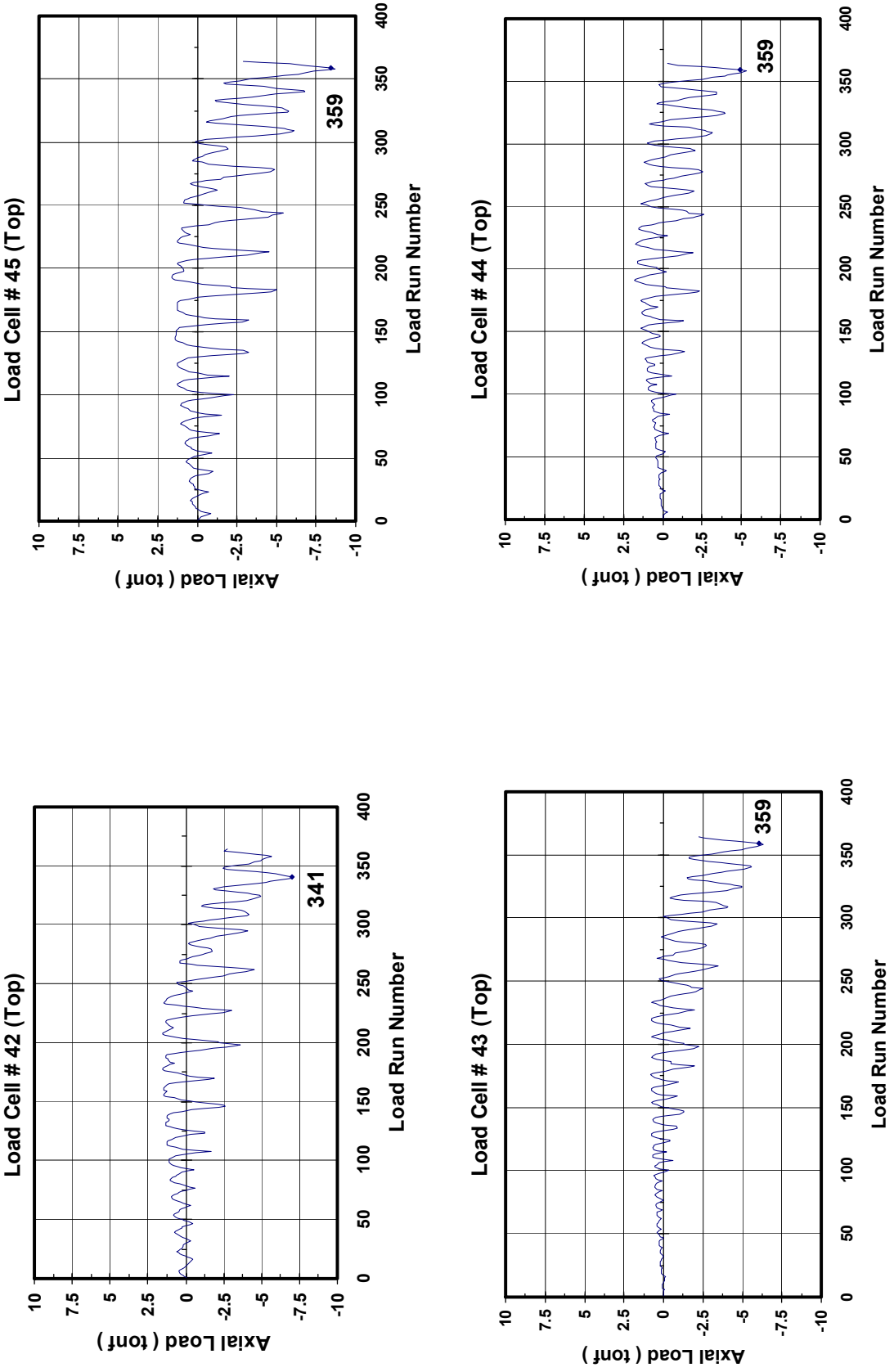

Figure A.13. Axial load at VSL thread lock bars of URM-wall Unit-1

APPENDIX B :

LATERAL FORCE AND DISPLACEMENT OR STRAIN OUTPUT DATA FROM URM-WALL UNIT 2

A total of Fifty one LVDTs were used to monitor the in-plane displacements, and diagonal deformations of the Unit-2. The recorded responses of all transducers and diagrams of lateral load vs. lateral displacement and also strain value are shown on the following pages.

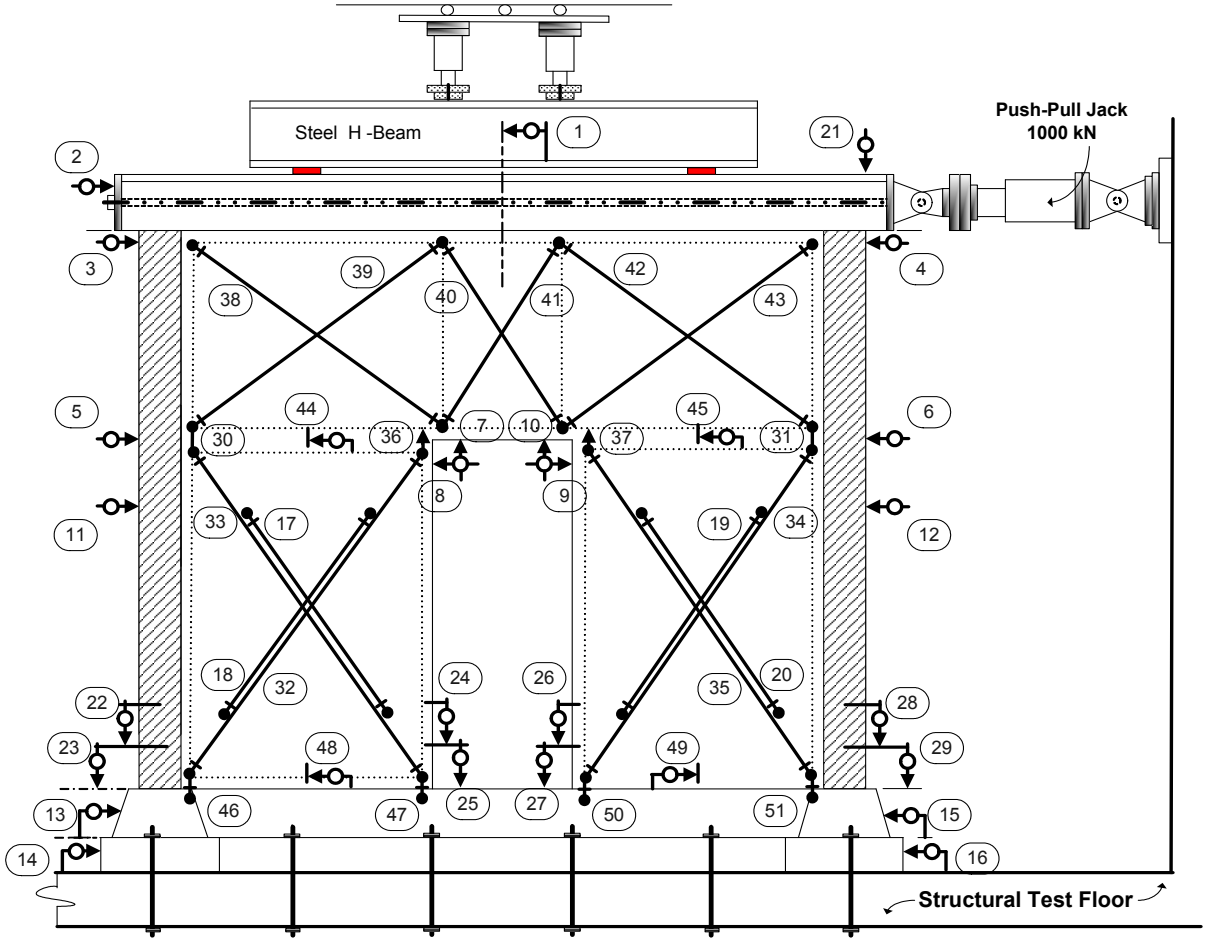

Figure B.1. Position of displacement transducers (LVDTs) at URM Unit-2

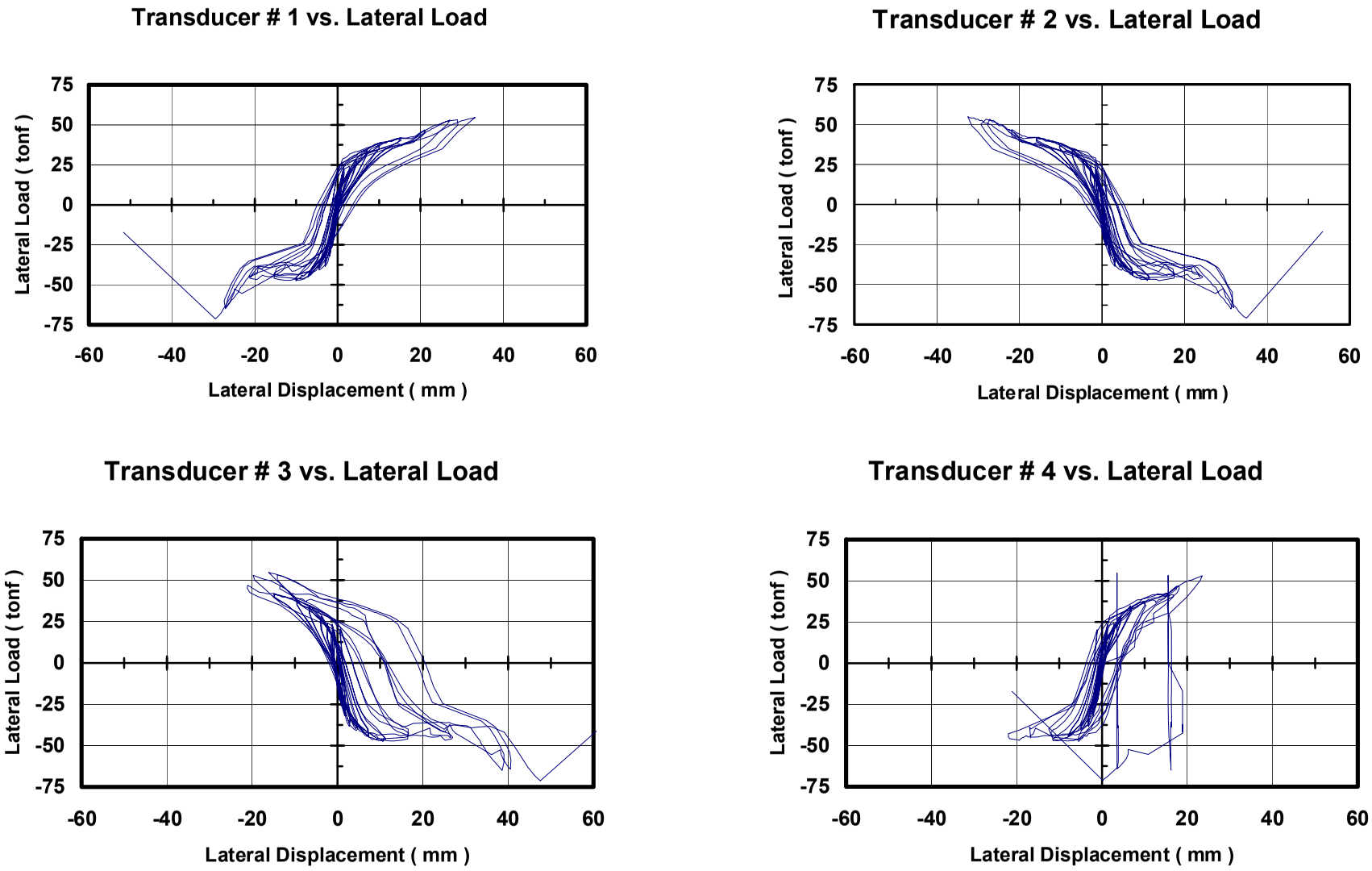

Figure B.2. Lateral force – displacement response of URM-wall Unit-2

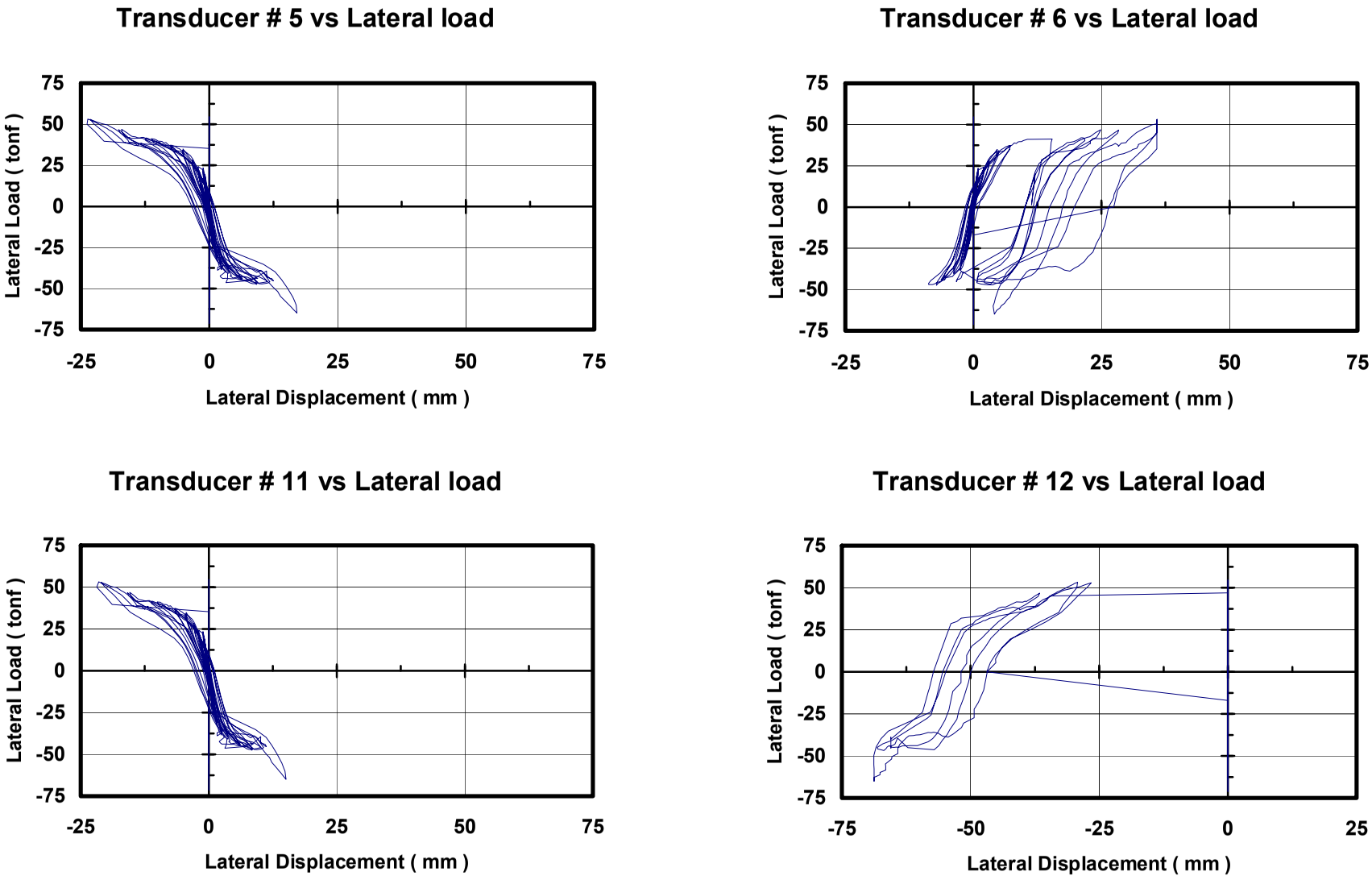

Figure B.3. Lateral force – displacement response of URM-wall Unit-2

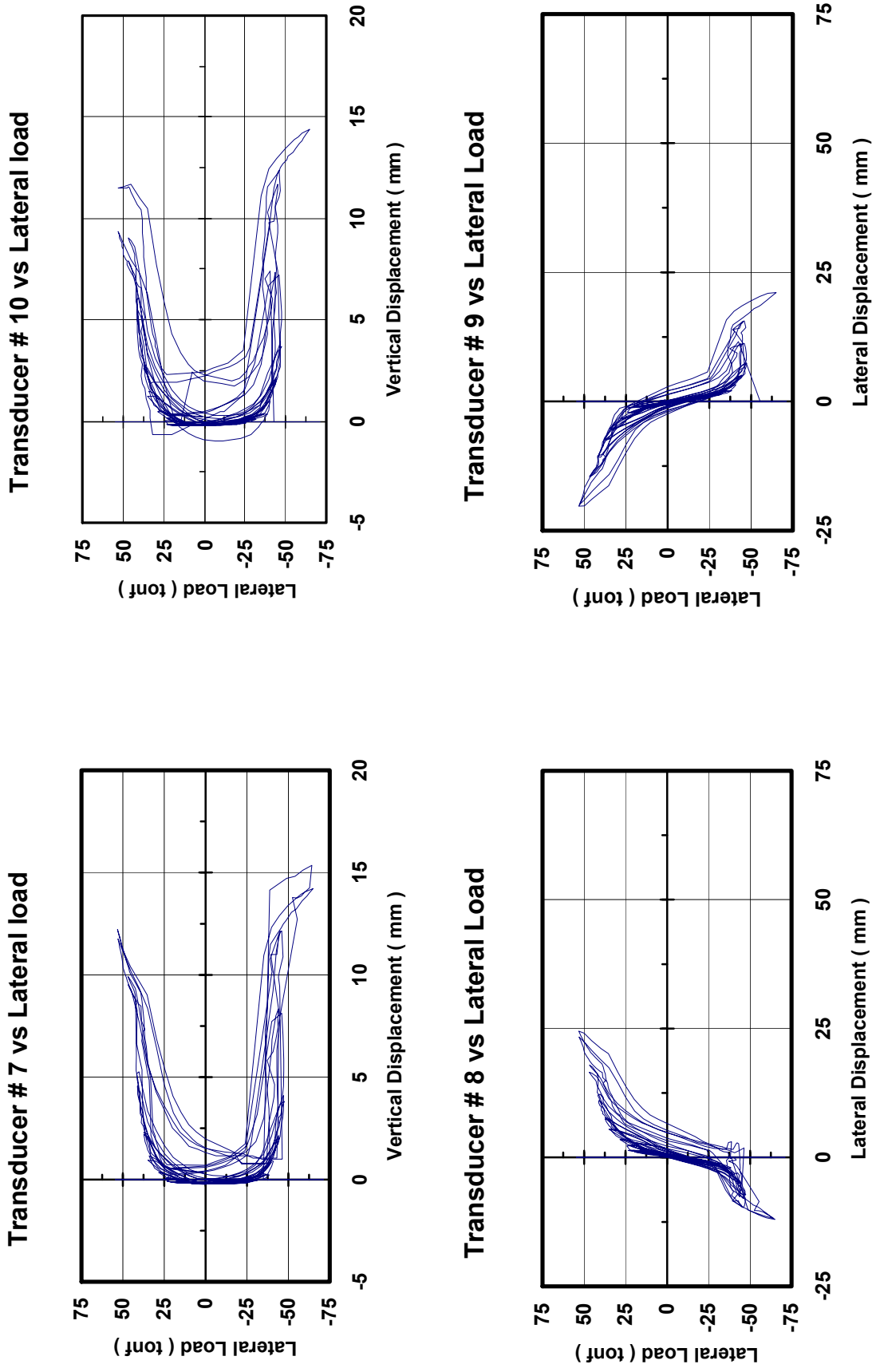

Figure B.4. Lateral force – displacement response of URM-wall Unit-2

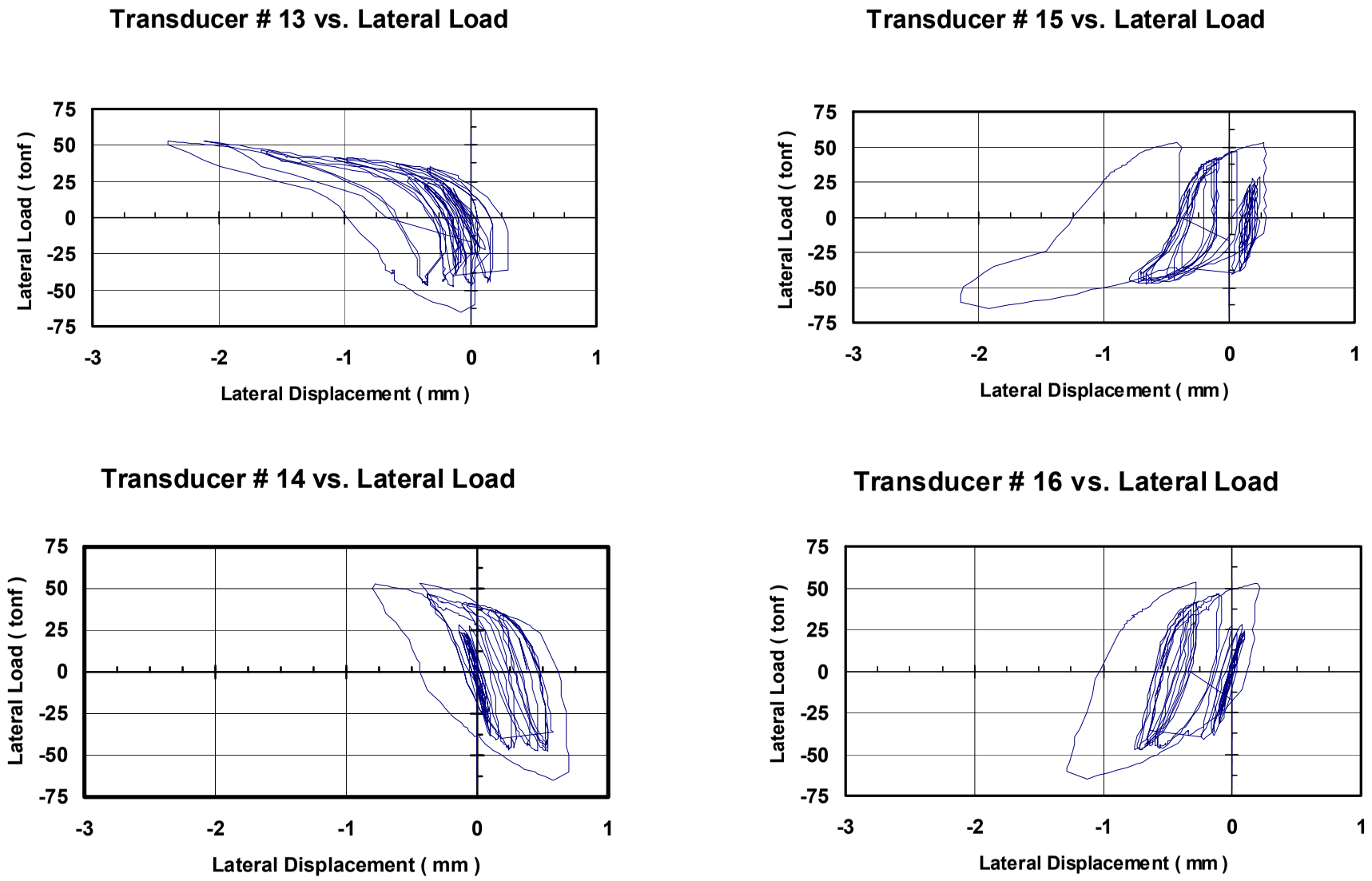

Figure B.5. Lateral force – displacement response of URM-wall Unit-2

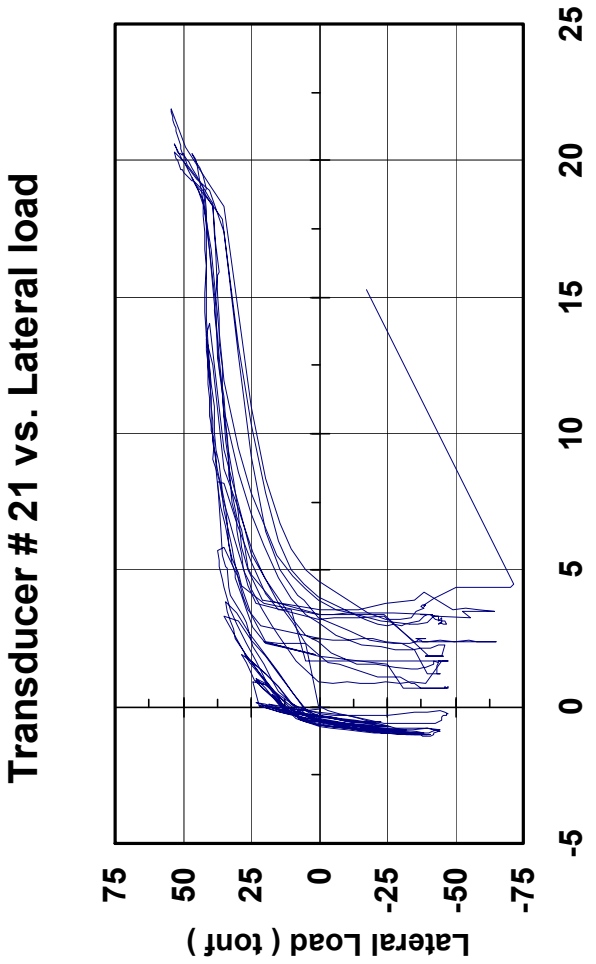

Figure B.6. Lateral force – displacement response of URM-wall Unit-2

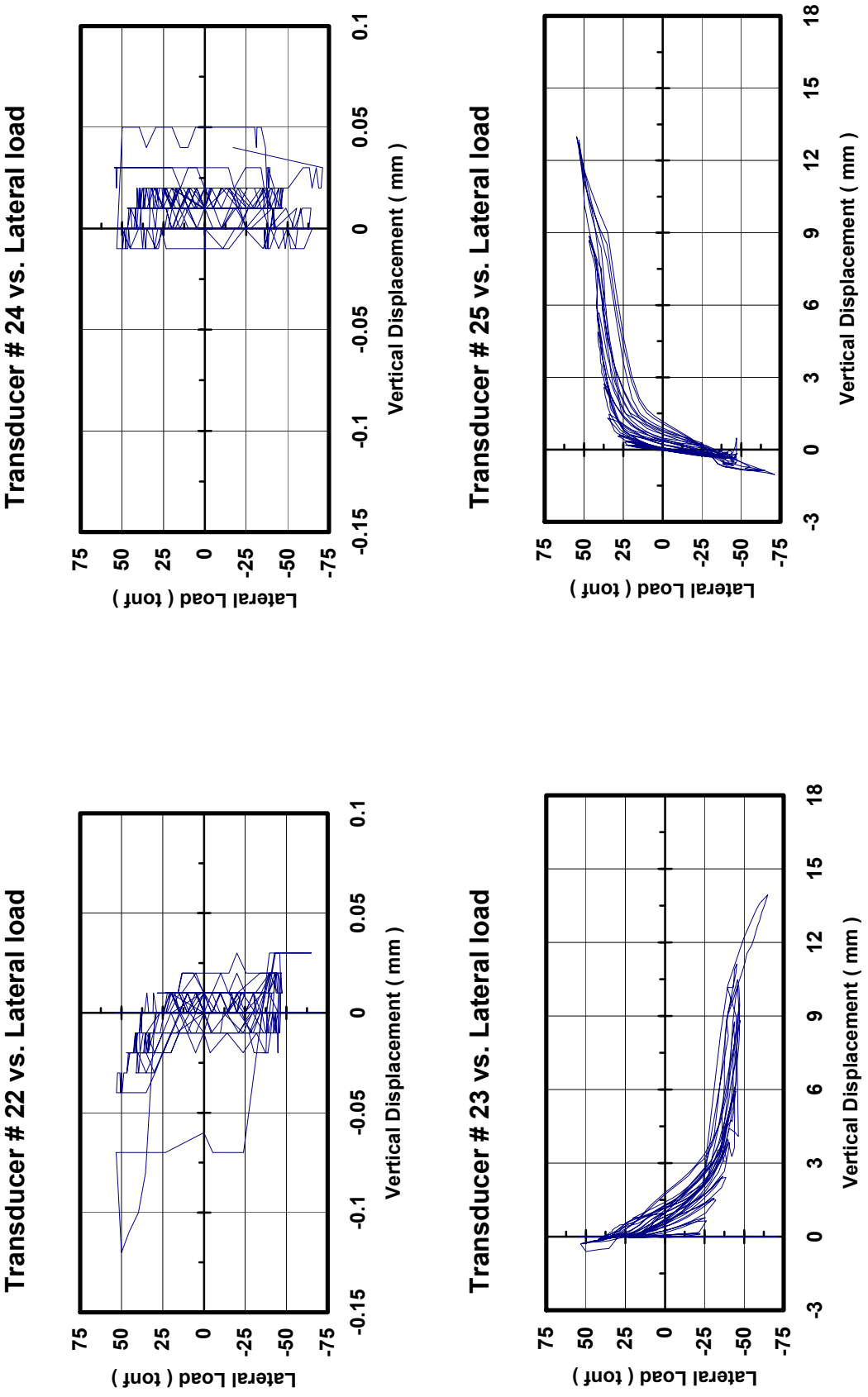

Figure B.7. Lateral force – displacement response of URM-wall Unit-2

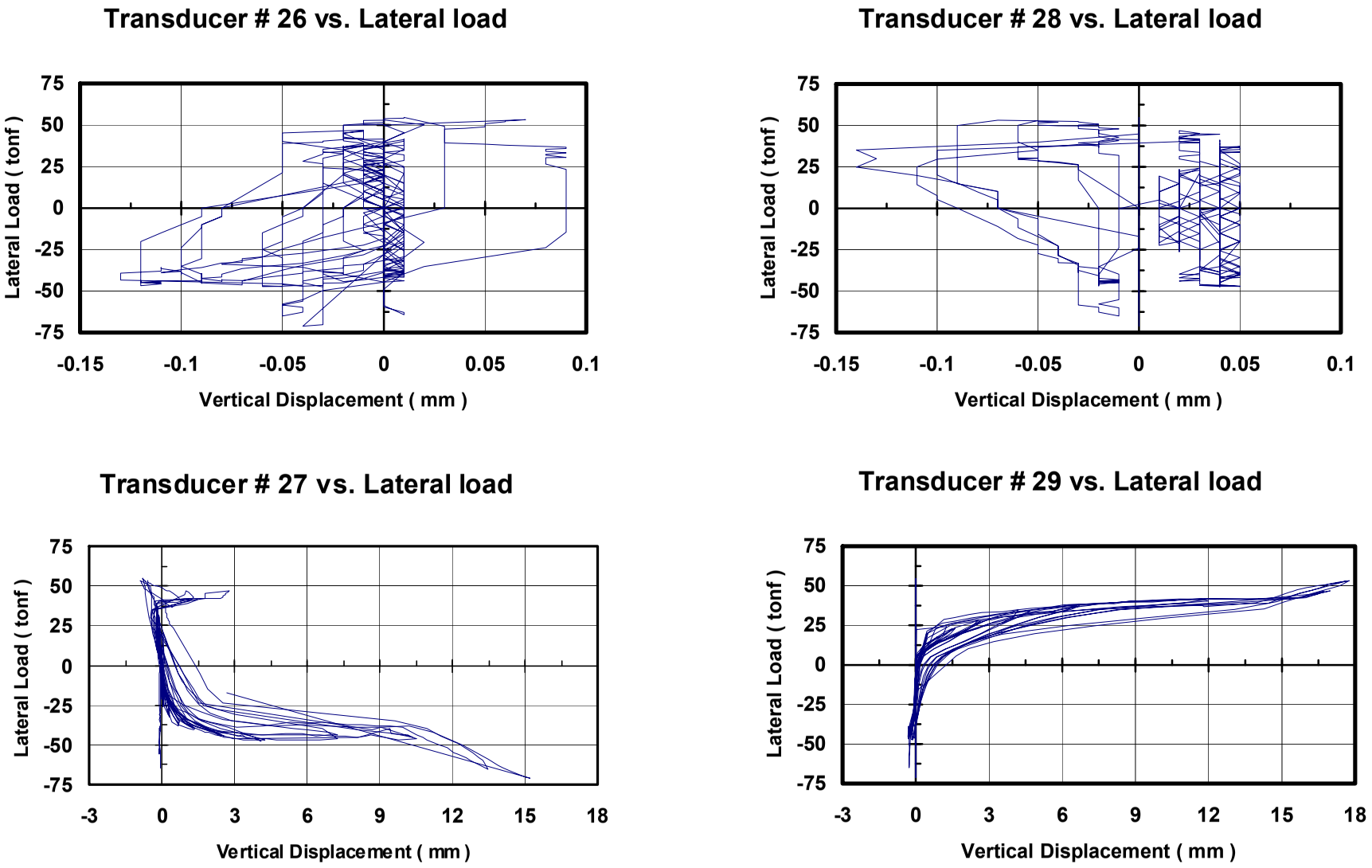

Figure B.8. Lateral force – displacement response of URM-wall Unit-2

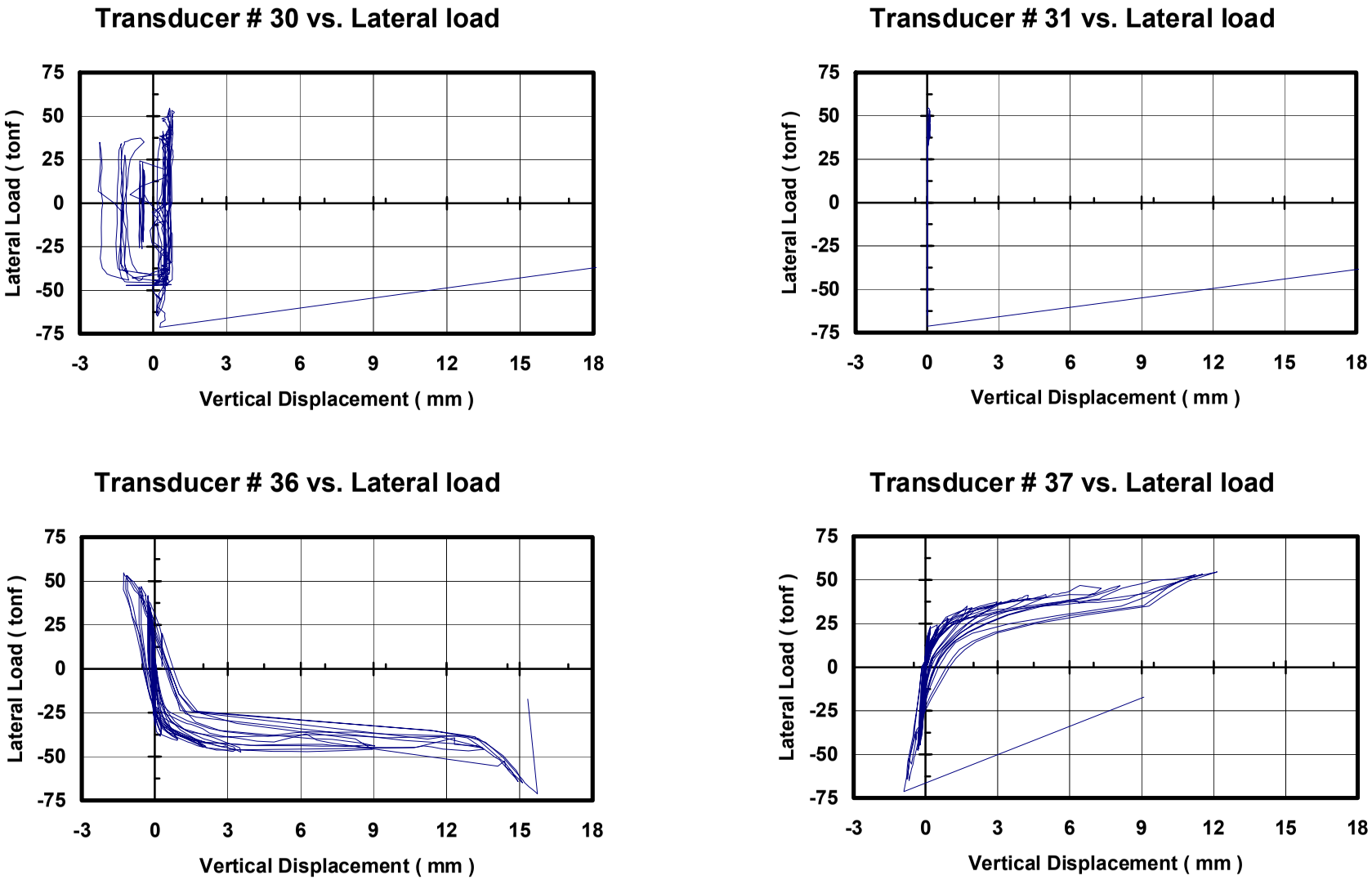

Figure B.9. Lateral force – displacement response of URM-wall Unit-2

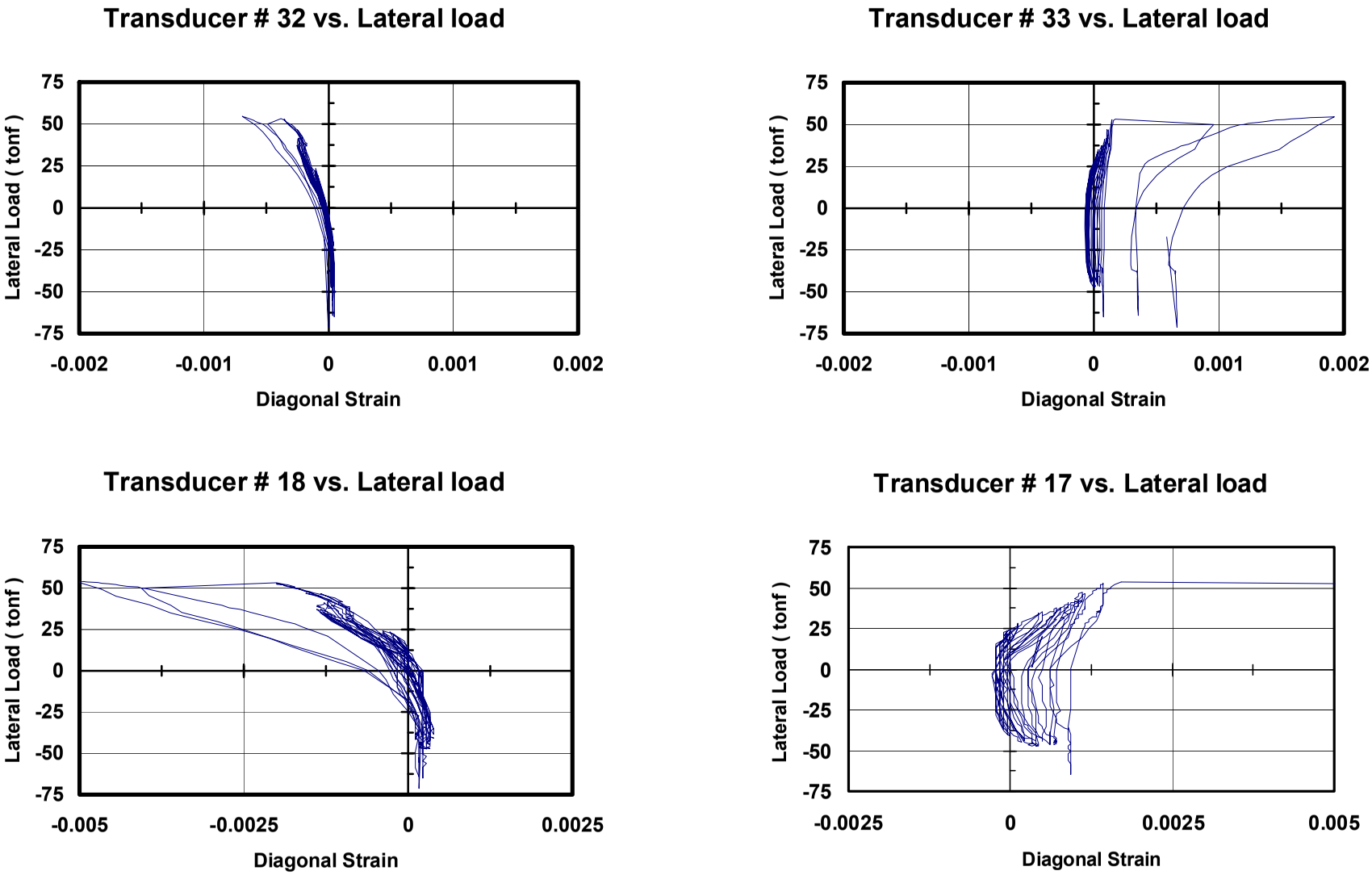

Figure B.10. Lateral force – diagonal strain response of URM-wall Unit-2

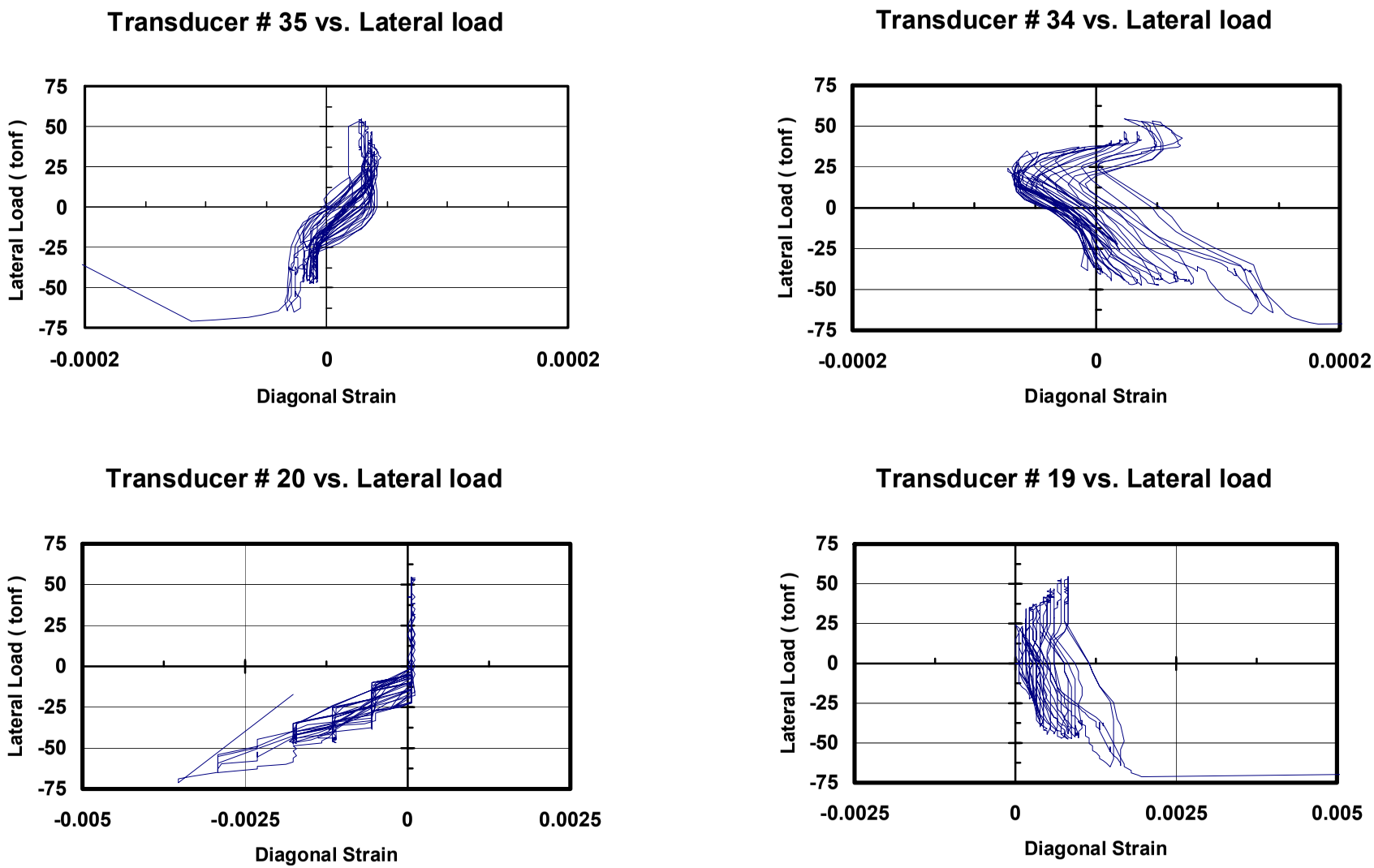

Figure B.11. Lateral force – diagonal strain response of URM-wall Unit-2

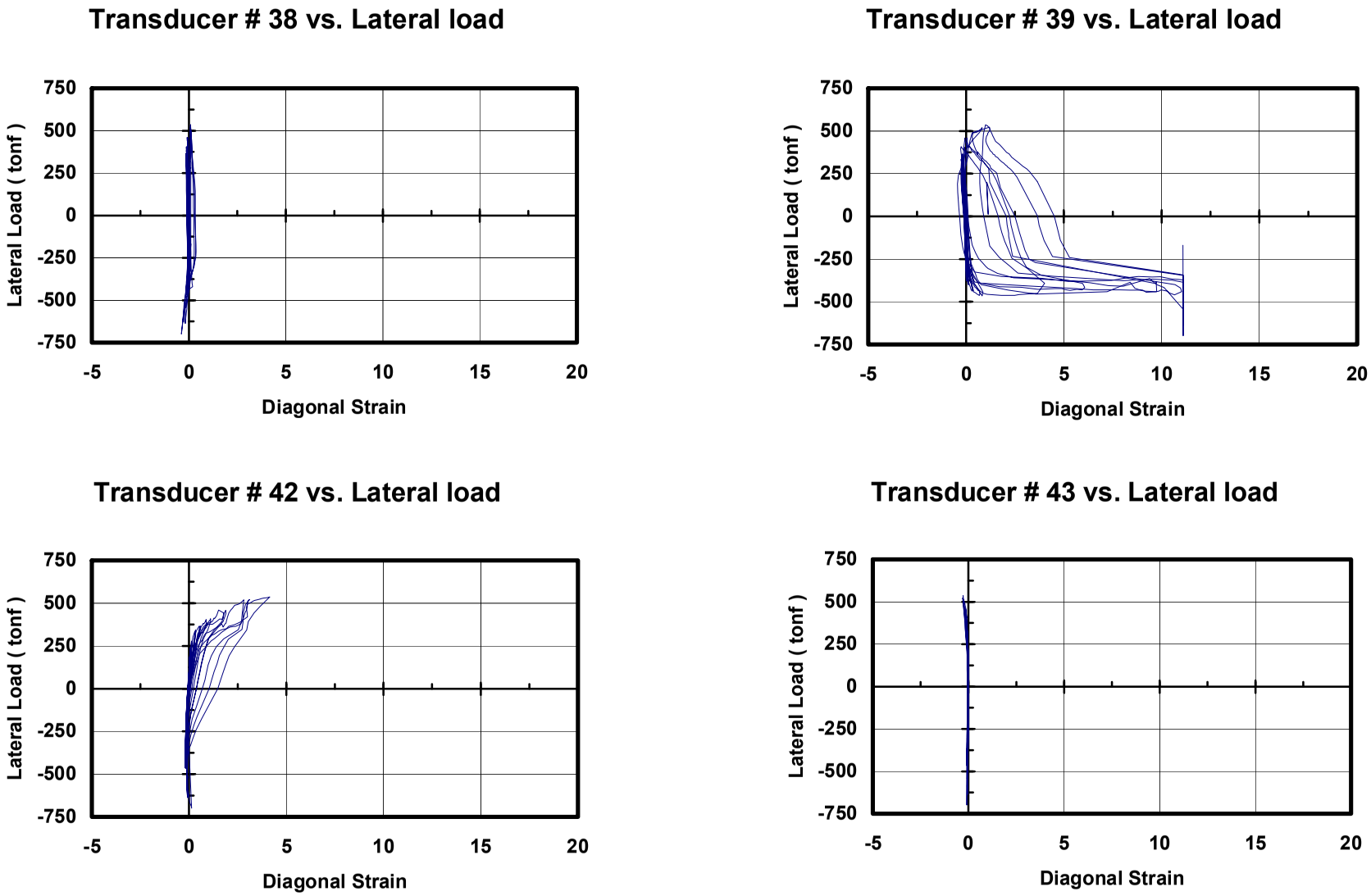

Figure B.12. Lateral force – diagonal strain response of URM-wall Unit-2

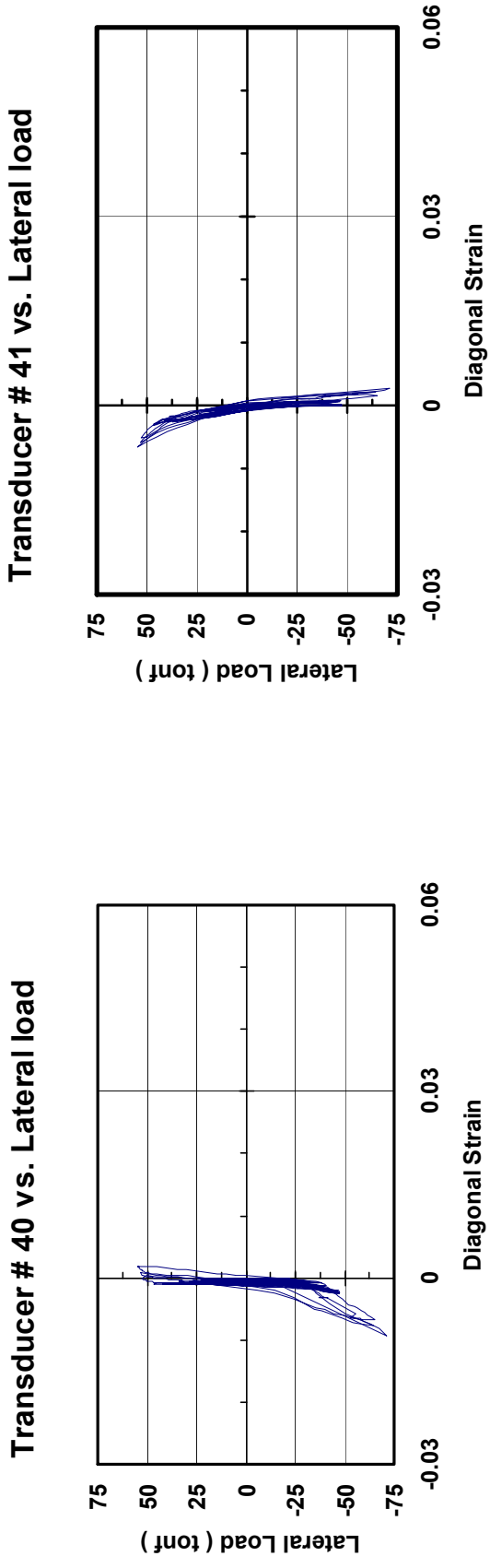

Figure B.13. Lateral force – diagonal strain response of URM-wall Unit-2

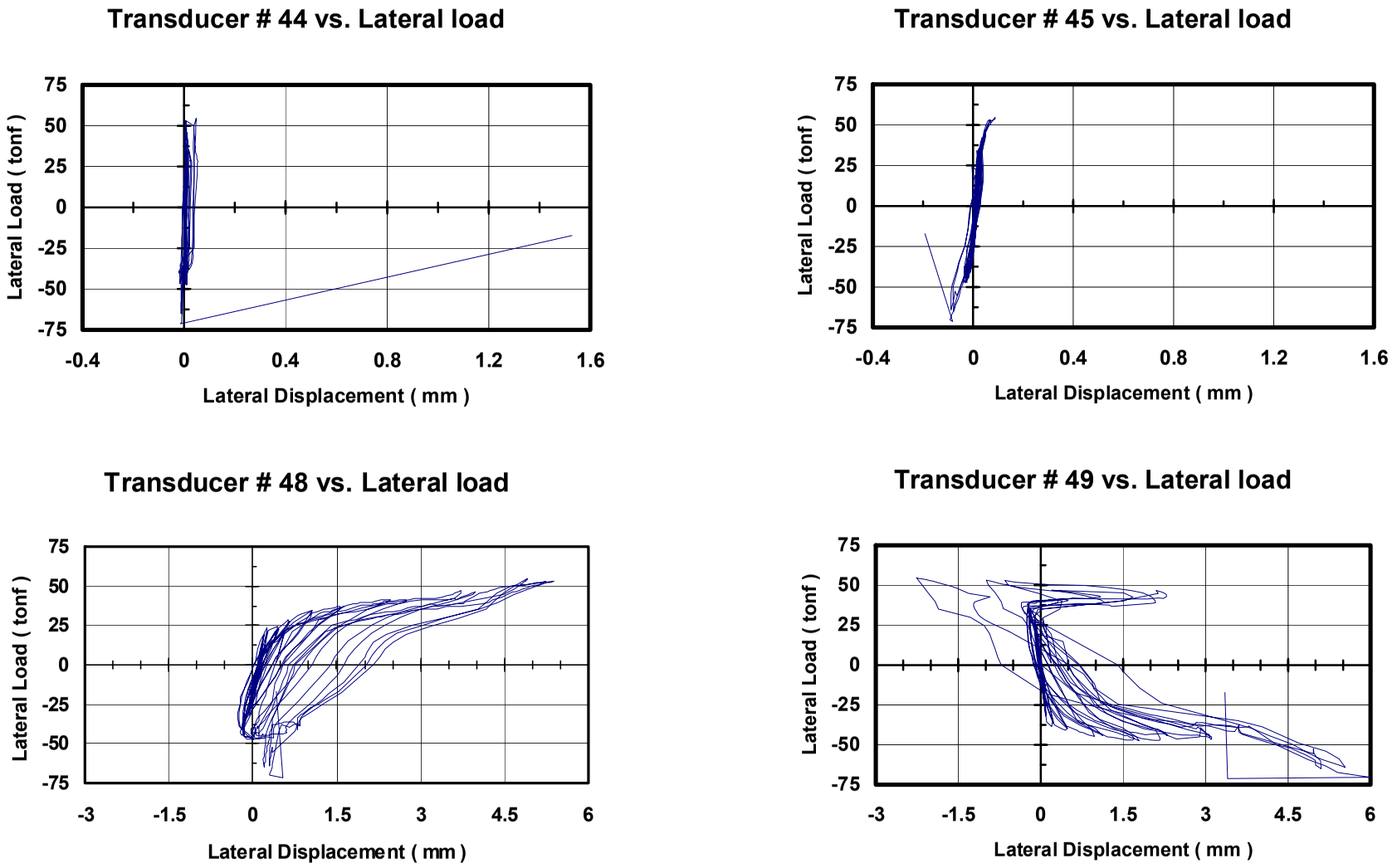

Figure B.14. Lateral force – displacement response of URM-wall Unit-2

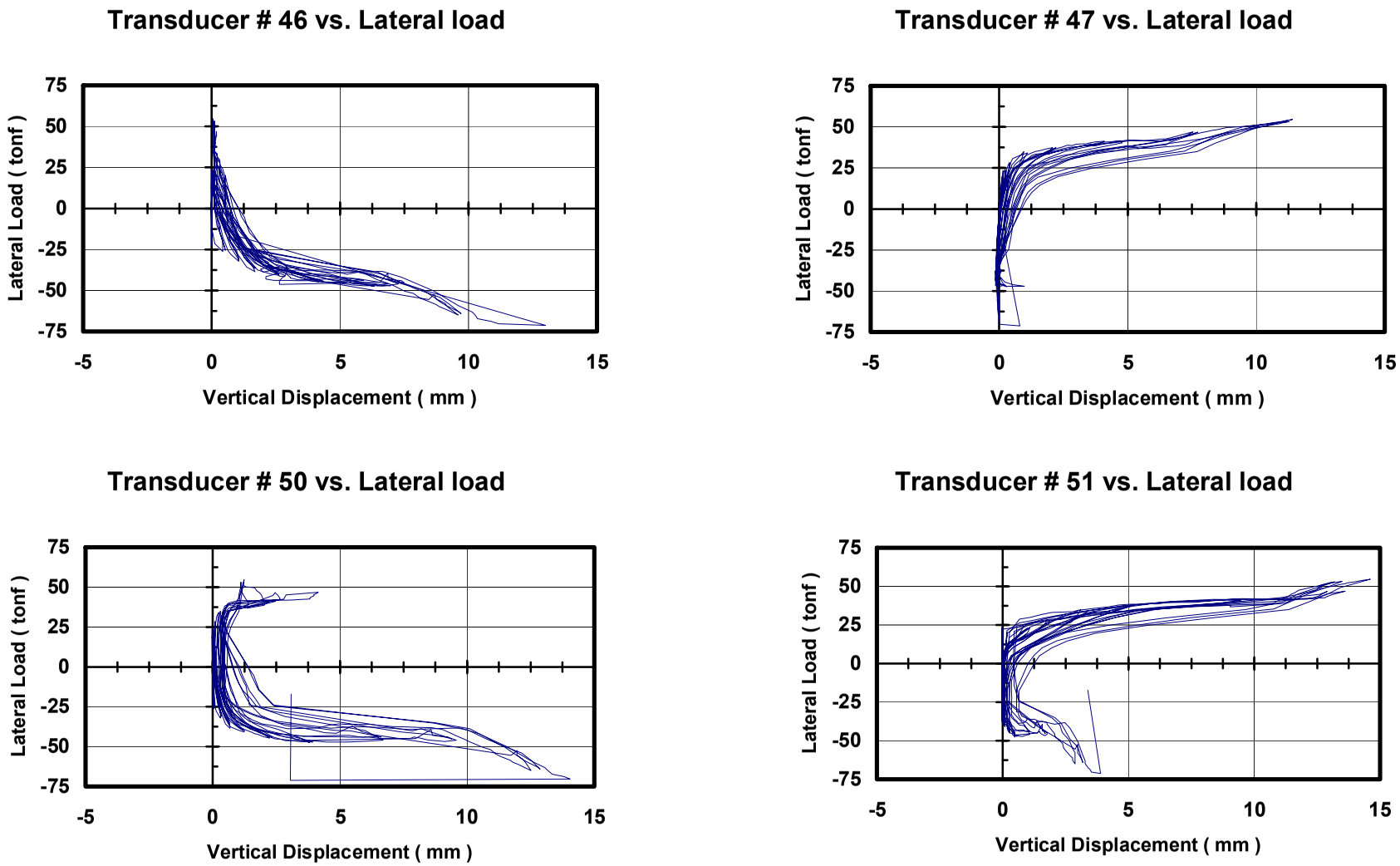

Figure B.15. Lateral force – vertical displacement response of URM-wall Unit-2

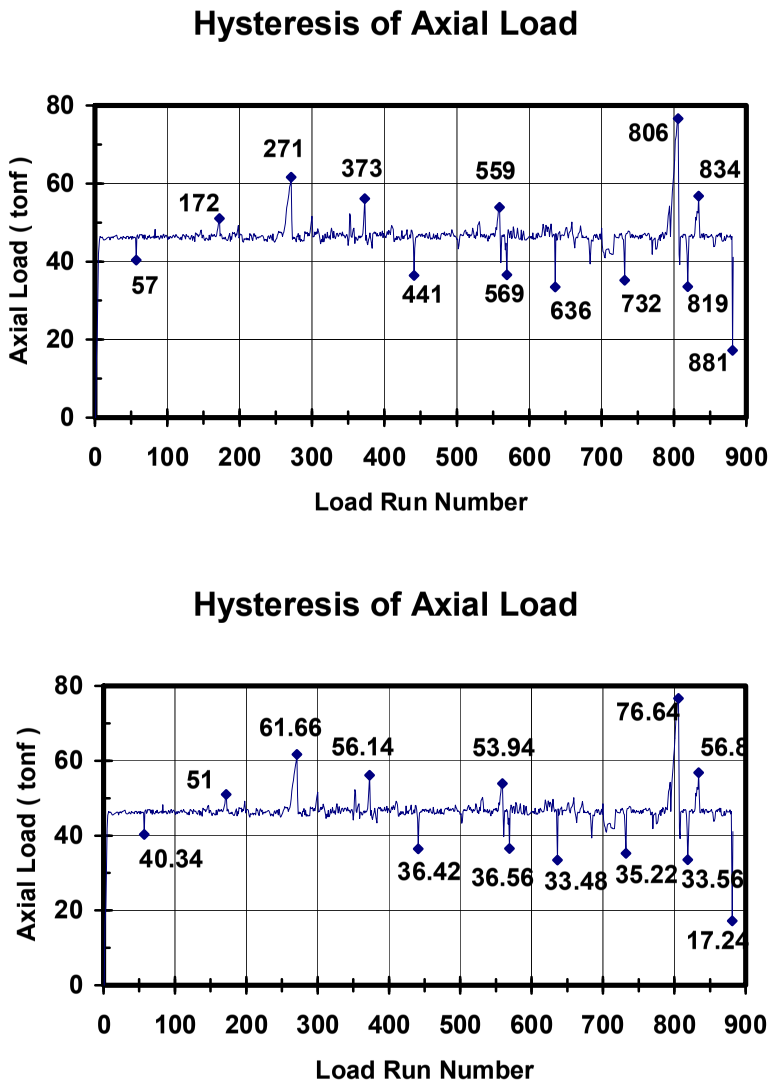

Figure B.16. Two axial jack-load response of URM-wall Unit-2